193A

HINDCAST STUDY OF HURRICANE ANDREW (1992) OFFSHORE GULF OF MEXICO

Oceanweather Inc.
Cos Cob, CT

November 10, 1992

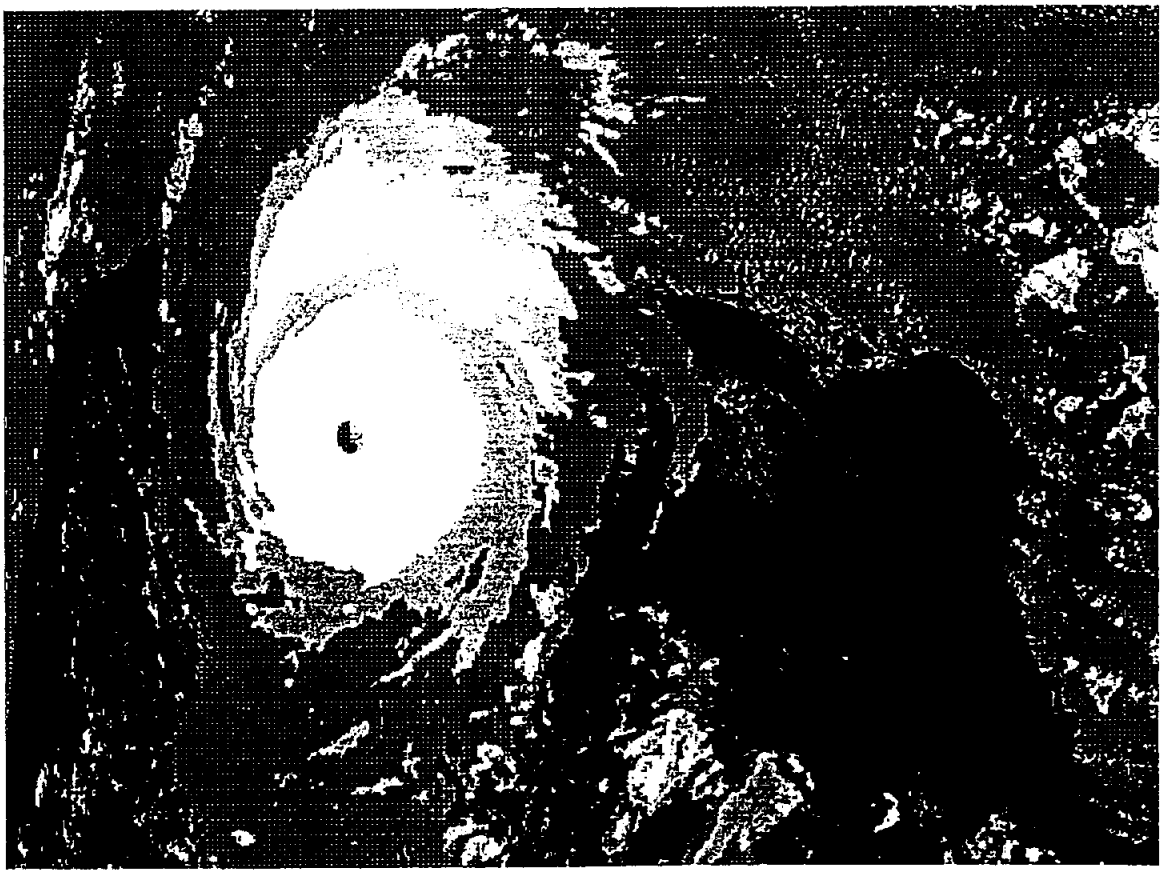

FINAL REPORT

HINDCAST STUDY OF HURRICANE ANDREW (1992)

OFFSHORE GULF OF MEXICO

prepared by

Vincent J. Cardone
and
Andrew T. Cox

Oceanweather Inc.
Cos Cob, CT

November 10, 1992

Table of Contents

1. INTRODUCTION

Hurricane Andrew was the costliest natural disaster in United States history. This perception is formed primarily by the devastation caused by this storm in South Florida. The loss of life and damage in the Gulf Coast states was an order of magnitude smaller than in South Florida. This study, however, is prompted by the striking impact of Andrew on offshore platforms, and associated infrastructure, located in Federal waters of the Gulf of Mexico. At least 249 of 3,800 offshore platforms were damaged by the storm, though there was no associated loss of life offshore, less than 500 barrels of oil spilled (with virtually no residual pollution therefrom), and production of oil and gas were minimally affected.

The exposure and response of the offshore infrastructure to Hurricane Andrew is, and will remain, of intense interest to the structural engineering community and to relevant government agencies. Intensive studies will be directed toward gaining an understanding of the structural response of damaged and collapsed platforms as well as of those platforms that survived in the area of greatest damage.

The experience of Hurricane Andrew provides an opportunity to quantitatively evaluate the adequacy of older design practices and possibly to validate the effectiveness of present design practices. Such studies will be severely hampered, however, without reliable data on environmental conditions (sustained wind speed and peak gust, significant wave height, maximum wave height, maximum wave crest heights, storm surge and storm driven ocean currents) at each site affected. Unfortunately, there were no instrumental measurements made offshore of surface winds, waves, currents or surge within about 50 miles of the track of the center of Hurricane Andrew. The objective of this study is to provide a reliable base of environmental data in the offshore

areas affected by the application of hindcast models which have been previously calibrated and validated against Gulf of Mexico hurricanes.

This report is organized as follows. Section 2 gives a general description of the hindcast approach applied. Section 3 describes the data assembled for the hindcast, and our analysis of that data to develop the storm meteorological parameters required by our hindcast models, but only as Andrew traversed the Gulf of Mexico. The reader interested in a more general description of the track, intensity and impact of this storm throughout its long history should read the NOAA National Hurricane Center Preliminary Report on Hurricane Andrew, included here as Appendix A, and perhaps the summary of airborne track and storm structure data included here as Appendix B. Section 4 presents the result of the hindcasts themselves, including comparison of hindcast and measured (as available to this study) data and a summary of hindcast extremes. Extensive hindcast results are also submitted separately on magnetic media.

2. THE HINDCAST APPROACH

This study may be viewed within the context of the Ocean Data Gathering Program (ODGP), which began in 1969 and included an extensive measurement program, a hindcast model development and calibration phase and an analysis phase which culminated in the establishment of reliable estimates of extreme wave heights and wave periods, associated with hurricane generated sea states in deeper parts of the Gulf of Mexico continental shelf between the Mississippi Delta and the Texas/Mexico border. The measured data acquired in the ODGP provided a basis for the development and calibration of numerical models for the accurate specification of surface wind and wind stress fields in historical Gulf of Mexico hurricanes. In addition, it was demonstrated that numerical spectral ocean wave prediction models

could be used to provide an accurate description of the complex pattern of sea states generated by and travelling with tropical cyclones (Cardone et al., 1976). The extremal analysis of the results of hindcasts of the most extreme historical hurricanes which had occurred between 1900 and 1970 carried out with the ODGP hindcast models, provided the design estimates (Ward et al., 1979; Haring and Heideman, 1978).

The ODGP was one of the earliest applications of the "hindcast-approach" to the specification of extremes. Since then, the hindcast approach has been widely adopted by the offshore and coastal engineering communities as a way to develop reliable extreme wind, wave, surge and current design estimates for offshore and coastal structure design. For example, the recently completed joint industry project "Gulf of Mexico Storm Hindcast of Oceanographic Extremes" (GUMSHOE) served to update the ODGP study and provide more reliable extreme design data in shallow water. In GUMSHOE a total of 100 tropical cyclones over the 90-year period 1900-1989 were hindcast. The statistical analysis of the hindcast data base provided definitive estimates of extremes of significant wave height, maximum individual wave height, maximum crest height, wind speed, current speed and storm surge height at over a 1000 grid points spaced nominally 12 nautical mile (nm) apart, covering all lease areas of current and future interest in deep and shallow water (water depths greater than 7.5 meters).

ODGP and GUMSHOE included substantial hindcast model validation studies because wind, wave, surge and current measurements have been made in some notable historical Gulf of Mexico storms (Audrey, 1957; Bertha, 1957; Carla, 1961, Camille, 1969; Edith, 1971, Delia, 1973, Frederic, 1979, Danny, 1985, Juan 1985). These validation studies (e.g. Reece and Cardone, 1982) suggest that our hindcast method typically specifies peak sea states (significant wave height) at an arbitrary site in a Gulf

of Mexico hurricane with bias of less than 0.5 m, mean abolute error of than 1.0 m and scatter index of 10-15% (scatter index is 100 x s.d/avg. where s.d. is the standard deviation of differences between hindcast and measured peak wave heights and avg. is the average of measured heights in the validation population of heights). The period and directional properties of peak storm generated seas appear to be specified with comparable accuracy.

The hindcast of an historical storm consists of three basic steps. First, the wind field is specified in a process which requires considerable work by a meteorologist both to develop required input parameters for a numerical model of the cyclone wind field, and to produce kinematic analyses for use when, and for areas in which, the numerical solution is not sufficiently accurate. The wind fields are specified on two grid systems, one used in the spectral wave model whose execution is the second part of the hindcast, and another used in the storm surge/current model, whose execution is the third part of the process. Appendix C gives concise descriptions of each of these processes, as specifically adapted to this problem.

3. METEOROLOGICAL CHARACTERISTICS OF HURRICANE ANDREW.

3.1 Data Sources

Our analysis referred to the following data, acquired from the indicated sources in the indicated format:

Vortex messages from U. S. Air Force Reserve aircraft reconnaissance of Hurricane Andrew . Received at OWI over its real time data link to the Global Telecommunications System, or GTS). Hard copy.

Continuous 1-minute average flight level wind speed, direction, D-value, air temperature. NHC. Hard copy and diskette file.

Synoptic observations from NOAA buoy and C-MAN stations. OWI GTS. Hard copy and hard disk files.

NOAA NHC advisories, including intensity and position at 3-hourly intervals. OWI GTS. Hard copy.

Synoptic observations from coastal and land stations. OWI-GTS. Hard copy.

Hourly composite radar images. WSI NOWRAD system. Hard disk files.

Loops of NOAA GOES visual, infrared and water vapor channel images. University of Wisconsin McIdas system. VHS tape.

Bullwinkle platform (Green Canyon Block 65) wind and wave measurements. NOAA C-MAN GTS and Shell. Hard copy.

Lena platform (28.2, 89.1) wind and pressure measurements. NOAA C-MAN and Exxon. Hard copy.

Jolliet Platform (Green Canyon Block 184) wave measurements. Conoco Inc.(These data remain confidential to Conoco Inc.)

3.2 General Storm Characteristics.

The NOAA NHC Preliminary Report gives a concise synoptic history of Hurricane Andrew from its formation out of a tropical wave which exited the west coast of Africa on August 14 to its demise on August 28 over the mid-Atlantic states. That report also includes vital meteorological statistics on the storm,

casualty and damage statistics, a critique of forecasts and warnings issued in real time, and a map and table of "best track" and intensity.

Of particular interest to this study is the period of time that the storm was in the Gulf of Mexico, or basically the 48-hour period between the time the storm exited south Florida near 1200 UT August 24, and the time it entered the Gulf Coast near 1200 UT August 26. During that period, the Air Force Reserve mounted twice-daily missions into Andrew, yielding no less than 28 center "fixes" and copious flight level data, mainly at 700 mb of wind, pressure and temperature defining the structure of the storm (at flight level).

Hurricane Andrew emerged into the Gulf of Mexico as an intense storm despite having passed over land through South Florida. Shortly after exiting the west coast of Florida, the central pressure was about 950 mb, maximum flight level winds were 117 knots, and the radius of maximum wind was still very small at about 10 nm. The aircraft fix data served as the principal source of data for specification of storm track and central pressure time histories in the Gulf of Mexico. We developed our own smoothed "best track" from the fix data, augmented by radar and satellite loops, to yield the track shown in Figure 1.

The observations of central pressure are shown in Figure 2, which also indicates the history implied in real time NHC advisories and the history ultimately used for our hindcast (as explained further below). Evidently, Andrew underwent one cycle of slight deepening shortly after leaving South Florida, and a more pronounced and sudden intensification when the center passed due south of the Delta. It is quite interesting that the central pressure reached its minimum (for the Gulf of Mexico phase) when the center was still about 60 nm offshore at about 2100 UT on

August 25. The central pressure then filled rapidly so that when the center actually crossed the coast, the pressure was close to 955 mb. This behavior is unlike most storms which maintain intensity until very near coast crossing. Andrew's behavior may be related to the oblique incidence angle of the track with the shoreline which placed much of the right front quadrant over land well before landfall, or perhaps to some other effect. Filling continued as the storm moved north through Louisiana on the 26th.

Maximum flight level winds in the Gulf of Mexico of about 130 knots were measured after the first round of deepening early on the 25th, and winds of 135 knots were measured at the end of the second round of deepening late on the 25th. However, as the central pressure filled early on the 26th, flight level winds appeared to decrease commensurately only to the left of the center, with the aircraft reporting maximum flight level winds of between 130 and 135 knots up until 0600 UT when the eye was just crossing Atchafalaya Bay. Aircraft data, satellite and radar imagery all supported a gradual expansion of the eye and eyewall diameter as the storm crossed the Gulf of Mexico, so that by the time the storm entered the Louisiana coast, the radius of maximum winds (in the boundary layer) was estimated to be 15 nm.

3.3 Detailed Storm Parameters

The bulk of the labor involved in our hindcast method as applied here is the development of the time history of the parameters required by our numerical vortex model of the boundary layer wind field. These consist mainly of the three-hourly coordinates of the storm center, and time histories of the central pressure, peripheral pressure, scale radius of the analytical form used to describe the axisymmetric part of the pressure field, the ambient circulation in which the storm is embedded described in terms of an equivalent geostrophic "steering flow", and a time backward weighted storm motion vector

(see Appendix C for a more detailed explanation of the model initialization).

The specification of storm parameters was most heavily influenced by the aircraft flight level and eye dropsonde data. For this study, the magnetic media files of virtually continuous flight level data were processed in much the same manner as they are processed at the NOAA National Hurricane Research Division. Figure 3 shows a typical flight pattern. To produce this plot, we first repositioned the individual measurements to a storm center relative coordinate system, using the sequence of fixes provided by the particular mission to determine the continuous position of the center over the approximately 8 hour duration of this flight. For this plot the flight level wind speeds were reduced by 75% to approximate 60-minute average winds at 20 m height. This reduction factor was taken from extensive empirical comparisons of flight level and surface winds reported by Powell and Black (1989).

In the storm relative coordínate system, individual legs were also plotted as a function of distance from the center as shown in Figure 4, which shows the reduced sea level pressure (extrapolated from 700 mb height) and surface wind speed distributions along flight legs taken north and south of the eye late on the 25th. The pressure plot shows a trial fit of the exponential profile to the reduced flight level data. The parameters of the pressure profile ultimately selected for the hindcast were not exclusively based upon fits to aircraft data for several reasons. It is possible, for example, that the structure of the inner core at the surface is different from that exhibited at flight level. In some storms the eyewall slopes inward toward the surface. A second consideration was the desire to compensate for the steady state aspect of the vortex model which implies instantaneous adjustment of the wind field to the pressure field. In the 9 hours before landfall, wind field

changes evidently lagged the rapid filling in central pressure especially to the right of the center where maximum wave generation occurs. Therefore, we introduced a lag in the pressure center (see Figure 2) in the modeled central pressure time history during the prelandfall filling stage. Since the wind response appeared to be asymmetrical, introduction of this lag should improve the accuracy of the modelled winds to the right of the center at the expense perhaps of slightly degrading the accuracy of the wind field to the left of the track.

The final parameter specification adopted for the hindcast (a result of many trial iterations) is given in Table 1. The ultimate objective of the model initialization was to provide a vortex description which provided the most accurate hindcast of ocean response parameters. Direct verification of the modeled wind field was given lower priority because available surface wind data are woefully inadequate for this purpose. Unfortunately, the inner core of Andrew weaved a path which avoided the buoy and platform stations equipped with calibrated recording anemometers (see Figure 1).

Table 1 gives the parameters used to calculate a series of ten numerical model wind field solutions on a storm-centered relative nested rectangular coordinate system (inner mesh spacing of 5 km), which are then interpolated in space and time to provide wind fields at 30-minute intervals on the rectangular grids of regular spacing of the wave and surge/current models. The 30-minute center coordinates are interpolated linearly from the 3-hourly positions in the "storm track table" of Table 1.

The hindcast extends from 1200 UT August 24 to 1800 UT August 26. The first snapshot specifies a vortex with central pressure of 947 mb, azimuthal averaged peripheral pressure of 1016 mb, scale radius of 9 nm, movement toward the west-northwest at 13 knots, and ambient geostrophic steering "flow" from the

east-southeast at 7 m/s. As the storm reached its maximum intensity at 1800 UT August 24, indicated in Table 1 by "snapshot" number 5, the central pressure had lowered to 932 mb, the scale radius had increased to 15 nm, the steering flow increased to 11 m/s and forward motion slowed to 11 knots, now directed toward the northwest. Since Andrew was accompanied by greater than normal peripheral pressures and ambient steering gradients, the effective intensity (i.e. in terms of wind, and ocean response) was somewhat greater than indicated merely by its central pressure.

4. HINDCAST RESULTS

4.1 Wind Field

In this study, all winds are referred to the effective over-water 60-minute average winds at a height of 20 m above sea level. Wind speeds at 10 m height are about 8% lower. Wind speeds at shorter averaging intervals may be derived by applying the following "gust" factors to the 60-minute average wind speed:

10 minute average	x 1.09
1 minute average	x 1.22
3-second gust	x 1.53

The hindcast wind fields are shown at two scales in this report. Appendix D shows the pattern over the whole Gulf at 6-hourly intervals, with wind vectors plotted at every other row and column of points of the wave hindcast model grid. Appendix E shows the winds at 3-hourly intervals at every model grid point over a more limited domain and only for the hindcast period during which the hurricane passed through this domain. Conventional "wind barb" representation (each full barb denotes ten knots, each half barb 5 knots and each flag 50 knots) is followed, which limits read resolution to about 5 knots. However,

on the high resolution plots, the two digits plotted adjacent to each vector allow the actual wind speed and direction to be read (the first digit is the tens place of the direction, the second digit is the units place of the speed). For example, at 1800 UT August 25 (map labelled as 92082518), the grid point with maximum wind speed is located due north of the storm center (center of cyclonic circulation), at which the wind direction is 070 degrees (from which) and the wind speed is 98 knots. Due south of the center maximum wind speeds are only 68 knots, indicating the asymmetry usually found in a Gulf hurricane if it is not heavily influenced by an extratropical weather system. The wind direction pattern is also quite asymmetrical with strong inflow in the right and rear quadrants and minimal inflow to the front and left of the center.

The evolution of the wind speed field is shown in a different way in Figures 5 (large domain) and Figure 6 (limited domain). These plots show contours of the maximum wind speeds experienced at each grid point over the entire storm history. For example, Figure 6 shows that winds exceeded 50 m/s only over a small area southwest of the Mississippi Delta, where the minimum central pressure was observed. Using the rough empirical ratio between surface and flight level winds speeds of 0.75, (Powell and Black, 1989) maximum flight level winds in the range of 130-135 knots are consistent with surface winds of about 99 knots, or about 51 m/s, which is very close to the maximum wind speed modeled.

Appendix F gives comparisons of modeled and measured (adjusted to 20 m) wind time histories at open-sea sites, including NOAA buoys 42001 and 42003, and Bullwinkle and Lena platforms. Only Lena was located to the right of the track, and only wind speed measurements are available there. There were two anemometers on Bullwinkle, and comparisons are presented for both. In general, there is excellent agreement between modeled

and observed wind direction histories, and a tendency for the modeled wind speeds to run higher than observed. However, as noted above, we judged it more important to model the inner core and right sides of the circulation accurately, and therefore decided not to compromise the storm parameters to achieve closer fits at sites left of the track, at the expense of lowering peak wind speeds closer to the center. Also, as noted below, this wind field provides generally unbiased hindcasts of peak storm significant wave heights at these same sites.

4.2 Surface Waves

The execution of the wave hindcast model provides directly the two-dimensional wave spectrum at hourly intervals, on the wave model grid (see Appendix C), an array of points spaced nominally 12 nm apart. Integrated properties of the spectrum are calculated from the 2-D spectra at all grid points and archived as part of the hindcast run. For example, Appendix G shows the pattern of hindcast HS and associated vector mean wave direction.

In a post-processing step, and only at points at which the peak HS in the storm exceeds at least 3 m, time histories of the 2-D spectra are used to calculate the probable maximum individual wave height, HM, and maximum individual crest height, HC. The entire time history at a point is used in this calculation following the method of Borgman (1973). The empirical statistical distribution of Forristall (1978) is used to specify HM and the empirical distribution of Haring et al. (1978) is used for HC. These calculations yield probability distributions for the respective heights. We have selected the median value (or 50% cumulative probability level) of the fitted distributions. Thus, even if the hindcast is perfect, it is quite possible that the median maximum HM or HC may be exceeded at a particular site.

The spatial distribution of the maximum hindcast HS and the maxima calculated (median) HM and HC are shown in Figures 7, 8 and 9 respectively on the large Gulf domain, and in Figures 10, 11 and 12 respectively for the limited domain of most interest. The hindcast shows maxima of HS increasing from about 8 m just off the west coast of Florida to a peak just above 13 m south of the Delta where the storm intensity peaked. The calculated maximum individual wave height and crest height just exceed 21 m and 13 m respectively. The absolute maximum sea state hindcast was at grid point 3748, at 28.25 degree N, 89.88 degrees W, where the hindcast HS is 13.26 m, HM is 22.04 m, and where HC is 12.79 m, though HC of 13.92 m was specified at an adjacent grid point . The hindcast and calculated storm maxima of winds and all ocean response parameters of interest at all grid points within the limited domain are given in Appendix G.

It is possible to compare measured and hindcast waves at only three offshore sites, none located closer than about 50 nm from the track. These comparisons are shown in Figures 13-15, for buoys 42001, 42003, and Bullwinkle platform respectively. At 42001 the agreement in HS is excellent throughout except for a slight lag and underspecfication of peak HS with respect to that measured. At 42003 the peak is slightly overpredicted and the lag is smaller. At Bullwinkle, the peak HS is well specified, with a lag of about 2 hours. Figure 16 is a scatter plot of measured and hindcast HS based upon all sites, and Table 2 compares just the peaks. Though the data sample is quite small, Table 2 suggests that this hindcast comes within the typical error characteristics for specification of storm peak HS at a site of the ODGP hindcast method. Over the three sites, the mean hindcast-measured difference in specification of peak HS is .32 m, and the mean absolute difference is only .38 m.

4.3 Storm Surge/Currents

The results of the hindcast of storm surge and vertically integrated currents are shown in Figures 17 and 18 for the large domain, and in Figures 19 and 20 for the limited domain. The latter figures show the hindcast peak at every model grid point. Figure 19 shows the peak hindcast current (plot threshold of 25 cm/sec) and the hindcast peak positive storm surge at the time of the peak current, and Figure 20 shows the peak hindcast storm surge (plot threshold of 20 cm) and the associated current.

No measurements of the surge offshore are available for comparison with this hindcast. The indicated positive surge near the storm track of 50-75 cm in deep water is associated with the "inverted barometer effect". Maximum positive storm surge increased with decreasing water depth near the track, exceeding 1 meter to the right of the track on the shelf and up to 3 meters at one grid point near the coast south of Houma near Terrebone Bay. The pattern of open coast surge is close to that observed (see Figure 21, from Haag Engineering Co., 1992). Higher resolution in the surge model would be required to make quantitative comparisons between observed and hindcast surge at gage locations right at the shoreline, but the general agreement between hindcast and measured peak positive surge between Grand Isle and Vermillion Bay is encouraging. The maximum vertically integrated current was specified to be 1.60 m/sec (3.1 knots) offshore Vermillion Bay.

5. DISCUSSION

The objective of providing an environmental data base for study of platform response to Hurricane Andrew has been satisfied by the hindcast method. The very limited field data available for validation of this hindcast suggests that errors in specification of wind fields and sea states are equal to or smaller than errors

typical of the hindcast method applied. No validation of currents was possible, but the profile of peak hindcast storm surge along the open coast of Louisiana appears to be in close agreement with the limited measurements available at this time.

By almost any standard measure (e.g. central pressure, peak winds, destructive potential) Hurricane Andrew was a very intense Gulf of Mexico hurricane. In this century we estimate that only 5 other hurricanes attained central pressure of 932 mb or lower in the Gulf of Mexico. The storm is also very highly ranked in terms of wave generation. If we use the ODGP historical hindcasts as a reference (Ward et al., 1979) the maximum hindcast HS at the shelf break south of the Mississippi Delta of 13.2 m (43.5 ft) was exceeded in only 7 storms this century anywhere in the Gulf. Off the central Gulf coast, only Betsy (1965) and Camille (1969), both with peak hindcast HS of (14 m) 46 ft, exceeded the peak hindcast HS in Andrew. The maximum calculated individual wave height of 22 m (72 ft) at the shelf break is equal to the site-specific 100-year return period maximum individual wave height estimated for deep water by Ward et al. (1979). Participants in the more recent joint industry projects which extended the ODGP results into shallow water (e.g. GUMSHOE) may make comparable comparisons in shallow water.

Finally, while this hindcast was carried out to support the platform response studies, there is the potential that the studies of platform damage and response may be used in a synergistic way to further validate the hindcast models and existing design data derived therefrom. We fully encourage the offshore industry efforts to utilize indirect methods to estimate the peak environmental conditions seen by their platforms, and recommend that such data be pooled to reveal the spatial pattern of peak environmental loads exerted by this hurricane. Such data might even by useful for reevaluation of some of the fundamental

physical mechanisms incorporated in the wave and hydrodynamic models exercised herein.

References

Borgman, L. E. 1973. Probabilities for the highest wave in a hurricane. J. Waterways, Harbors and Coastal Engineering Division, ASCE, 185-207

Cardone, V. J., W. J. Pierson, and E. G. Ward. 1976. Hindcasting the directional spectra of hurricane generated waves. J. of Petrol. Tech., 28, 385-394.

Forristall, G. Z. 1978. On the statistical distribution of wave heights in a storm. J. of Geophys. Res., 83, 2353 - 2358.

Haring, R. E. and J. C. Heideman. 1978. Gulf of Mexico rare wave return periods. OTC Paper 3280.

Haag Engineeering Co. 1992. Hurricane Andrew Storm Damage Survey. Informal report.

Powell, M. D. and P. G. Black. 1989. The relationship of hurricane resonnaissance flight-level wind measurements to winds measured by NOAA's oceanic platform. 6th National Conference on Wind Engineering. March 7-10, 1989. Houston, TX.

Reece, A. M. and V. J. Cardone. 1982. Test of wave hindcast model results against measurements during four different meteorological systems. OTC #4323, 14th Annual OTC (Offshore Technology Conference), Houston, Texas, May 3 - 6.

Ward, E. G., L. E. Borgman, and V. J. Cardone. 1979. Statistics of hurricane waves in the Gulf of Mexico. J. Petrol. Tech., May, 632 - 642.

Table 1. Storm parameters and track used for numerical model simulation of boundary layer wind field

Tropical Cyclone Input Data — Project *ANDREW JIP*
Storm # *9208* Name *ANDREW* Duration of Hindcast *60 hours*

SNAP	1	EYELAT = *26* .,	DIREC = *280* .,	SPEED = *13* .,	EYPRES = *947*.,
		RADIUS = *9* .,	PFAR =*1016* .,	SGW = *7* .,	AN1 = *120*.,
SNAP	2	EYELAT = *26* .,	DIREC = *280* .,	SPEED = *13* .,	EYPRES = *943*.,
		RADIUS = *9* .,	PFAR =*1016* .,	SGW = *7* .,	AN1 = *120*.,
SNAP	3	EYELAT = *27* .,	DIREC = *295* .,	SPEED = *13* .,	EYPRES = *948*.,
		RADIUS = *12* .,	PFAR =*1016* .,	SGW = *8* .,	AN1 = *125*.,
SNAP	4	EYELAT = *28* .,	DIREC = *295* .,	SPEED = *13* .,	EYPRES = *944*.,
		RADIUS = *15* .,	PFAR =*1016* .,	SGW = *9* .,	AN1 = *125*.,
SNAP	5	EYELAT = *28* .,	DIREC = *305* .,	SPEED = *11* .,	EYPRES = *932*.,
		RADIUS = *15* .,	PFAR =*1016* .,	SGW = *11* .,	AN1 = *125*.,
SNAP	6	EYELAT = *29* .,	DIREC = *320* .,	SPEED = *10* .,	EYPRES = *936*.,
		RADIUS = *15* .,	PFAR =*1016* .,	SGW = *9* .,	AN1 = *140*.,
SNAP	7	EYELAT = *30* .,	DIREC = *340* .,	SPEED = *9* .,	EYPRES = *958*.,
		RADIUS = *15* .,	PFAR =*1016* .,	SGW = *8* .,	AN1 = *155*.,
SNAP	8	EYELAT = *30* .,	DIREC = *355* .,	SPEED = *9* .,	EYPRES = *973*.,
		RADIUS = *15* .,	PFAR =*1016* .,	SGW = *8* .,	AN1 = *160*.,
SNAP	9	EYELAT = *30* .,	DIREC = *5* .,	SPEED = *8* .,	EYPRES = *982*.,
		RADIUS = *15* .,	PFAR =*1016* .,	SGW = *8* .,	AN1 = *170*.,
SNAP	10	EYELAT = *31* .,	DIREC = *5* .,	SPEED = *8* .,	EYPRES = *990*.,
		RADIUS = *16* .,	PFAR =*1016* .,	SGW = *8* .,	AN1 = *175* ,

Storm Track Table

TIME STEP	LAT	LONG	SNAP	ROT	(YMDH)
0	25 36	-81 12	1	0	92082412
6	25 41	-82 10		0	2415
12	25 46	-83 09	1	0	2418
18	26 00	-84 03		0	2421
24	26 08	-85 02	2	0	2500
30	26 23	-85 54		0	2503
36	26 38	-86 47		0	2506
42	26 56	-87 38	3	0	2509
48	27 16	-88 24		0	2512
54	27 31	-89 08	4	0	2515
60	27 47	-89 42	5	0	2518
66	28 10	-90 09	5	0	2521
72	28 33	-90 39		0	2600
78	28 47	-91 03	6	0	2603
84	29 09	-91 19		0	2606
90	29 37	-91 34	7	0	2609
96	30 06	-91 42	8	0	2612
102	30 29	-91 40	9	0	2615
108	30 54	-91 36	10	0	2618

File: G:\05ANDREW.TAB, Thursday 5-Nov-1992 11:38am

Table 2.

Hurricane ANDREW
Comparision of Hindcast vs. Measured
Peak-to-Peak Significant Wave Heights

Measured			Hindcast				
Station	Time	Hs	Grid Pt	Time	Hs	Time Diff (Meas-Hind)	Hs Diff (Meas-Hind
BUSL1	2519	7.86	3664	2521	7.76	-2	.10
42001	2513	4.50	2896	2517	3.84	-4	-.66
42003	2502	6.50	2896	2503	6.98	-1	-.39

File: G:\COMPPEAK.WPF, Monday 9-Nov-1992 4:28pm

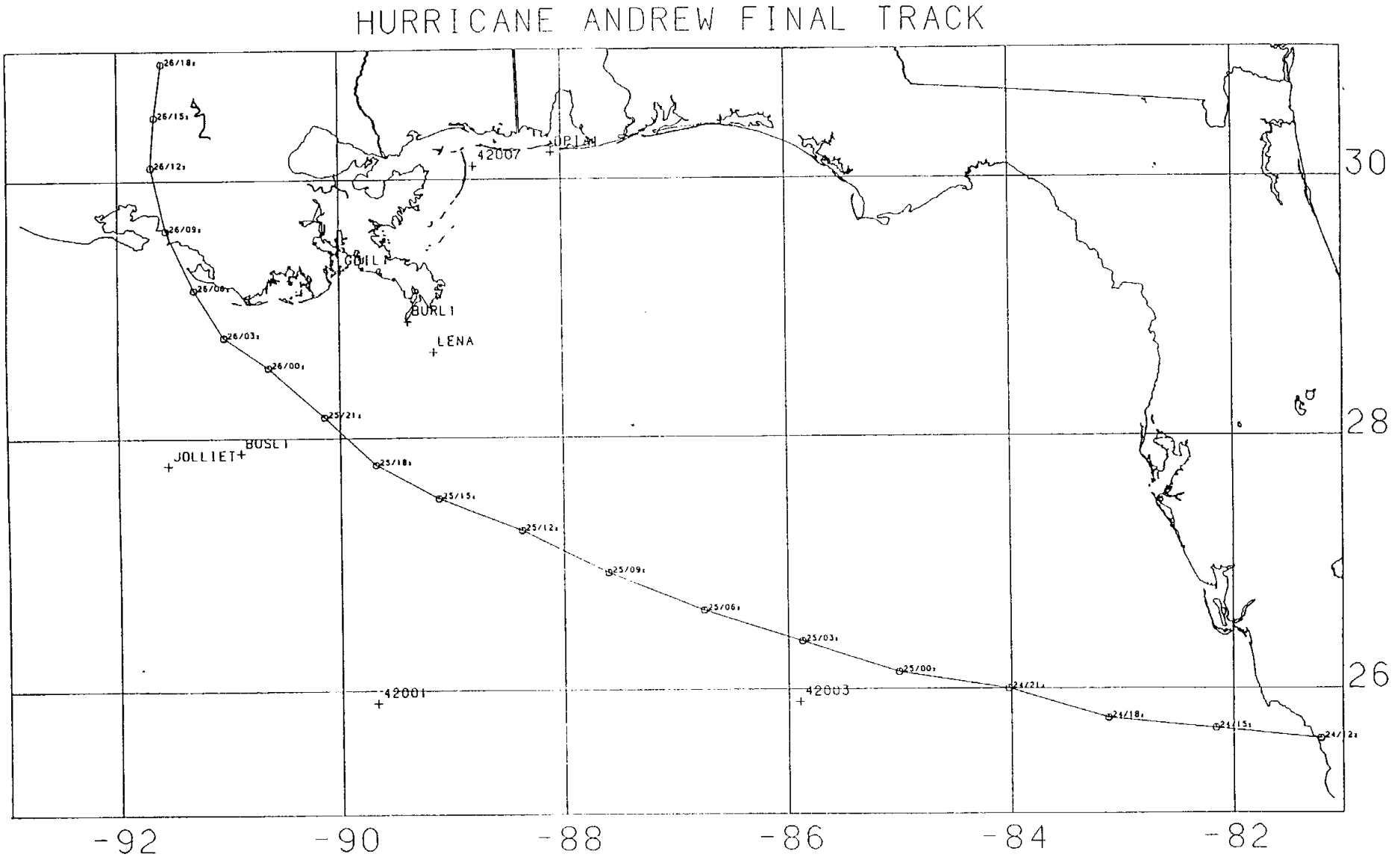

Figure 1. Storm track used for hindcast. 3-hourly positions and locations of known buoy and platform measurement sites.

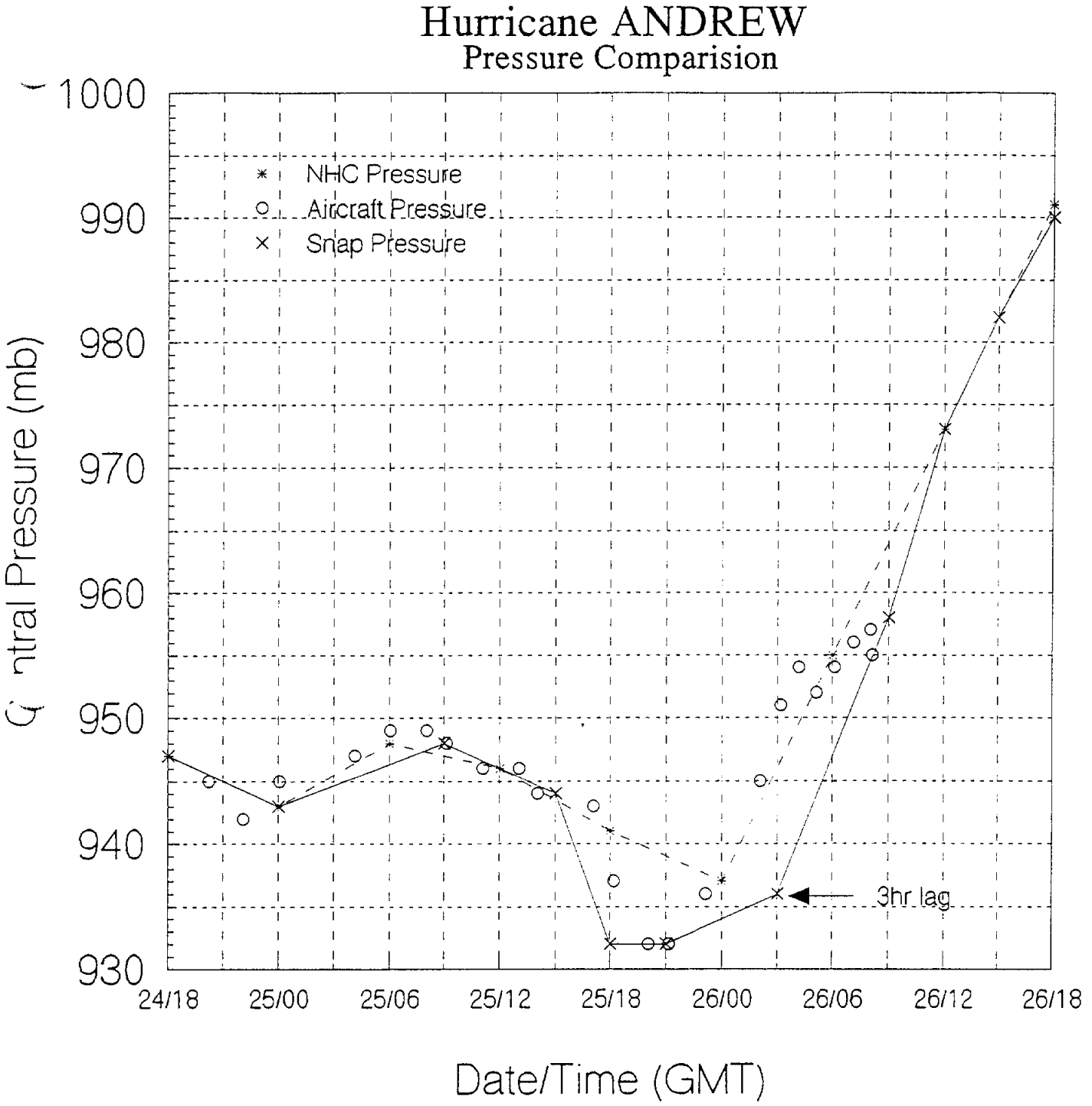

Figure 2. Observed central pressures, NHC advisory central pressures, and central pressure time history used for hindcast, with lag during filling stage to model lag in decay of peak winds.

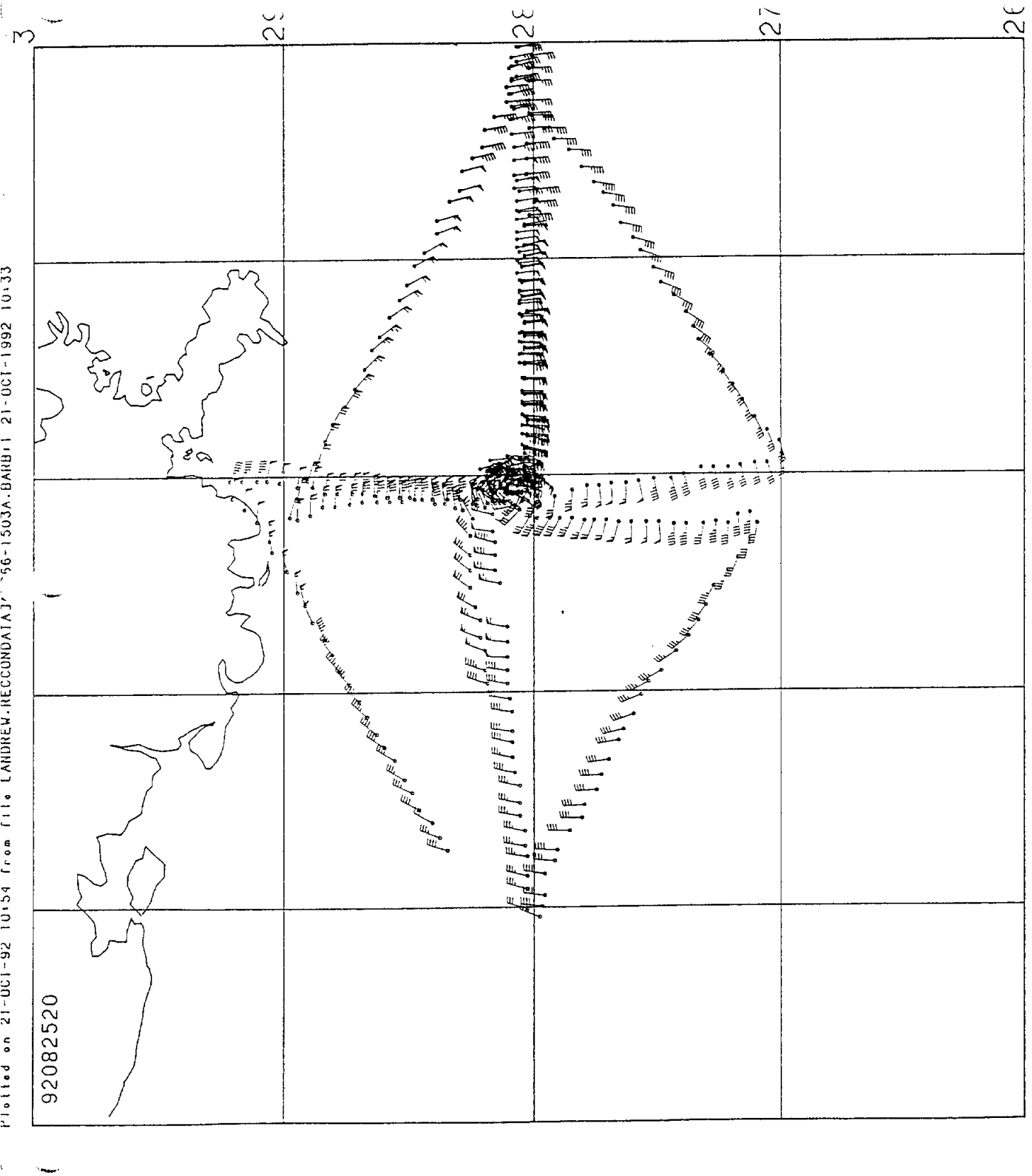

Figure 3. Flight path and measured winds (reduced to 20 m level) in a mission into Hurricane Andrew by Air Force Research aircraft late on August 25.

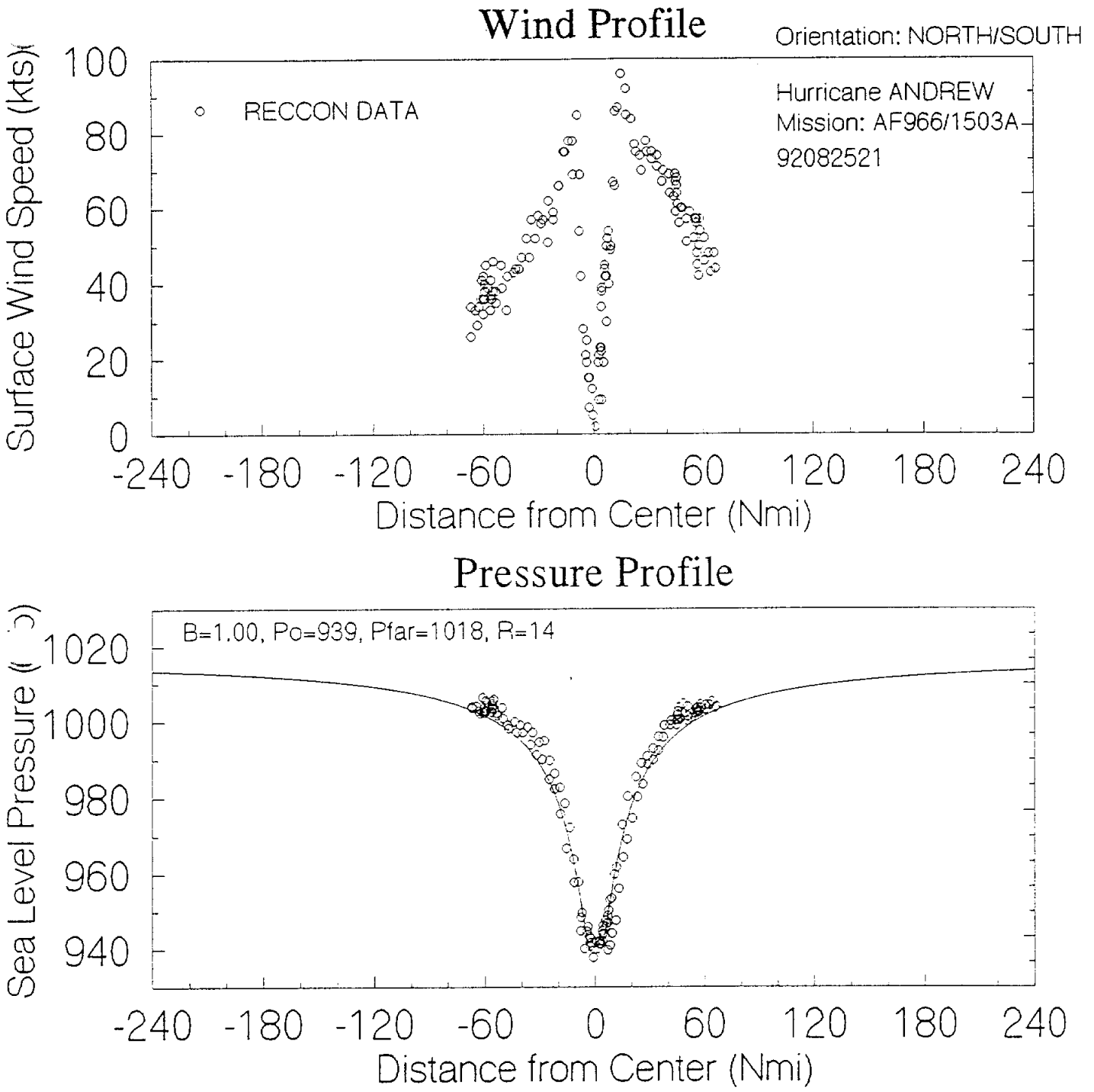

Figure 4. Flight level data reduced to surface level and repositioned with respect to the center of Hurricane Andrew for a north-south flight leg through the eye. A trial fit of the exponential pressure profile is shown through the pressure data.

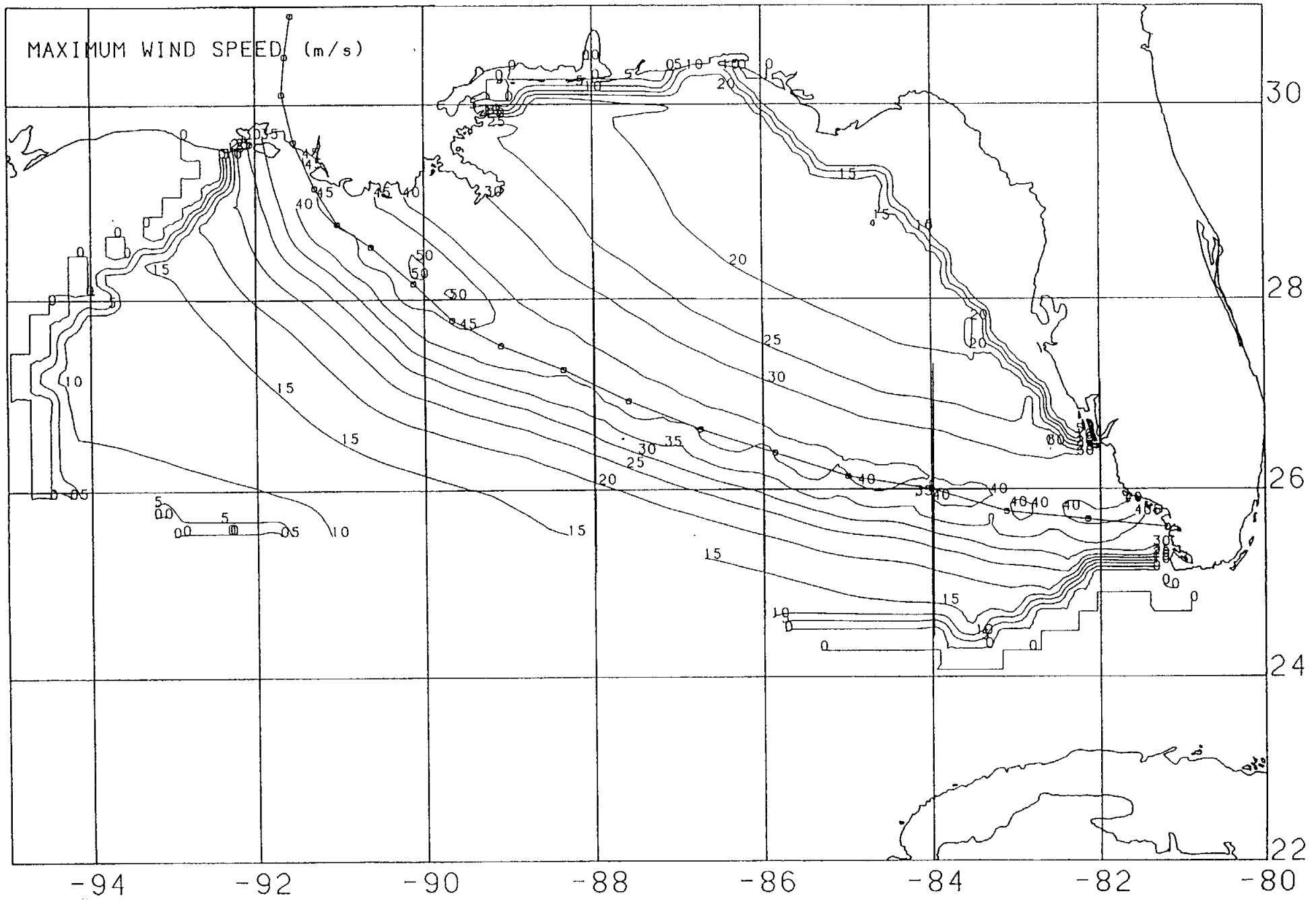

Figure 5. Contours of maximum modeled 20-m average wind speed. Contours less than 15 m/s are spurious and should be disregarded. Storm track is superimposed.

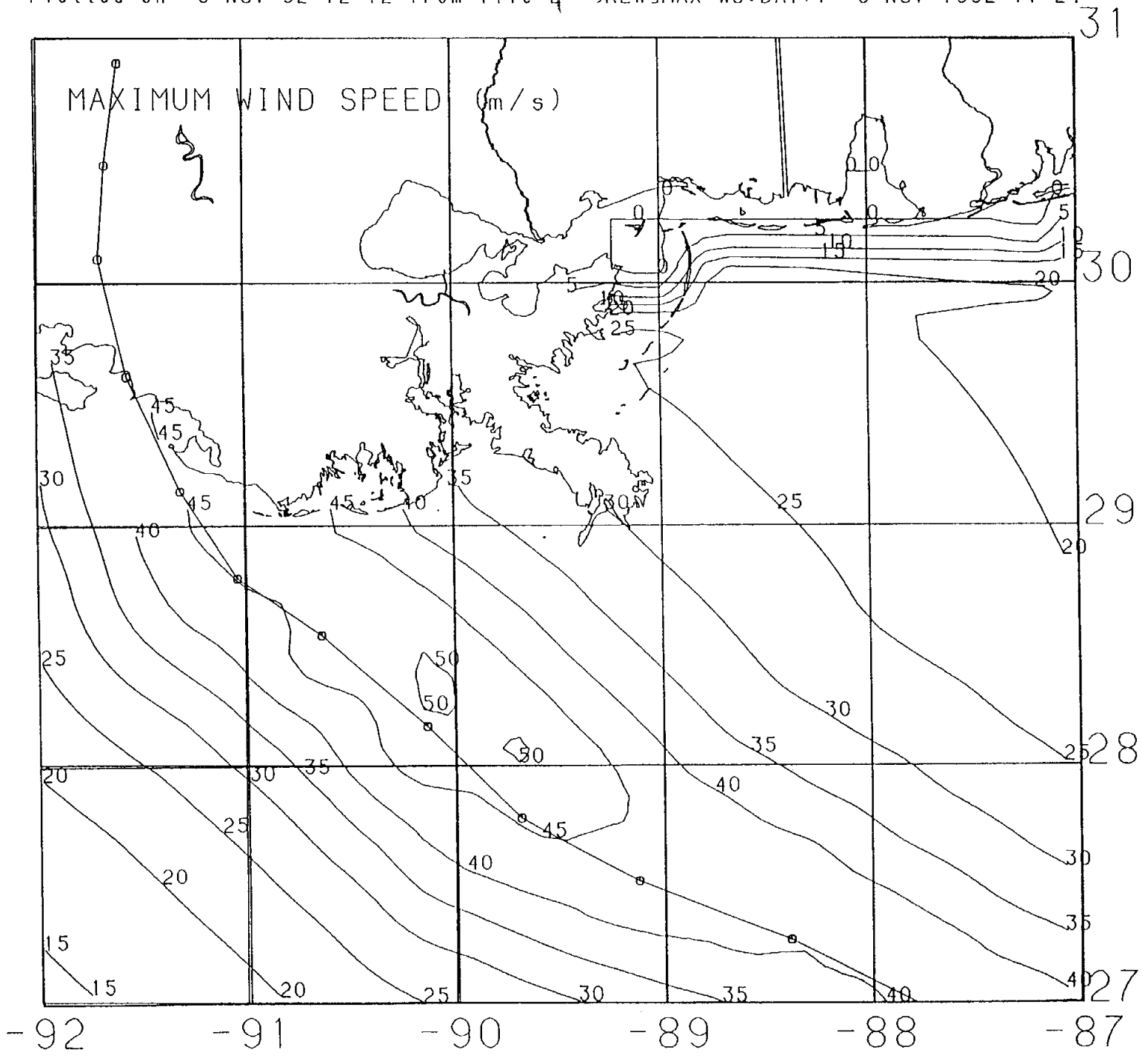

Figure 6. Same as Figure 5, but for a more a limited domain.

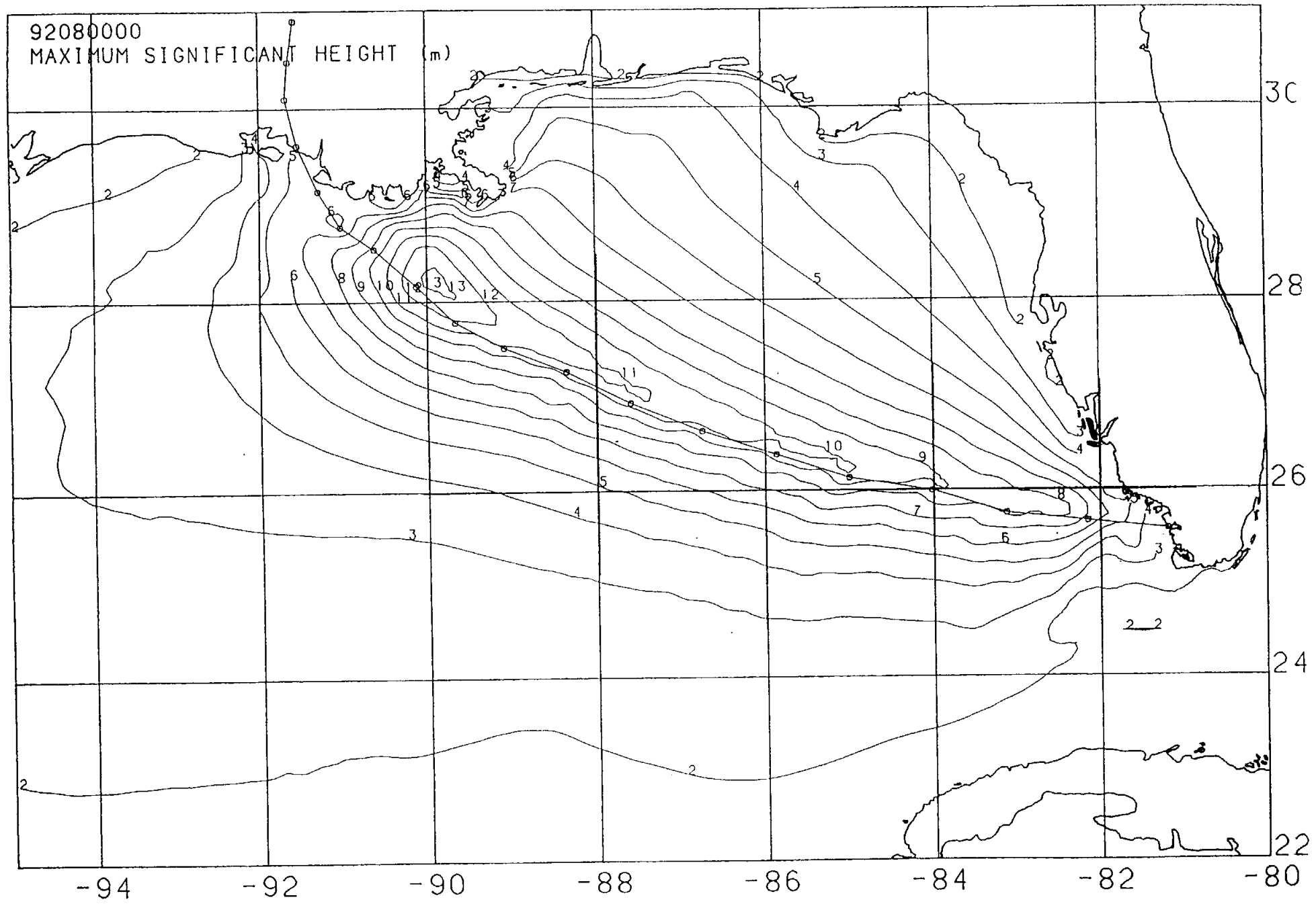

Figure 7. Contours of maximum hindcast significant wave height.

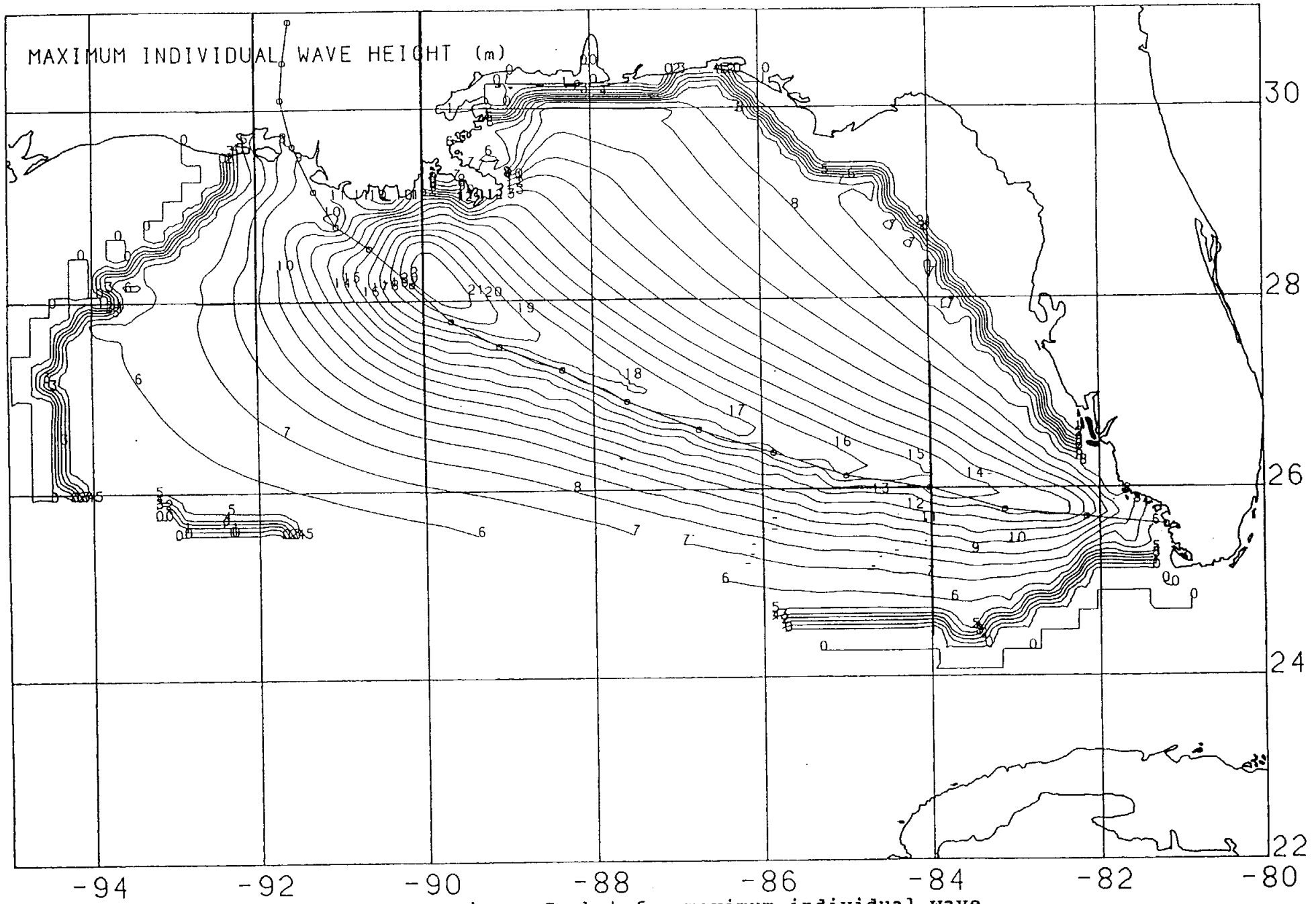

Figure 8. Same as Figure 7, but for maximum individual wave height. Contours of heights lower than 7 m are spurious and should be disregarded.

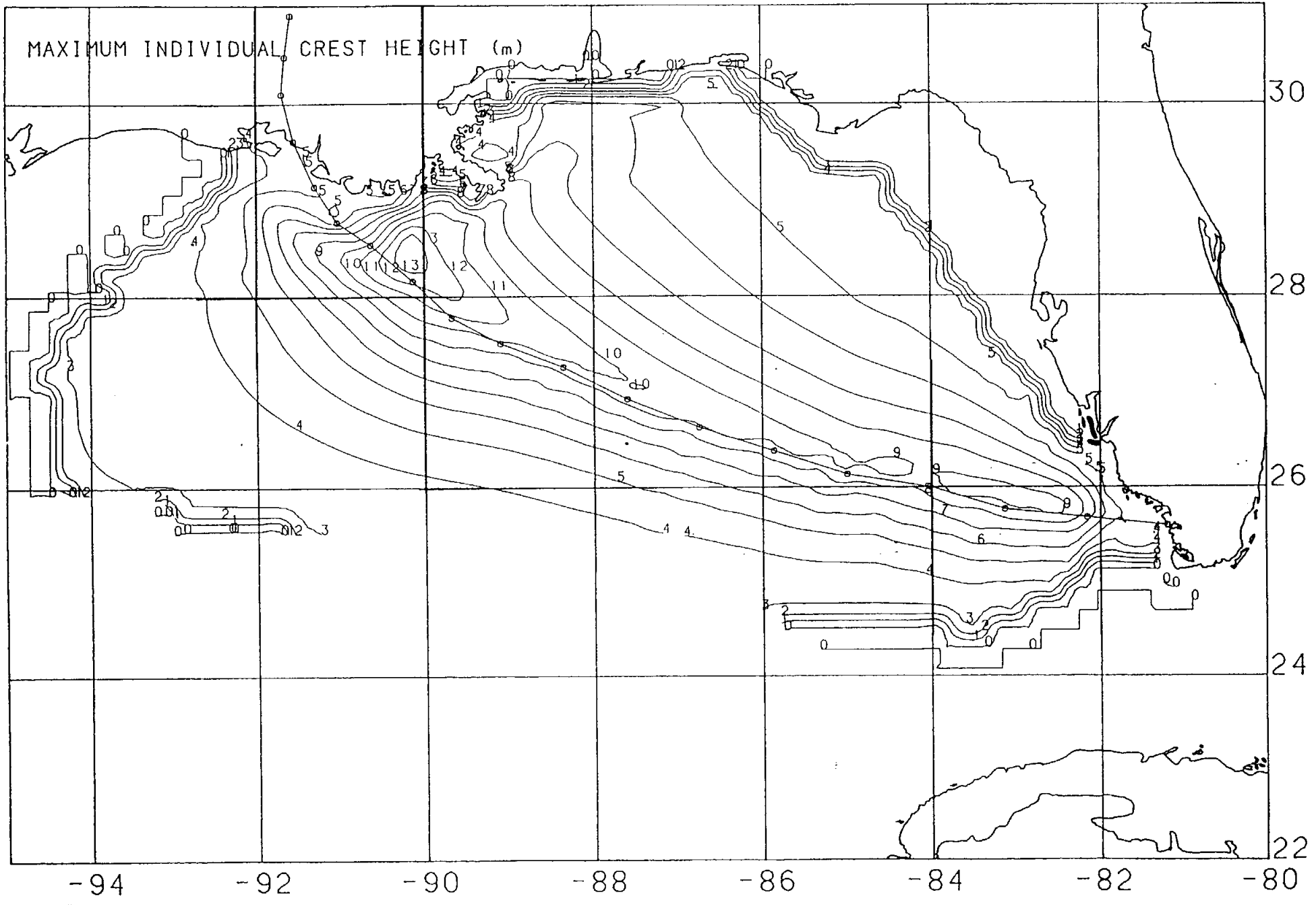

Figure 9. Same as Figure 7, but for maximum crest height, above mean sea level. Contours of heights lower than 4 meters are spurious and should be disregarded.

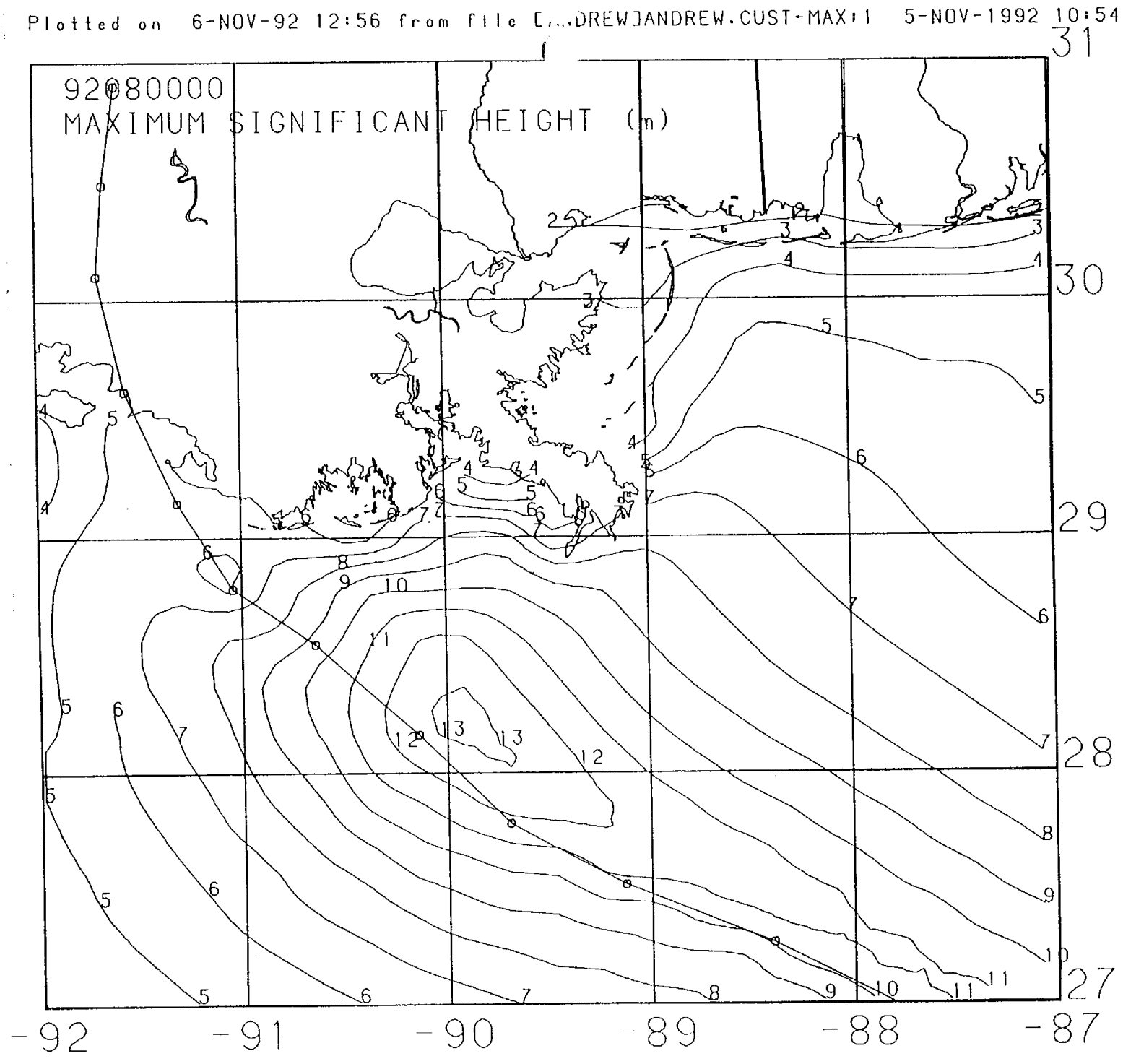

Figure 10. Same as Figure 7, but on more limited domain.

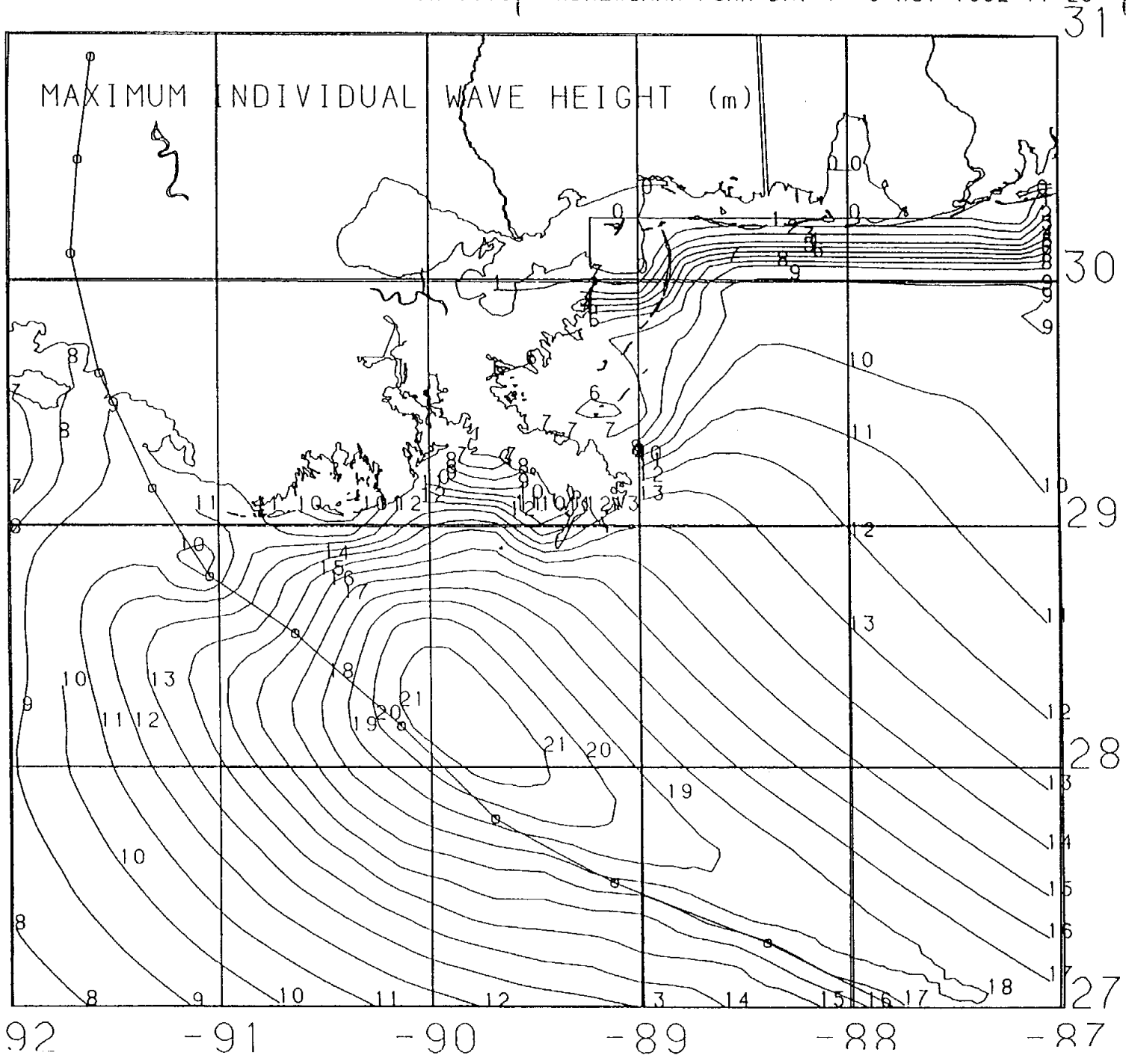

Figure 11. Same as Figure 8, but on more limited domain.

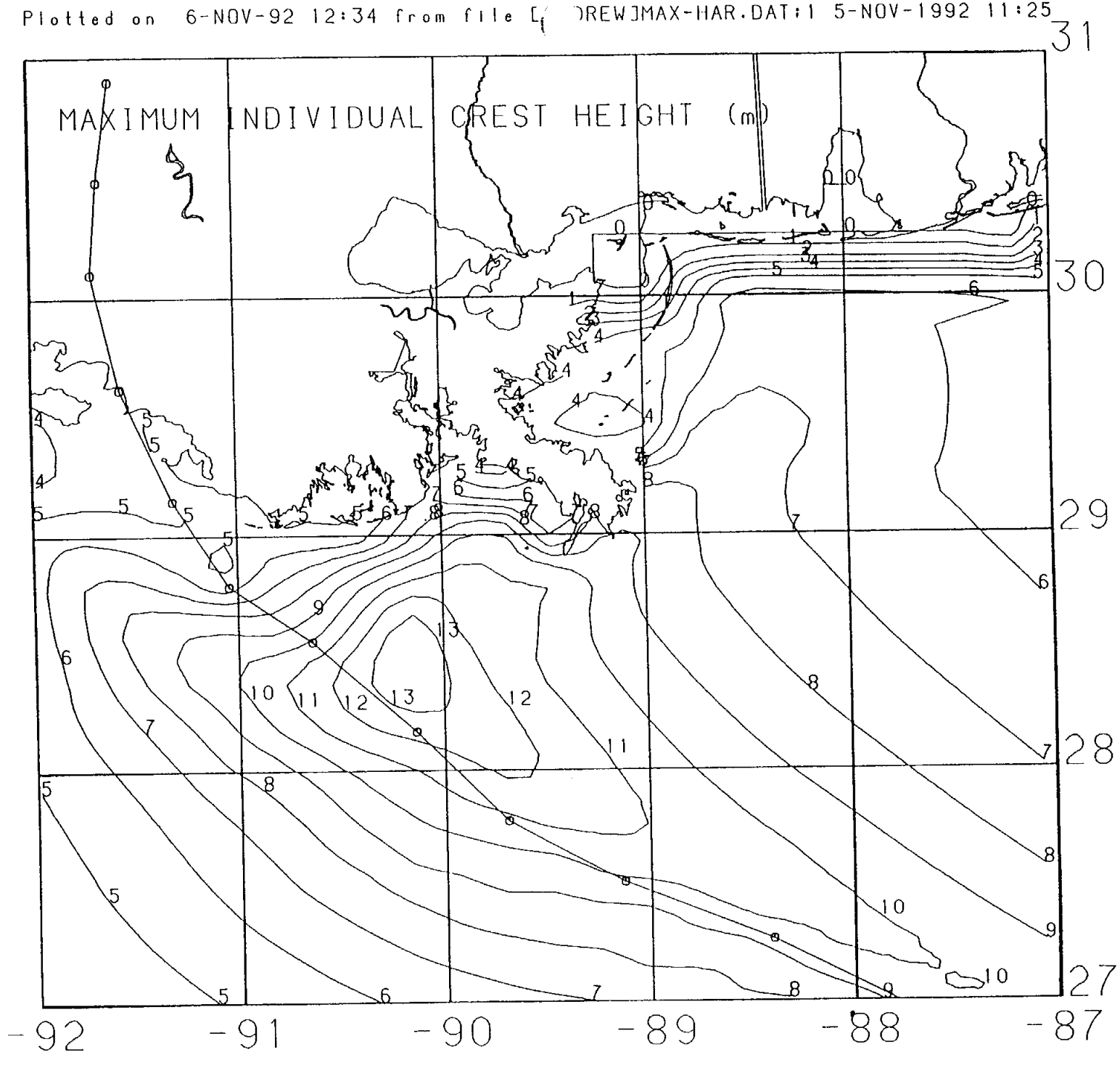

Figure 12. Same as Figure 9, but on more limited domain.

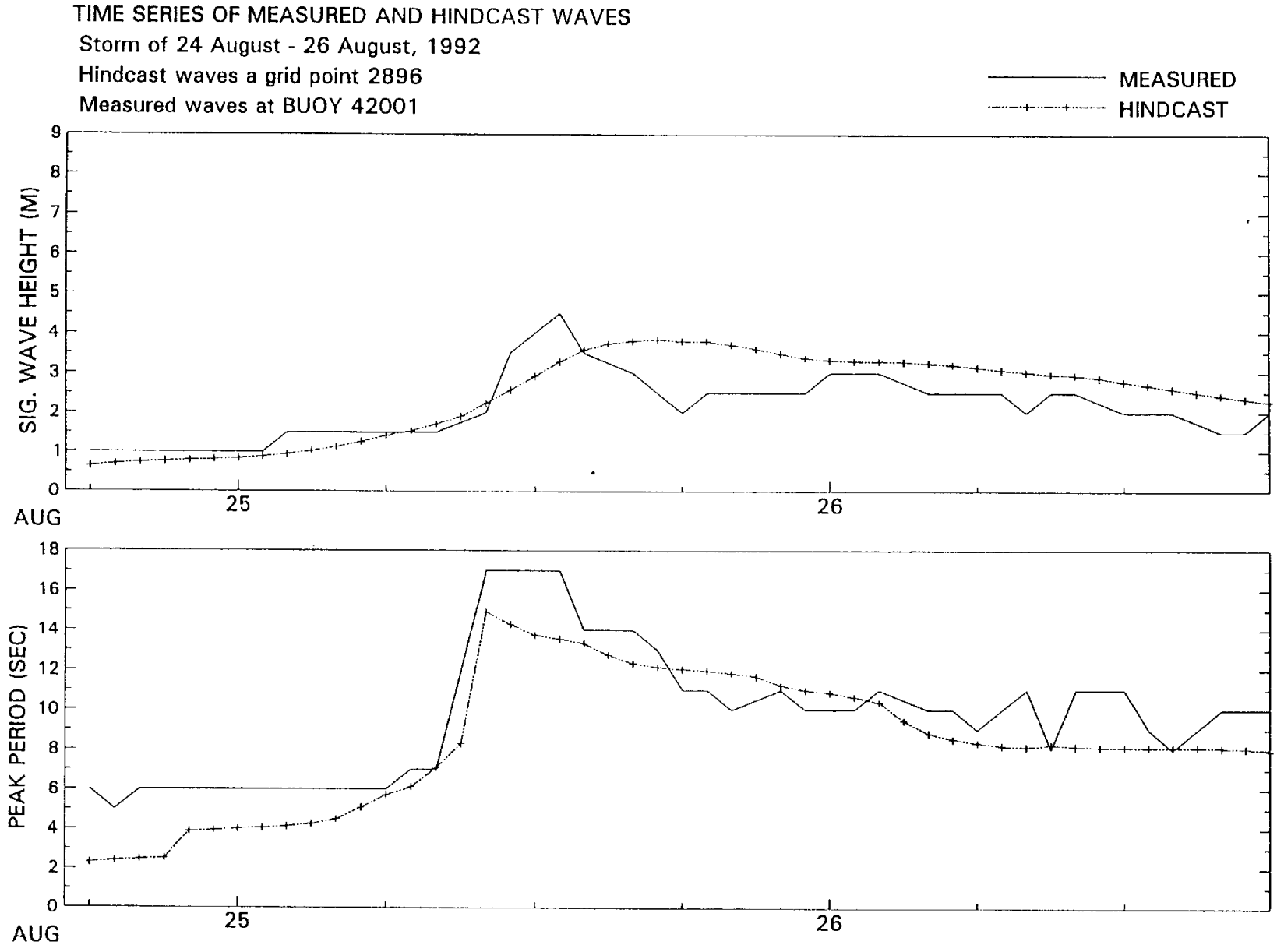
TIME SERIES OF MEASURED AND HINDCAST WAVES
Storm of 24 August - 26 August, 1992
Hindcast waves a grid point 2896
Measured waves at BUOY 42001
MEASURED
HINDCAST
SIG. WAVE HEIGHT (M)
PEAK PERIOD (SEC)
AUG
25
26
PLOTTED ON 9-NOV-92 16:05:35 (42001wave.hind & 42001_hstp.meas)

Figure 13.

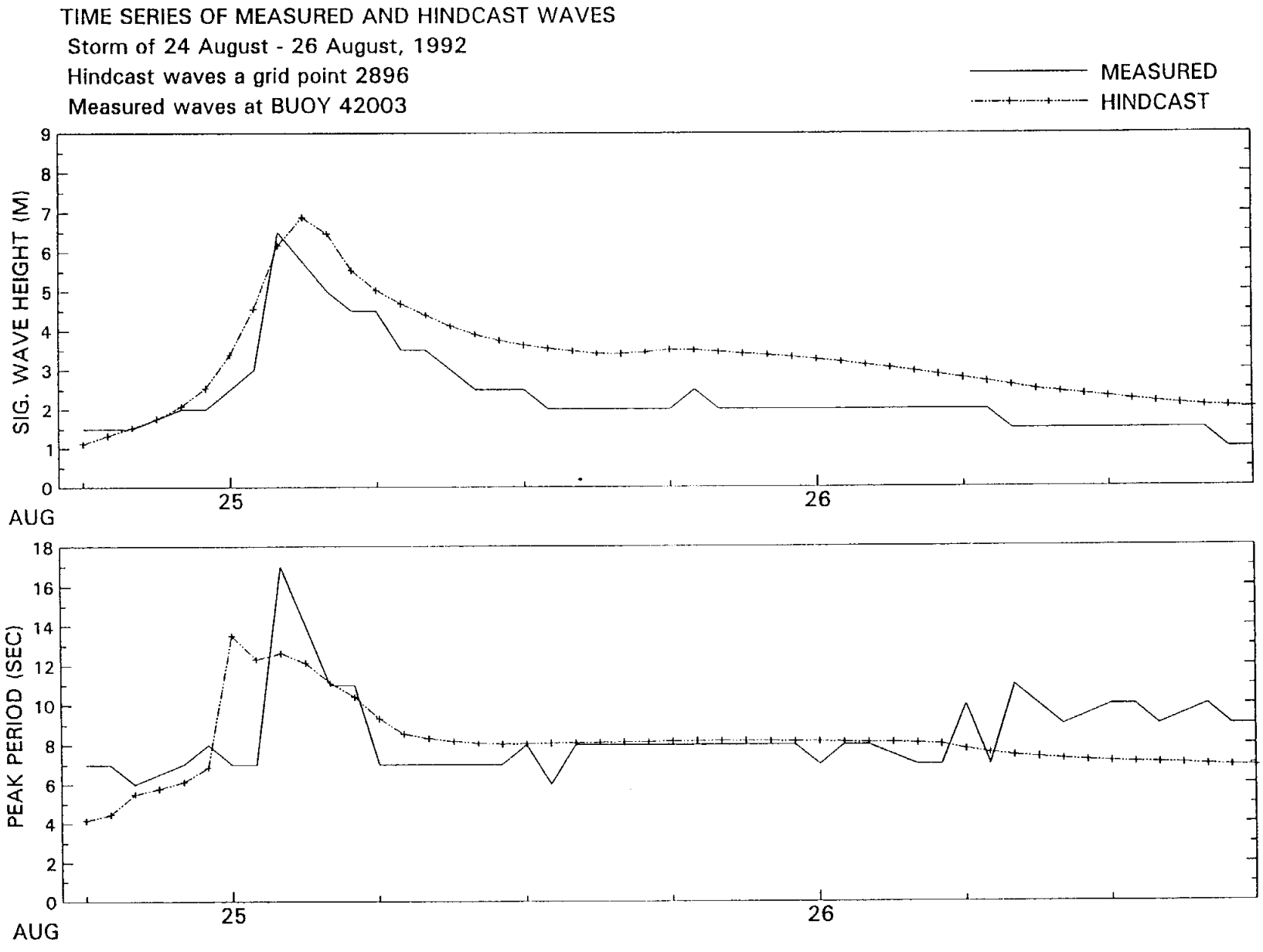
TIME SERIES OF MEASURED AND HINDCAST WAVES
Storm of 24 August - 26 August, 1992
Hindcast waves a grid point 2896
Measured waves at BUOY 42003
MEASURED
HINDCAST
SIG. WAVE HEIGHT (M)
0
1
2
3
4
5
6
7
8
9
25
26
AUG
PEAK PERIOD (SEC)
0
2
4
6
8
10
12
14
16
18
25
26
AUG
PLOTTED ON 9-NOV-92 16:05:28 (42003wave.hind & 42003_hstp.meas)

Figure 14.

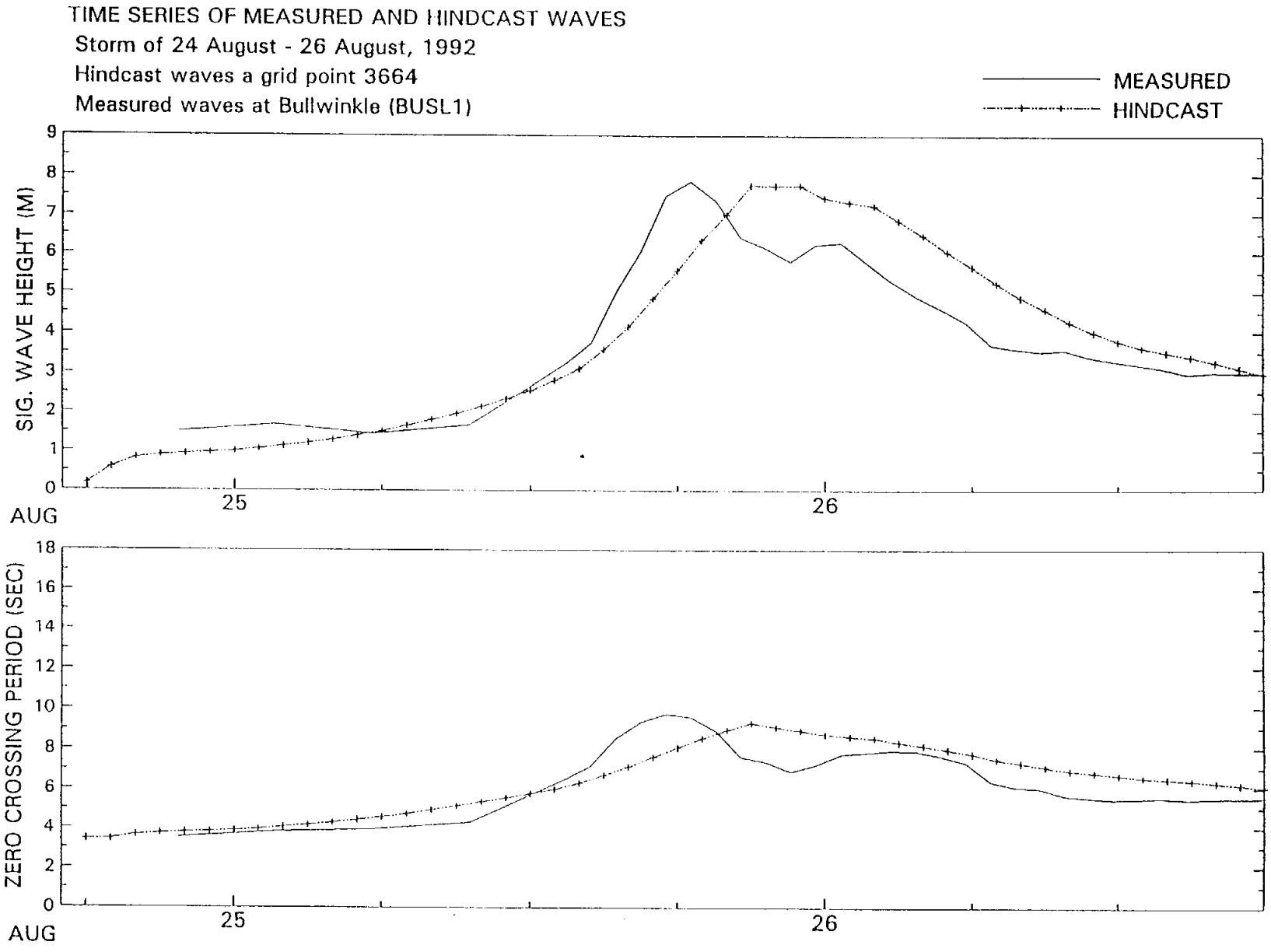
TIME SERIES OF MEASURED AND HINDCAST WAVES
Storm of 24 August - 26 August, 1992
Hindcast waves a grid point 3664
Measured waves at Bullwinkle (BUSL1)
MEASURED
HINDCAST
SIG. WAVE HEIGHT (M)
0
1
2
3
4
5
6
7
8
9
AUG
25
26
ZERO CROSSING PERIOD (SEC)
0
2
4
6
8
10
12
14
16
18
AUG
25
26
PLOTTED ON 4-NOV-92 16:50:06 /bull_hstz.mass & bus/1/hstzwave.HIND/

Figure 15.

HURRICANE ANDREW
ODGP HINDCAST PERIOD 92082418-2618
COMPARISION OF HINDCAST AND MEASURED WAVES AT BUOYS

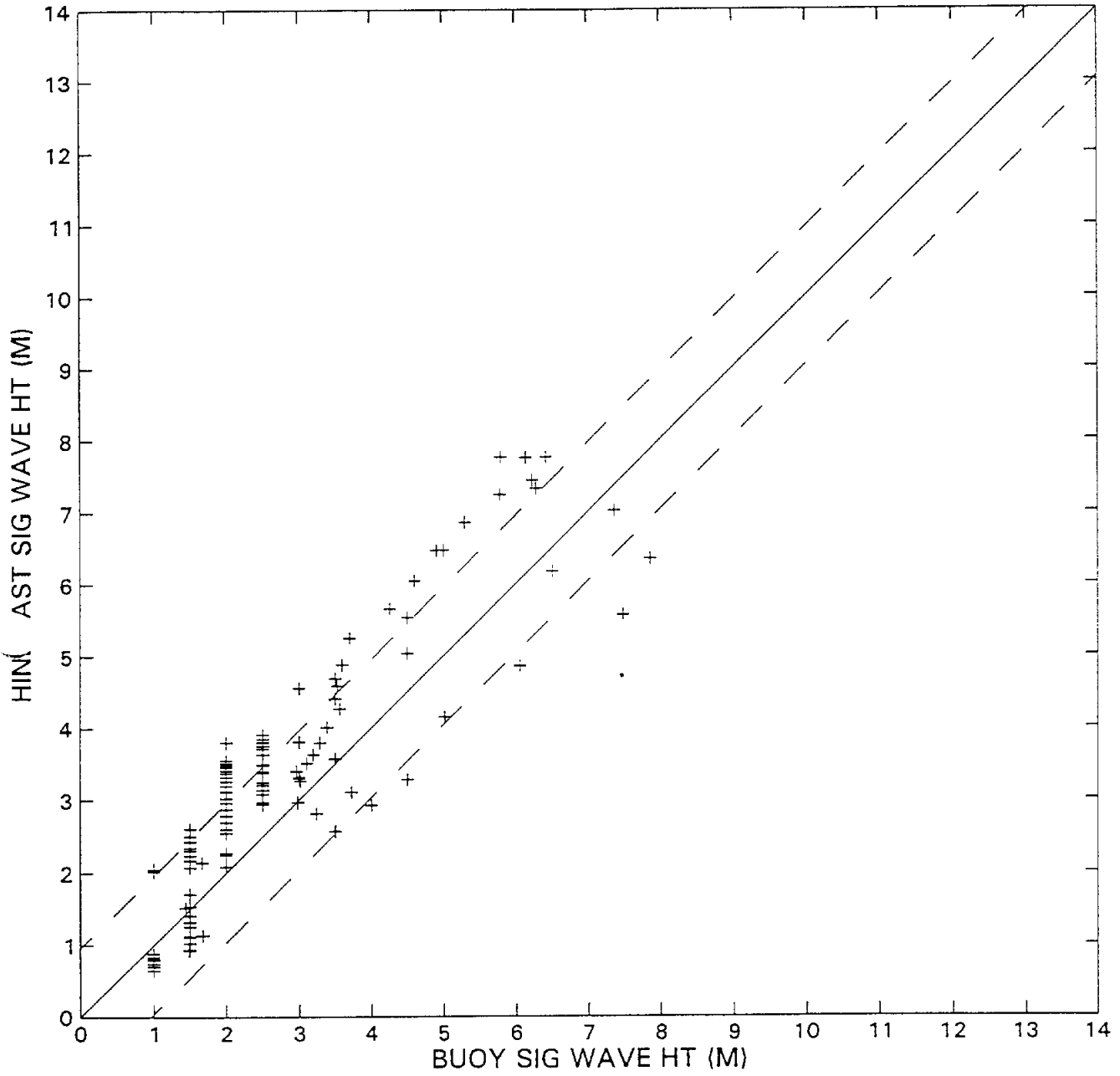

Total number of points:	115
Average measurement:	2.80
Average hindcast:	3.37
Mean difference:	-.56
Root mean square:	.96
Standard deviation:	.78
Scatter index:	.28
Ratio:	.24

PLOTTED ON 6-NOV-92 16:02:57 (%%%%% COMVAV_PC)

Figure 16.

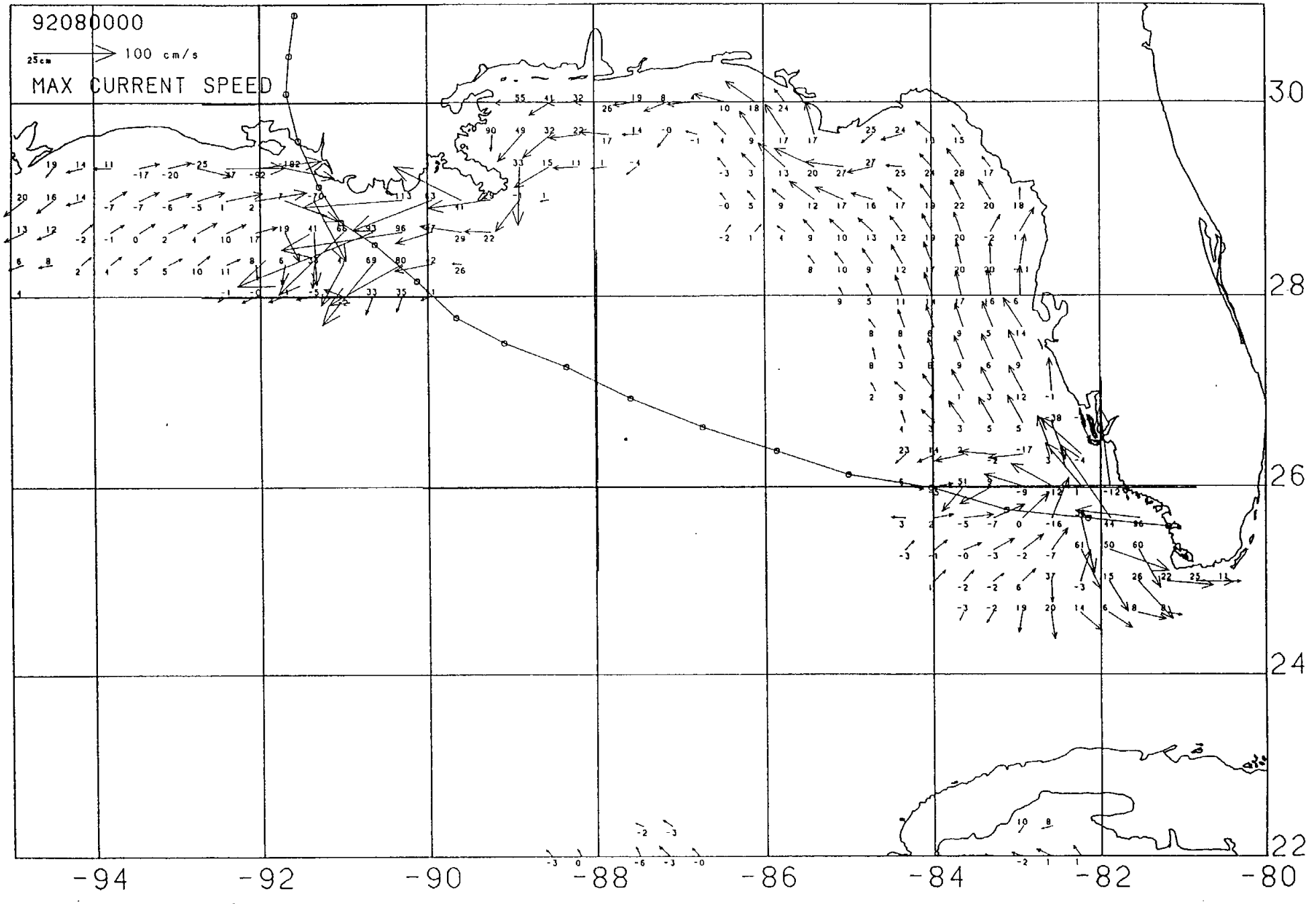

Figure 17. Maximum hindcast vertically averaged currents and associated storm surge.

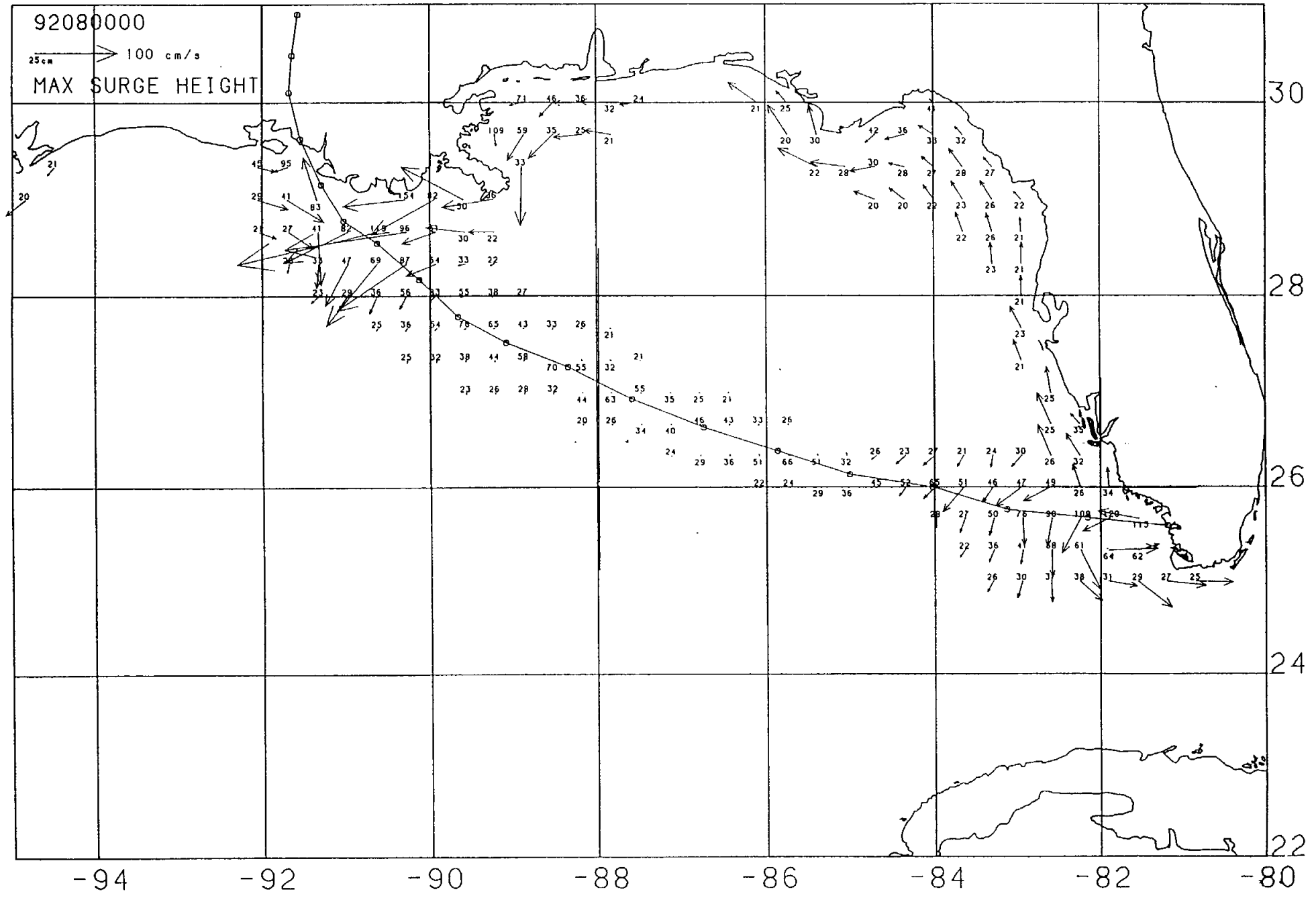

Figure 18. Maximum hindcast positive storm surge and associated vertically averaged current.

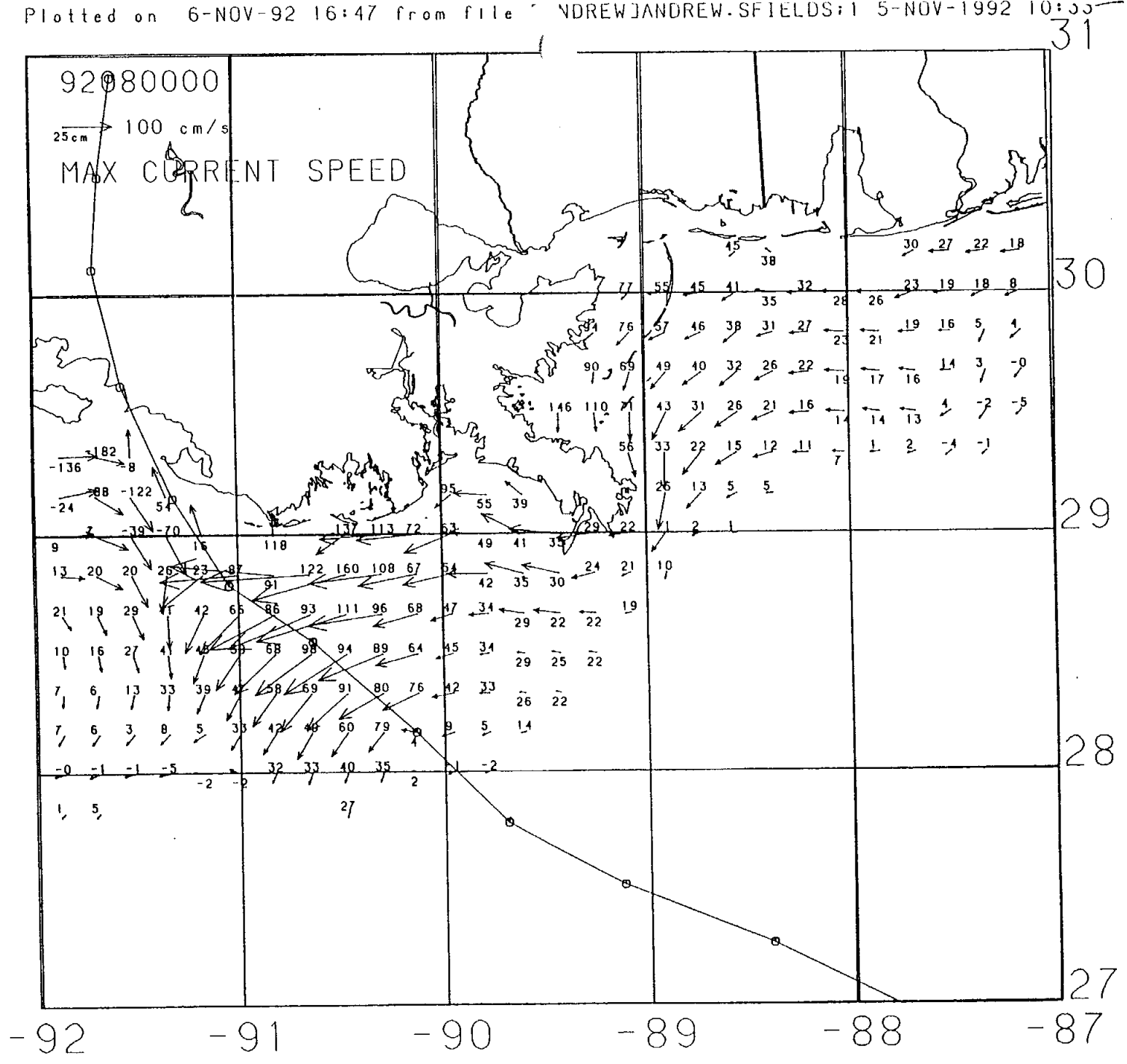

Figure 19. Same as Figure 17, but on more limited domain

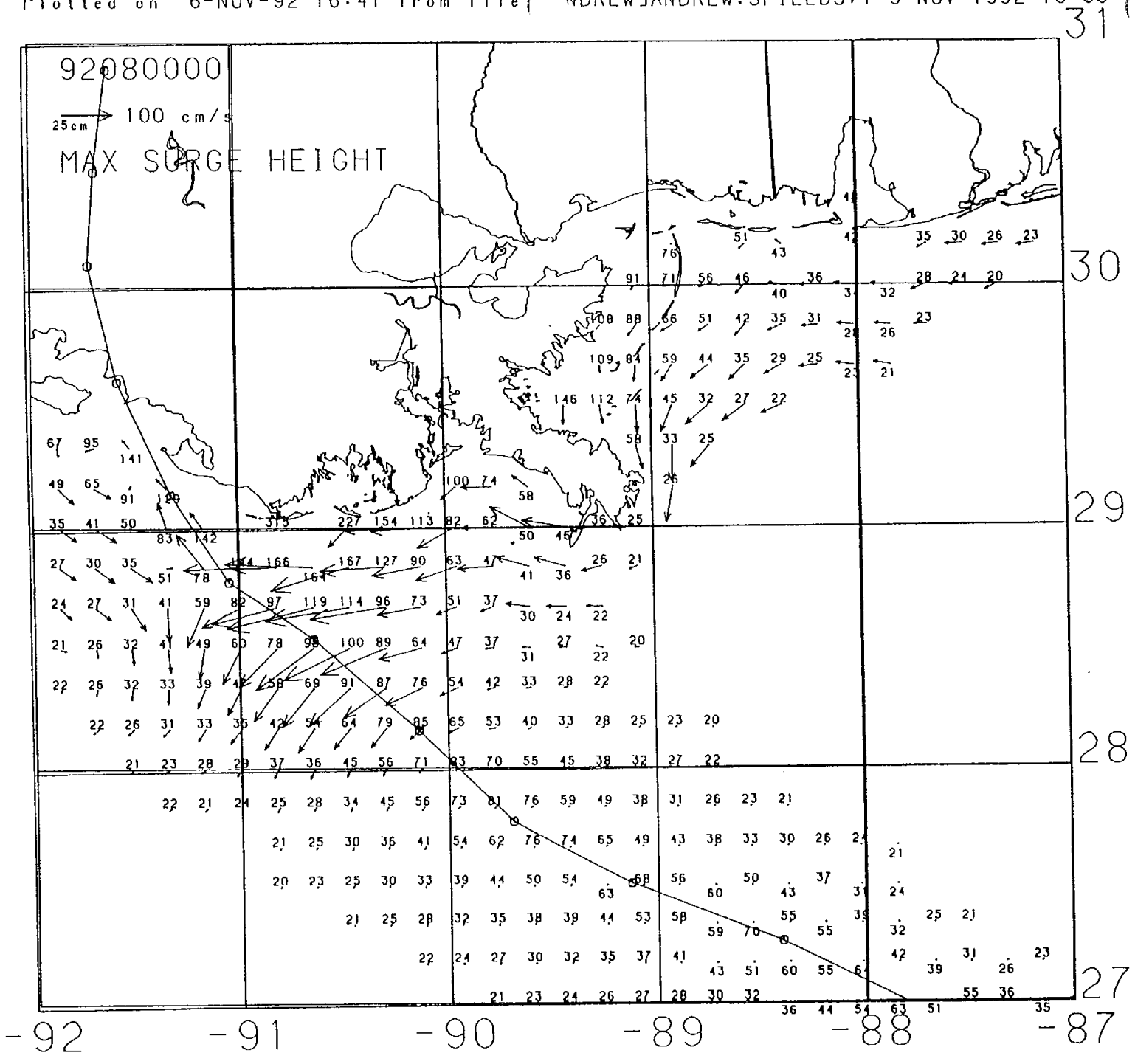

Figure 20. Same as Figure 18, but on more limited domain

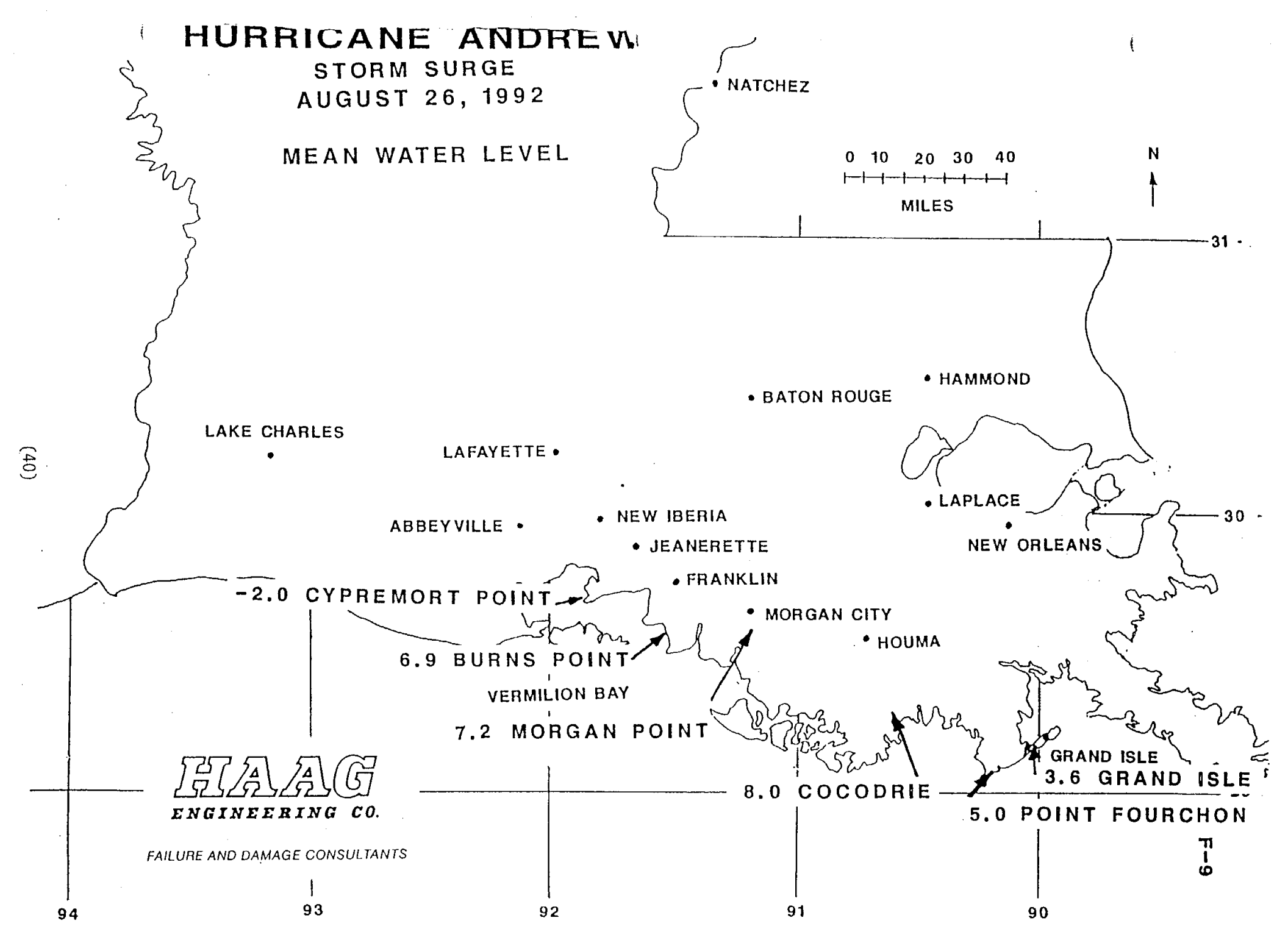

Figure 21. Preliminary estimates of maximum storm surge along Louisiana coast (Haag Engineering, 1992)

Appendix A

NOAA National Hurricane Center Preliminary Report on Hurricane Andrew 16-28 August, 1992

Preliminary Report
Hurricane Andrew
16 - 28 August 1992

Andrew was a small and ferocious Cape Verde hurricane that wrought unprecedented economic devastation along a path through the northwestern Bahamas, the southern Florida peninsula, and south-central Louisiana. Preliminary damage estimates in the United States range from $15-30 billion, making Andrew the most expensive natural disaster in U.S. history. The tropical cyclone struck southern Dade County, Florida, especially hard, with violent winds and storm surges characteristic of a category 4 hurricane on the Saffir-Simpson intensity scale, and with a central pressure (926 mb) that is the third lowest this century for a hurricane at landfall in the United States. In Dade County alone, the forces of Andrew resulted in 15 deaths and one-quarter million people homeless. An additional 25 lives were lost in Dade County from the indirect effects of Andrew, but the total of 40 lives lost there seems remarkably low considering the destruction caused by this hurricane.

a. Synoptic History

Hurricane Andrew formed from a tropical wave that satellite pictures and upper-air data indicate crossed from the west coast of Africa to the tropical North Atlantic Ocean on 14 August. The wave moved westward at about 20 kt, steered by a swift and deep easterly current on the south side of an area of high pressure. The wave passed to the south of the Cape Verde Islands on the following day. At that point, meteorologists at the National Hurricane Center (NHC) Tropical Satellite Analysis and Forecast (TSAF) unit and the Synoptic Analysis Branch (SAB) of the National Environmental Satellite Data and Information Service (NESDIS) found the wave sufficiently well-organized to begin classifying the intensity of the system using the Dvorak (1984) analysis technique.

Convection subsequently became more focused in a region of cyclonic cloud rotation. Narrow spiral-shaped bands of clouds developed around the center of rotation on 16 August. At 1800 UTC on the 16th, both the TSAF unit and SAB calculated a Dvorak T-number of 2.0 and the "best track" (Table 1 and Fig. 1) shows that the transition from tropical wave to tropical depression took place at that time.

The depression was initially embedded in an environment of easterly vertical wind shear. By midday on the 17th, however, the shear diminished. The depression grew stronger and, at 1200 UTC 17 August, it became Andrew, the first Atlantic tropical storm of the 1992 hurricane season. The tropical cyclone continued moving rapidly on a heading which turned from west to west-northwest. This course was in the general direction of the Lesser Antilles.

Between the 17th and 20th of August, the tropical storm passed south of the center of the high pressure area over the eastern Atlantic. Steering currents carried Andrew closer to a strong

upper-level low pressure system centered about 500 n mi to the east-southeast of Bermuda and to a trough that extended southward from the low for a few hundred miles. These currents gradually changed and Andrew decelerated on a course which became northwesterly. This change in heading spared the Lesser Antilles from an encounter with Andrew. The change in track also brought the tropical storm into an environment of strong southwesterly vertical wind shear and quite high surface pressures to its north. Although the estimated maximum wind speed of Andrew varied little then, a rather remarkable evolution occurred.

Satellite images suggest that Andrew produced deep convection only sporadically for several days, mainly in several bursts of about 12 hours duration. The deep convection also did not persist. Instead, it was stripped away from the low-level circulation by the strong southwesterly flow at upper levels. Air Force Reserve unit reconnaissance aircraft investigated Andrew and, on the 20th, found that the cyclone had degenerated to the extent that only a diffuse low-level circulation center remained. Andrew's central pressure rose considerably (Fig. 2). Nevertheless, the flight-level data indicated that Andrew retained a vigorous circulation aloft. Wind speeds near 70 kt were measured at an altitude of 1500 ft near a convective band lying to the northeast of the low-level center. Hence, Andrew is estimated on 20 August to have been a tropical storm with 40 kt surface winds and an astonishingly high central pressure of 1015 mb.

Significant changes in the large-scale environment near and downstream from Andrew began by 21 August. Satellite imagery in the water vapor channel indicated that the low aloft to the east-southeast of Bermuda weakened and split. The bulk of the low opened into a trough which retreated northward. That evolution decreased the vertical wind shear over Andrew. The remainder of the low dropped southward to a position just southwest of Andrew where its circulation enhanced the upper-level outflow over the tropical storm. At the same time, a strong and deep high pressure cell formed near the U.S. southeast coast. A ridge built eastward from the high into the southwestern Atlantic with its axis lying just north of Andrew. The associated steering flow over the tropical storm became easterly. Andrew turned toward the west, accelerated to near 16 kt, and quickly intensified.

Andrew reached hurricane strength on the morning of 22 August, thereby becoming the first Atlantic hurricane to form from a tropical wave in nearly two years. An eye formed that morning and the rate of strengthening increased. Just 36 hours later, Andrew reached the borderline between a category 4 and 5 hurricane and was at its peak intensity (Table 1). From 0000 UTC on the 21st (when Andrew had a barely perceptible low-level center) to 1800 UTC on the 23rd the central pressure had fallen by 92 mb, down to 922 mb. A fall of 72 mb occurred during the last 36 hours of that period and qualifies as rapid deepening (Holliday and Thompson, 1979).

The region of high pressure held steady and drove Andrew nearly due west for two and a half days beginning on the 22nd. Andrew was a category 4 hurricane when its eye passed over northern Eleuthera Island in the Bahamas late on the 23rd and then over the southern Berry Islands in the Bahamas early on the 24th. After leaving the Bahamas, Andrew continued moving westward toward southeast Florida.

Andrew weakened when it passed over the western portion of the Great Bahama Bank and the pressure rose to 941 mb. However, the hurricane rapidly reintensified during the last few hours preceding landfall on Florida as it moved over the Straits of Florida. Radar, aircraft and satellite data showed a decreasing eye diameter and strengthening eyewall convection. Aircraft data also suggest that the deepening trend continued up to the coast. The eye temperature was at least 1-2°C warmer at 1010 UTC (an hour after the eye made landfall) than it was in the last "fix" about 15 n mi offshore at 0804 UTC. It is estimated that the central pressure was 926 mb at landfall near Homestead AFB, Florida at 0905 UTC (5:05 A.M. EDT) 24 August.

The maximum sustained surface wind speed (1-min average at 10 meters elevation) during landfall over Florida is estimated at 125 kt (about 145 mph), with gusts at that elevation near 150 kt (about 175 mph). The sustained wind speed corresponds to a category 4 hurricane on the Saffir-Simpson scale. Locally stronger winds occurred at heights more than 10 meters (about 30 ft) above the ground, such as on taller structures. Several unofficial reports of stronger gusts are being evaluated. The landfall intensity is discussed further in Section b.

Andrew moved nearly due west when over land and crossed the extreme southern portion of the Florida peninsula in about four hours. Although the hurricane weakened about one category on the Saffir-Simpson scale during the transit over land, and the pressure rose to about 950 mb, Andrew was still a major hurricane when its eyewall passed over the extreme southwestern Florida coast.

The first of two cycles of modest intensification commenced when the eye reached the Gulf of Mexico. Also, the hurricane continued to move at a relatively fast pace while its track gradually turned toward the west-northwest.

As Andrew reached the north-central Gulf of Mexico, the high pressure system to its northeast weakened and a strong mid-latitude trough approached the area from the northwest. Steering currents began to change. Andrew turned toward the northwest and its forward speed decreased to about 8 kt. The hurricane struck a sparsely populated section of the south-central Louisiana coast with category 3 intensity at about 0830 UTC on the 26th. The landfall location is about 20 n mi west-southwest of Morgan City.

Andrew weakened rapidly after landfall, to tropical storm strength in about 10 hours and to depression status 12 hours later. During this weakening phase, the cyclone moved northward and then

accelerated northeastward. Andrew and its remnants continued to produce heavy rain that locally exceeded 10 inches near its track (Table 2c). By midday on the 28th, Andrew had begun to merge with a frontal system over the mid-Atlantic states.

b. Meteorological Statistics

The best track intensities were obtained from the data presented in Figs. 2 and 3. Those figures show the curves of Andrew's central pressure and maximum sustained one-minute wind speed, respectively, versus time, along with the observations on which they were based. The figures contain relevant surface observations and intensity estimates derived from analyses of satellite images performed by the TSAF unit, SAB and the Air Force Global Weather Central (USAF in figures). The aircraft data came from reconnaissance flights by the U.S. Air Force Reserve unit based at Keesler AFB, Mississippi. Additional data were collected aboard a NOAA aircraft.

Table 2 lists a selection of surface observations. The anemometer at Harbour Island, near the northern end of Eleuthera Island in the Bahamas, measured a sustained wind speed of 120 kt shortly after 2100 UTC on the 23rd. That wind speed was the maximum that could be registered by the instrument. A higher speed may have occurred at a later time.

Unfortunately, there were no official observations of sustained surface winds in the region of maximum wind speeds at the U.S. landfall sites. However, there is considerable evidence supporting a maximum sustained wind speed of about 125 kt over southeastern Florida. The strongest reported sustained wind near the surface occurred at the Fowey Rocks C-MAN station at 0800 UTC. The station sits about 11 n mi east of the shoreline and, at that time, was within the northern eyewall. The 0800 UTC data included a 2-min sustained wind of 123 kt (141 mph) with a gust to 147 kt (169 mph) at a platform height of 43 meters. The National Data Buoy Center converted this observation to a two-min wind of 108 kt (124 mph) at 10 meters elevation using a boundary-layer model. The peak one-minute wind during that period at Fowey Rocks was likely a few knots higher. Moreover, it is unlikely that this point observation was so fortuitously situated that it represents a sampling of the absolute strongest wind. Indeed, Fowey Rocks ceased transmitting data only 3 minutes later, presumably when even stronger winds disabled the instrumentation. A subsequent visual inspection indicated that the mast supporting the anemometer had become bent 90 degrees from vertical.

Reconnaissance aircraft data from a flight level of about 10,000 ft are also compatible with a 125 kt estimate. The maximum wind speed along 10 seconds of flight track (equated to a 1-min wind speed at a stationary site) on the last pass prior to landfall was 162 kt. That wind occurred at 0810 UTC in the eyewall region 11 n mi to the north of the center of the eye (almost directly above Fowey Rocks). As with the observation from Fowey Rocks, it

must be kept in mind that the aircraft provided a series of "point" observations (i.e., no lateral extent). Almost assuredly, somewhat higher wind speeds occurred elsewhere in the northern eyewall, a little to the left and/or to the right of the flight track. A wind speed at 10,000 ft is usually reduced in order to obtain a surface wind estimate. The findings of a preliminary analysis of the aircraft and low-level observations by the Atlantic Oceanographic and Meteorological Laboratory (AOML) Hurricane Research Division is consistent with 125 kt.

Two indirect measures of intensity support a sustained wind speed of at least 125 kt. First, a standard pressure-wind relationship applied to 926 mb yields around 135 kt (155 mph). Second, a special TSAF unit Dvorak technique classification at landfall provided a T-number of 6.5, or 127 kt.

It is estimated that maximum gusts (of 3-5 seconds duration) were near 150 kt (175 mph) at the 10-meter level at landfall in Florida. Unofficial observations in Table 2b support locally higher, more instantaneous, peak gusts.

Several unofficial pressure observations read at the surface near Homestead support a landfall central pressure of 926 mb (Table 2b). The observations also suggest that the 932 mb central pressure report from reconnaissance aircraft one hour prior to landfall came from a dropsonde that probably did not sample the lowest pressure within the eye. In this century, only Camille in 1969 and the Labor Day (Keys') Storm in 1935 had lower pressures at the time of landfall in the United States (Hebert et al., 1992).

The maximum 10-second flight-level wind speed reported during Andrew was 170 kt at about 1500 UTC on 23 August. The aircraft data indicate that the lowest pressure in Andrew was 922 mb near 1700 UTC that day.

Andrew came ashore in the northwest Bahamas and southeast Florida near high tide and was accompanied by a locally huge storm surge. The surge at Current Island, near the northern end of Eleuthera Island, reached a phenomenal 23 ft. Figure 4 shows a cross section of the height of the storm tide (which is the sum of the storm surge and astronomical tide) over the southeast Florida coastline. The 16.9 ft storm tide which headed inland from Biscayne Bay is a record maximum for the southeast Florida peninsula. Storm tides in Louisiana were at least 7 ft (Table 2a) and caused flooding from Lake Borgne westward through Vermillion Bay. Results from storm surge surveys in southwest Florida were incomplete at the time of this writing.

There have been no confirmed reports of tornadoes associated with Andrew over the Bahamas or Florida. Funnel sightings, some unconfirmed, were reported in the Florida counties of Glades, Collier and Highlands, where Andrew crossed in daylight. In Louisiana, one tornado occurred in the city of Laplace several hours prior to Andrew's landfall. That tornado killed 2 people and injured 32 others. Tornadoes in the Ascension, Iberville, Baton

Rouge, Pointe Coupee, and Avoyelles parishes of Louisiana reportedly did not result in casualties. Numerous reports of funnel clouds were received by officials in Mississippi and tornadoes were suspected to have caused damage in several Mississippi counties. In Alabama, the occurrence of two damaging tornadoes has been confirmed over the mainland while another tornado may have hit Dauphin Island. As Andrew and its remnants moved northeastward over the eastern states, it continued to produce severe weather. For example, several damaging tornadoes in Georgia late on 27 August were attributed to Andrew.

Andrew dropped sufficient rain to cause local floods even though the hurricane was relatively small and generally moved rather fast. Rainfall totals in excess of seven inches were recorded in southeast Florida, Louisiana, and Mississippi (Table 2c). Rainfall amounts near five inches occurred in several neighboring states. Hammond, Louisiana reported the highest total, 11.92 inches.

c. Casualty and Damage Statistics

Table 3 lists a preliminary count of casualties and damages associated with Andrew. The death toll currently stands at 54.

Damage estimates are fluctuating within the $15-30 billion range. Andrew's impact on southern Dade County was extreme from the Kendall district southward through Homestead and Florida City, to near Key Largo. Insured losses alone in southern Florida have been preliminarily estimated at $7.3 billion by the Property Claims Division of The American Insurance Services Group, Inc. Recent news reports indicate that this total may rise. Reports by Florida Governor Chiles and the American Red Cross, summarized in The Miami Herald, delineate the extent of damage in Florida. The loss to South Florida's agricultural industry was $1.04 billion. Andrew destroyed 25,524 homes and damaged 101,241 others. About 670,000 customers lost power in Dade County alone (one customer may represent multiple users). The State of Florida requested $2 billion in federal aid for cleanup of debris. The Miami Herald reported $0.5 billion in losses to boats in southeast Florida.

The damage to Louisiana is estimated at $1 billion.

Damage in the Bahamas has been estimated at $0.25 billion.

Extensive damage occurred to numerous offshore platforms near the south-central Louisiana coast.

Figure 5 displays a radar reflectivity pattern (similar to rainfall intensity) about 30 minutes prior to landfall, superimposed on a map of southern Florida. The figure shows that the most devastated areas correspond closely in location to the region overspread by Andrew's eyewall and its accompanying core of destructive winds and, near the coastline, decimating storm surges. Flight-level data about an hour prior to landfall place the radius of maximum wind at 11 n mi (in the northern eyewall at 10,000 ft

altitude). The radius of maximum wind at the surface was likely a little less than 11 n mi. Areas of southern Florida well-outside the eyewall experienced less severe damage and fewer casualties.

Table 3 reveals that about one-half of the fatalities were "indirect". The indirect deaths occurred primarily during the recovery phase following Andrew's passage.

Hurricanes are notoriously capricious. Andrew was a compact system. A little larger system, or one making landfall just a few nautical miles further to the north, would have been catastrophic for heavily populated, highly commercialized and no less vulnerable areas to the north. That area includes downtown Miami, Miami Beach, Key Biscayne and Fort Lauderdale. Andrew also left the highly vulnerable New Orleans region relatively unscathed.

d. Forecast and Warning Critique

Track forecast errors by the NHC and by the suite of track prediction models are given in Table 4. On average, the NHC errors were about 30% smaller than the current 10-year average. The most significant changes in Andrew's track and intensity (see Fig. 1, Table 1) were generally well anticipated (noted in NHC's Tropical Cyclone Discussions) and the forecast tracks generally lie close to the best track. However, the rate of Andrew's westward acceleration over the southwestern Atlantic was greater than initially forecast. In addition, the NHC forecast a rate of strengthening that was less than what occurred during Andrew's period of rapid deepening.

Several of the dynamic track models had stellar performances during this hurricane. The Aviation Model (AVNO) performed especially well. However, recent modifications to this model (including the incorporation of a simulated vortex at the hurricane location) give the AVNO a rather short "track history". Hence, the operational reliability of this model for hurricane forecasting is not established. The GFDL and QLM models also had small errors. It should be pointed out, however, that the NHC works on a six-hourly forecast cycle and that the models mentioned above are run just once per 12 hours. Moreover, the output from these models becomes available to forecasters no earlier than the following six-hour forecast cycle.

Historically, the NHC90 statistical-dynamical model has been the most accurate of NHC's track guidance models. The NHC90 errors were rather large during Andrew. Because the NHC90 uses output from the Aviation Model it is possible that the recent changes in the latter model may be responsible for NHC90's degraded performance.

Table 5 lists a chronology of watches and warnings issued by the National Hurricane Center and the Government of the Bahamas. The associated lead times (based on landfall of the eye) are given in Table 6.

Massive evacuations were ordered in Florida and Louisiana as the likelihood of Andrew making landfall in those regions increased (Table 7). About 55,000 people left the Florida Keys. Evacuations were ordered for 517,000 people in Dade County, 300,000 in Broward County, 315,000 in Palm Beach County and 15,000 in St. Lucie County. For counties further west in Florida, currently available evacuation totals exceeding one thousand people are Collier (25,000), Glades (4,000) and Lee (2,500).

It is estimated that 1,250,000 people evacuated from parishes in southeastern and south-central Louisiana.

About 250,000 people evacuated from Orange and Jefferson Counties in Texas.

The recovery process continues in several areas. Nevertheless, it is not too early to emphasize an important point. The winds in Hurricane Andrew wreaked tremendous structural damage, particularly in southern Dade County. Notwithstanding, the loss of life in Hurricane Andrew, while very unfortunate, was far less than has previously occurred in hurricanes of comparable strength. Historical data suggests that storm surge is the greatest threat to life. Clearly, lives were saved by the large evacuation along the coastline of southeast Florida. The relatively small loss of life there serves as testimony to the success and importance of coordinated programs of hurricane preparedness.

References

Dvorak, V. F., 1984: Tropical cyclone intensity analysis using satellite data. NOAA Technical Report NESDIS 11, National Oceanic and Atmospheric Administration, U. S. Department of Commerce, Washington, DC, 47 pp.

Hebert, P. J., J. D. Jarrell, and M. Mayfield, 1992: The deadliest, costliest, and most intense hurricane of this century (and other frequently requested facts). NOAA Technical Memorandum NWS NHC-31, National Oceanic and Atmospheric Administration, U.S. Department of Commerce, Washington, DC, 40 pp.

Holliday, C. R., and A. H. Thompson, 1979: Climatological characteristics of rapidly intensifying typhoons. Mon. Wea. Rev., 107, 1022-1034.

Acknowledgments

Much of the data in this summary was provided by NWS WSFO/WSO reports from MIA, EYW, MLB, PBI, TBW, SIL, BTR, LCH, JAN, BHM, MOB, MEM, BPT and ATL. Sam Houston of the AOML Hurricane Research Division collected additional observations. Jerry Kranz of the NOAA Aircraft Operations Center performed the calibration tests noted in Table 2b.

Ed Rappaport
National Hurricane Center
16 September 1992

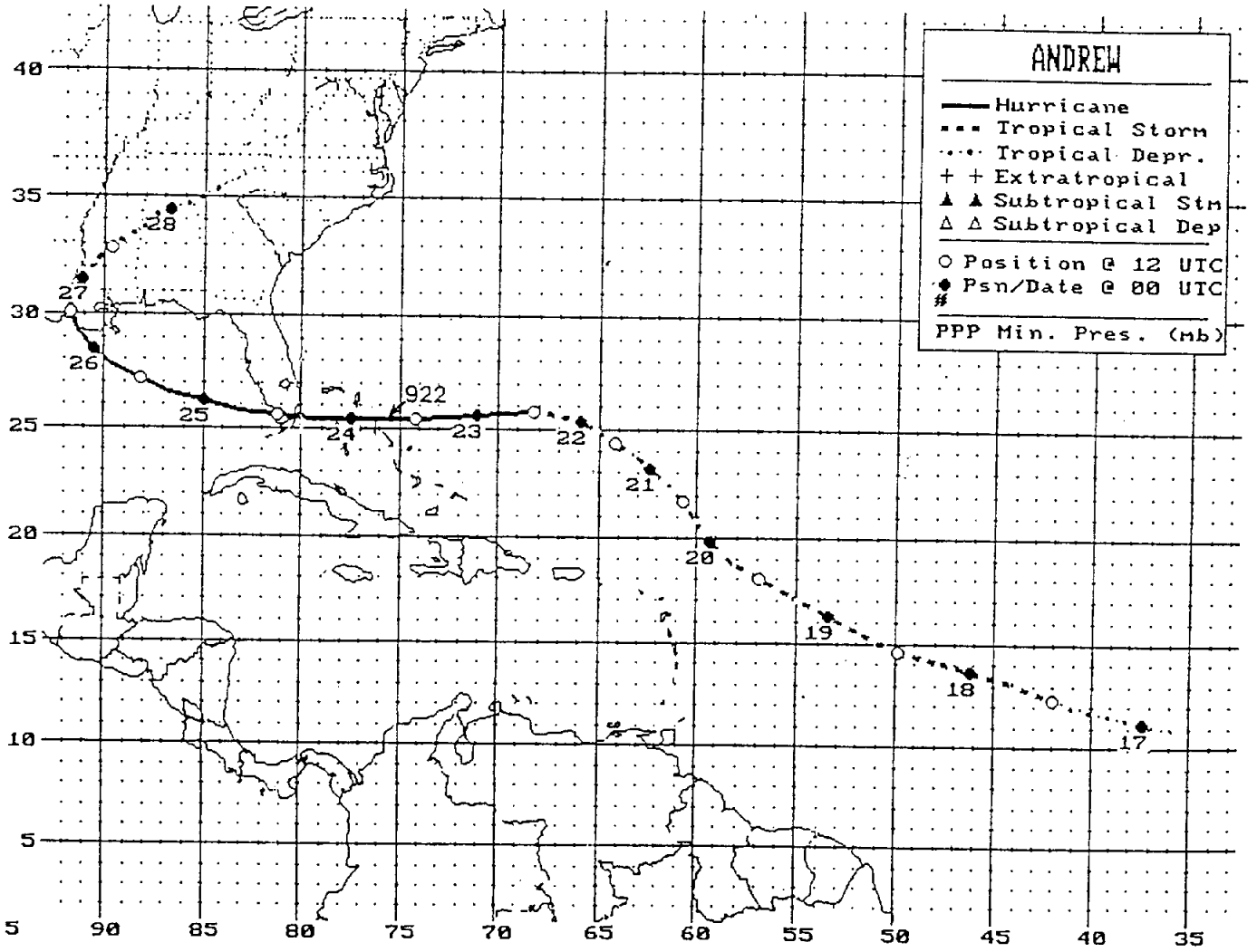

Figure 1. Best track positions for Hurricane Andrew.

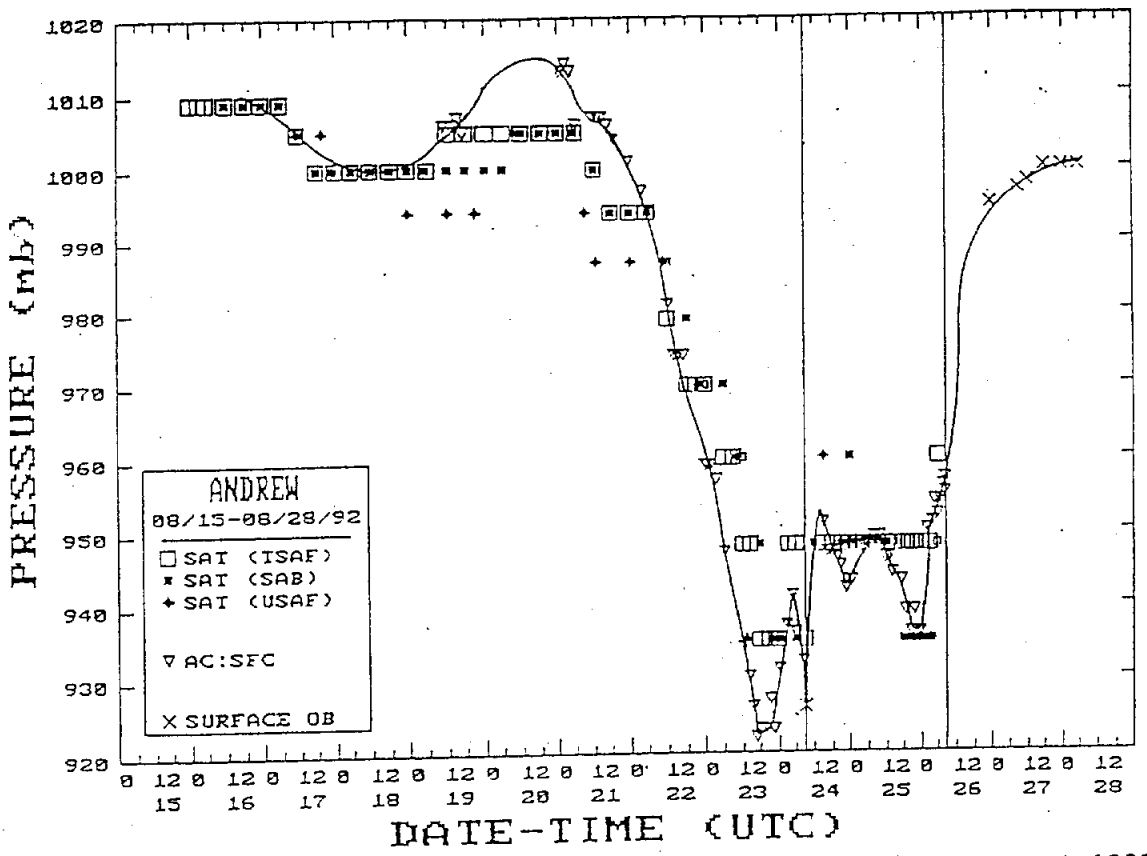

Figure 2. Best track central pressure curve for Hurricane Andrew, August 1992. Landfalls on mainland noted by vertical lines.

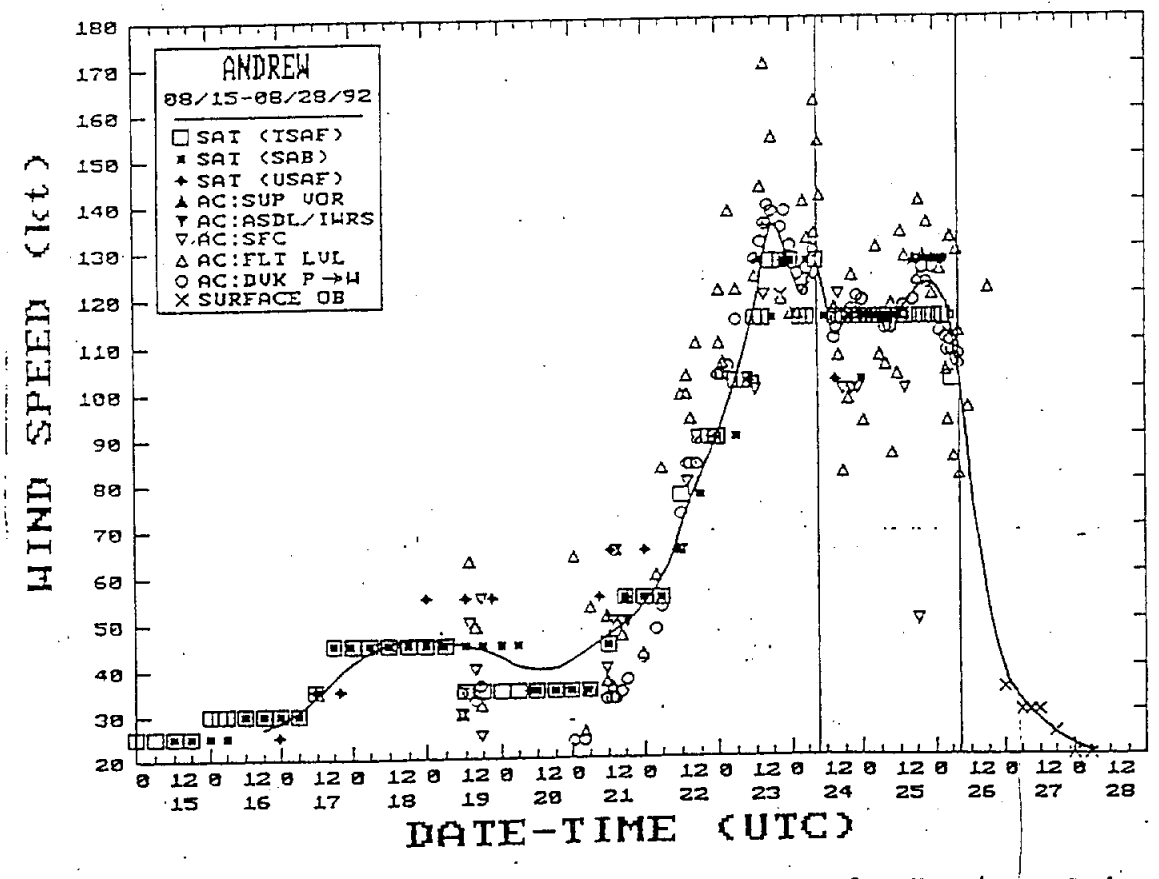

Figure 3. Best track maximum sustained wind speed curve for Hurricane Andrew, August 1992. Not all aircraft observations are a sampling of the maximum wind. Landfalls on mainland noted by vertical lines.

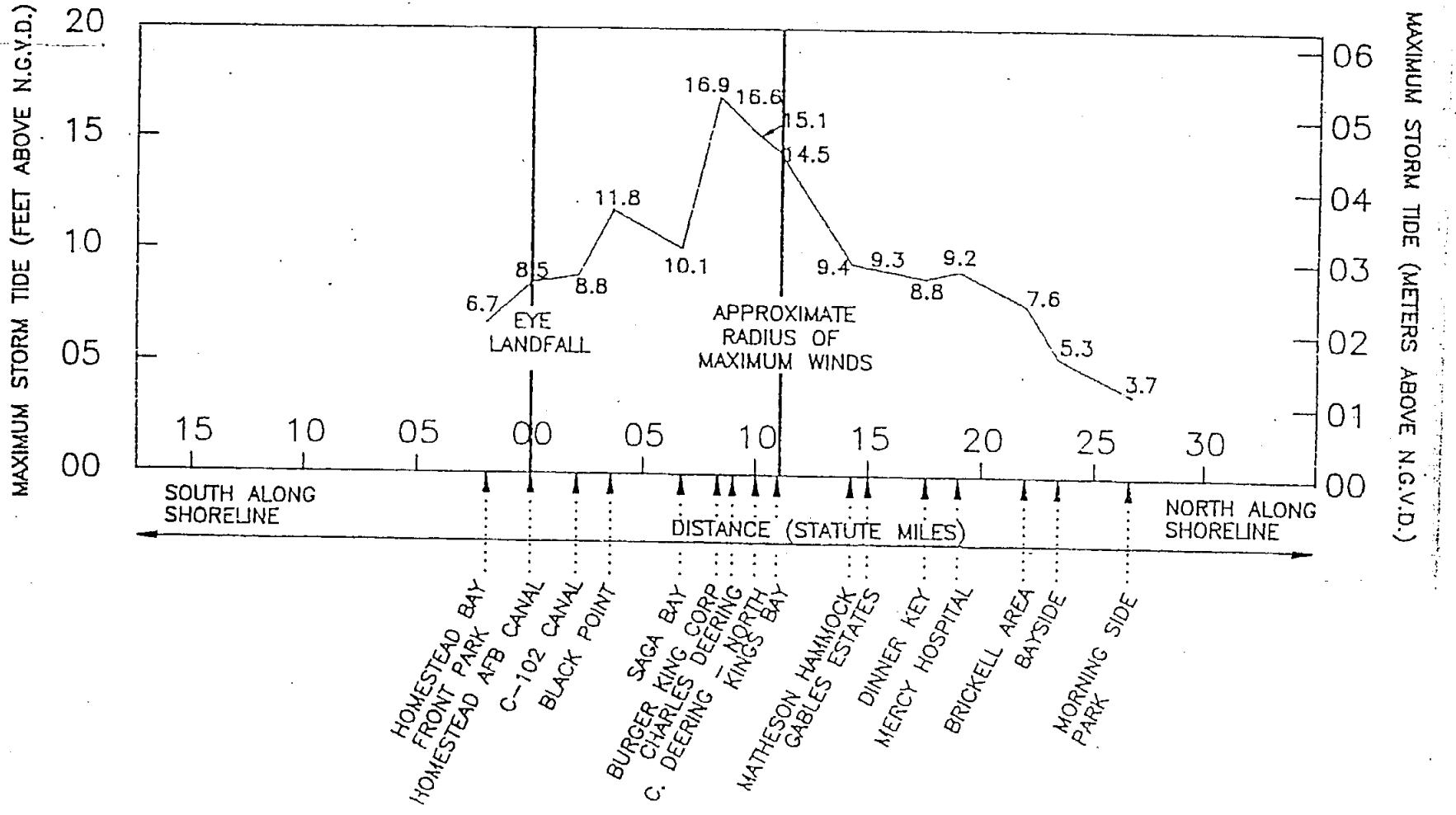

Figure 4. Plot of preliminary storm tide heights along western shore of Biscayne Bay associated with Hurricane Andrew, 24 August 1992. (Provided by the U.S. Geological Survey under a mission assignment from FEMA.) (Heights in feet above NGVD - National Geodetic Vertical Datum - zero elevation - i.e., mean sea level of 1929.)

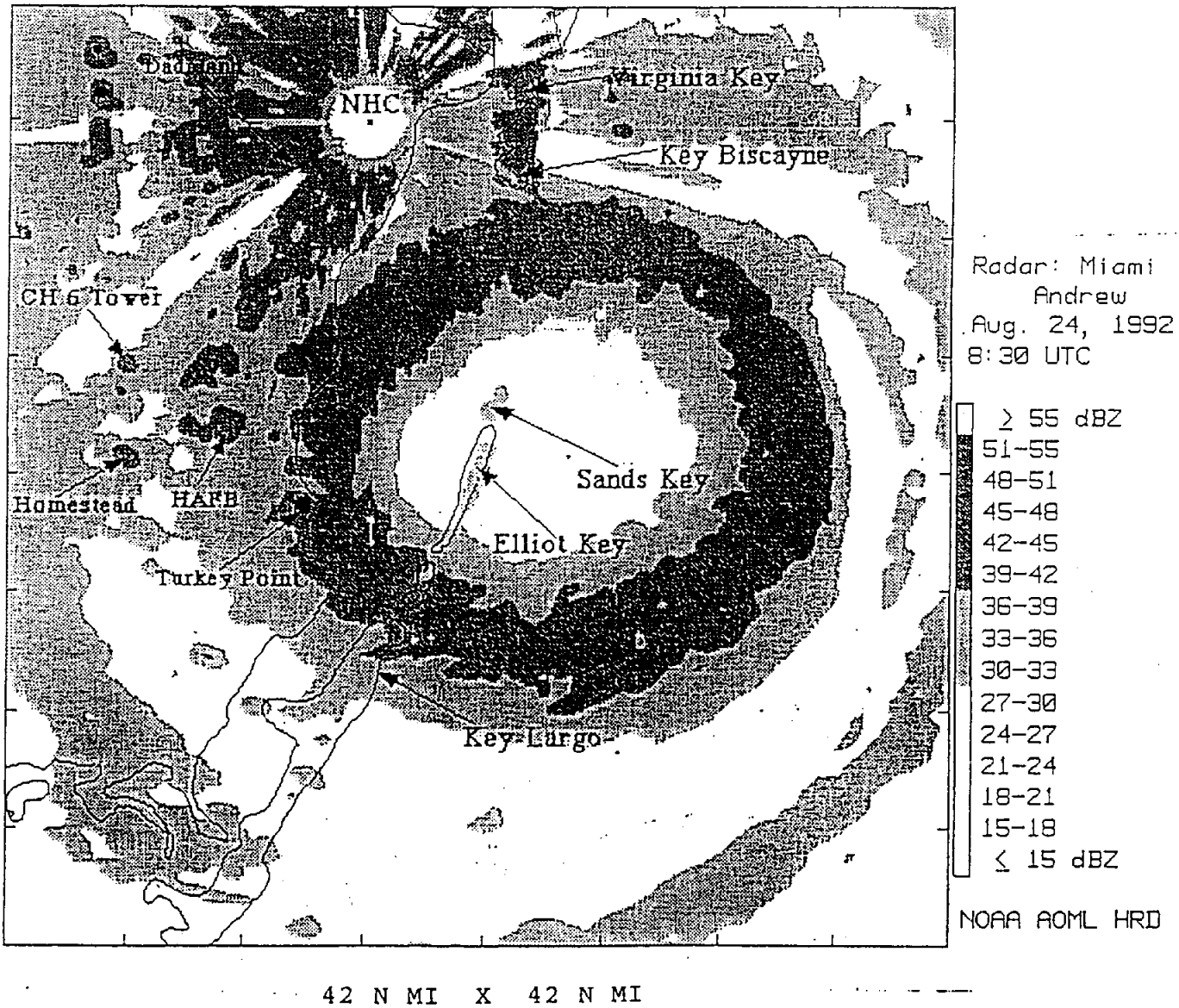

Figure 5. Miami radar reflectivity factor (similar to rainfall intensity) pattern of Hurricane Andrew at about 0830 UTC 24 August 1992. Andrew made landfall near Homestead AFB about 30 minutes later. Variations in reflectivity factor (dBZ) denoted by shades of gray. Figure provided by NOAA-AOML Hurricane Research Division.

Table 1. Preliminary best track, Hurricane Andrew, 16-28 August 1992.

Date/Time (UTC)	Position Lat. (°N)	Position Lon. (°W)	Pressure (mb)	Wind Speed (kt)	Stage
16/1800	10.8	35.5	1010	25	Tropical Depression
17/0000	11.2	37.4	1009	30	" "
0600	11.7	39.6	1008	30	" "
1200	12.3	42.0	1006	35	Tropical Storm
1800	13.1	44.2	1003	35	" "
18/0000	13.6	46.2	1002	40	" "
0600	14.1	48.0	1001	45	" "
1200	14.6	49.9	1000	45	" "
1800	15.4	51.8	1000	45	" "
19/0000	16.3	53.5	1001	45	" "
0600	17.2	55.3	1002	45	" "
1200	18.0	56.9	1005	45	" "
1800	18.8	58.3	1007	45	" "
20/0000	19.8	59.3	1011	40	" "
0600	20.7	60.0	1013	40	" "
1200	21.7	60.7	1015	40	" "
1800	22.5	61.5	1014	40	" "
21/0000	23.2	62.4	1014	45	" "
0600	23.9	63.3	1010	45	" "
1200	24.4	64.2	1007	50	" "
1800	24.8	64.9	1004	50	" "
22/0000	25.3	65.9	1000	55	" "
0600	25.6	67.0	994	60	" "
1200	25.8	68.3	981	70	Hurricane
1800	25.7	69.7	969	80	"
23/0000	25.6	71.1	961	90	"
0600	25.5	72.5	947	105	"
1200	25.4	74.2	933	120	"
1800	25.4	75.8	922	135	"
24/0000	25.4	77.5	930	125	"
0600	25.4	79.3	937	120	"
1200	25.6	81.2	951	110	"
1800	25.8	83.1	947	115	"
25/0000	26.2	85.0	943	115	"
0600	26.6	86.7	948	115	"
1200	27.2	88.2	946	115	"
1800	27.8	89.6	941	120	"
26/0000	28.5	90.5	937	120	"
0600	29.2	91.3	955	115	"
1200	30.1	91.7	973	80	"
1800	30.9	91.6	991	50	Tropical Storm
27/0000	31.5	91.1	995	35	" "
0600	32.1	90.5	997	30	Tropical Depression
1200	32.8	89.6	998	30	" "
1800	33.6	88.4	999	25	" "
28/0000	34.4	86.7	1000	20	" "
0600	35.4	84.0	1000	20	" "
1200					Merging with frontal system
23/1800	25.4	75.8	922	135	Minimum Pressure
Landfall: northern Eleuthera Island, Bahamas					
23/2100	25.4	76.6	923	130	Hurricane
southern Berry Islands, Bahamas					
24/0100	25.4	77.8	931	125	Hurricane
Homestead Air Force Base, Florida					
24/0905	25.5	80.3	926	125	Hurricane
Point Chevreuil, Louisiana (20 n mi west-southwest of Morgan City)					
26/0830	29.6	91.5	956	105	Hurricane

Table 2a. Hurricane Andrew selected surface observations, August 1992.

Location	Minimum sea-level pressure		Maximum surface wind speed (kt)			Storm surge** (ft)	Storm tide** (ft)	Rain (storm total) (in)
	Pressure (mb)	Date/time (UTC)	1-minute average	Peak gust	Date/time (UTC)*			
Bahamas								
Harbour Island	935-	23/2100	120***		23/shortly after 2100			
Nassau	999-	24/0000	80	100	24/0025			
Current Island						23		
Lower Bogue (1 n mi inland)						16		
Florida East Coast and Keys								
Miami WSFO/NHC	982-	24/0900	N100***	N142***	24/0850			
NOAA/AOML	984							
Miami I. Arpt. (MIA)	992.6	24/0900	E75	E100	24/0950			2.04
Tamiami Airport (TMB)	988-		50***	70***	24/0833			
Miami Beach DARDC			65	92	24/0816			
Haulover NOS NGWLMS			U58	85	24/0900			
Palm Beach (PBI)	1010.8	24/0259,0420	43	51	24/1033			
Palm Beach ASOS			42		24/1036			
Key West WSO (EYW)	1010.1	24/1400	25	37	24/1614			0.33
Patrick AFB (COF)			15	31	24/0735			
Orlando (MCO)				30	24/1850			
NASA Shuttle (X68)			11	23	24/1755			
Titusville (TIX)			8	14	24/1149			0.80+
Melbourne (MLB)								
East Perrine							16.9 (see Fig. 4)	
Florida West Coast								
Collier County (EOC)				N87	24/			
Fort Myers (RSW)	1010.2	24/1347,1446	30	45	24/1446,1547.			0.56
Glades County EOC				44	24/between 1100 and 1200			
Clrwtr./St. P. Arpt.			30	40	24/1625			
Goodland							6 (MLW)	
Everglades City							6 (MLW)	
Fort Myers Beach							2.0	
Venice							1.8	
Anna Marie Island							1.5	
Homosassa							1.5	
Gulf Harbors							1.5	
Indian Rocks Beach							1.0	

Table 2a (cont.). Hurricane Andrew selected surface observations, August 1992.

Location	Minimum sea-level pressure		Maximum surface wind speed (kt)			Storm surge** (ft)	Storm tide** (ft)	Rain (storm total) (in)
	Pressure (mb)	Date/time (UTC)	1-minute average	Peak gust	Date/time (UTC)*			
Louisiana								
P42 (Morgan City)			N80	N94				
Baton Rouge (BTR)	996.5	26/1427	42	61	26/1452			5.70
New Orleans (MSY)	1006.6	26/0805	39	57	26/0950			5.70
Bayou Bienvenue								6.28
Salt Point AMOS (P92)			40	72	26/0728			
Lafayette (LFT)	990.5	26/1250	46	62	26/1057			5.51
Lake Charles (LCH)	1008.8		21	34	26/2152			0.05
Cocodrie							E7	
Burns Point (St. Mary Parish)							6.8 (MWL)	
Bayou Dupre							6.5	
Bayou Bienvenue							6.3	
NWS HANDAR east N. Orleans							5.6	
Port Fourchon							5.0 (MWL)	
N end of causeway							4.9	
Industrial canal							4.4	
Marina							4.3	
Rigolets							4.2	
Grand Isle							3.5 (MWL)	
Alabama								
Huntsville (HSV)	1000.3	27/2250	22	36	27/1742			0.92
Birmingham (BHM)	1001.7	27/2215	19	35	27/1640			1.77
Montgomery (MGM)	1008.8	27/2045	23	31	27/2307			1.55
Mobile (MOB)	1010.1	27/2051	26	35	25/1844			0.64
Mobile State Docks						2.6	3.5	
Dauphin Island							6	
Georgia								
Atlanta (ATL)	1005.4	28/0400		39	27/2039			

Table 2a (cont.). Hurricane Andrew selected surface observations, August 1992.

Location	Minimum sea-level pressure		Maximum surface wind speed (kt)			Storm surge** (ft)	Storm tide** (ft)	Rain (storm total) (in)
	Pressure (mb)	Date/time (UTC)	1-minute average	Peak gust	Date/time (UTC)*			
Mississippi								
Jackson (JAN)	998.6	26/0750	28	49	27/0219			4.79
Tupelo (TUP)			24	36	27/2000			1.86
Meridian (MEI)	1004.4		25	48	27/0945			5.29
State Port (Gulfport)				39	27/1951			
Bay St. Louis							E4.5	
Texas								
Port Arthur (BPT)	1011.5	26/1000	22	30	26/1953			
Sabine Pass						1.1	1.3	
Ship reports								
OYGK2 (29.5°N 80.6°W)			U60		25/1200			
ELLE2 (19.4°N 56.6°W)	1013.5	19/1500	U35		19/1500			
C6KD (28.1°N 79.2°W)	1015.5	24/0600	U35		24/0600			
Gulf of Mexico platforms (+, U, N)								
SS 198G (28.2°N 92.0°W)			78	100	26/0330			
EC 83H (28.2°N 92.0°W)			46	49	26/0330			
EC 42B (29.5°N 92.8°W)			38	88	26/0430			
SM 136B (28.2°N 92.0°W)			38	44	25/2230			

+,– A more extreme value may have occurred unnoticed.
E Estimated.
U Unknown averaging period.
N Non-standard elevation.
MLW Above Mean Low Water.
MWL Above Mean Water Level.
* Time of 1-minute wind speed unless only gust is given.
** Storm surge is water height above normal tide level. Storm tide is water height relative to National Geodetic Vertical Datum (NGVD) which is defined as mean sea level in 1929.
*** Equipment became inoperable after this measurement.

Table 2b. Additional rainfall totals and unofficial weather reports on Hurricane Andrew, August 1992.

Location	Maximum surface wind speed (kt)			Minimum pressure (mb)		Total Rain (in.)
	Sustained	Peak gust	Date/time (UTC)*	P	Date/time (UTC)	
Florida						
Perrine		184**				
Princeton		155**	24/0935			
Virgina Key	85	98	24/0930	992	24/0830	
Turkey Point		85**	24/0820			
Fort Lauderdale	66	76				
Homestead				A925		
Princeton				A926		
Redlands				A926		
Leisure City				928	24/0945	
Homestead				929	24/0925	
Redlands				A930		
Homestead				933		
Perrine				948		
Cutler Ridge				949		
South Richmond Hts.				956		
Angelfish Creek				957	24/0940	
Southwest Kendall				962		
South Miami Hts.				965		
Kendall				967		
Tamiami Lakes				985	24/0930	
South Miami				997-	24/0930	
Cape Coral		45				
S-124 (Broward County)						7.79
S-21A (Dade County)						7.41
S-20G (Dade County)						5.19
S-37A (Broward County)						5.14
S-39 (Broward/Palm Beach Counties)						5.12
S-80 (Martin-St. Lucie)						4.94
Everglades Park (Collier County)						E4.50
S-18C (Dade County)						4.48
Marco Island						E3.50
S-20F (Dade County)						4.12
S-308 (Lake Okeechobee area)						3.47
Cudjoe Key						2.02
Louisiana						
Berwick Fire Stn.	N83	N104				
Jeanerette	71	78+		975		
Jeanerette	67	75	26/0845			
Near Brusly	69	90+	26/1310	990.2	26/1337	5.05
Lafayette courthouse		N90				
Mooring 17 (29.2°N 92.0°W)				994.9	26/0930	
Hammond						11.92
Robert						11.02
Amite						10.36
Morgan City						9.31
Manchac						8.75
Jeanerette						7.96
Butte La Rose						7.90
Ponchatoula						7.54
Mt. Herman						7.50
Franklin						7.03

Table 2b (cont.). Additional rainfall totals and unofficial weather reports on Hurricane Andrew, August 1992.

Location	Maximum surface wind speed (kt) Sustained	Peak gust	Date/time (UTC)*	Minimum pressure (mb) P	Date/time (UTC)	Total Rain (in.)
						5.06
WSFO Slidell						4.42
Jena 4WSW						
Alabama						
						4.40
Aliceville						3.60
Tuscaloosa						3.46
MRGA1 Morgan						3.21
MRZA1 Mount Roszell						2.90
CDCA1 Red Bay Creek						2.89
WRTA1 Wright						2.75
CBTA1 Colbert						2.66
AKDA1 Lexington						2.62
OAKA1 Oakland						
Georgia						
						5.24
Hurst						4.60
Mountain City						4.31
Burton						4.30
Clayton						3.83
Nacoochee Pwr						3.40
Helen						3.32
SCHG1 Suches G. Creek						3.13
TUSG1 Titus						3.05
Tallulah						2.67
Jasper						2.65
BRDG1 Blue Ridge Dam						2.64
EPWG1 Epworth H. Store						
Kentucky						
						2.56
BLWK2						
Mississippi						
						9.30
Sumrall						8.20
Pelahatchie (gage)						7.63
Yazoo City						7.24
Crystal Springs						7.07
Pelahatchie (co-op)						7.04
Collins						7.04
Union Church						7.02
Brookhaven						6.71
Mize						6.36
Rockport						6.36
Monticello						6.30
Booneville						6.14
Good Hope						5.95
Vicksburg						5.93
McComb						5.82
Ofahoma						5.72
Bay St. Louis						5.65
White Oak						5.59
Forest						5.59
Liberty						5.52
Goshen Springs						5.51
Port Gibson						

Table 2b (cont.). Additional rainfall totals and unofficial weather reports on Hurricane Andrew, August 1992.

Location	Maximum surface wind speed (kt) Sustained	Peak gust	Date/time (UTC)*	Minimum pressure (mb) P	Date/time (UTC)	Total Rain (in.)
Meadville						5.45
Tylertown						5.38
Columbia						5.32
Philadelphia						5.06
North Carolina						
HDSN7 Highlands						4.68
WLGN7 F-Wallace Gap						2.73
RMNN7 Rosman						2.62
Tennessee						
ELKT1 Elkton						3.80
WNBT1 Waynesboro						3.64
GEOT1 Georgetown						3.43
IRCT1 Iron City-S.C.						3.33
BGLT1 Big Lick						3.25
CBOT1 Crab Orchard						3.07
CLLT1 Collinwood						3.07
PSKT1 Pulaski						3.03
LNVT1 Lynnville						2.97
PICT1 Pickwick Dam						2.95
CLET1 Cleveland						2.91
CLBT1 Columbia						2.80
DYNT1 Dime						2.74
LEWT1 Lewisburg						2.58
CSV Crossville Arpt.						2.57
PKVT1 Pikeville						2.50

A Corrected value based on laboratory test of instrument conducted by the NOAA Aircraft Operations Center.
E Estimated.
+,- A more extreme value may have occurred unnoticed.
* Time of sustained wind speed unless only gust is given.
** Value was at upper limit of equipment range, or equipment became inoperable beyond this value.

Table 2c. Hurricane Andrew selected NDBC observations, August 1992.

Platform/ Location	Minimum sea-level pressure		Maximum wind speed (kt)		
	Pressure (mb)	Date/time (UTC)	average*	Peak gust	Date/time (UTC)
Fowey Rocks C-MAN FWYF1/ 25.6°N 80.1°W	967.5**	24/0800	123**	147**	24/0800
Bullwinkle Platform BUSL1/ 27.9°N 90.9°W	998.5	25/2300	52	63	25/2200
Molasses Reef C-MAN MLRF1/ 25.0°N 80.4°W	998.5	24/0900	48	56	24/1000
Eastern Gulf Buoy 42003/ 25.9°N 85.9°W	1000.5**	25/0200	45**	56**	25/0200
Grand Isle C-MAN GDIL1/ 29.2°N 89.9°W	1005.2	25/2300	48	59	25/2200
Southwest Pass C-MAN BURL1/ 28.9°N 89.4°W	1006.1	25/2200	56	64	25/2100
Sombrero Key C-MAN SMKF1/ 24.6°N 81.2°W	1007.7	24/1100	34	39	24/1130
Lena Platform C-MAN LNEL1/ 28.2°N 89.1°W	1007.7	25/1600			
Eleuthera Buoy 41016/ 24.6°N 76.5°W	1007.9	23/2100	29	35	24/0100
Sand Key C-MAN SANF1/ 24.5°N 81.9°W	1010.2	24/1100,1400	30	35	24/1600
Settlement Point C-MAN SPGF1/ 26.7°N 79.0°W	1012.7	24/0600	38	44	24/0500
Dauphin Island C-MAN DPIA1/ 30.2°N 88.1°W	1016.1	26/0000	32	38	25/2100

* NOAA buoys report an 8-minute average wind. C-MAN stations report a 2-min average wind at the top of the hour and 10-min averages at other times.

** Equipment became inoperable shortly after observation.

Table 3. Initial estimates of casualties and damages incurred in association with Hurricane Andrew.

	Deaths			Damage
	Direct	Indirect	Missing	($Billion)
Bahamas	3	1		0.25
Florida	15	29		15–30
Dade County	15	25		15–30
Broward County	0	3		0.1
Monroe County	0	1		0.131
Collier County	0	0		0.03
Louisiana	6		2	1
St. J. the B. Parish	2			
Offshore	4		2	
Lafayette Parish				0.017
Vermillion Parish				0.001
Georgia				0.001
Total	24	30	2	15–30

Table 4. Hurricane Andrew average track forecast errors (nautical miles), non-homogeneous sample.

	Forecast period (hours)				
Model	12	24	36	48	72
Official	33	65	106	141	243
(no. of cases)	(37)	(35)	(33)	(31)	(27)
CLIPER	35	81	148	233	437
	(37)	(35)	(33)	(31)	(27)
AVNO	60	75	89	97	132
	(15)	(15)	(14)	(13)	(11)
BAMD	45	93	141	182	268
	(37)	(35)	(33)	(31)	(27)
BAMM	40	81	121	151	229
	(37)	(35)	(33)	(31)	(27)
BAMS	39	77	114	135	197
	(37)	(35)	(33)	(31)	(27)
QLM	39	64	93	130	192
	(19)	(18)	(17)	(16)	(14)
NHC90	35	77	135	197	330
	(37)	(35)	(33)	(31)	(27)
VBAR	32	60	93	138	287
	(23)	(23)	(23)	(23)	(23)
GFDL	36	71	93.	117	209
	(9)	(9)	(9)	(9)	(7)

Table 5. Watch and warning summary, Hurricane Andrew.

Date/Time(UTC) /Action	
22/1500 Hurricane Watch	Northwest Bahamas from Andros and Eleuthera Islands northward through Grand Bahama and Great Abaco
22/2100 Hurricane Warning	Northwest Bahamas from Andros and Eleuthera Islands northward through Grand Bahama and Great Abaco
22/2100 Hurricane Watch	Florida east coast from Titusville southward through the Florida Keys including the Dry Tortugas
23/0600 Hurricane Warning	Central Bahamas including Cat Island, Great Exuma, San Salvador, and Long Island
23/1200 Hurricane Warning	Florida east coast from Vero Beach southward through the Florida Keys to the Dry Tortugas including Florida Bay
23/1200 Tropical Storm Warning	Florida east coast north of Vero Beach to Titusville
23/1200 Hurricane Watch	Florida west coast south of Bayport including the greater Tampa area to north of Flamingo
23/1800 Hurricane Warning	Florida west coast south of Venice and Lake Okeechobee
23/1800 Tropical Storm Warning	Florida west coast north of Venice to Bayport
24/0900 Hurricane Warning discontinued	Bahamas except for Bimini and Grand Bahama
24/1300 Hurricane Warning discontinued	Remainder of the Bahamas
24/1300 Hurricane Warning discontinued	Florida except for Lake Okeechobee and the west coast south of Venice to Flamingo
24/1300 Tropical Storm Warning and Hurricane Watch discontinued	Florida east coast from Vero Beach to Titusville and Florida west coast from Venice to Bayport
24/1300 Hurricane Watch	Northern Gulf coast from Mobile, Alabama to Sabine Pass, Texas
24/1800 Hurricane Warning discontinued	Remainder of Florida
24/2100 Hurricane Warning	Northern Gulf coast from Pascagoula, Mississippi to Vermillion Bay, Louisiana
25/0900 Hurricane Warning	Vermillion Bay, Louisiana to Port Arthur, Texas
25/0900 Hurricane Watch	West of Port Arthur through High Island, Texas
25/1500 Hurricane Warning	West of Port Arthur through the Bolivar Peninsula Texas
25/1500 Hurricane Watch	West of the Bolivar Peninsula to Freeport, Texas
26/0700 Hurricane Warning discontinued	East of Grand Isle, Louisiana
26/0700 Hurricane Watch discontinued	West of the Bolivar Peninsula
26/1100 Hurricane Warning discontinued	West of Port Arthur, Texas
26/1300 Hurricane Warning discontinued	West of Cameron, Louisiana
26/1700 Hurricane Warning discontinued	Remainder of Gulf coast

Table 6. Watch and warning lead times for landfall sites during Hurricane Andrew. Lead time refers to time lapsed from advisory to landfall.

Location	Type	Lead Time (hours)
Northwest Bahamas	Hurricane Watch	30
	Hurricane Warning	24
Southeast Florida	Hurricane Watch	36
	Hurricane Warning	21
South-central Louisiana	Hurricane Watch	43
	Hurricane Warning	24

Table 7. Chances of the center of Hurricane Andrew passing within 65 miles of listed locations by date and time (EDT) indicated; probabilities in percent with X for less than 2 percent.

ADVISORY ISSUE TIME: / PROBABILITY END TIME:	16/11PM 19/8PM	17/5AM 20/2AM	17/11AM 20/8AM	17/5PM 20/2PM	17/11PM 20/8PM
SVMG 110N 640W	4	5	7	6	X
TTPP 106N 614W	7	8	9	6	X
TTPT 112N 608W	8	10	11	8	X
TGPY 120N 618W	8	10	11	9	X
TBPB 131N 595W	11	14	15	14	4
TVSV 131N 612W	9	11	14	12	3
TLPL 138N 610W	10	12	15	14	5
TFFF 146N 610W	10	12	15	15	8
TDPR 153N 614W	10	12	15	15	10
TFFR 163N 615W	10	12	16	16	13
TAPA 171N 618W	9	11	15	16	15
TKPK 173N 627W	8	10	14	15	14
TNCC 122N 690W	X	X	3	2	X
TNCM 181N 631W	X	X	14	14	14
TISX 177N 648W	X	X	12	12	9
TIST 183N 650W	X	X	X	12	X

ADVISORY ISSUE TIME: / PROBABILITY END TIME:	18/5AM 21/2AM	18/11AM 21/8AM	18/5PM 21/2PM	18/11PM 21/8PM	19/5AM 22/2AM
TBPB 131N 595W	4	3	X	X	X
TVSV 131N 612W	3	3	X	X	X
TLPL 138N 610W	6	6	2	X	X
TFFF 146N 610W	9	9	4	2	2
TDPR 153N 614W	11	13	7	4	3
TFFR 163N 615W	15	18	13	8	6
TAPA 171N 618W	18	21	17	14	10
TKPK 173N 627W	16	20	17	14	12
TNCM 181N 631W	17	21	19	19	17
TISX 177N 648W	12	16	14	14	12
TIST 183N 650W	13	17	16	16	15
TJPS 180N 666W	8	13	12	12	11
MDSD 185N 697W	X	6	7	8	8
MDCB 176N 714W	X	2	3	3	3
MTPP 186N 724W	X	X	3	3	3
TJSJ 184N 661W	X	X	X	14	14

Table 7 (cont.). Chances of the center of Hurricane Andrew passing within 65 miles of listed locations by date and time (EDT) indicated; probabilities in percent with X for less than 2 percent.

ADVISORY ISSUE TIME:	19/11AM	19/5PM	19/11PM	20/5AM	20/11AM
PROBABILITY END TIME:	22/8AM	22/2PM	22/8PM	23/2AM	23/8AM
TAPA 171N 618W	2	X	X	X	X
TKPK 173N 627W	4	X	X	X	X
TNCM 181N 631W	7	3	X	X	X
TISX 177N 648W	6	3	2	2	2
TIST 183N 650W	9	5	3	3	3
TJPS 180N 666W	7	5	4	4	4
MDSD 185N 697W	6	7	6	6	6
MDCB 176N 714W	3	4	3	3	4
MTPP 186N 724W	3	6	4	4	5
TJSJ 184N 661W	9	6	4	4	4
MDPP 198N 707W	8	11	9	9	9
MUCM 214N 779W	X	3	X	X	2
MTCA 183N 738W	X	4	3	3	3
MUGM 200N 751W	X	6	3	3	4
MBJT 215N 712W	X	16	13	13	12
MYMM 224N 730W	X	14	11	12	11
MYSM 241N 745W	X	14	9	X	10
MYEG 235N 758W	X	10	X	X	7
MYAK 241N 776W	X	7	X	X	X

ADVISORY ISSUE TIME:	20/5PM	20/11PM	21/5AM	21/11AM	21/5PM
PROBABILITY END TIME:	23/2PM	23/8PM	24/2AM	24/8AM	24/2PM
MDSD 185N 697W	4	X	X	X	X
MDCB 176N 714W	2	X	X	X	X
MTPP 186N 724W	4	X	2	2	2
MDPP 198N 707W	7	3	3	3	2
MUCM 214N 779W	4	X	2	5	5
MTCA 183N 738W	3	X	2	2	X
MUGM 200N 751W	5	X	3	4	3
MBJT 215N 712W	12	6	8	6	6
MYMM 224N 730W	13	7	9	8	8
MYSM 241N 745W	13	8	12	11	12
MYEG 235N 758W	10	5	8	9	10
MYAK 241N 776W	7	2	6	8	9
MYNN 251N 775W	8	3	7	9	10
MYGF 266N 787W	6	2	6	9	9
MUHA 230N 824W	X	X	X	3	3
MKJS 185N 779W	X	X	X	2	2
MWCG 193N 814W	X	X	X	2	X
MUCF 221N 805W	X	X	X	4	4
MUSN 216N 826W	X	X	X	2	2
BERMUDA	2	X	3	2	2
MIAMI FL	X	X	2	7	7
W PALM BEACH FL	X	X	3	7	8
MARATHON FL	X	X	X	5	6
FT PIERCE FL	X	X	X	X	8
COCOA BEACH FL	X	X	X	X	7
DAYTONA BEACH FL	X	X	X	X	6

Table 7 (cont.). Chances of the center of Hurricane Andrew passing within 65 miles of listed locations by date and time (EDT) indicated; probabilities in percent with X for less than 2 percent.

ADVISORY ISSUE TIME:	21/11PM	22/5AM	22/11AM	22/5PM	22/11PM
PROBABILITY END TIME:	24/8PM	25/2AM	25/8AM	25/2PM	25/8PM
MUCM 214N 779W	4	5	6	7	2
MUGM 200N 751W	3	X	X	X	X
MBJT 215N 712W	3	2	X	X	X
MYMM 224N 730W	6	6	5	X	X
MYSM 241N 745W	11	12	16	19	21
MYEG 235N 758W	9	10	12	15	11
MYAK 241N 776W	9	11	14	22	27
MYNN 251N 775W	11	13	17	27	35
MYGF 266N 787W	11	13	17	24	24
MUHA 230N 824W	4	5	8	14	16
MWCG 193N 814W	X	X	X	4	X
MUCF 221N 805W	4	5	8	12	10
MUSN 216N 826W	2	3	6	10	9
MUAN 219N 850W	2	3	5	9	11
MMCZ 205N 869W	X	X	3	5	5
BERMUDA	2	X	X	X	X
MIAMI FL	8	10	14	21	23
W PALM BEACH FL	9	11	15	20	20
MARATHON FL	6	8	12	19	23
FT PIERCE FL	9	11	15	18	16
COCOA BEACH FL	9	11	14	16	13
DAYTONA BEACH FL	8	10	12	13	10
JACKSONVILLE FL	7	8	9	9	7
SAVANNAH GA	6	7	7	5	4
CHARLESTON SC	X	7	6	3	2
MMMD 210N 897W	X	X	2	3	5
MYRTLE BEACH SC	X	X	5	X	X
WILMINGTON NC	X	X	4	X	X
KEY WEST FL	X	X	X	18	21
MARCO ISLAND FL	X	X	X	19	21
FT MYERS FL	X	X	X	18	19
VENICE FL	X	X	X	17	17
TAMPA FL	X	X	X	X	14
CEDAR KEY FL	X	X	X	X	11

ADVISORY ISSUE TIME:	23/5AM	23/5AM	23/11AM	23/11AM	23/5PM
PROBABILITY END TIME:	26/2AM	26/2AM	26/8AM	26/8AM	26/2PM
MYSM 241N 745W	26	26	13	13	X
MYEG 235N 758W	12	12	2	X	X
MYAK 241N 776W	34	34	34	34	17
MYNN 251N 775W	51	51	68	68	99
MYGF 266N 787W	36	36	43	43	61
MUHA 230N 824W	18	18	15	15	10
MUCF 221N 805W	10	10	5	5	X
MUSN 216N 826W	9	9	5	5	X
MUAN 219N 850W	11	11	9	9	6
MMCZ 205N 869W	5	5	4	X	X
MIAMI FL	34	34	40	40	56
W PALM BEACH FL	30	30	33	33	47
MARATHON FL	30	30	32	32	37
FT PIERCE FL	23	23	23	23	28
COCOA BEACH FL	17	17	16	16	16

Table 7 (cont.). Chances of the center of Hurricane Andrew passing within 65 miles of listed locations by date and time (EDT) indicated; probabilities in percent with X for less than 2 percent.

ADVISORY ISSUE TIME:	23/5AM	23/5AM	23/11AM	23/11AM	23/5PM
PROBABILITY END TIME:	26/2AM	26/2AM	26/8AM	26/8AM	26/2PM
DAYTONA BEACH FL	11	11	10	10	9
JACKSONVILLE FL	7	7	6	6	X
SAVANNAH GA	3	3	2	X	X
CHARLESTON SC	X	X	X	X	X
MMMD 210N 897W	5	5	5	5	X
MMSO 238N 982W	2	2	3	X	X
MMTM 222N 979W	X	X	2	X	X
KEY WEST FL	27	27	28	28	31
MARCO ISLAND FL	28	28	31	31	42
FT MYERS FL	25	25	27	27	37
VENICE FL	21	21	22	22	29
TAMPA FL	17	17	17	17	20
CEDAR KEY FL	13	13	12	12	13
ST MARKS FL	X	X	X	10	9
APALACHICOLA FL	X	X	X	12	12
PANAMA CITY FL	X	X	X	X	11
PENSACOLA FL	X	X	X	X	11
ADVISORY ISSUE TIME:	24/5AM	24/5AM	24/11AM	24/11AM	24/5PM
PROBABILITY END TIME:	27/2AM	27/2AM	27/8AM	27/8AM	27/2PM
MYGF 266N 787W	30	30	X	X	X
MUHA 230N 824W	X	2	X	X	X
MUAN 219N 850W	X	3	X	X	X
MMCZ 205N 869W	X	2	X	X	X
MIAMI FL	99	99	X	X	X
W PALM BEACH FL	73	73	X	X	X
MARATHON FL	62	62	X	X	X
FT PIERCE FL	8	8	X	X	X
COCOA BEACH FL	4	4	X	X	X
DAYTONA BEACH FL	3	3	X	X	X
JACKSONVILLE FL	3	3	X	X	X
SAVANNAH GA	X	X	X	X	X
CHARLESTON SC	X	X	X	X	X
MMMD 210N 897W	X	3	X	X	X
MMSO 238N 982W	X	3	X	X	X
KEY WEST FL	37	37	X	X	X
MARCO ISLAND FL	83	83	99	99	X
FT MYERS FL	67	67	94	94	X
VENICE FL	46	46	62	62	X
TAMPA FL	19	19	6	6	X
CEDAR KEY FL	10	10	4	4	X
ST MARKS FL	8	8	6	6	6
APALACHICOLA FL	12	12	9	9	8
PANAMA CITY FL	11	11	11	11	10
PENSACOLA FL	12	12	15	15	16
MOBILE AL	12	X	17	17	18
GULFPORT MS	13	X	19	19	21
BURAS LA	X	X	24	24	26
NEW ORLEANS LA	X	X	21	21	23
NEW IBERIA LA	X	X	20	20	21

Table 7 (cont.). Chances of the center of Hurricane Andrew passing within 65 miles of listed locations by date and time (EDT) indicated; probabilities in percent with X for less than 2 percent.

ADVISORY ISSUE TIME:	24/5AM	24/5AM	24/11AM	24/11AM	24/5PM
PROBABILITY END TIME:	27/2AM	27/2AM	27/8AM	27/8AM	27/2PM
PORT ARTHUR TX	X	X	16	16	17
GALVESTON TX	X	X	X	15	15
FREEPORT TX	X	X	X	X	13
PORT O CONNOR TX	X	X	X	X	10
ADVISORY ISSUE TIME:	24/11PM	25/5AM	25/11AM	25/5PM	25/11PM
PROBABILITY END TIME:	27/8PM	28/2AM	28/8AM	28/2PM	28/8PM
FT PIERCE FL	2	X	X	X	X
COCOA BEACH FL	2	X	X	X	X
DAYTONA BEACH FL	3	X	X	X	X
JACKSONVILLE FL	4	X	X	X	X
SAVANNAH GA	3	X	X	X	X
CHARLESTON SC	2	X	X	X	X
MMSO 238N 982W	X	3	X	X	X
MARCO ISLAND FL	2	X	X	X	X
FT MYERS FL	2	X	X	X	X
VENICE FL	3	X	X	X	X
TAMPA FL	4	X	X	X	X
CEDAR KEY FL	6	X	X	X	X
ST MARKS FL	9	5	X	X	6
APALACHICOLA FL	11	7	6	4	6
PANAMA CITY FL	13	8	7	6	7
PENSACOLA FL	16	13	11	9	11
MOBILE AL	18	16	14	13	13
GULFPORT MS	20	20	18	16	15
BURAS LA	23	32	50	44	64
NEW ORLEANS LA	21	25	36	37	66
NEW IBERIA LA	X	23	38	50	76
PORT ARTHUR TX	X	18	24	28	30
GALVESTON TX	X	17	20	19	11
FREEPORT TX	X	16	17	15	X
PORT O CONNOR TX	X	13	13	10	X

RECONNAISSANCE FIX LOG

CYCLONE NAME ANDREW
CYCLONE DATES

ACFT	MISSION IDENT	OB #	DATE/TIME (GMT)	LAT °N	LON °W	MAX WIND SFC	MAX WIND FL	MIN SLP	STD. SFC HT.	MAX TEMP OUT °C	MAX TEMP IN °C	DEW PT. °C	EYE SHAPE	EYE CHAR.	ACFT. ALT.	ACCURACY NAV./MET.
				(DEGS-MINS)		(KT)		(MB)	(M)							(N. MI.)
EXAMPLE AF980	0503 ALICIA	12	17/0902	2753	9401	65	75	986	1303	19	22	18	C20	CLSD	850MB	5/5
			25/1405	27°25'	88°54'	100	128	944	2619	10	15	11	C30	CLSD	700	1/2
			25/1717	27°42'	89°37'	-	127	943	2535	11	16	14	C25	CLSD	700	1/2
			25/1840	27°51'	89°50'	50	123	939/E937	2561	11	17	11	C20	CLSD	700	1/2
			25/2010	28°05'	90°04'	-	128	936/E932	2536	9	18	13	C22	CLSD	700	1/2
			25/2135	28°15'	90°15'	-	135	939/E932	2544	12	20	10	C19	[illegible]	[illegible]	1/3
			25/2329	28°31'	90°36'	-	120	940/E936	2569	12	[illegible]	11	C23	[illegible]	[illegible]	1/3
			26/0207	28°42'	90°59'	-	125	950/E9445	2633	8	16	13	C23	[illegible]	[illegible]	2/2
			26/0344	28°51'	91°07'		104	/E951	2663	9	13	13	C25	CLSD	700	2/2
			26/0458	28°58'	91°13'		73	959	2682	11	14	14	C25	CLSD	700	2/2
			26/0526	29°04'	91°17'		132	E952	2695	3	14	14	C18	CLSD	700	2/2
			26/0624	29°14'	91°22'		55	954F	2703	12	14	13	C18	[illegible]	700	2/2
			26/0729	29°21'	91°27'		129	956	2714	11	15	13	C22	CLSD	700	2/2
			26/0806	29°33'	91°33'		81	E157	2731	8	15	13	C22	CLSD	700	3/3
			26/0931	29°33'	91°32'		112	955	2722	11	14	14	C20	CLSD	700	3/3
			26/1102	29°52	91 39	-	96	—	—	9	13	11	C12	11	11	1/3
			26/1228	30°12	91°44	Radar fix							C12			
			26/1325	30°12	91°31	Radar fix						—	—			

CYCLONE NAME _____

CYCLONE DATES _____

ACFT	MISSION IDENT	OB #	DATE/TIME (GMT)	LAT °N	LON °W	MAX WIND SFC	MAX WIND FL	MIN SLP	STD. SFC HT.	MAX TEMP OUT °C	MAX TEMP IN °C	DEW PT. °C	EYE SHAPE	EYE CHAR.	ACFT. ALT.	ACCURACY NAV./MET.
				(DEGS-MINS)		(KT)		(MB)	(M)							(N. MI.)
EXAMPLE AF980	0503 ALICIA	12	17/0902	2753	9401	65	75	986	1303	19	22	18	C20	CLSD	850MB	5/5
984	0703 ANDREW	10	22/1334	25 50	68 42	80	99	974	1211	18	23	14	C10	<45D	850	1/2
984	0703 ANDREW	13	22/1519	2551	6910	-	94	974	2665	8	15	7	C10	CLSD	700	1/2
	0703 ANDREW	17	22/1709	2549	6931	90	110	974 (977)E	2863	8	16	7	C15	CLSD	700	1/2
NOAA2			22/2102	25.7	70.4		89						C15	CLOSED	20000'	
AF966	0803A ANDREW	06	23/0006	25°35'	71°05'		89	959	2784	10	18	5	C13	"	700	1/1
"	"	40?	23/0021	25°34'	71°08'	—	121	959	2778	10	17	10	C13	"	"	1/1
"	"	08	23/0315	25°34'	71°30'		106	959	2765	9	16	8	C12	"	"	1/1
		13	23/0549	25 30	71 59	—	139	959	2787	8	15	10	C11	"	700	1/1
		17	23/0543	25 31	72 32	—	121	951	2838	9	18	8	C12	"	700	1/1
AF984	0903A ANDREW	7	23/1124	25°22	74°19	100	124	934	2545	9	19	4	C11	"	700	1/3
"	0903A ANDREW	11	23/1403	25°19	74°45	—	143	930	2509	9	19	8	C8		700	1/3
"	"	14	23/1527Z	25°24'	75°01'	120	170	926	2469	10	21	3	C8	"	700	1/2
"	0903	21	23/1648Z	25°24'	75°29	136	170	922	2462	12	22	3	C8	"	700	1/2 * LIX
"	"	24	23/1753Z	25°27'	75°42'	—	154	923	2461	12	22	4	C8	"	700	1/2
AF-366	1003	5	23/2045	25°28'	76°32'	—	110	927	2461	10	20	7	C0 8-20 (double)	"	700	1/2
	1003	9	23/2232	25°27	76°59	—	127	923	2462	8	15	10	C0 8-20	"	700	1/2
	1003A	13	24/0013	25°25'	77°32'		116	931	2487	7	14	12	C0 8-20	"	"	1/2

CYCLONE NAME ANDREW

CYCLONE DATES

ACFT	MISSION IDENT	OB #	DATE/TIME (GMT)	LAT °N	LON °W	MAX WIND SFC	MAX WIND FL	MIN SLP	STD. SFC HT.	MAX TEMP OUT	MAX TEMP IN	DEW PT.	EYE SHAPE	EYE CHAR.	ACFT. ALT.	ACCURACY NAV./MET.
				(DEGS-MINS)		(KT)		(MB)	(M)	°C	°C	°C				(N. MI.)
EXAMPLE AF980	0503 ALICIA	12	17/0902	2753	9401	65	75	986	1303	19	22	18	C20	CLSD	850MB	5/5
			24/0230	25 26	78 13	—	116	DROP 937	2552	7	15	13	C20	CLSD	700MB	3/3
			24/0710	25 22	78 49	—	140	EXTRA 941	2569	7	13	13	C2[illegible]	CLSD	700MB	5
			24/0546	25 22	77 20	—	W154 F132	936	2547	6	14	14	C20	CLSD	700	3/2
			24/0341	2526	3001		133	932	2497	4	16	13	C13	CLSD	700	5/5
			24/1502	25°39'	82°13	[illegible]	117	951/EXT 948E	2658	9	15	12	C14	CLSD	700	1/5
			24/1632	25°41	82°41	120	107	947	2656	9	16	15	C17	CLSD	700	1/1
			24/1751	25°46	83°06	100	117	947	2655	10	14	14	C17	CLSD	700	1/1
			24/1919	25°50'	83°34'	NA	98	[illegible]	2641	10	15	14	C16	CLSD	700	1/1
			24/2051	26°03'	84°03'	100	124	945	2611	9	15	15	C14	CLSD	700	1/1
			24/2220	26°22'	84°30'	100	117	945	2611	9	16	15	C12	CLSD	700	1/1
			25/0017	26°09'	85°09'	NA	93	945	2609	9	16	13	C13	CLSD	700	1/1
			25/0429	26°33'	86°24'	—	130	947	953	13	23	19	C13	CLSD	850	3/6
			25/0611	26°40	86°51'		107	949	2643							
			25/0807	2652	8728	—	105	949	2652							
			25/0957	2659	8748		86	948	2641	11	12	11	C12 (EYE OUTER EYE FORMING)	OPEN E	700	1/3
			25/1120	27°13'	88°14'	—	103	946	2636	10	13	11	C10	OPEN S	700	1/3
			25/1310	27°22'	88°38'	—	133	946	2629	10	13	12	C30	CLSD	700	1/3

Appendix C.

Hindcast Methodology

Appendix C.

Hindcast Methodology

Introduction

The hindcast of a historical storm consists of three basic steps. First, the wind field is specified in a process which requires considerable work by a meteorologist both to develop required input parameters for a numerical model of the cyclone wind field, and if necessary and warranted to produce kinematic analyses for use when, and for areas in which the numerical solution is not sufficiently accurate. The wind fields are specified on two grid systems, one used in the spectral wave model whose execution is the second part of the hindcast, and another used in the storm surge/current model, whose execution is the third part of the process. In this section we give concise descriptions of each of these processes, as specifically adapted to this problem. More extensive mathematical treatments are reserved to cited references.

Wind Field Specification

We have two approaches available to the specification of wind fields in tropical cyclone regimes. In the first approach, a numerical model of the boundary layer flow in a moving vortex is adapted to specify the time and space varying wind associated with a propagating cyclone. Some account of the ambient flow in the far-field surrounding the cyclone is incorporated in this approach through the specification of the ambient pressure field; the background flow is prescribed in terms of a constant equivalent geostrophic pressure gradient limiting this scheme to relatively simple superpositions of tropical cyclones and surrounding systems. For example, the case of a tropical cyclone travelling around the periphery of the sub-tropical anticyclone is well handled by this approach, a configuration characteristic of Andrew through most of its history.

In recent years, detailed aircraft reconnaissance has revealed quite complicated wind fields in some tropical cyclones. For example, some storms exhibit two distinct maxima in the radial variation of boundary layer wind, one often very close to the eye of the storm (10-15 n.mi.), and the second perhaps 50 to 100 miles away from the center. Other storms exhibit a single maximum near the center, but with a much slower decrease in wind speed with radial distance outside of the radius of maximum wind. For such storms, we have developed a second approach which utilizes kinematic analysis of over-water wind observations (often aircraft observations are extrapolated down to the 20-meter reference level), to develop a description of the wind field about the translating cyclone, which is then used to provide a time varying wind field, by propagating the complicated wind field distribution with the moving storm center. Fortunately, on the scale at which we are attempting to resolve

the wave and surge fields (that is, as dictated by the resolution of the wave and surge models), Andrew exhibited neither double concentric wind maxima nor anomalous outer core radial wind profiles, so the wind specification could be made with the wind model. However, many iterations of the model solution were made in order to achieve a wind field in reasonable agreement with the limited observations of surface winds and with surface winds reduced from aircraft measurements. Therefore, we next describe the numerical cyclone model.

Numerical Cyclone Wind Field Model

The model developed in the Ocean Data Gathering Program (ODGP) provides a complete description of the surface winds in the boundary layer of a tropical cyclone from the simple model parameters available in historical storms. The model is an application of a theoretical model of the horizontal air flow in the boundary layer of a moving vortex. That model solves, by numerical integration, the vertically averaged equations of motion that govern a boundary layer subject to horizontal and vertical shear stresses. The equations are resolved in a Cartesian coordinate system whose origin translates at constant velocity, v_f , with the storm center of the pressure field associated with the cyclone. Variations in storm intensity and motion are represented by a series of quasi-steady state solutions.

The non-linear system of equations is solved numerically on a fine-mesh nested grid system (inner nest grid spacing is prescribed). Transformation of steady solution to earth fixed coordinates provides the vertically integrated wind field.

The Ocean Data Gathering Program wind model included an empirical scaling of the 20-meter wind speed from the vertically integrated wind. In a later study we replaced the empirical scaling by replacing the surface drag treatment (Cardone et al., 1979) with a similarity boundary layer parameterization.

The model pressure field is described as the sum of an axially symmetric part, $\tilde{p}$, and a large-scale pressure field, $\overline{p}$, of constant gradient. The symmetric part is described in terms of an exponential pressure profile

$$\tilde{p} = p_0 + \Delta p \exp(-r_a/r)$$

where p_0 is central pressure, Δp is storm anomaly and

r_a is a scaling radius nearly equivalent to the radius of maximum wind. The model, therefore, can be initialized from parameters that are usually available from historical meteorological records:

p_0, r_a, v_f and the ambient pressure field $\overline{p}$. The entire wind field history is computed from knowledge of the variation of those parameters along the storm track.

For each hindcast, so-called "snapshots" are specified to describe the surface wind distribution on the nested grid as often as is necessary to describe different stages of intensity.

The interpolation of winds to the hindcast wave and current model grids from the snapshot wind fields, which are generated on a moving nested grid, proceeds in three stages. First, the hourly coordinates of the storm center are linearly interpolated from a track table. Second, at each interval, the model wind components are linearly interpolated in time between adjacent snapshots. Third, for each grid point each hour, given the latitude and longitude of the eye and the latitude and longitude of the point, the smallest nest is found within which the grid point lies and the wind components are interpolated bi-linearly to the grid point from the four surrounding nest positions.

The model was validated originally against winds measured in several Ocean Data Gathering Program storms. It has since been applied to nearly every recent hurricane to affect the United States offshore area. Comparisons with over-water measurements from buoys and rigs support an accuracy specification of +/- 20 degrees in direction and +/- 2 meters/second in wind speed (1-hour average at 20-meter elevation). Most comparisons have been published (see e. g., Cardone et al., 1978; Ross and Cardone, 1978; Cardone and Ross, 1979; Forristall et al., 1977; 1978; 1980).

The cyclone wind model has also been applied to the study of tropical cyclones in foreign basins. The model has been used by the U. S. National Aeronautics and Space Administration (NASA) and by the National Oceanic and Atmospheric Administration (NOAA) to evaluate marine winds sensed remotely from SKYLAB and SEASAT in several Pacific Ocean typhoons. More recently, in over three-dozen proprietary industry-sponsored studies, the model has been applied to model tropical cyclones offshore Borneo, in the Gulf of Thailand, the Arafura Sea, offshore NW Australia, and in several studies for offshore China, including waters around Hainan Is. and Pearl River Basin.

As presently formulated, the wind model is free of arbitrary calibration constants which might link the model to a particular storm type. The variations in structure between tropical storm types manifest themselves basically in the characteristics of the pressure field of the vortex itself and of the surrounding region. The interaction of a tropical cyclone and its environment, except as noted above, can usually be accounted for by a proper specification of the input parameters. The assignable parameters of the planetary boundary layer (PBL) formulation, namely planetary boundary layer depth (in this case 500 m) and stability (air-sea temerature -2 degree C) and of the sea surface roughness formulation, are the same as we have used in several recent studies of Gulf of Mexico hurricanes.

The Wave Hindcast Model

Background

The wave hindcast model adapted for this study is a so-called fully-discrete spectral wave model. That is, the wave spectrum is resolved in discrete frequency-direction bins, a grid of points is laid out to represent the basin of interest, and a solution is obtained based upon integration of the spectral energy balance equation, a process which successively simulates, at each model grid point, and for each time step, the physical processes of wave growth and dissipation (through the source terms of the energy balance) and wave propagation.

Three classes of spectral models are generally recognized. First-generation models (1G), such as the ODGP model (Cardone, Pierson, and Ward, 1976), are part of the family of fully-discrete spectral models originally proposed by Pierson, Tick, and Baer (1966). This type of model is characterized by a source-term formulation which does not include an explicit representation of conservative transfers of energy between spectral components, believed to be associated with resonant non-linear wave-wave interactions. Second-generation models (2G) were introduced to include at least a parametric representation of a wave-wave interaction source term, while third-generation (3G) models, only recently introduced, attempt to model the wave-wave interaction source term rigorously.

The formulation of the ODGP model has been described in detail in past studies, most recently in MacLaren (1985). The skill of the model has also been documented in numerous studies, including Reece and Cardone (1982), and more recently by Cardone and Greenwood (1987), wherein the characteristics of the model are compared to those of recent 2G and 3G models.

While a number of 2G models and the so-called 3G-WAM model (WAMD1 Group, 1988) have been demonstrated in some applications

to achieve hindcast skill comparable to the ODGP 1G model, no clear superiority of these later formulations has been established in the specification of storm peak wave heights in a storm at a site. For example, the 2G model developed at Oceanweather for an international wave model comparison program (SWAMP, 1985), and known as the SAIL model (Greenwood, Cardone, and Lawson, 1985), has been calibrated against the same data base used for the ODGP model, and validated against wave measurements in some of the same validation storms used in this study with good skill, but only in a deep water mode. The 3G-WAM model was not considered for this study. It has been tested against three Gulf of Mexico hurricanes (WAMDI Group, 1988) and provides the same skill in specification of peak wave height and period as provided by ODGP when driven by identical wind fields, yet 3G-WAM requires a factor of 5 or more computer time than ODGP. The 3G-WAM model was also applied in a deep water mode for those tests. The shallow water version of 3G-WAM has not been tested against a wide range of wave regimes with any real success. ODGP was also applied in the recent Joint Industry Program - GUMSHOE including shallow water mechanisms.

Grid System

The wave model grid system is shown in Figure C1. The model has basically the following attributes:

grid domain: 18.3386-30.4554 degrees North latitude
97.7000-80.2200 degrees West longitude
grid spacing: 11.91 n. mi. at north edge, 13.09 n. mi. at south edge
projection: direct Mercator
time step: 30 minutes (15 minutes grow, 30 minutes propagation, 15 minutes grow)
angular spectral resolution: 24 directions, 15-degree bandwidth
frequency spectral resolution: 15 frequencies, binned as given in Table C1
spectral growth algorithms: ODGP2 (deep water); ODGPS (shallow water)
propagation: interpolatory, deep water and shallow water, great circle effects and refraction and shoaling included.

Basic Propagation Scheme

The propagation scheme is basically interpolatory. Convergence of meridians (great circle effects) is modelled. This scheme, whose dispersion properties are described in detail by Greenwood, Cardone, and Lawson (1985), has been used with success by Oceanweather in its wave models since it was first developed and described by Greenwood and Cardone (1977).

Deep-Water Source-Term Algorithms

Two variants of the ODGP spectral/growth model were applied in this model, one for deep water grid points, the second at shallow water grid points (points with water depth less than 200 m.)

The original ODGP algorithm was implemented in a wave model as a subroutine called CMPE24. While a few changes in the code and numerics of this subroutine have been effected since the original version was developed in the ODGP-Analysis Phase (ODGP-AP), the calibration of this spectral growth/ dissipation algorithm and the quantitative behavior of hindcasts of tropical and extratropical cyclones have not changed. The algorithm is described in most detail in the original ODGP-AP report (proprietary to ODGP-AP participants) and most recently in the public domain in MacLaren (1985).

A slightly modified version of the ODGP spectral/growth algorithm (ODGP2) was developed in 1983, and has been used operationally since then. The subroutine which implements the modified algorithm is called CMPE27. The changes affect only the behavior of the high-frequency part of the wave spectrum, and were made in order to make the so-called saturation range of the spectrum more responsive to the stage of wave development. CMPE27 differs from CMPE24 in the following three particulars:

1. The integrated band (0.24167 hz to 3.0 hz) is not automatically saturated by the local wind, but is subject to grow, propagate, and dissipate.

2. The f-4 range in the representation of the high-frequency tail of saturated spectrum in the ODGP algorithm is not used, as an f-5 representation throughout the tail is assumed.

3. Phillips' "constant" is allowed to float as a function of sea state, following Resio's (1981) correlation

Shallow-Water Propagation and Depth Grid

The propagation scheme of the shallow-water model is analogous to that used in the deep-water model. In the construction of the table of propagation coefficients at each grid point and for each frequency and direction bin, a numerical shallow-water tracing program is used instead of the simple spherical trigonometric calculation of the ray path in the deep-water program. Effects of shoaling and refraction over an irregular bathymetry as resolved on the model grid are included.

The depth field was derived from the digital data base produced at the U.S. National Geophysical Data Center (NGDC), known as ETOPO5. That data base is stored on one 6250 bpi

magnetic tape and resolves the global topography/bathymetry on a 5 minute grid. Previous studies have noted deficiencies in ETOPO5 in the vicinity of steep bottom slopes (NGDC are aware of the problem and are working on a revised ETOPO5), so prior to use, we corrected parts of the ETOPO5 grid which represents the Gulf. By displaying and contouring the ETOPO5 grid array, four areas in the Gulf of Mexico were identified as having been contaminated by NGDC's interpolation problem: (1) south and central Florida west coast; (2) both sides of the Mississippi Delta; (3) Campeche Bank; (4) offshore southeast Texas (25 to 27 degrees North). The correction procedure was simple. For the affected parts of the grid, depth values were read off (visual interpolation) hand contoured depth fields on the USGS 1100 series charts at ETOPO5 grid points, and the new values simply replaced the ETOPO5 values.

Depths were assigned to the wave model grid by simply averaging all ETOPO5 grid depths which lay within a grid box defined by each point. Since there are typically 6 or 9 ETOPO5 depths within a rectangle represented by each grid point, the binning effects considerable smoothing of the depth field, and no further smoothing was applied. At a few points near shore, the depth was limited to a minimum depth of 7.5 m, to avoid computational problems with the ray-tracing routine. Figure C2 shows contours of the depth field as resolved on the wave grid.

The assignment of grid points to land or sea was made by digitizing the coastline off standard charts, plotting the digitized coastline together with the entire grid array, then manually reading off those points which lie on land. The grid was then replotted to check the assignments. After deletion of land points, the grid contains 2969 active points.

Shallow Water Source Terms

A shallow-water version of the ODGP spectral growth algorithm (CMPE24/ CMPE27) has been under development since 1984. The first significant test of the algorithm against field measurements was made during the Canadian Atlantic Storms Project (CASP), which was carried out on the Canadian Scotian Shelf in the period January - March 1986. The performance of the model hindcasts, which were carried out as part of a real-time analysis/ forecast system, exceeded that of the several other operational and research shallow-water models which also participated in the experiment (Eid and Cardone, 1987).

The modifications of the ODGP deep-water routine spectral/growth subroutine made to extend the model to shallow water are:

1. transformation of the fully-developed Pierson-Moskowitz form to shallow water;

2. calculation of an explicit attenuation associated with bottom friction, which is modelled after the comprehensive treatment of Grant and Madsen (1982);

3. calculation of the exponential growth rate using the shallow-water celerity;

4. adoption of wave-number scaling of the high-frequency saturation range of the spectrum, with the equilibrium range coefficient expressed as a function of the stage of wave development.

5. modification of the equilibrium range treatment to include a dependence on significant wave steepness.

Numerical Storm Surge/Current Model

Oceanweather have applied, in several recent studies, a state-of-the-art current/surge model in problems of this type, including applications in the South China Sea and Bering Seas. The particular model adapted was developed at Texas A&M under the direction of Professor R. O. Reid, and is described in detail by Bunpapong, Reid, and Whitaker (1985). The model differs from most previous surge models, since it was designed for basin-wide simulations (such as Bunpapong's initial treatment of the problem of hurricane forcing on a grid covering the entire Gulf of Mexico), rather than models restricted to limited stretches of the continental shelf.

The theoretical formulation of the model is based upon the vertically-integrated momentum and conservation equations for quasi-hydrostatic large-scale disturbances in a basin of variable depth. The model is formulated to handle up to two layers, but was used in the single layer mode in this study.

The normal mode equations are solved by finite-difference on a time-marching model, employing an alternating direction implicit differencing scheme. The model is quasi-linear, and tides are not included. Variable bathymetry, variable coriolis parameter, and variable atmospheric pressure are modelled, however. The inverted barometric effect is therefore implicit in the model, and is automatically included in the modelled water-level anomalies. Surface-pressure anomalies are also used to stipulate barotropic height anomalies on the open boundaries of the model. A no-flow condition is taken at all solid boundaries.

The surge model is forced by specification of time histories of surface pressure and wind stress at the top boundary, and bottom friction at the bottom boundary.

The surge model incorporates a quadratic bottom-stress law with a constant friction coefficient. Bunpapong, Reid, and Whitaker (1985) used a coefficient of 2.5 E-3 in their Gulf of Mexico hurricane simulations. This was reduced to 1.0 E-3 in this study, which is at the lower end of the range of friction factors commonly adopted in models of this type. This value was used because we have found that when driven by wind stresses produced by our wind models, more accurate open coast surges were provided with the reduced friction factor.

The model was adapted to the Gulf on a grid covering the same domain as that of the wave model. However, the grid system, shown in Figure C3, is slightly different with points spaced 10 minutes in latitude and 10.5 minutes in longitude. Therefore, the surge model grid points and wave model grid points do not coincide; however, since the resolutions are comparable, it is easy to match grid points in order to produce a single archive of hindcast results referenced to the wave model grid point location. (The location of a surge model output point is somewhat ambiguous anyway, since the grid is staggered such that the x-component of current, the y-component of current and the water levels are specified at a different location within a grid box). Parts of the southern and eastern boundary are treated as open non-reflecting boundary conditions. The model time step is 15 minutes. Wind stresses and sea-level pressures are provided to the current/surge model at 30-minute intervals and interpolated linearly to 15 minutes.

References

Borgman, L. E. 1973. Probabilities for the highest wave in a hurricane. J. Waterways, Harbors and Coastal Engineering Division, ASCE, 185-207

Bunpapong, M., R. Reid, and R. Whitaker. 1985. An investigation of hurricane-induced forerunner surge in the Gulf of Mexico. Prepared for U.S. Army Engineer Waterways Experiment Station and the Coastal Engineering Research Center, Contract DACW39-82-K-0001, by Dept. of Oceanography, Texas A&M University, Ref. 85-2-T. Research conducted through Texas A&M Research Foundation, Project 4667, College Station, TX.

Cardone, V. J., W. J. Pierson, and E. G. Ward. 1976. Hindcasting the directional spectra of hurricane generated waves. J. of Petrol. Tech., 28, 385-394.

Cardone, V. J., D. B. Ross, and M. Ahrens. 1978. An experiment in forecasting hurricane generated sea states. In Proceedings of 11th Technical Conference on Hurricanes and Tropical Meteorology, Dec. 13 - 16, 1977, Miami Beach, Florida. American Meteorological Society, Boston, MA.

Cardone, V. J., C. V. Greenwood, and J. A. Greenwood. 1979. A unified program for the specification of hurricane boundary layer winds over surfaces of specified roughness. Final Report, Contract DACW-39-78-C-0100. Dept. of the Army, Waterways Experiment Station, Corps of Engineers, Vicksburg, MS.

Cardone, V. J. and D. B. Ross. 1979. State-of-the-art wave prediction methods and data requirements. Ocean Wave Climate, Edited by M. D. Earle and A. Malahoff. Plenum Publishing Corp., 1979, 61 - 91.

Cardone, V. J. and J. A. Greenwood. 1987. A sensitivity study of spectral wave growth algorithms. ESRF Report 065. Proceedings of the International Workshop on Wave Hindcasting and Forecasting, September 23-26, 1986. Halifax, NS, 133-143.

Eid, B. M., V. J. Cardone, J. A. Greenwood, and J. Saunders. 1987. Real-time spectral wave forecasting model test during CASP. ESRF Report 065. Proceedings of the International Workshop on Wave Hindcasting and Forecasting, September 23-26, 1986, Halifax, NS, 183-195.

Forristall, G. Z., R. C. Hamilton, and V. J. Cardone. 1977. Continental shelf currents in tropical storm Delia:

Observations and theory. J. of Phys. Oceanography, 7, 532 - 546.

Forristall, G. Z., E. G. Ward, V. J. Cardone, and L. E. Borgman. 1978. The directional spectra and kinematics of surface waves in Tropical Storm Delia. J. of Phys. Oceanography, 8, 888 - 909.

Forristall, G. Z., E. G. Ward, and V. J. Cardone. 1980. Directional wave spectra and wave kinematics in hurricanes Carmen and Eloise. 17th International Conference on Coastal Engineering, Sydney, Australia.

Grant, W. D., and O. S. Madsen, 1982. Movable bed roughness in unsteady oscillatory flow. J. of Geophys. Res. 87, C1, 469-481.

Greenwood, J. A. and V. J. Cardone. 1977. Development of a global ocean wave propagation algorithm. Final Report to U.S. Navy Fleet Numerical Weather Central, Monterey, California, Contract N-00228-76-C-3081.

Greenwood, W. J., V. J. Cardone, and L. M. Lawson. 1985. Intercomparison test version of the SAIL wave model. In Ocean Wave Modeling. The SWAMP Group. Plenum Press, New York, 221-233.

Haring, R. E. and J. C. Heideman. 1978. Gulf of Mexico rare wave return periods. OTC Paper 3280.

Maclaren Plansearch Ltd. 1985. Evaluation of the spectral ocean wave model (SOWM) for supporting real-time wave forecasting in the Canadian east coast offshore. Contractor's report submitted to the Atmospheric Environment Service, Environment Canada. Downsview, Ontario

Pierson, W. J., L. J. Tick, and L. Baer. 1966. Computer-based procedures for preparing global wave forecasts and wind field analysis capable of using wave data obtained by a spacecraft. In: Sixth Naval Hydrodynamic Symposium, ACRO-136. Office of Naval Research, Dept. of the Navy, Washington, D.C., 499-532.

Reece, A. M. and V. J. Cardone. 1982. Test of wave hindcast model results against measurements during four different meteorological systems. OTC #4323, 14th Annual OTC (Offshore Technology Conference), Houston, Texas, May 3 - 6.

Ross, D. B. and V. J. Cardone. 1978. A comparison of parametric and spectral hurricane wave prediction products.

Turbulent Fluxes through the Sea Surface, Wave Dynamics, and Prediction, A. Favre and K. Hasselmann, editors, 647 - 665.

SWAMP (The Sea Wave Modeling Project) Group (24 authors). 1985. Ocean Wave Modeling. Plenum Press, New York, NY.

WAMDI Group. 1988. The WAM model- a third generation ocean wave prediction model. J. of Phys. Oceanog. 18, 1776-1810.

Ward, E. G. 1974. Ocean Data Gathering Program - An Overview. OTC (Offshore Technology Conference) Paper No. 2108-B, Presented at the Sixth Annual OTC, Houston, TX, May 6 - 8, 1974.

Table C1

Frequency bands and bandwidths of ODGP wave model

BAND	NOMINAL FREQUENCY		BANDWIDTH
1	14/360 hz =	.03889 hz	1/180 hz
2	16/360	.04444	1/180
3	18/360	.05000	1/180
4	20/360	.05556	1/180
5	22/360	.06111	1/180
6	24/360	.06667	1/180
7	26/360	.07222	1/180
8	29/360	.08056	1/ 90
9	33/360	.09167	1/ 90
10	37/360	.10278	1/ 90
11	42/360	.11667	1/ 60
12	48/360	.13333	1/ 60
13	57/360	.15833	1/ 30
14	75/360	.20833	1/ 15
15	111/360	.30833	2/ 15

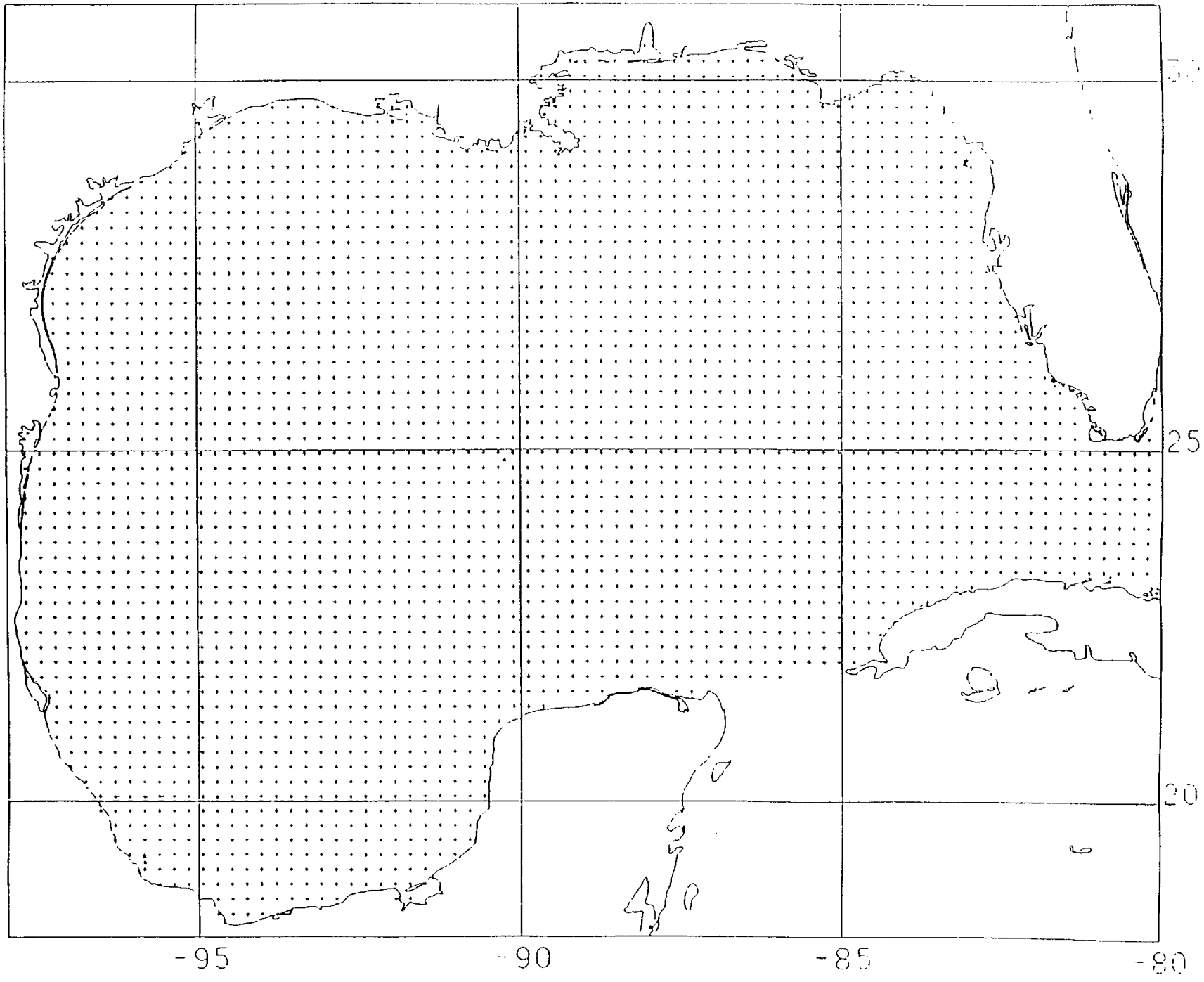

Figure C1 Wave hindcast model grid system.

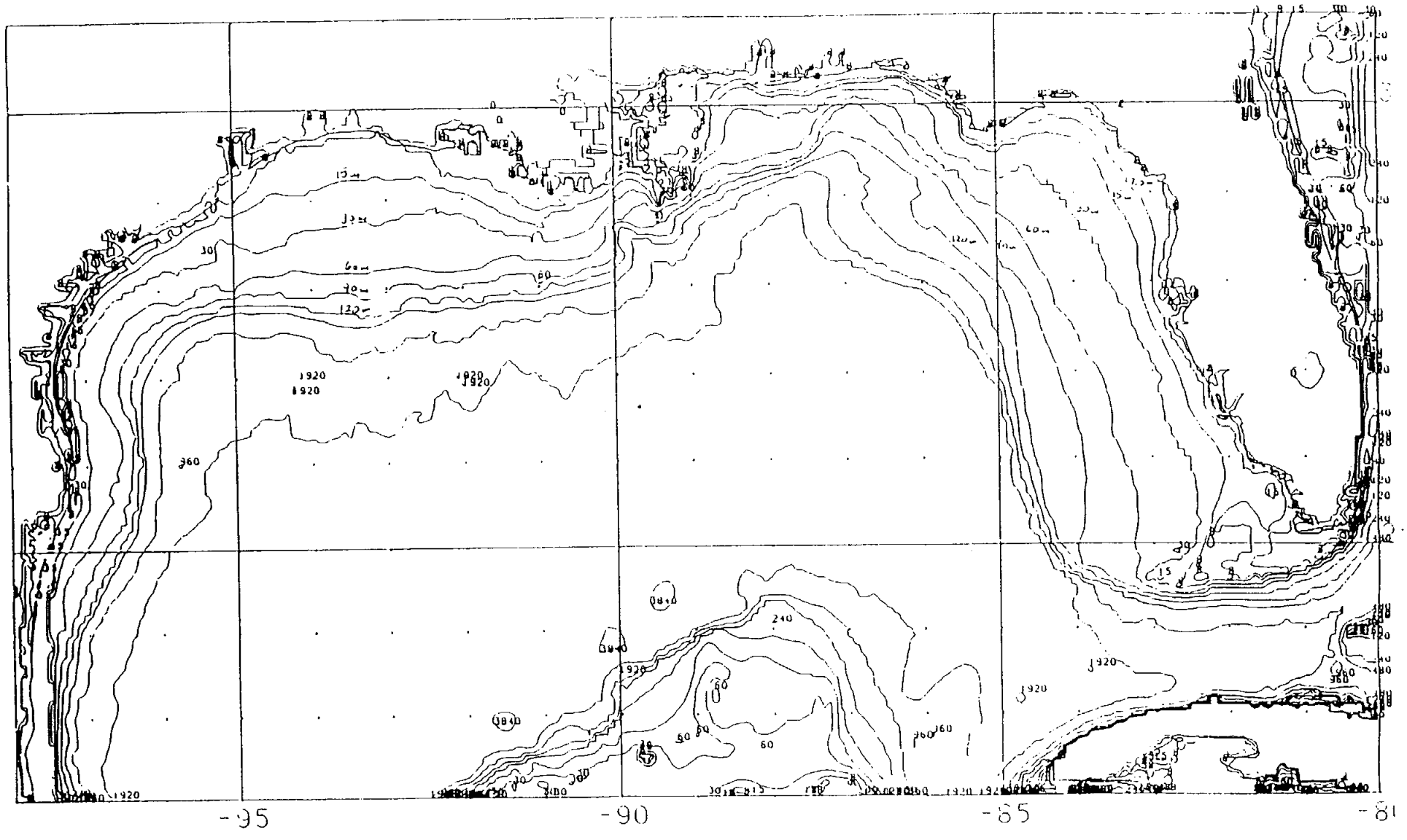

Figure C 2 Contours of depth field (meters) as resolved on GUMSHOE wave model grid.

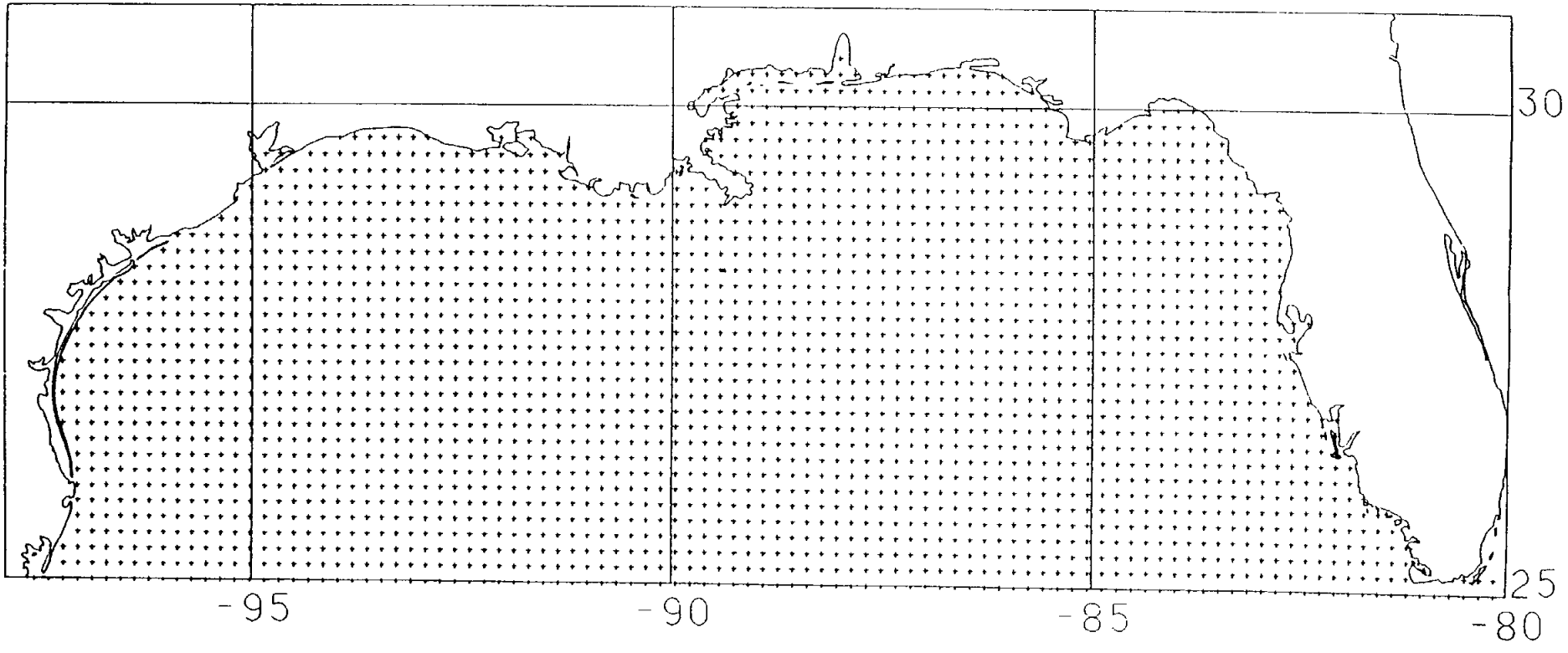

Figure C 3 Northern half of surge model grid system. (water level grid point shown)

Attachment D

Conventional "wind barb" representation of the surface wind field in Hurricane Andrew at 3-hourly intervals on the large domain. Winds are plotted at alternate rows and columns of grid points on the wave model grid. Areas devoid of winds lie outside the domain of the numerical vortex wind model used for the hindcast. Representation of speed is flag: 50 knots; each full barb: 10 knots, each half barb: 5 knots.

Winds plotted represent 60-minute average winds at an elevation of 20 meters. For average winds at 10 meters reduce speeds by about 8%. For other typical averaging intervals the 1-hour average wind speed may be increased by the following factors:

10 minute average	1.09
1 minute average	1.22
peak gust	1.53

Hurricane ANDREW 1992

92082412

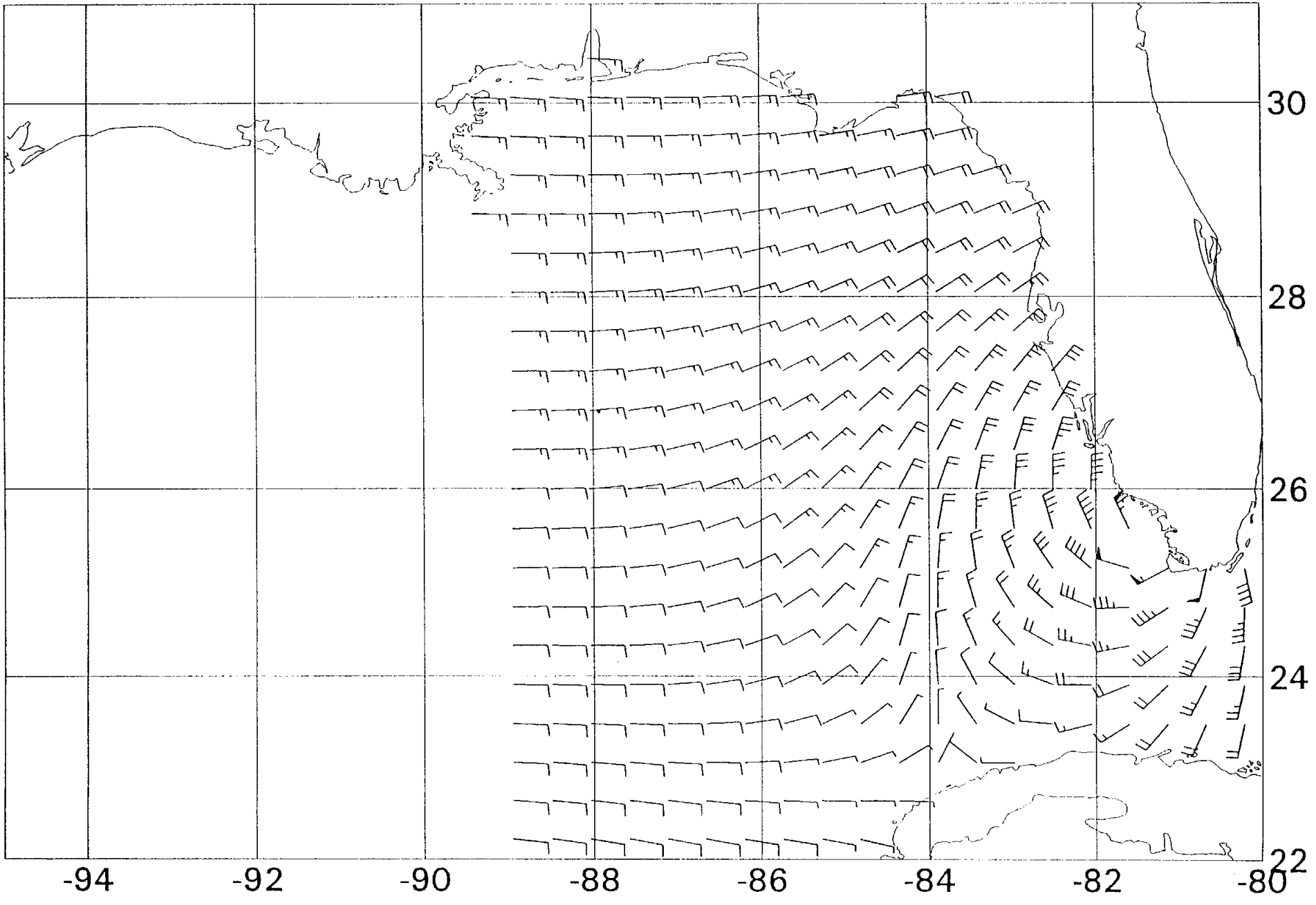

Hurricane ANDREW 1992

92082415

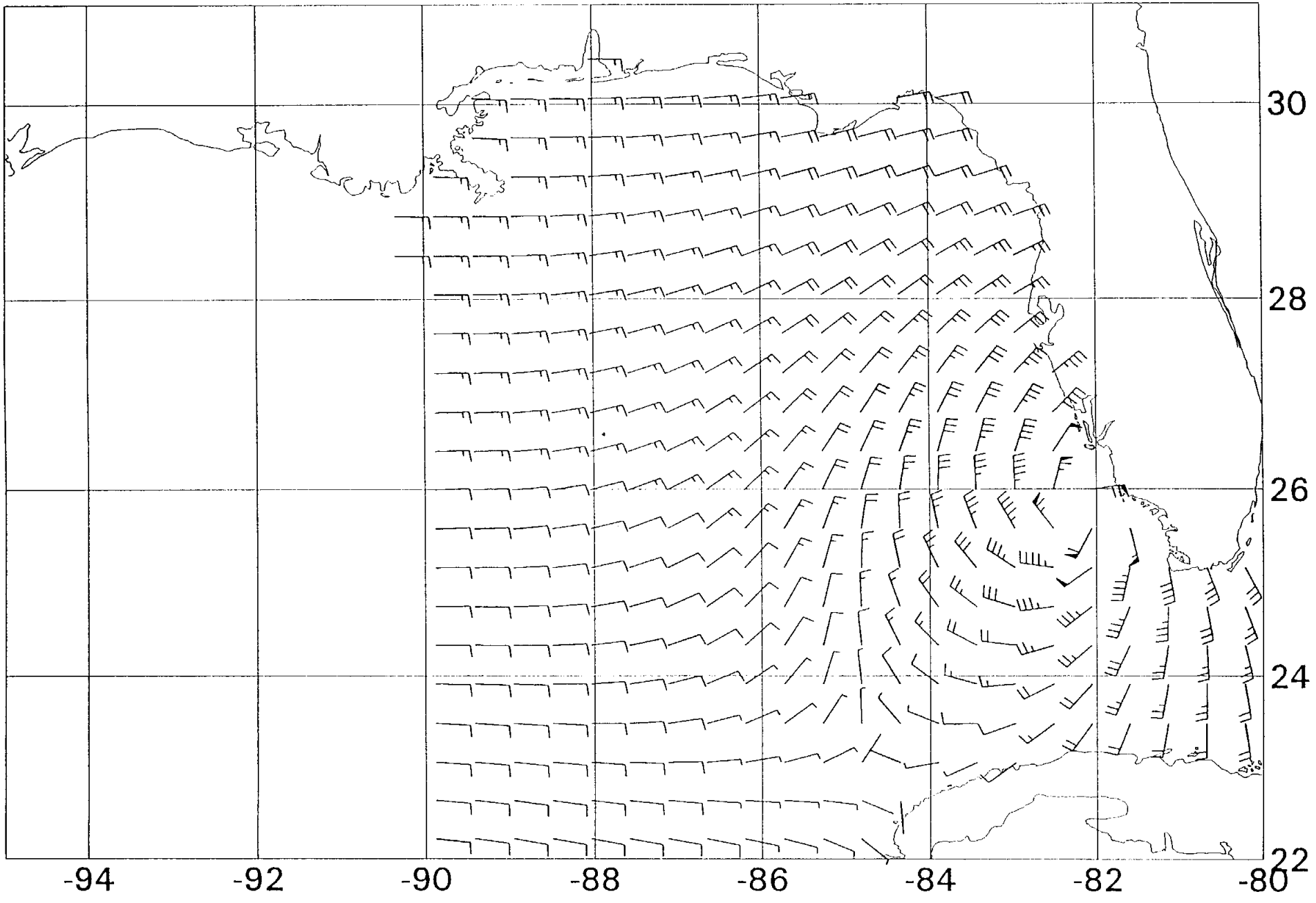

Hurricane A[illegible]DREW 1992

92082418

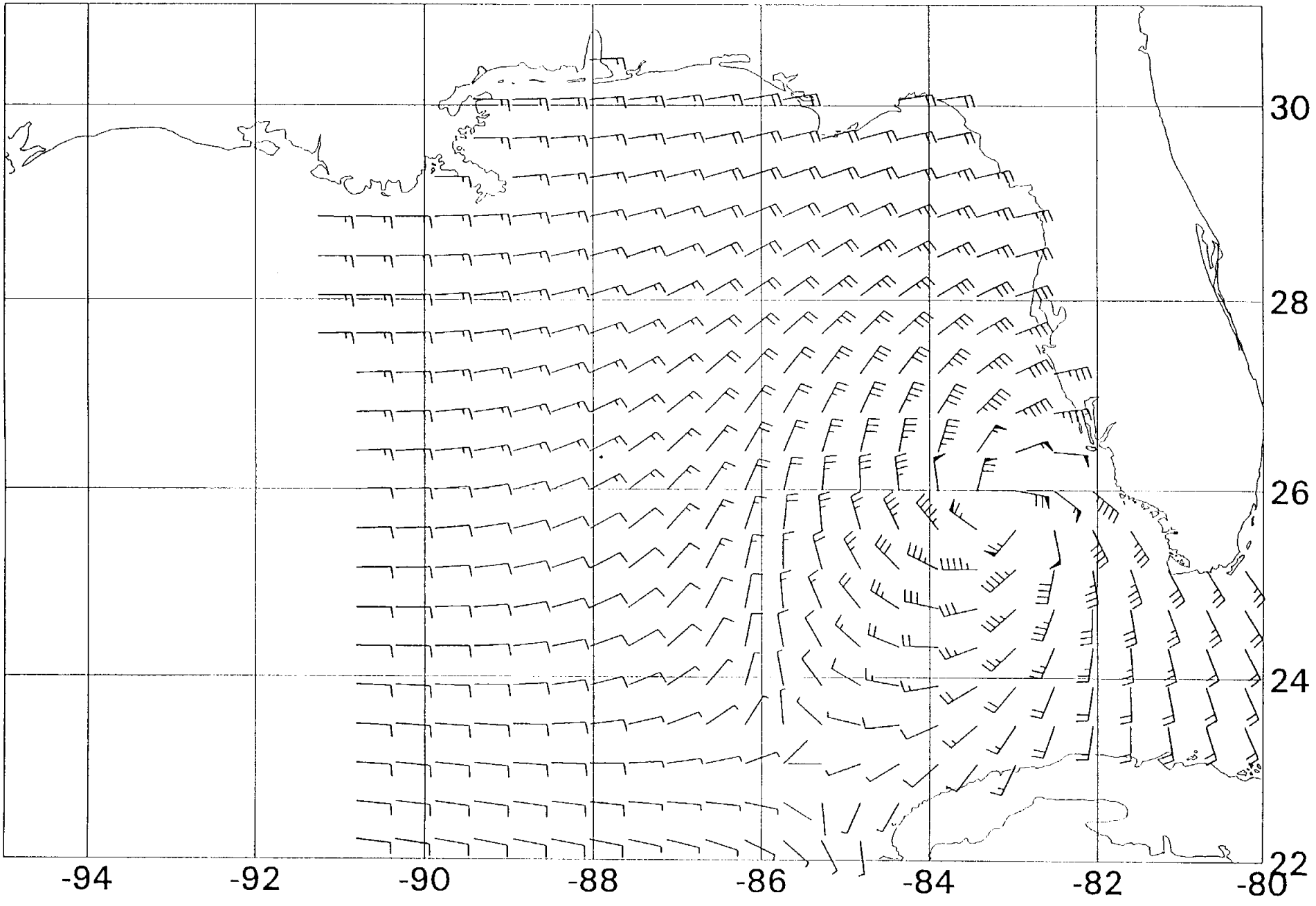

Hurricane ANDREW 1992

92082421

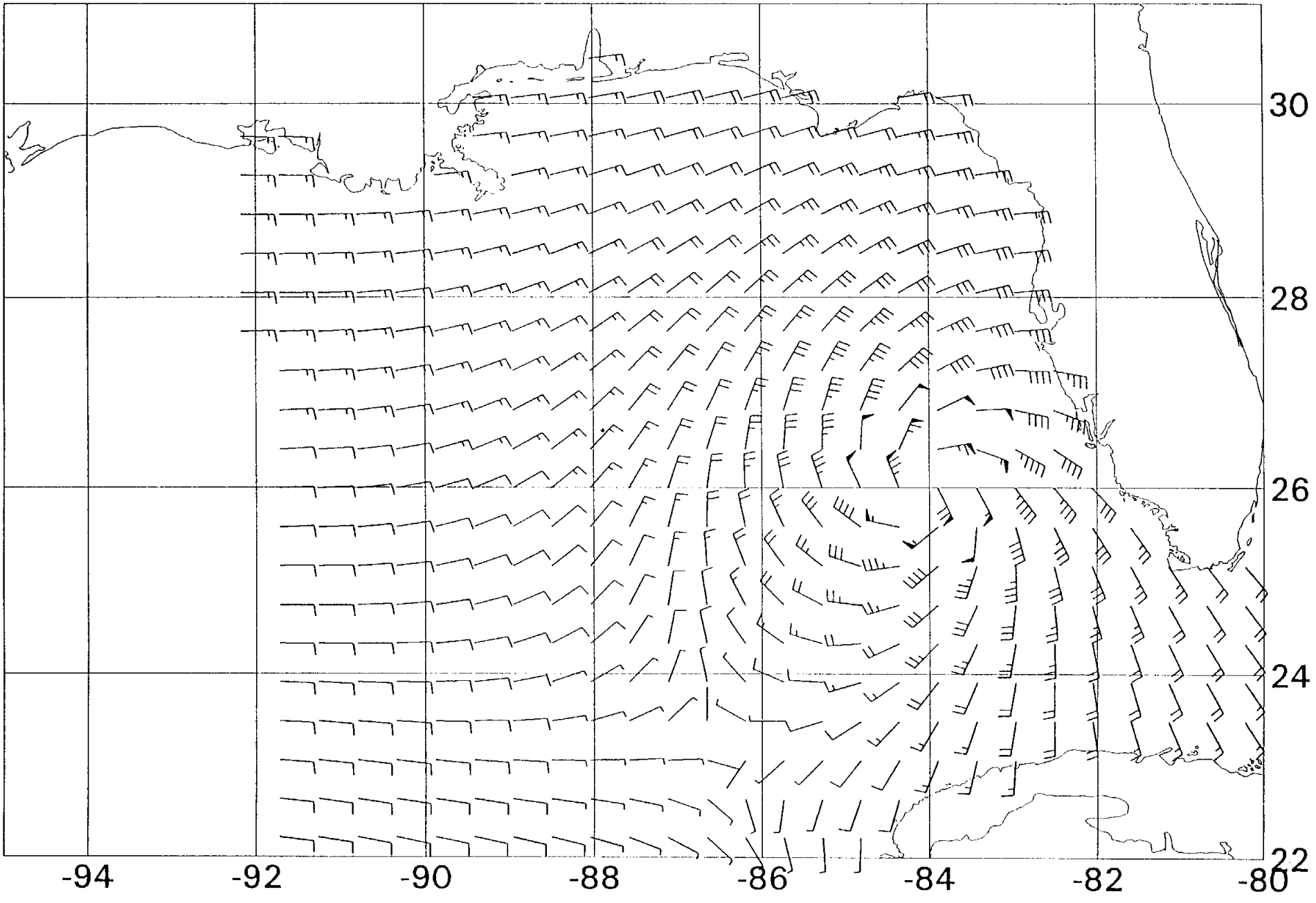

Hurricane ANDREW 1992

92082500

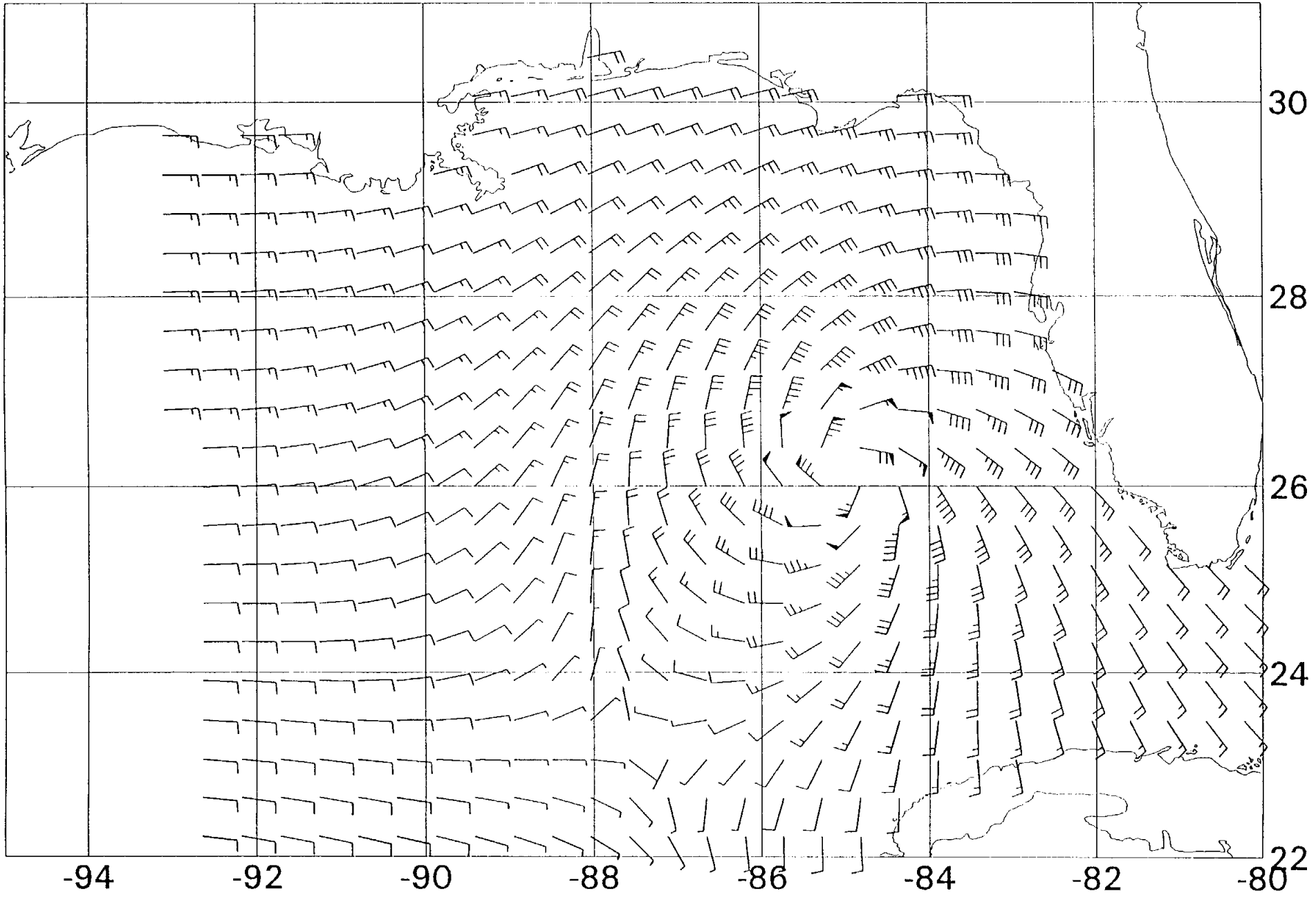

Hurricane ANDREW 1992

92082503

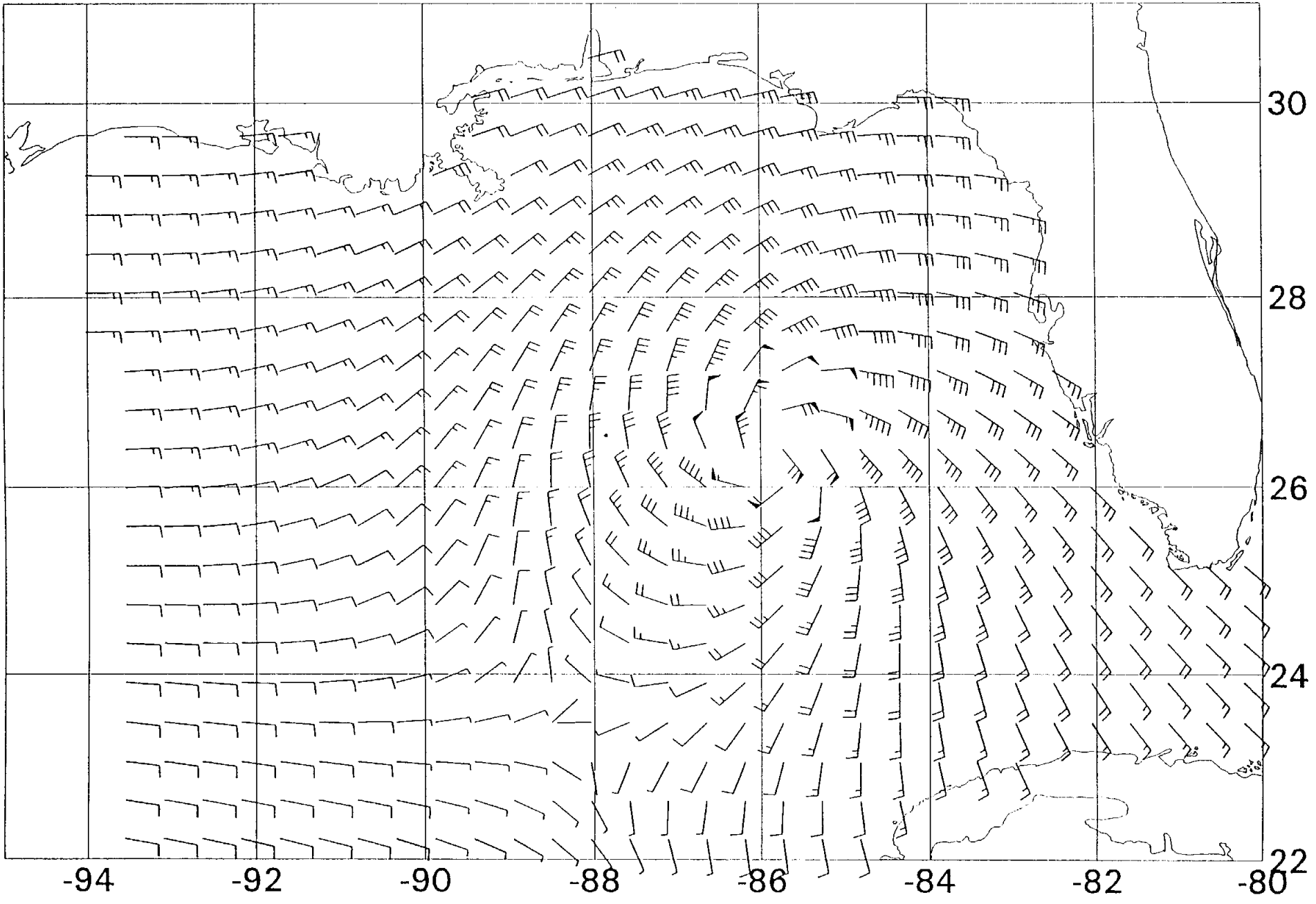

Hurricane ANDREW 1992

92082506

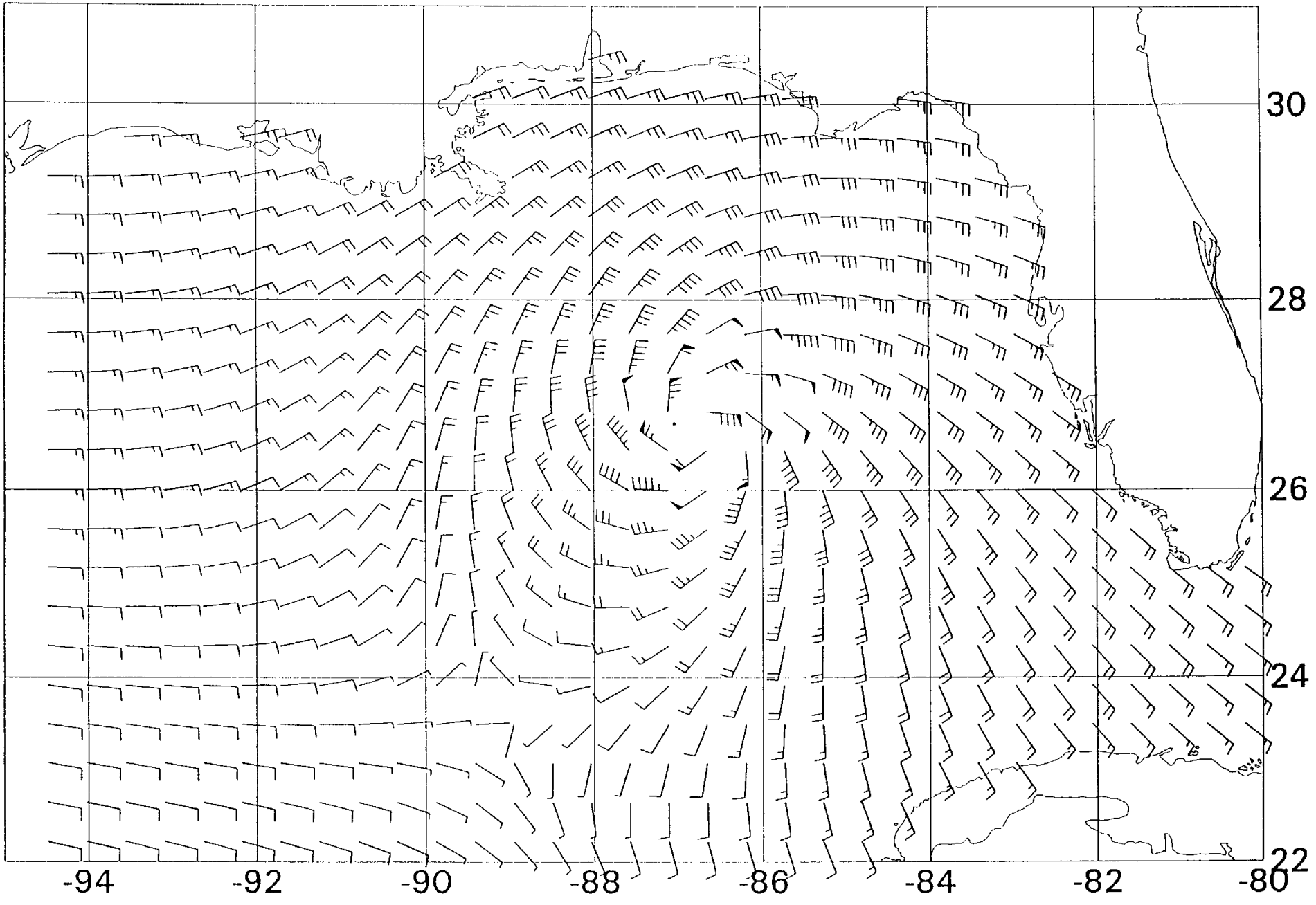

Hurricane A( )REW 1992

92082509

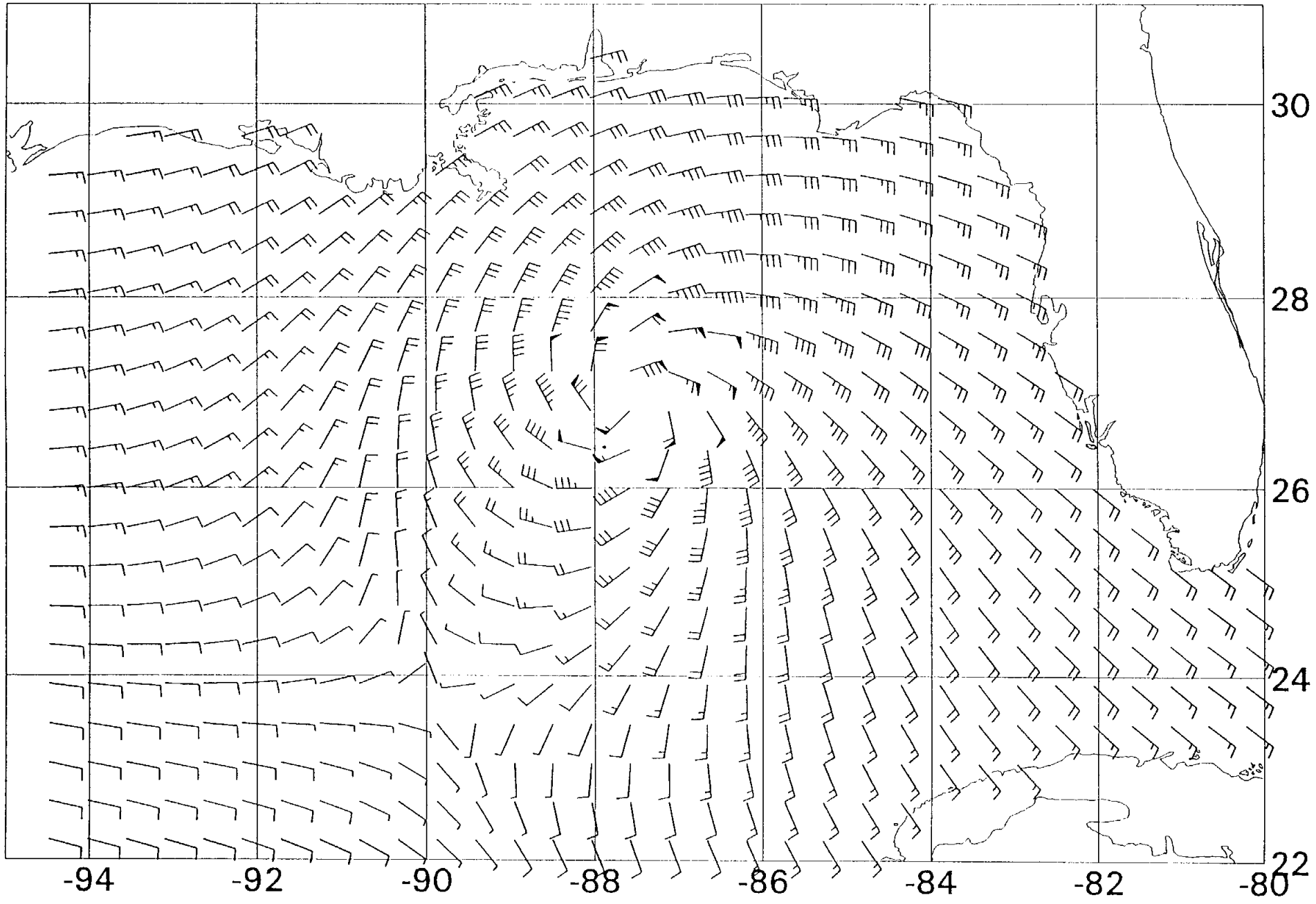

Hurricane ANDREW 1992

92082512

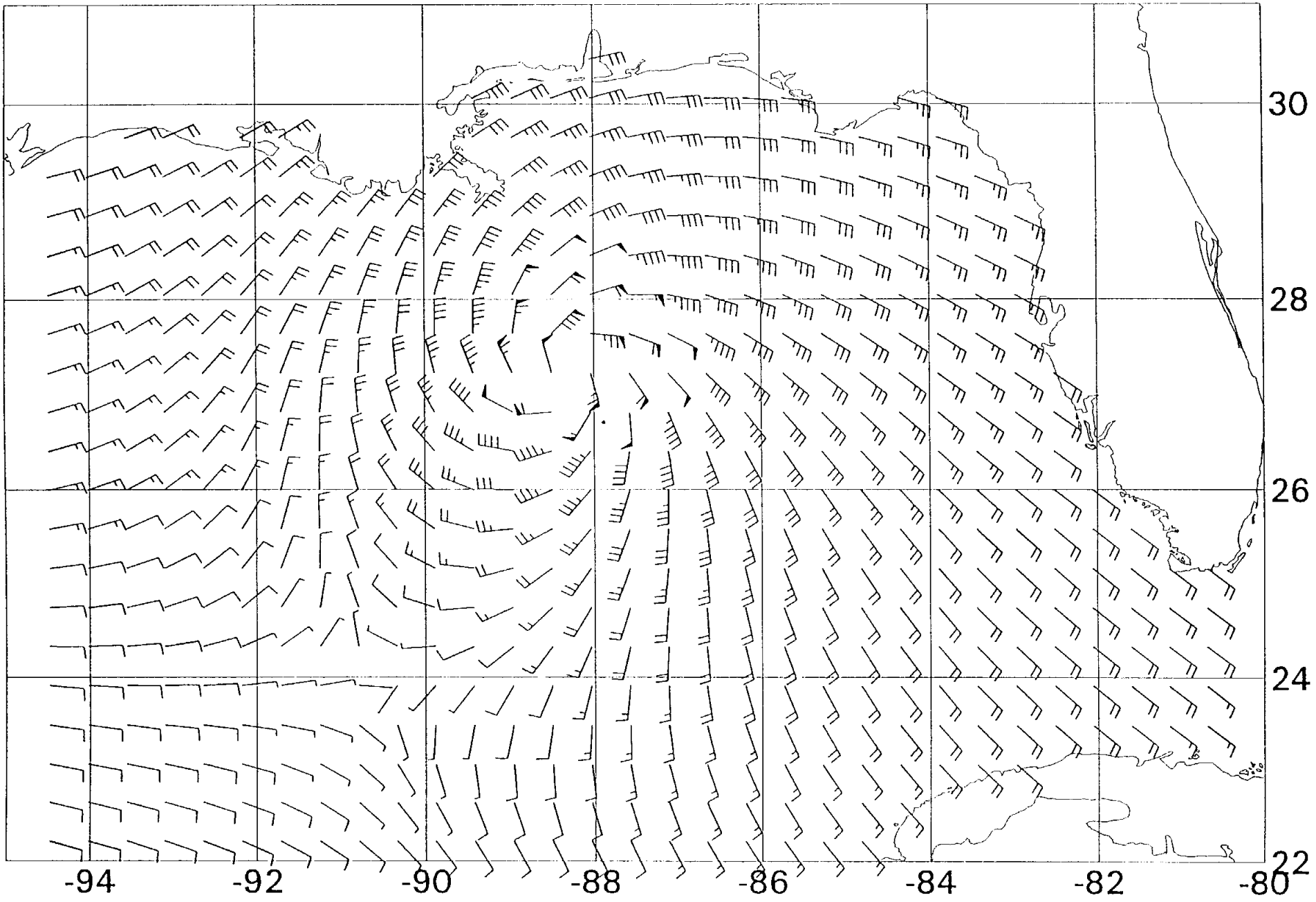

Hurricane A( )REW 1992

92082515

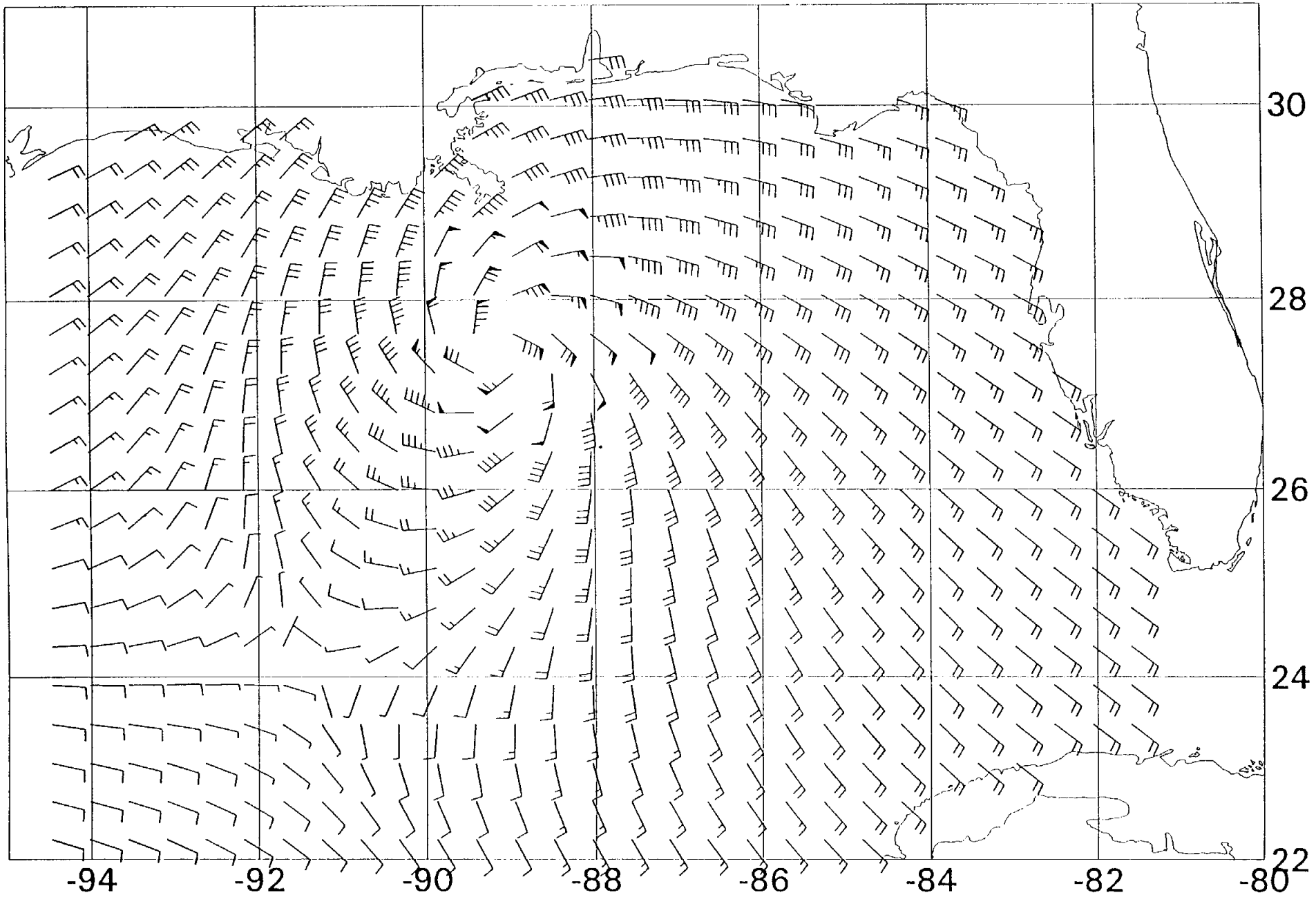

Hurricane A(DREW 1992

92082518

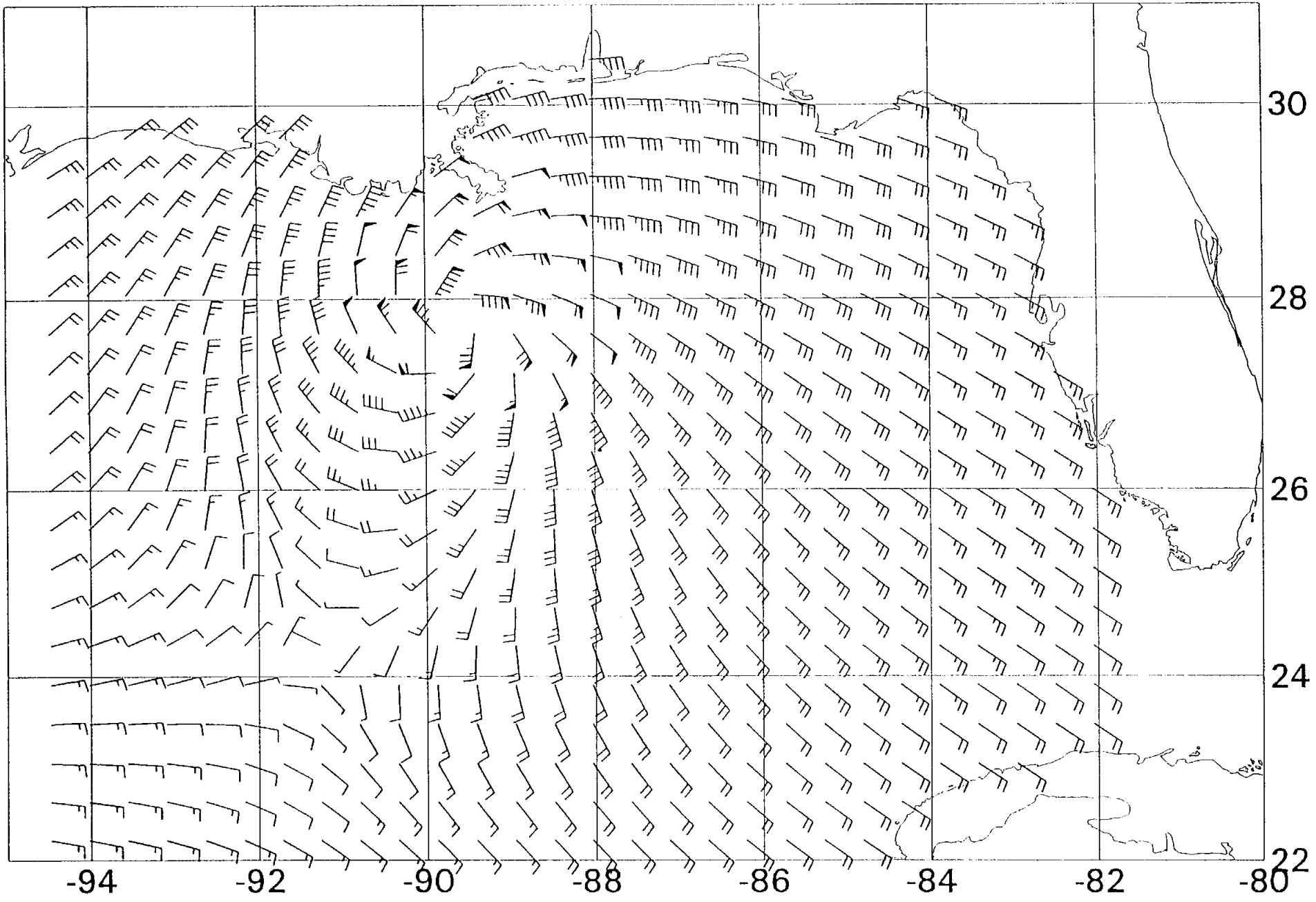

Hurricane ANDREW 1992

92082521

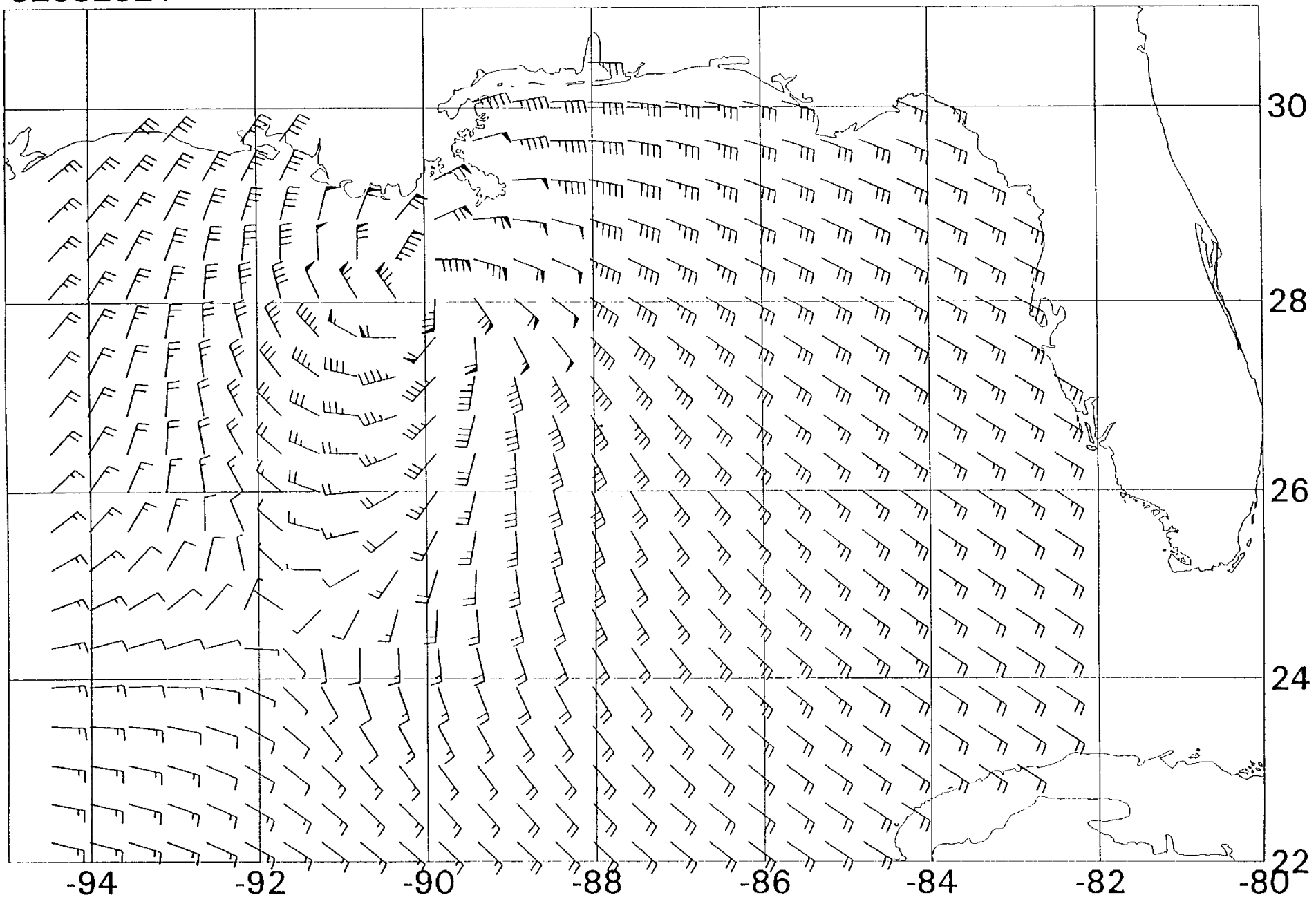

Hurricane A[illegible]DREW 1992

92082600

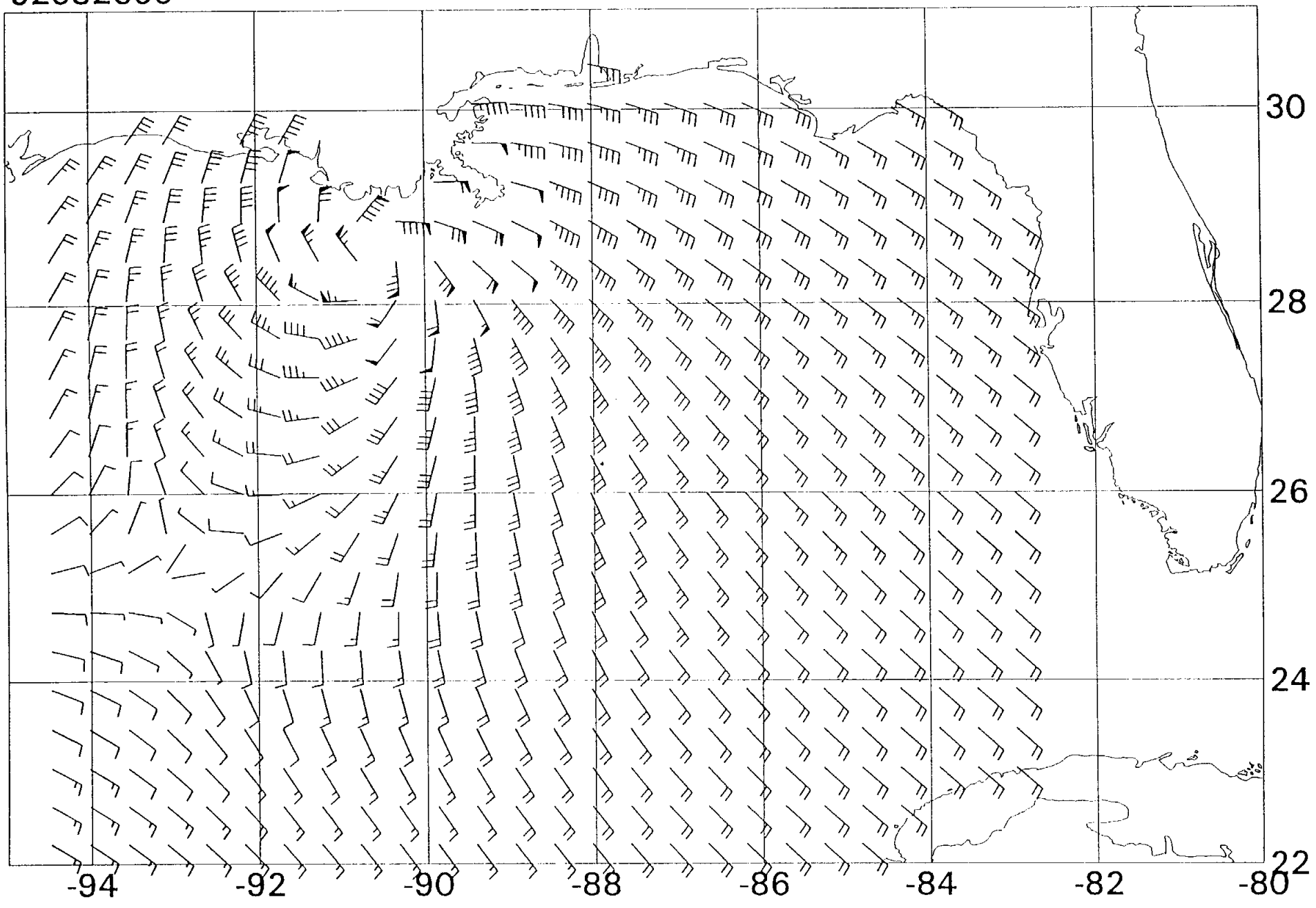

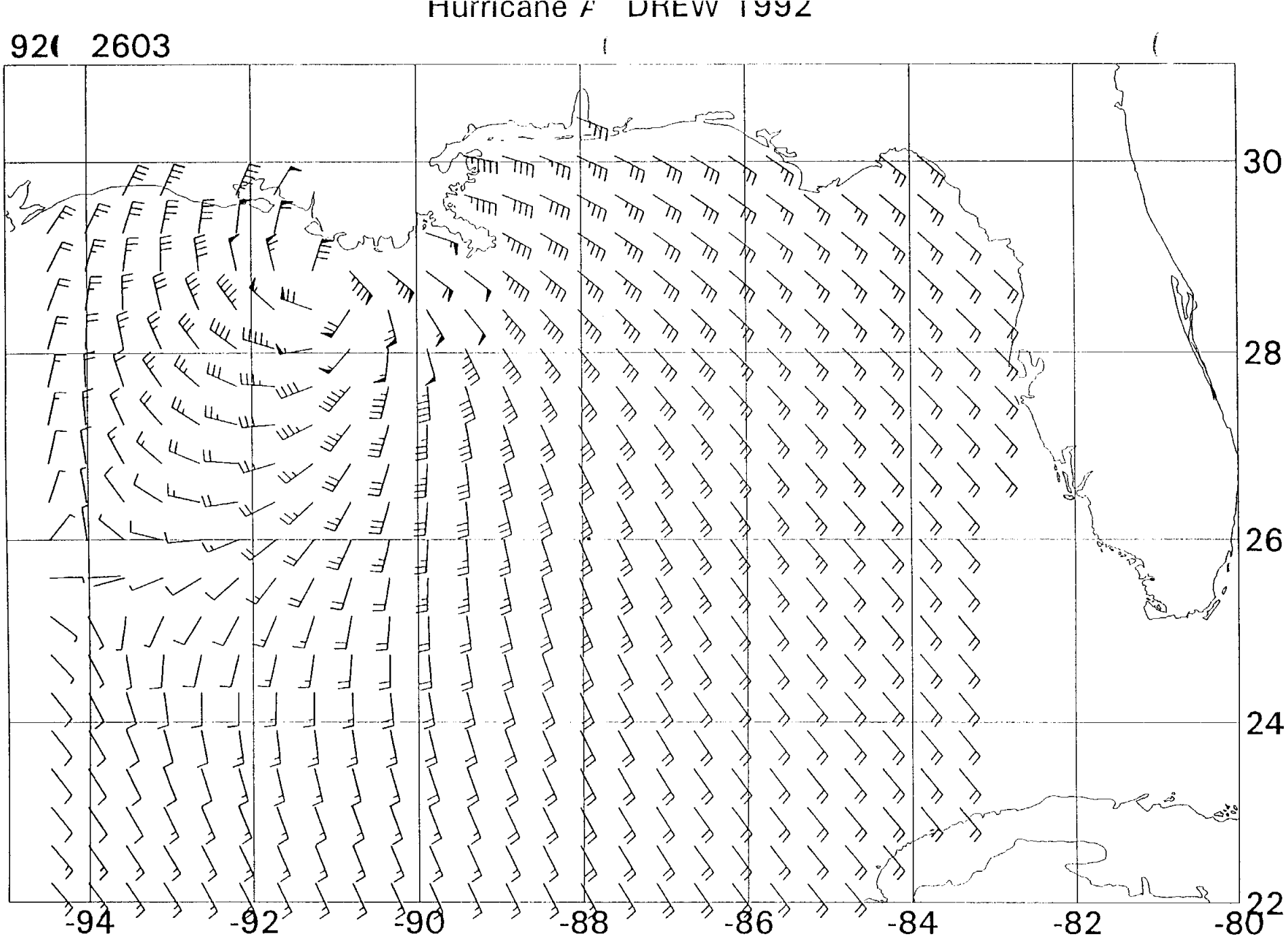
Hurricane ANDREW 1992
92(2603
30
28
26
24
22
-94
-92
-90
-88
-86
-84
-82
-80

Hurricane A DREW 1992

92082606

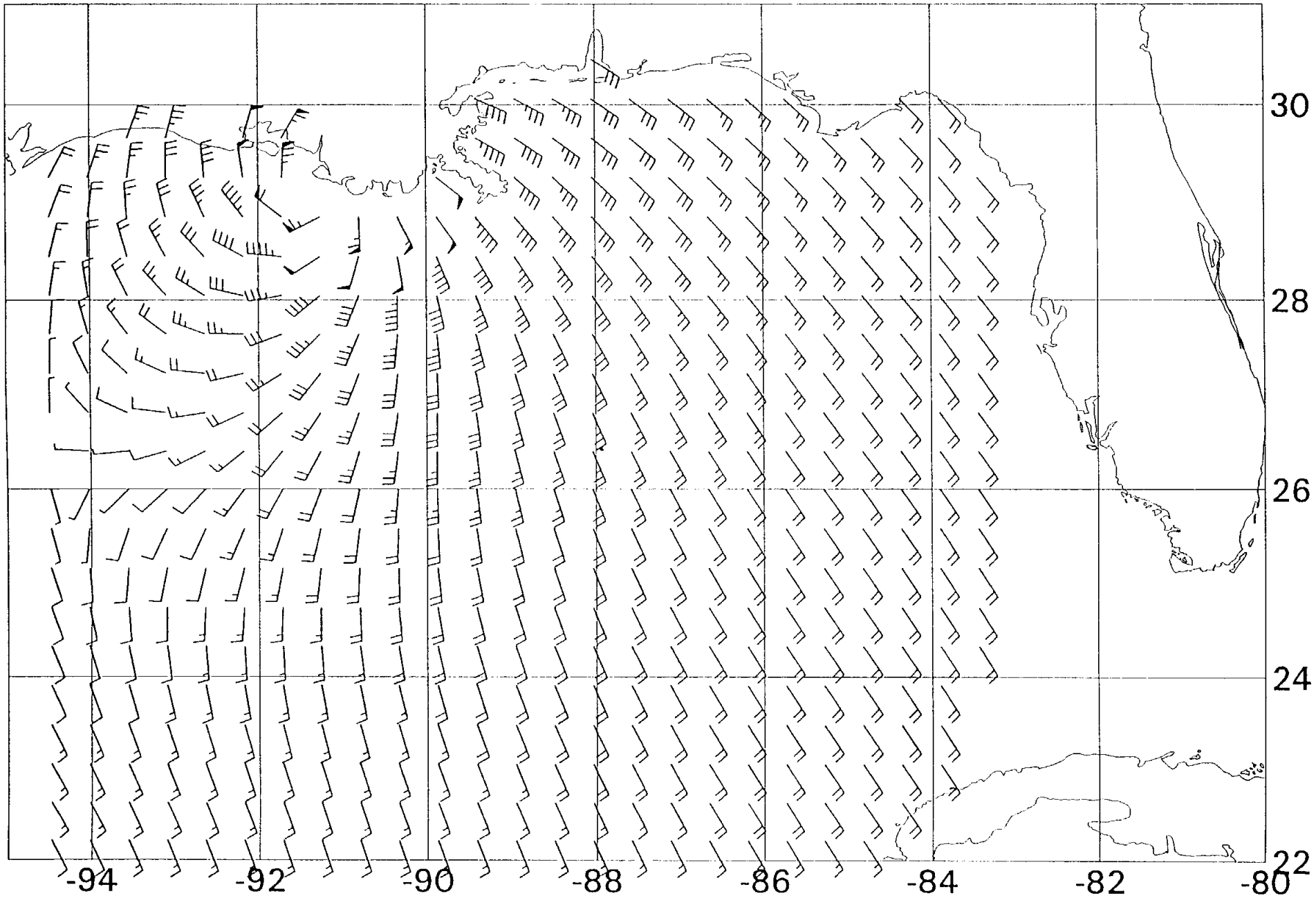

Hurricane ANDREW 1992

92082609

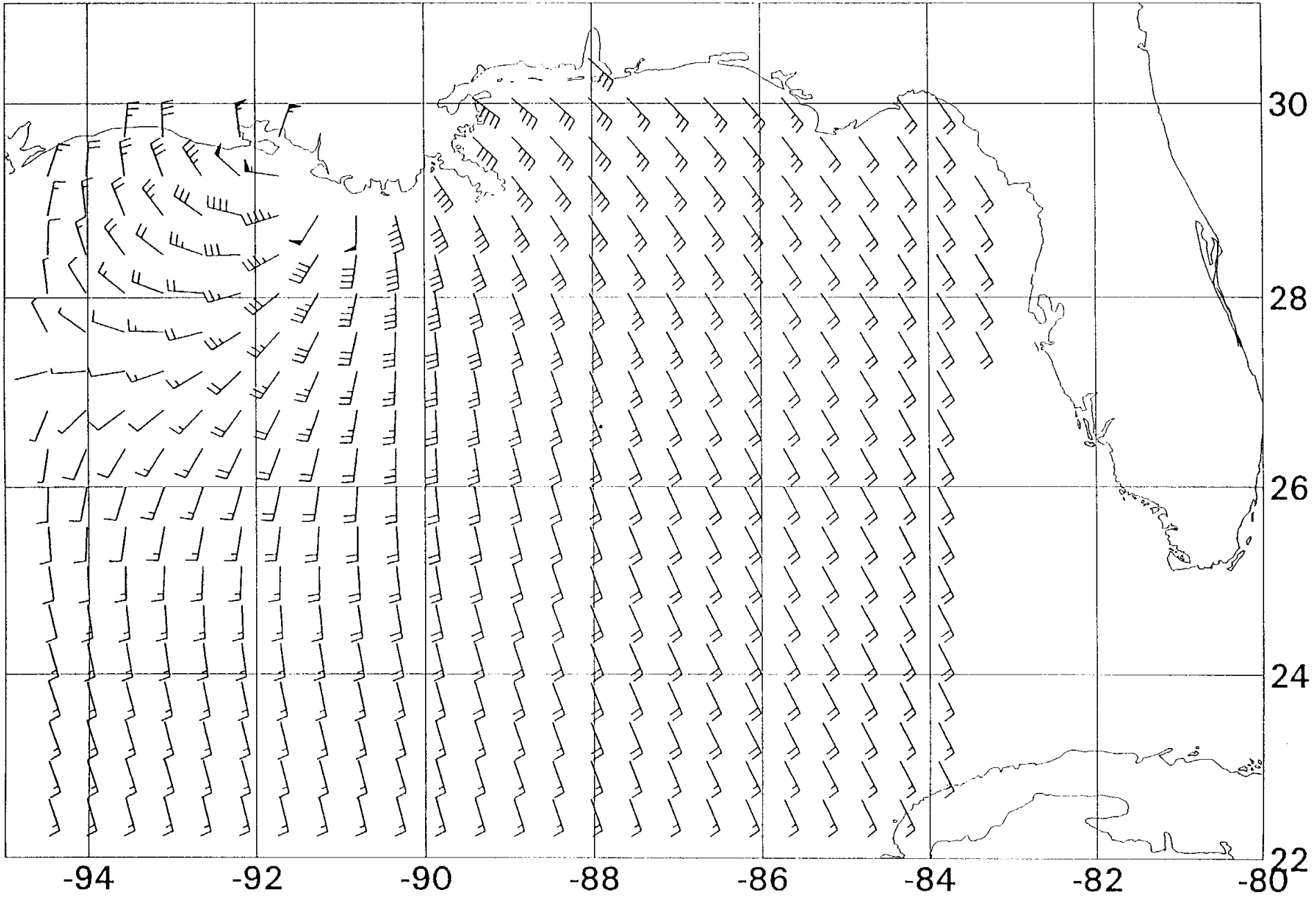

Hurricane ANDREW 1992

92082612

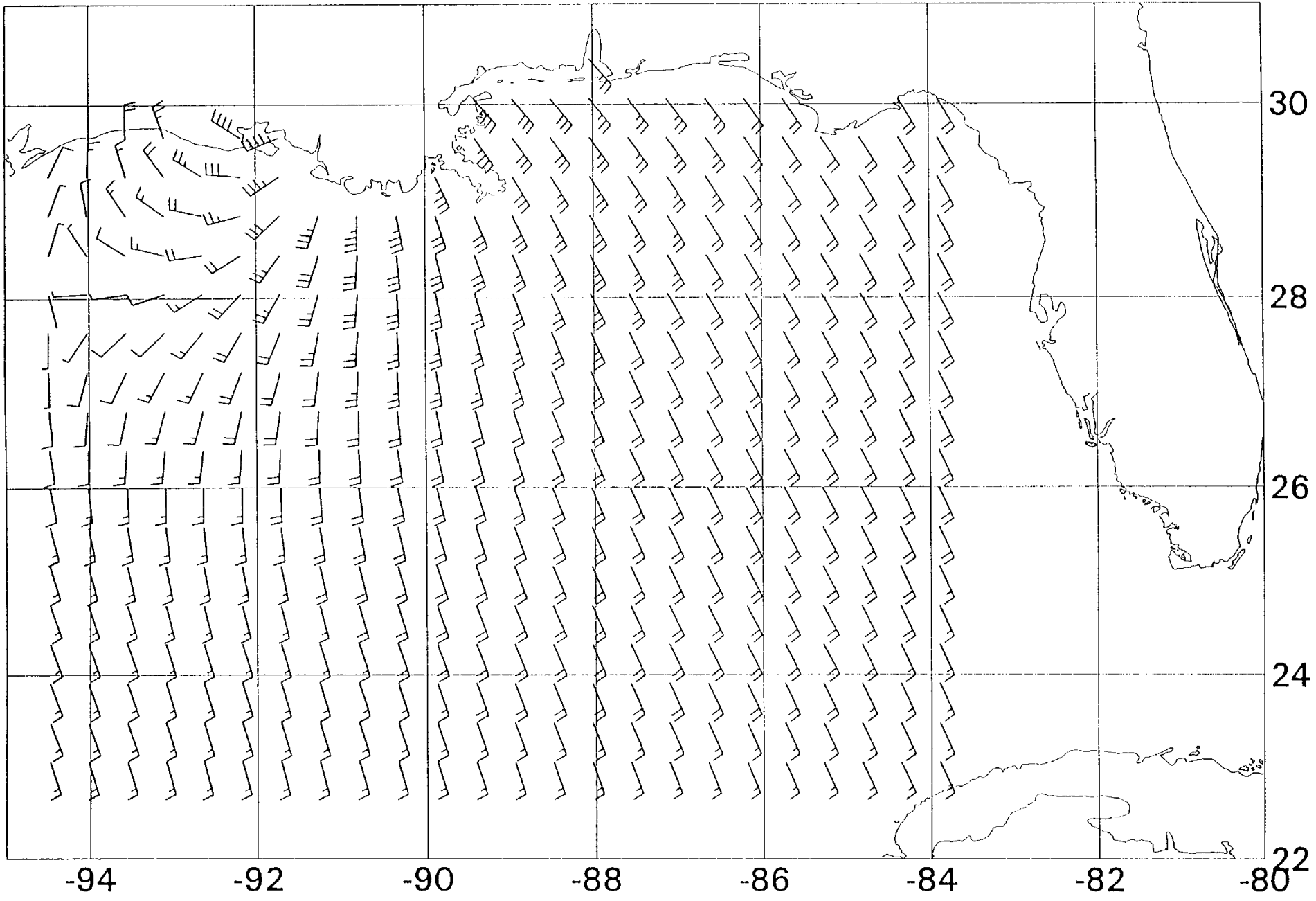

Hurricane A( )REW 1992

92082615

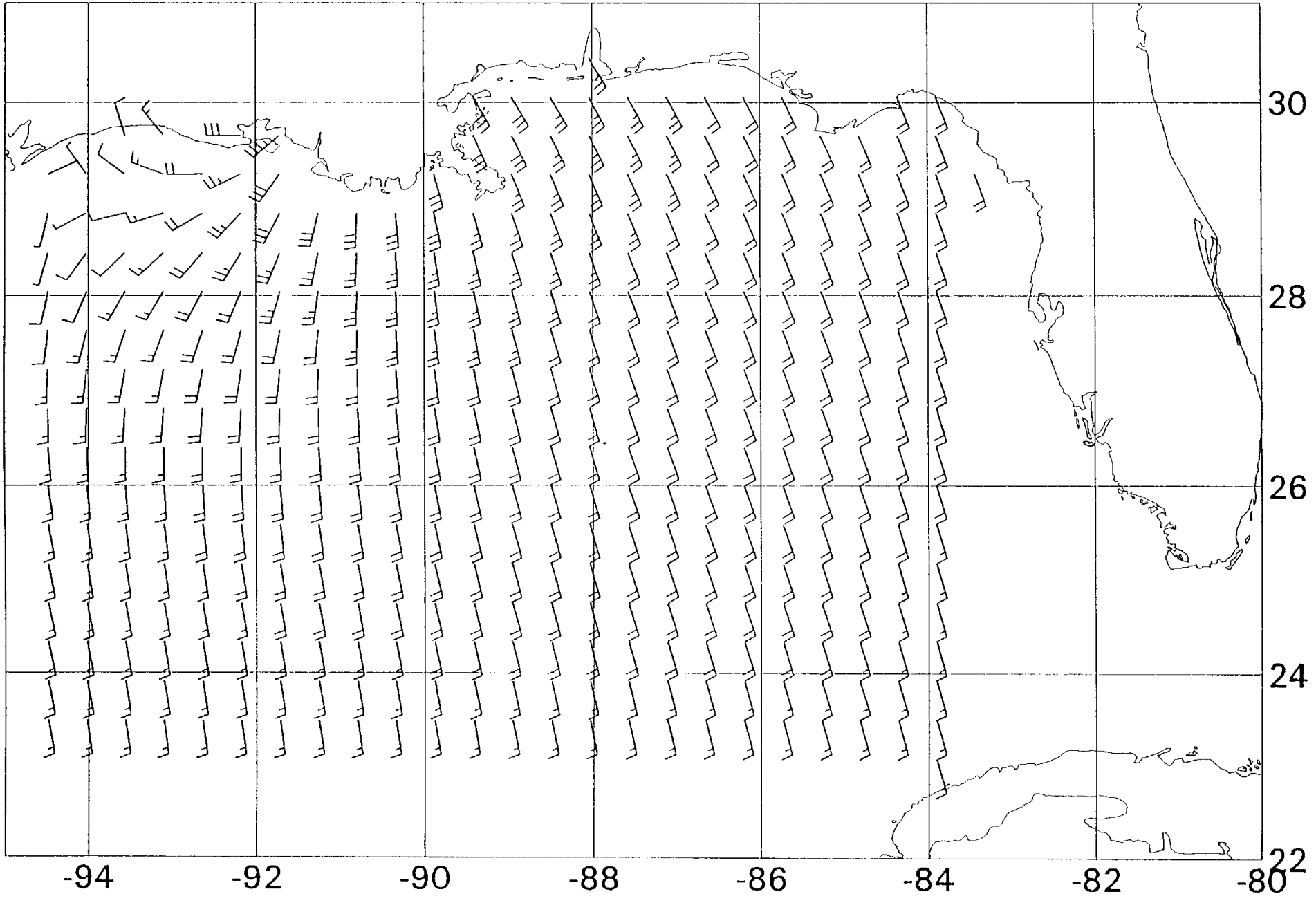

Hurricane A( )REW 1992

92082618

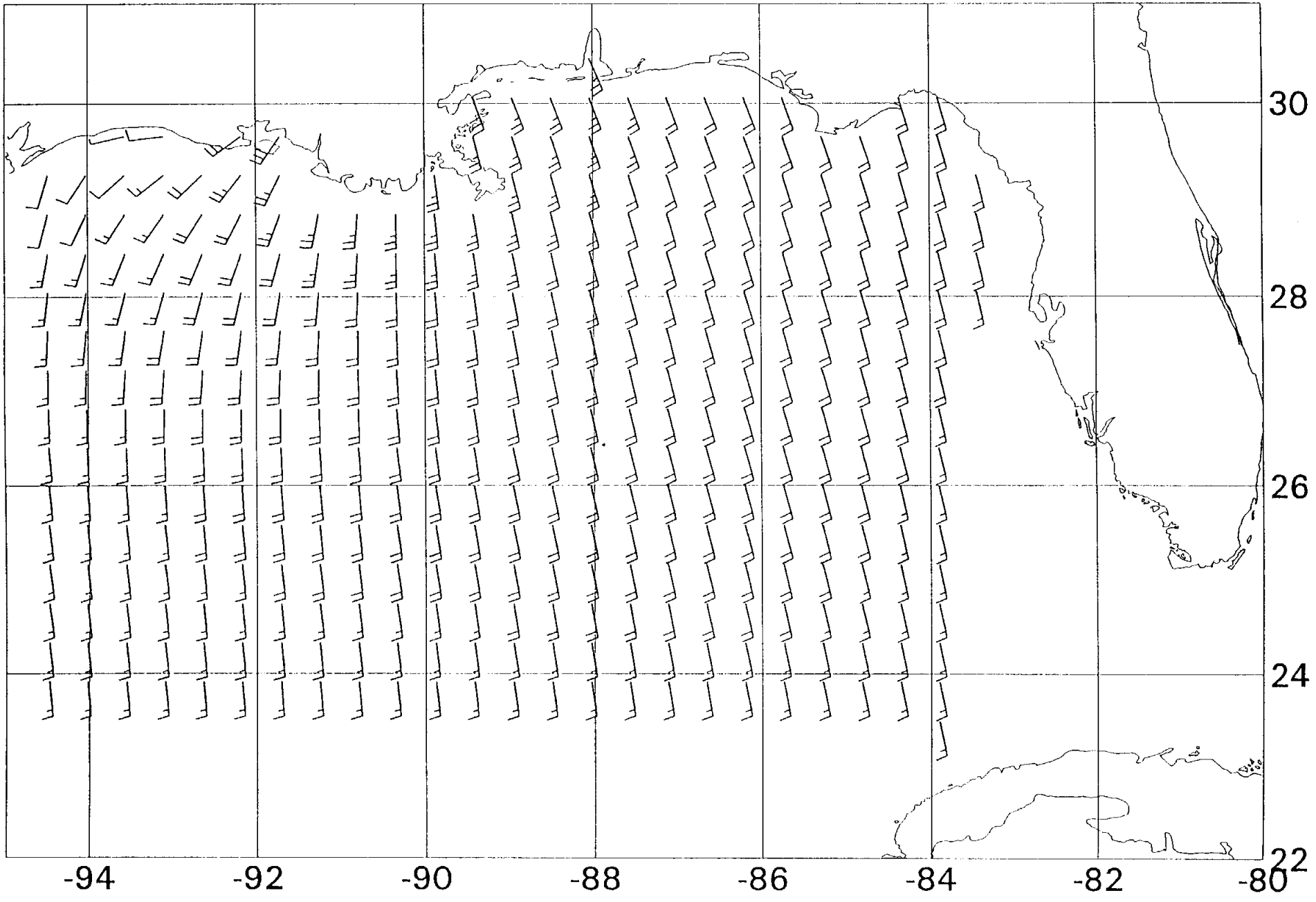

Attachment E

Conventional "wind barb" representation of the surface wind field in Hurricane Andrew at 3-hourly intervals on the small domain. Winds are plotted at every grid points of the wave model grid. Representation of speed is flag: 50 knots; each full barb: 10 knots, each half barb: 5 knots. The two digits plotted near each vector allow higher resolution of wind direction and speed. The first digit is the "tens" place of the wind direction (e.g. if the vector is in the first quadrant, 7 means the wind direction is 070 degrees) and the second digit is the units place of the speed (e.g if there is one full barb and one half barb, 6 means the wind speed is 16 knots).

Winds plotted represent 60-minute average winds at an elevation of 20 meters. For average winds at 10 meters reduce speeds by about 8%. For other typical averaging intervals the 1-hour average wind speed may be increased by the following factors:

10 minute average	1.09
1 minute average	1.22
peak gust	1.53

92082506

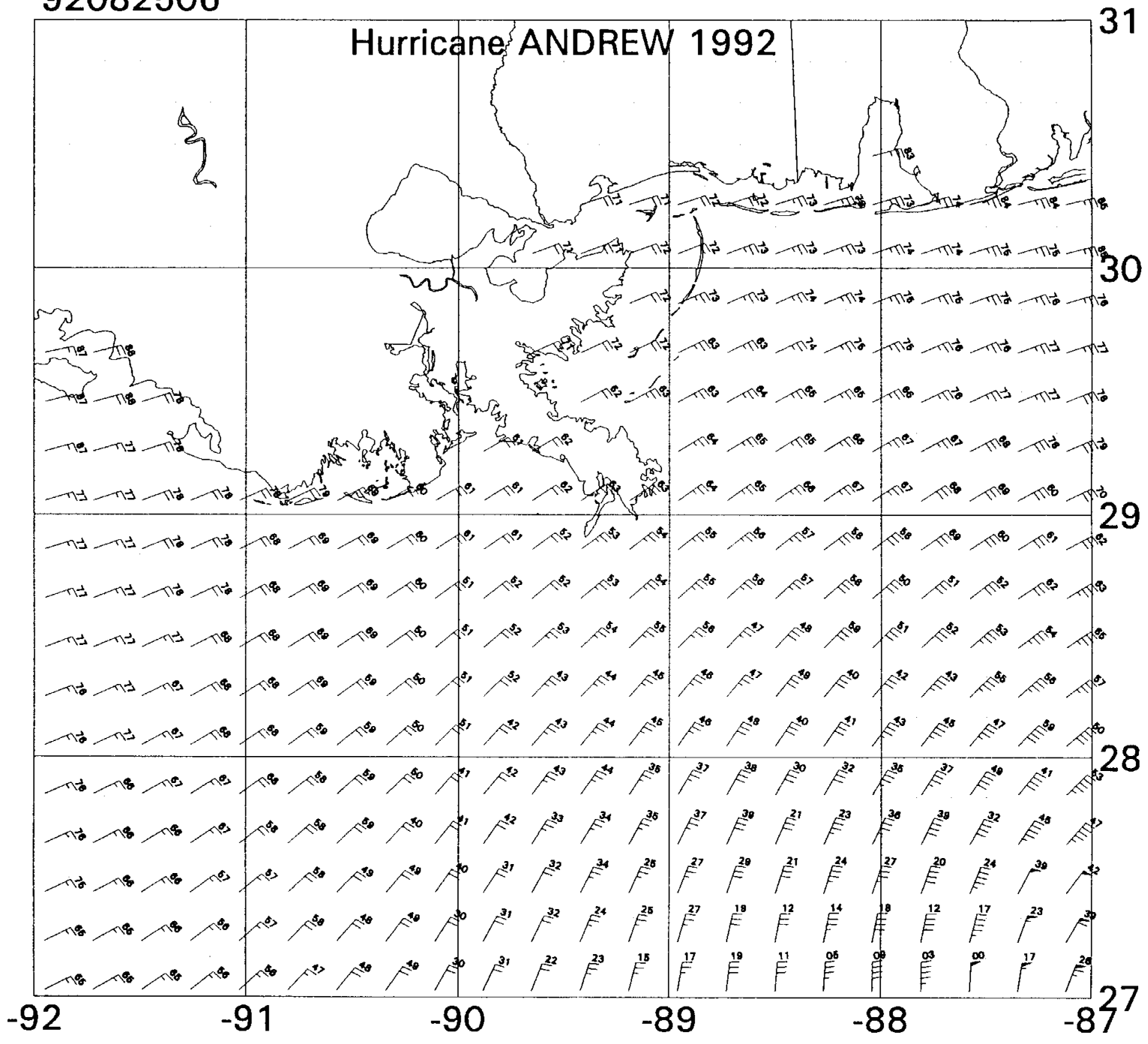

PLOTTED ON 6-NOV-92 11:53:22

92082509

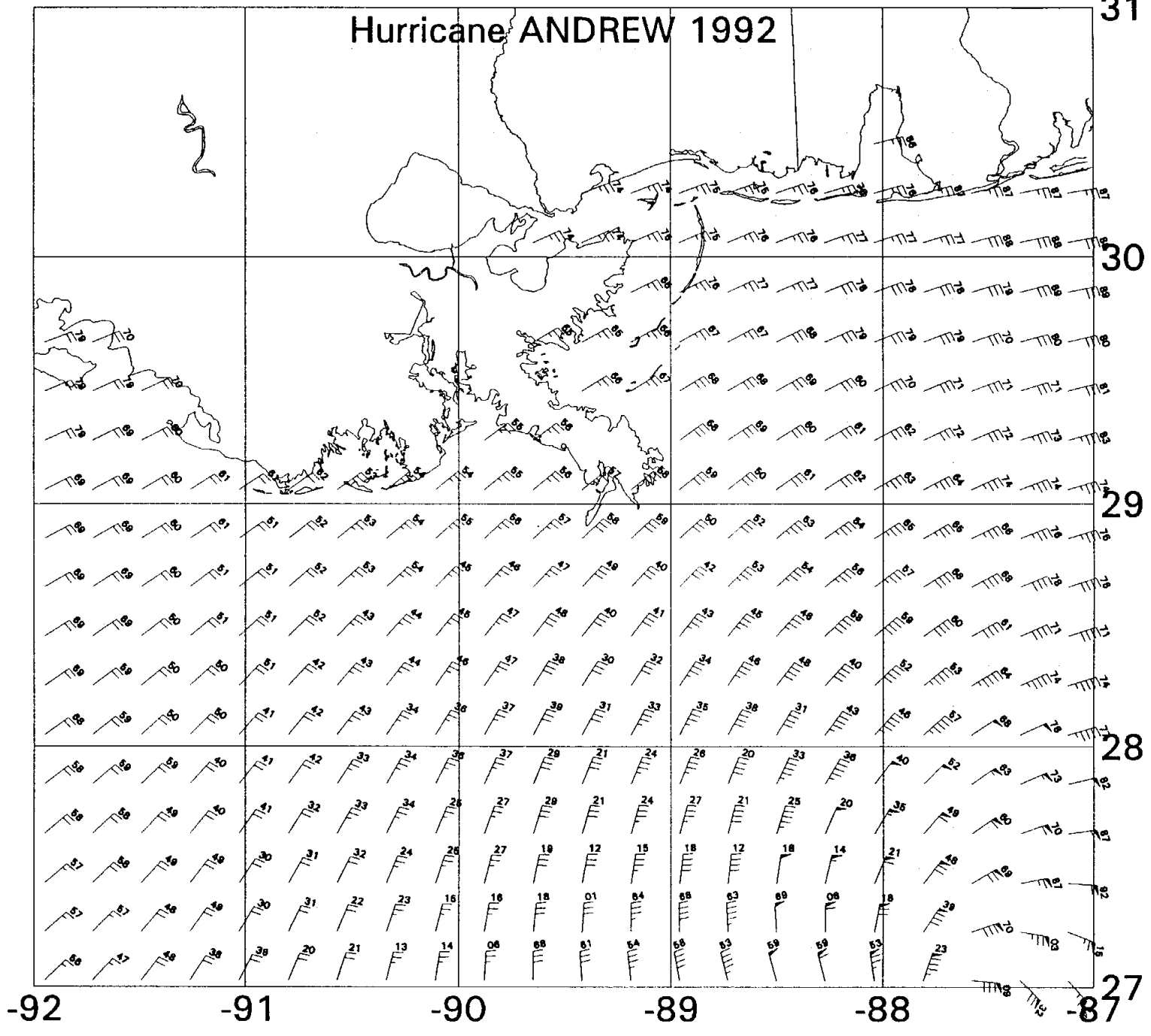

PLOTTED ON 6-NOV-92 11:57:00

92082512

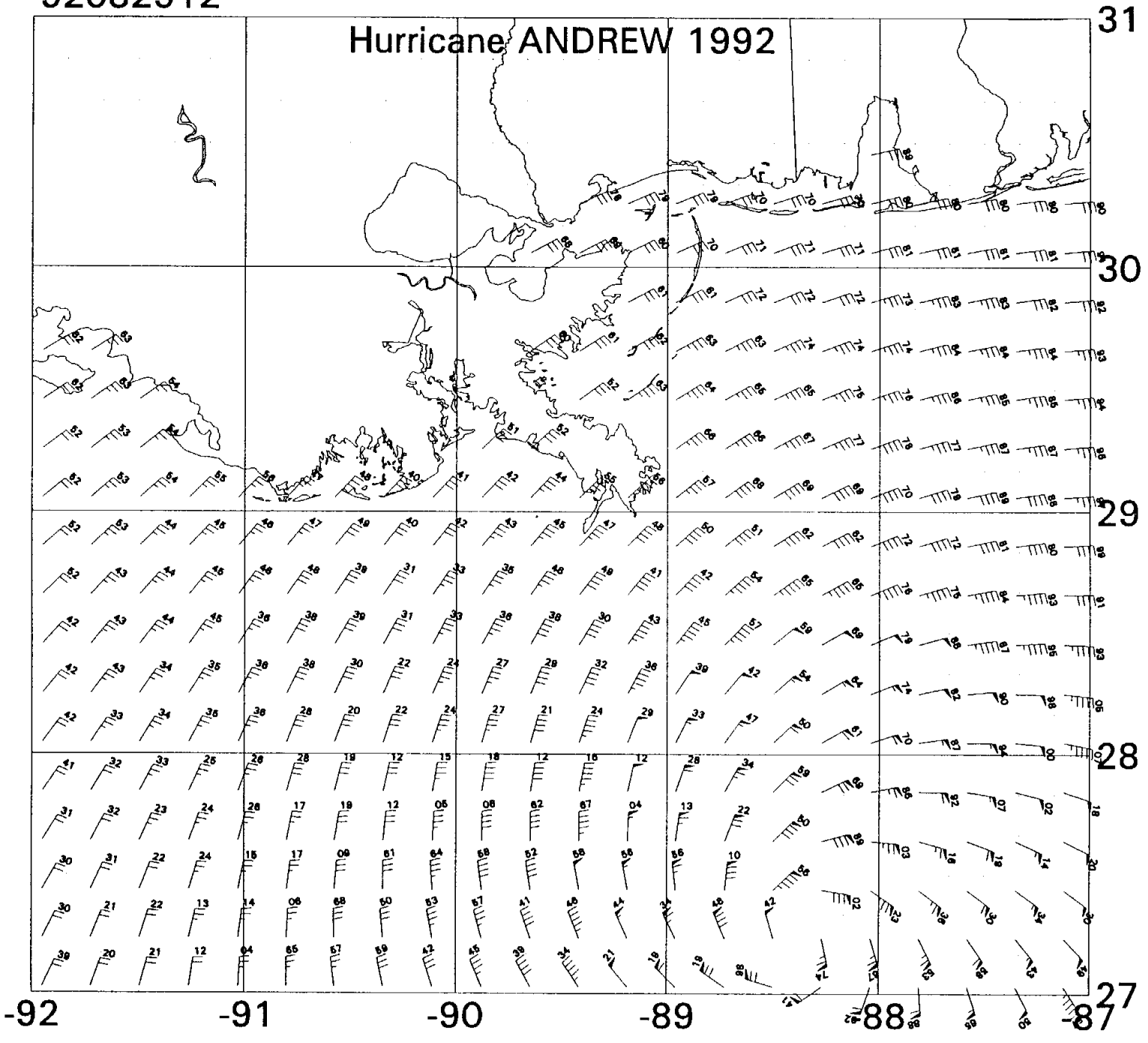

PLOTTED ON 6-NOV-92 12:05:15

92082515

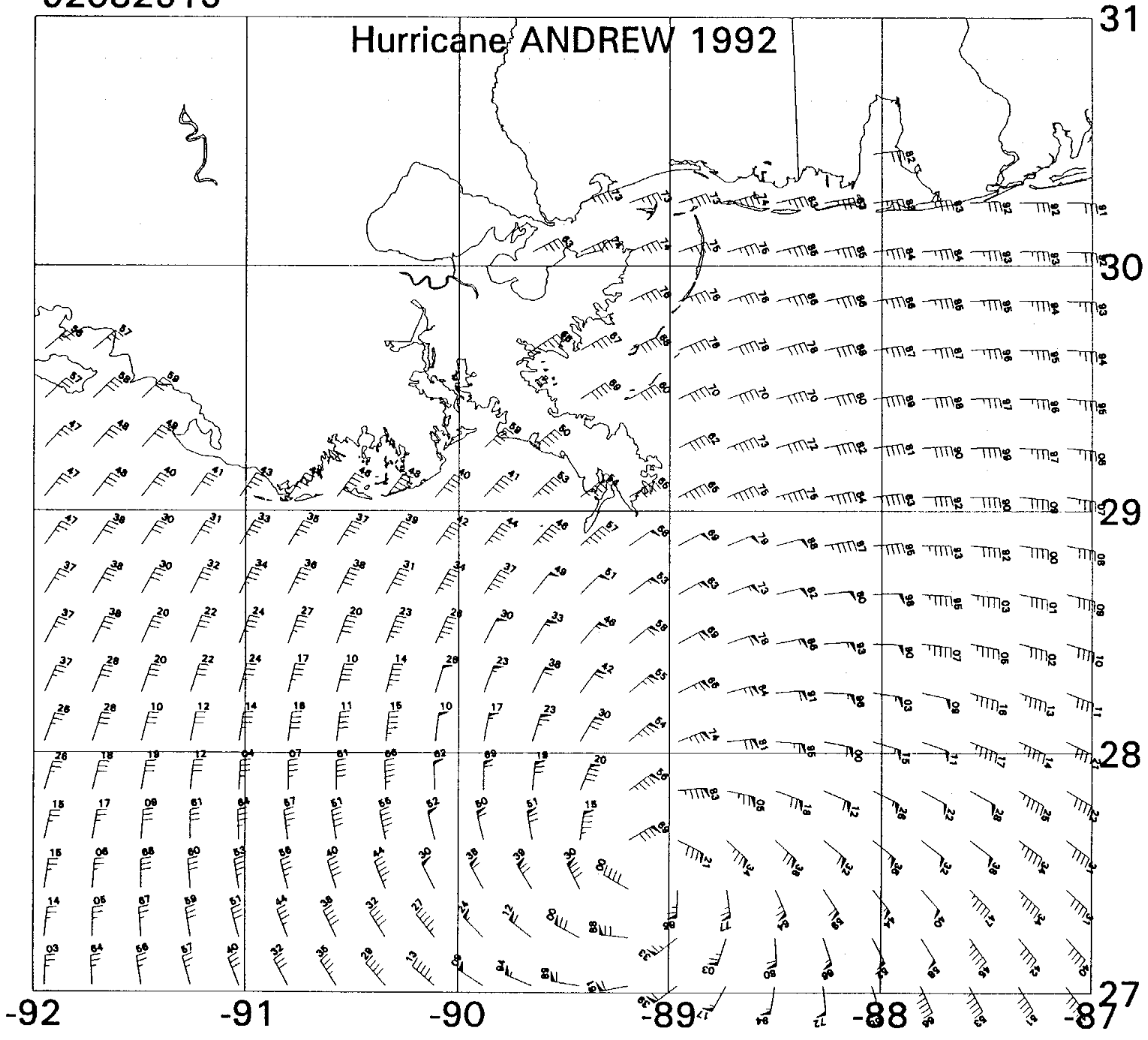

PLOTTED ON 6-NOV-92 12:07:53

92082518

Hurricane ANDREW 1992

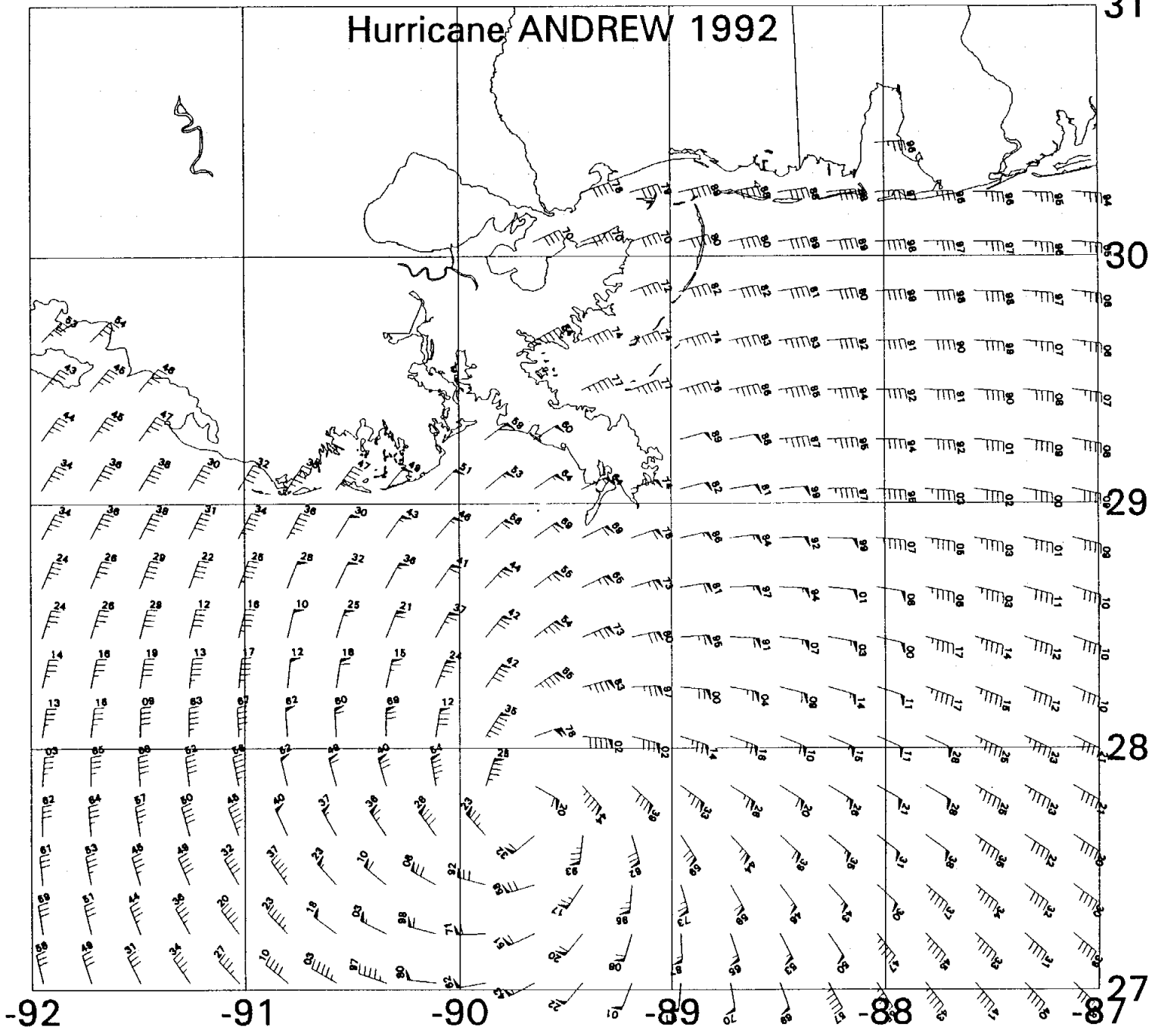

PLOTTED ON 6-NOV-92 12:10:38

92082521

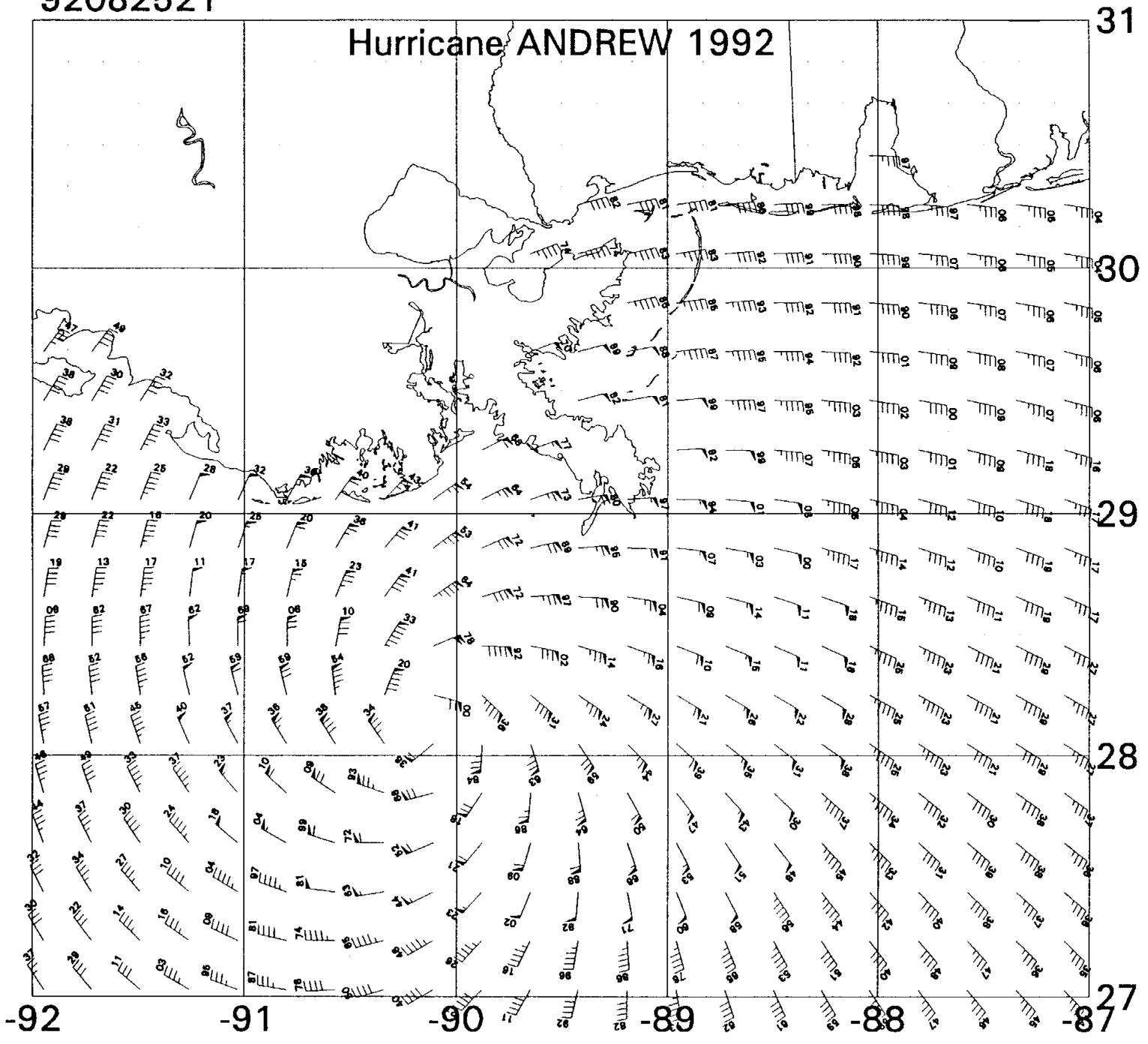

PLOTTED ON 6-NOV-92 12:13:09

92082600

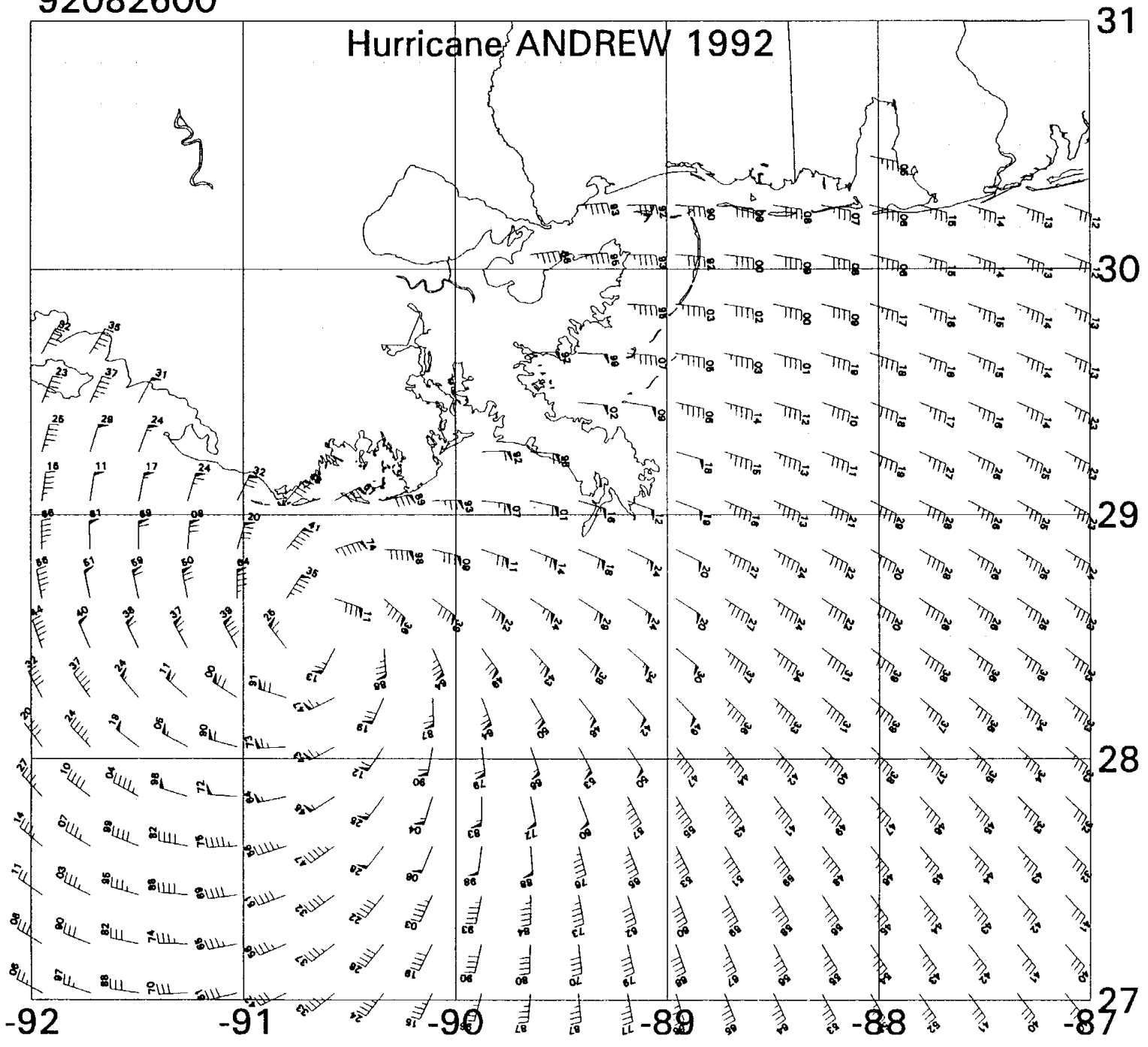

PLOTTED ON 6-NOV-92 12:15:40

92082603

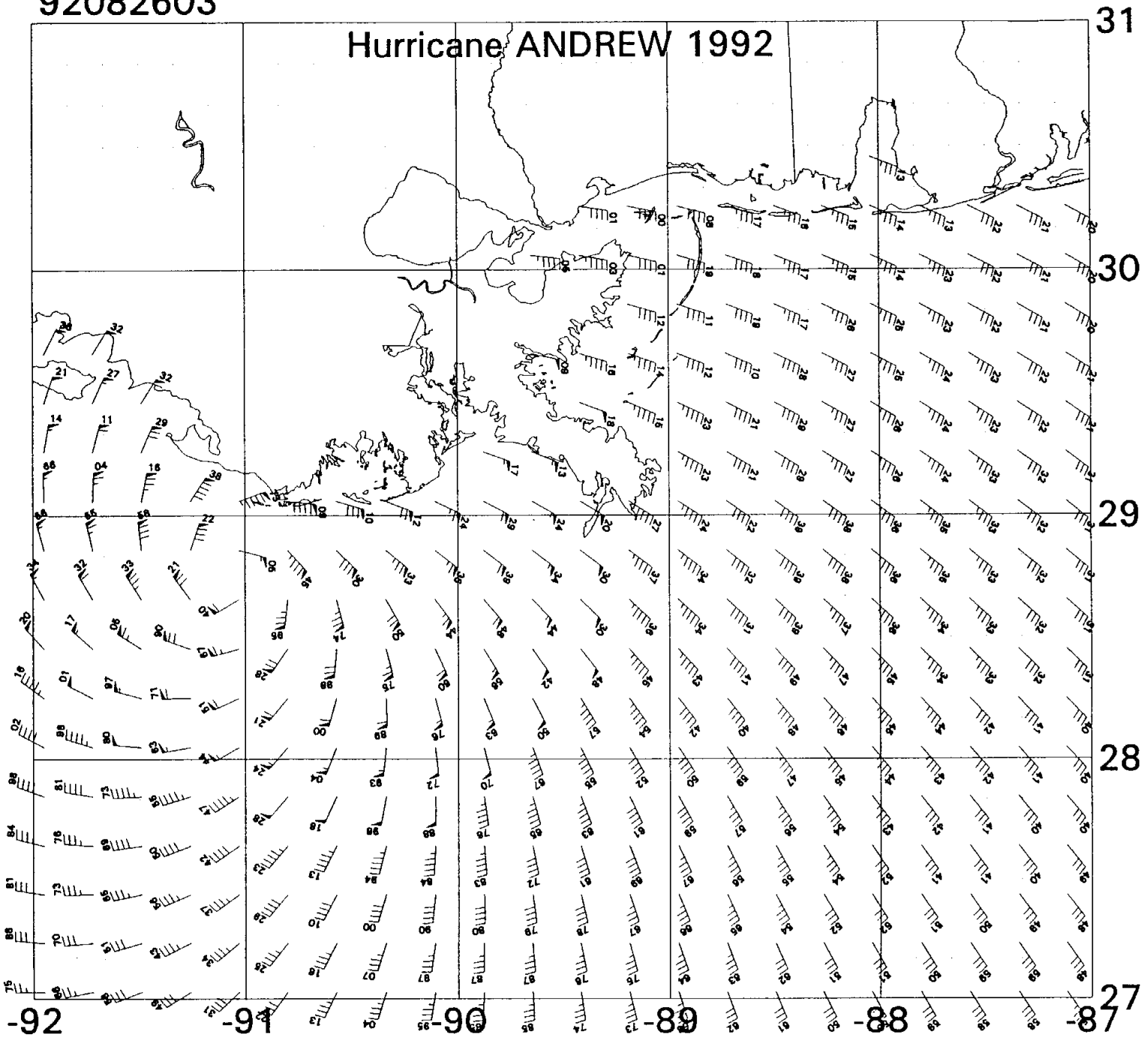

PLOTTED ON 6-NOV-92 12:25:04

92082606

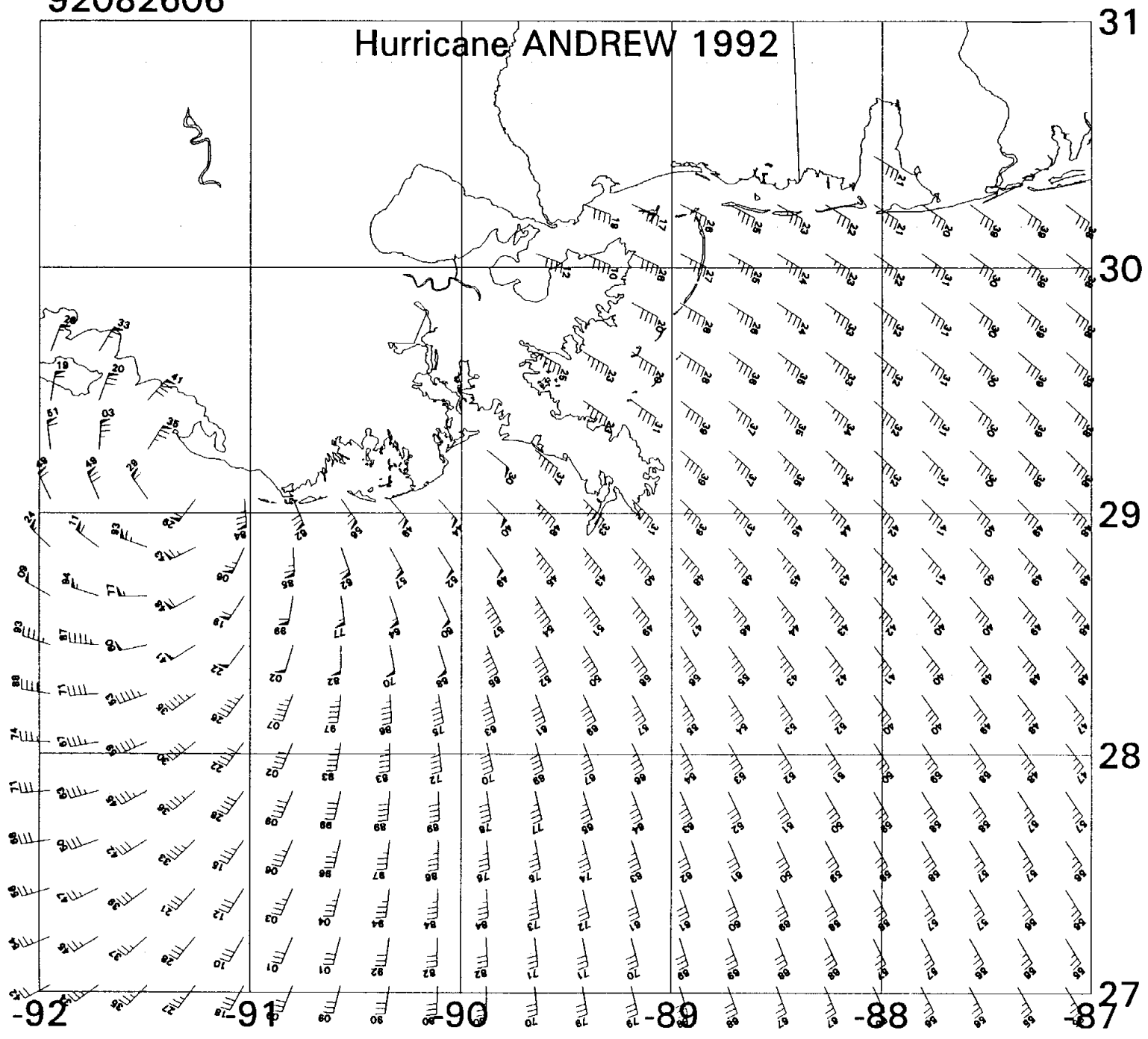

PLOTTED ON 6-NOV-92 12:27:32

92082609

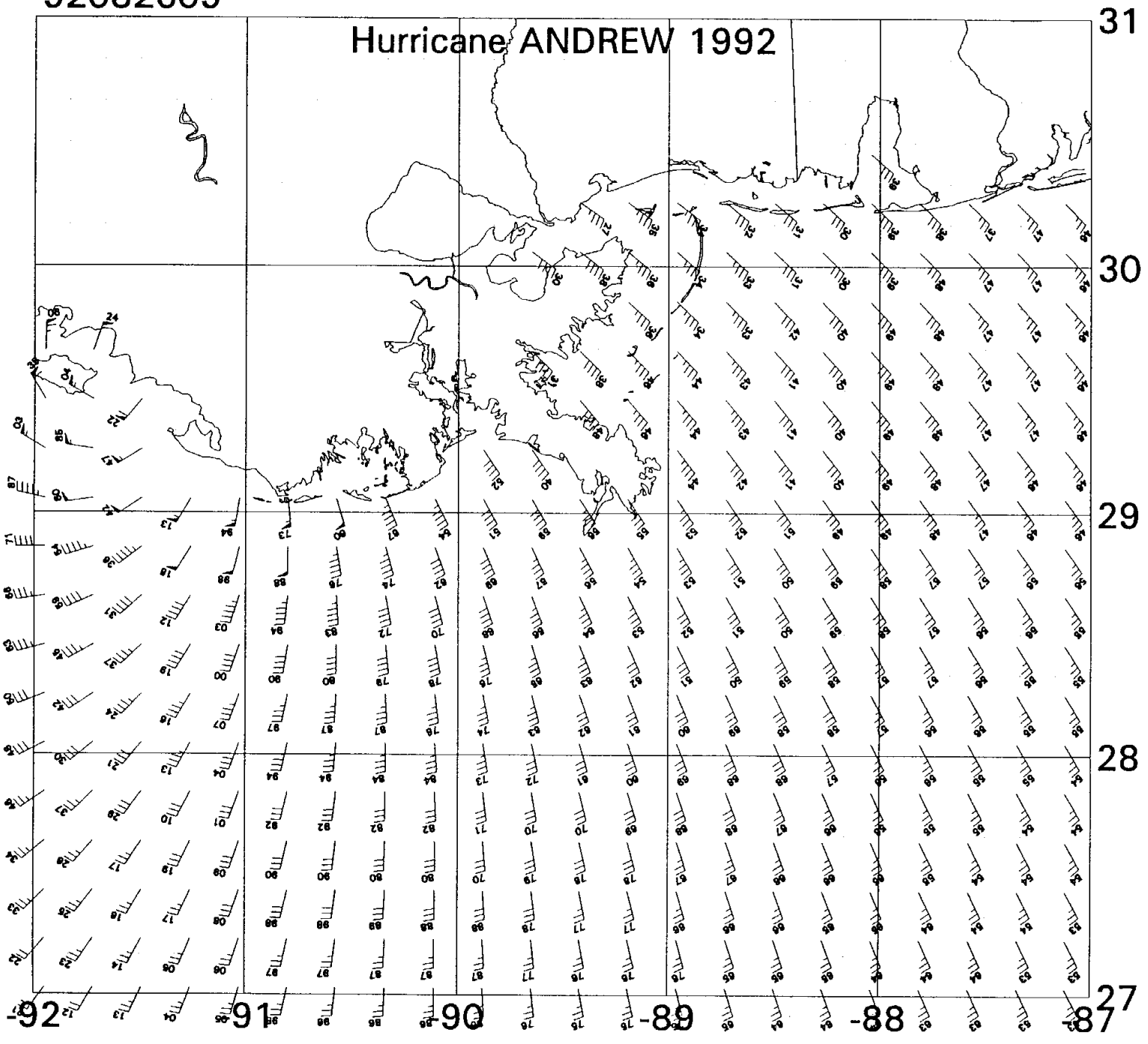

PLOTTED ON 6-NOV-92 12:30:02

92082612

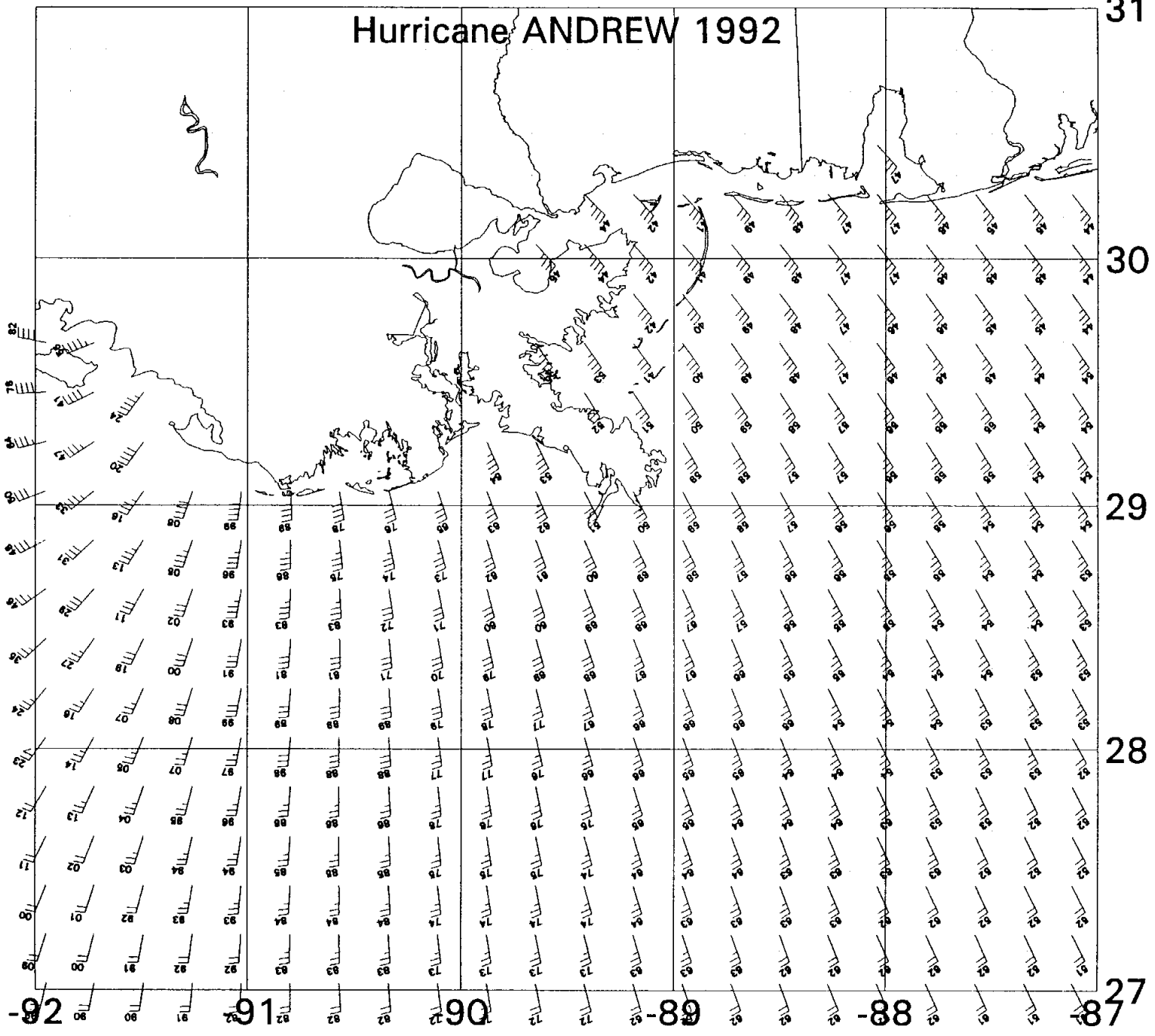

PLOTTED ON 6-NOV-92 12:34:26

Appendix F

Comparison of measured (after adjustment to 20 m) and hindcast time histories of wind speed and direction at NOAA buoys 42001, 42003, Bullwinkle and Lena platforms. (see Figure 1 for locations)

TIME SERIES OF MEASURED AND HINDCAST WINDS
Hurricane ANDREW 24 October - 26 October, 1992
Hindcast winds at grid point 2880
Measured winds at buoy 42001

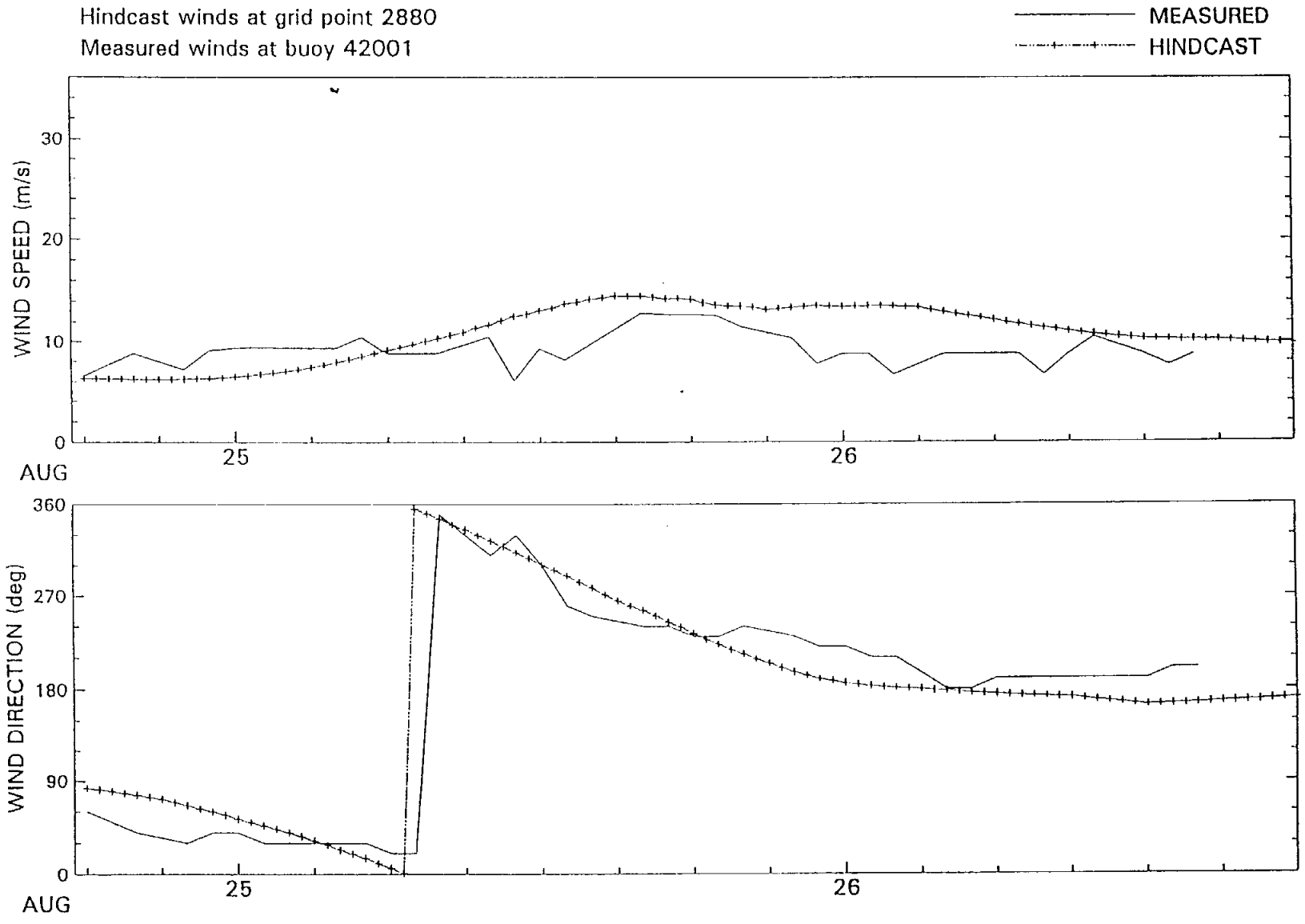

PLOTTED ON 4-NOV-92 16:54:14 (42001_92.MEAS_ADJ & 42001.HIND)

TIME SERIES OF MEASURED AND HINDCAST WINDS
Hurricane ANDREW 24 October - 26 October, 1992
Hindcast winds at grid point 2896
Measured winds at buoy 42003

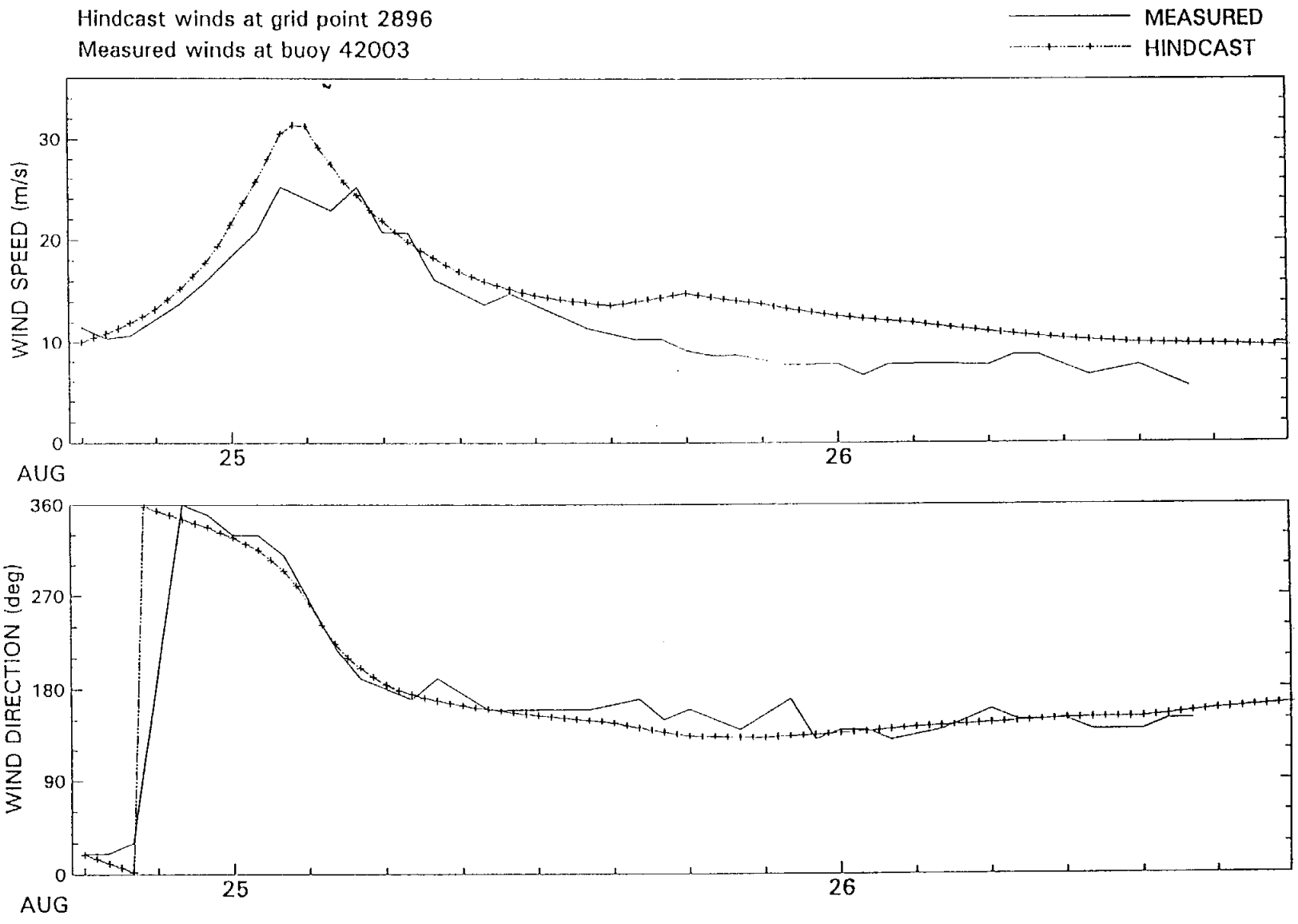

PLOTTED ON 4-NOV-92 16:54:21 (42003_92.MEAS_ADJ & 42003.HIND)

TIME SERIES OF MEASURED AND HINDCAST WINDS
Hurricane ANDREW 24 October - 26 October, 1992
Hindcast winds at grid point 3664
Measured winds at buoy BULLWINKLE ANEMOMETER#1

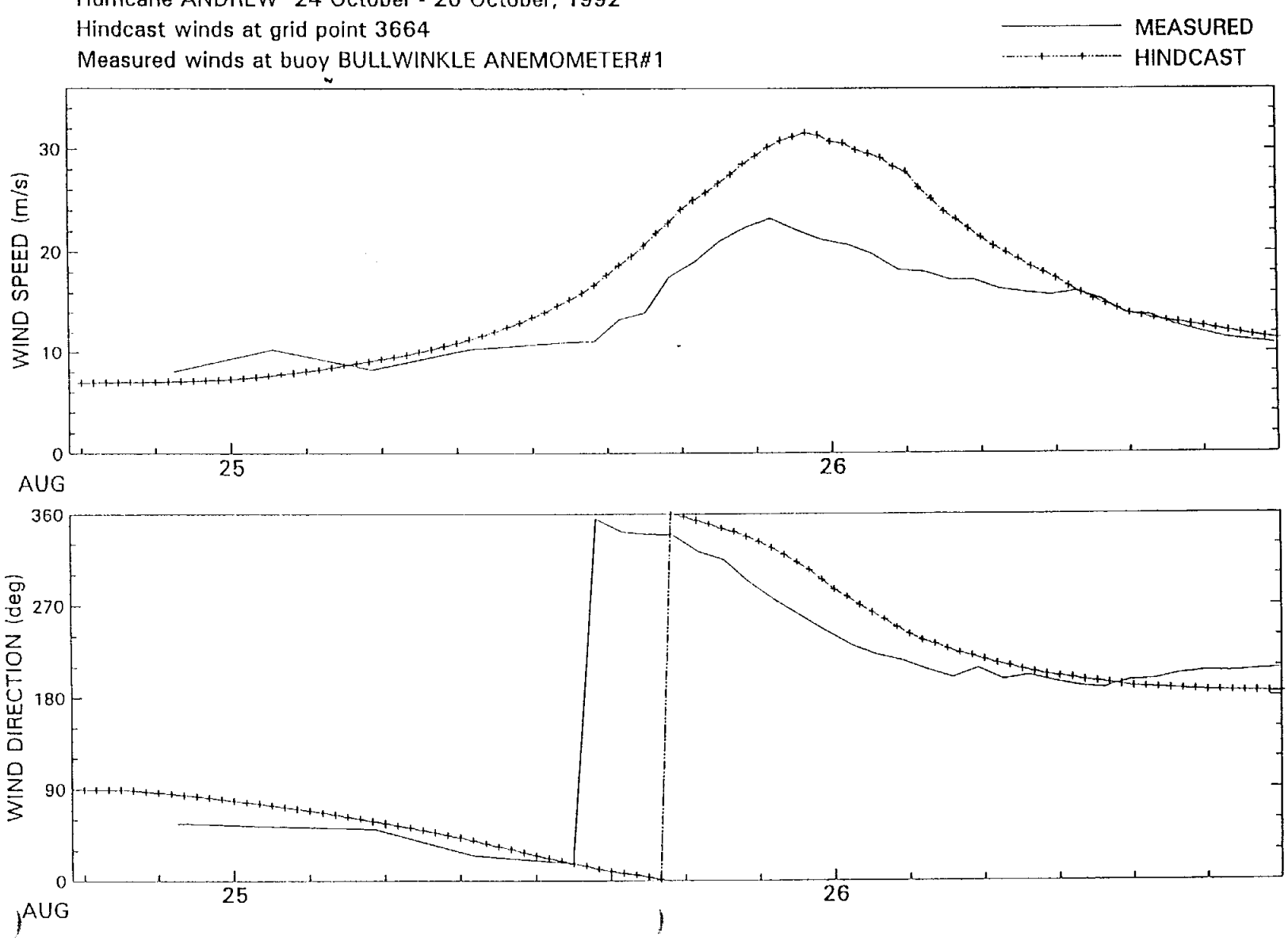

PLOTTED ON 4-NOV-92 16:54:53 /BULL_WSWD1.MEAS_ADJ & BULLWINK.HIND/

TIME SERIES OF MEASURED AND HINDCAST WINDS
Hurricane ANDREW 24 October - 26 October, 1992
Hindcast winds at grid point 3664
Measured winds at buoy BULLWINKLE ANEMOMETER#2

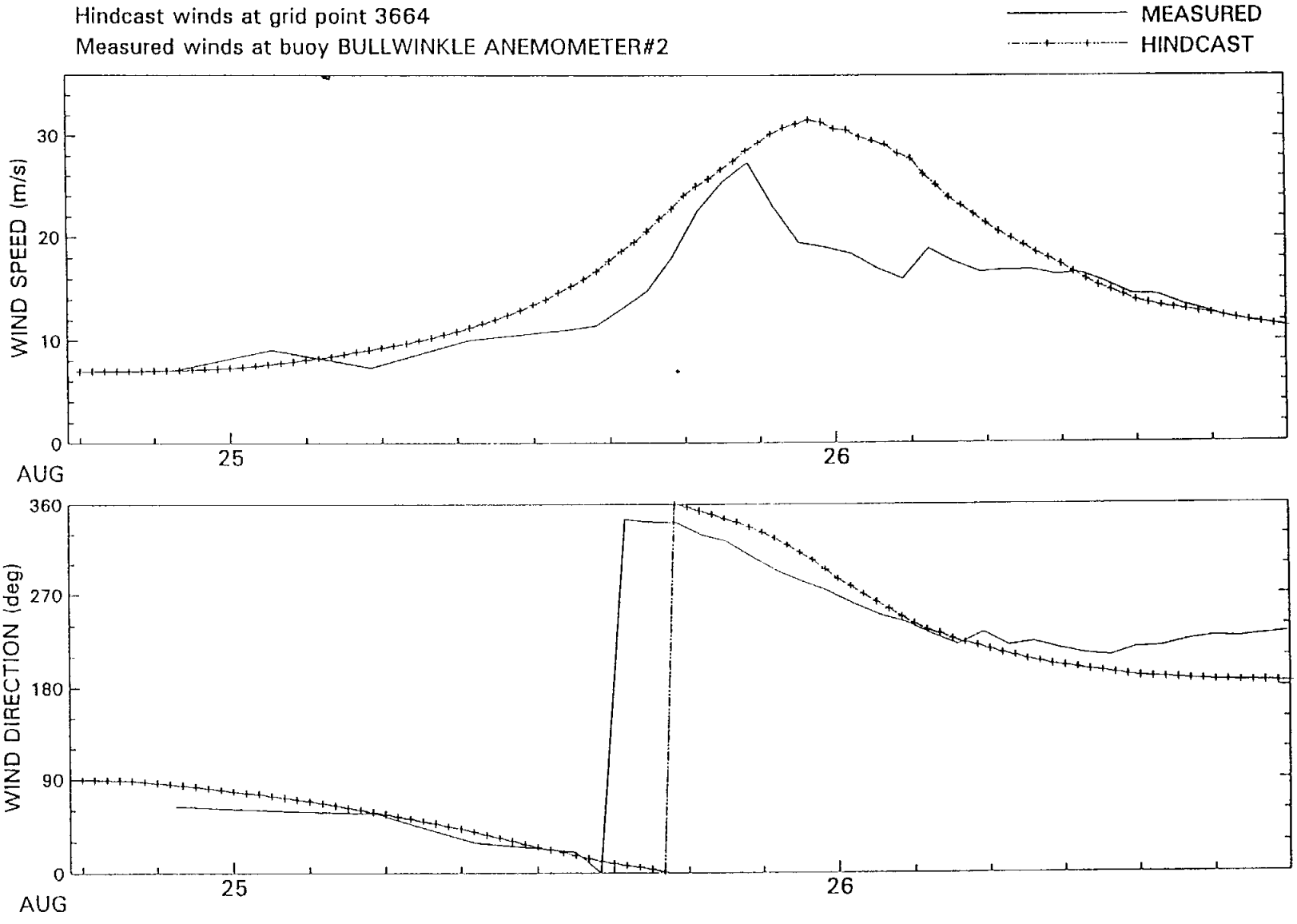

PLOTTED ON 4-NOV-92 16:54:59 (BULL_WSWD2_MEAS_ADJ & BULLWINK_HIND)

TIME SERIES OF MEASURED AND HINDCAST WINDS
Hurricane ANDREW 24 October - 26 October, 1992
Hindcast winds at grid point 3909
Measured winds at buoy LENA

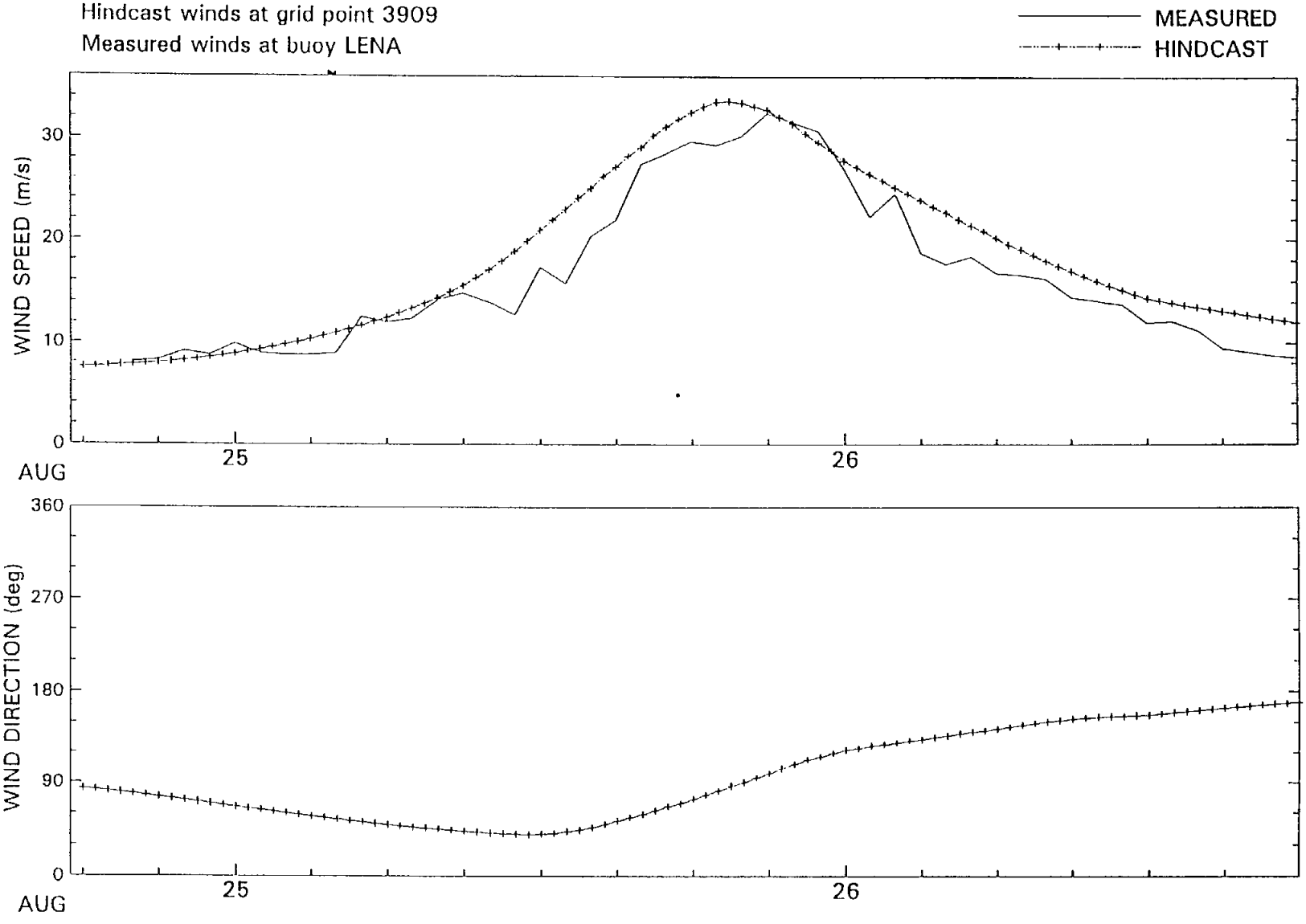

PLOTTED ON 4-NOV-92 16:55:07 (LENA_WSWD1.MEAS_ADJ & LENA.HIND)

Appendix G

Vector field plots of hindcast significant wave height and vector mean wave direction at 3-hourly intervals at alternate rows and columns of wave model grid system within the large domain. Numerals denote significant wave height in meters x 10. (i.e. 48 = 4.8 meters)

Plotted 3-NOV-92 15:05 from file [ANDREW]ANDREW.FIELDS;2 4-NO 92 12:18

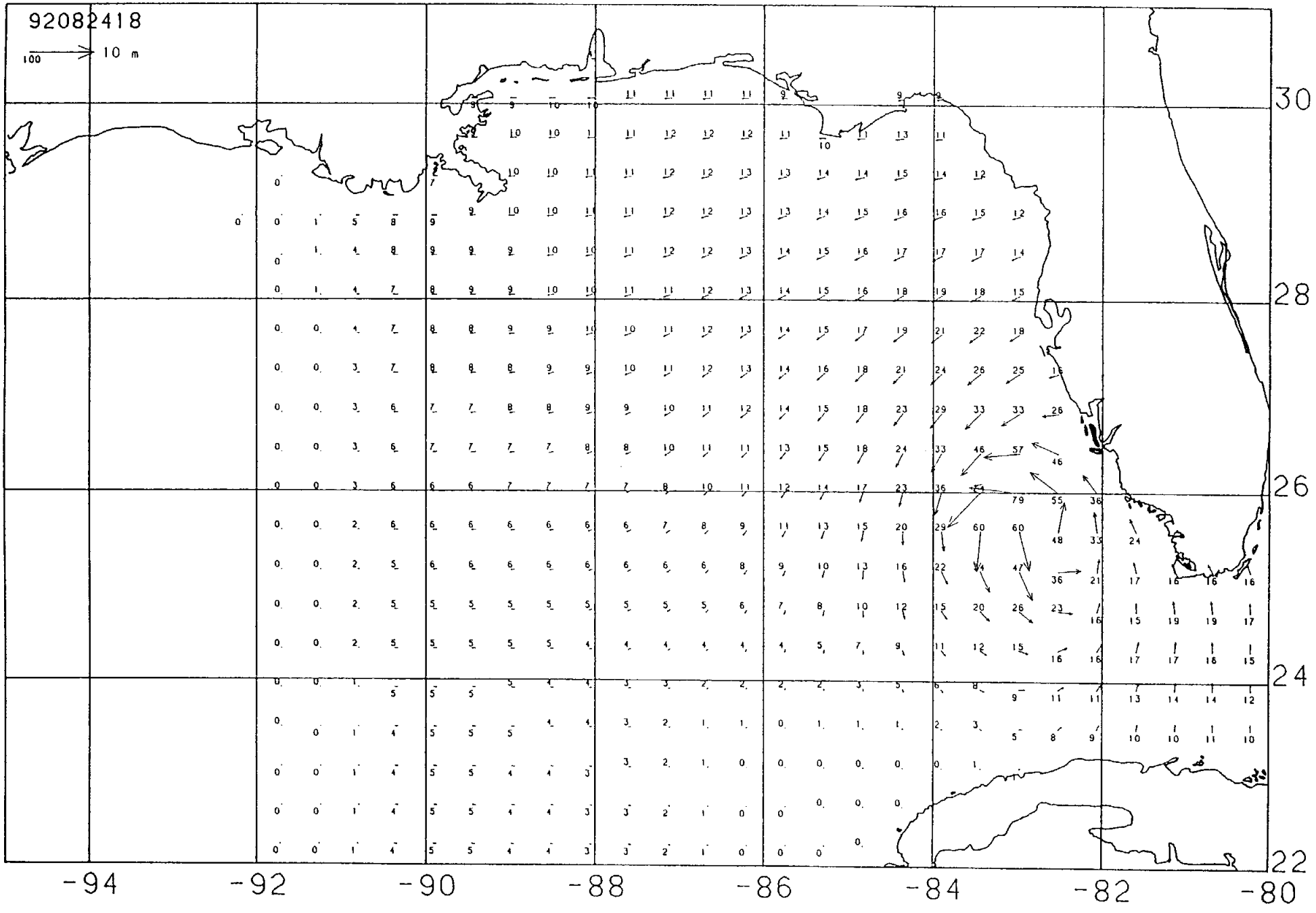

Plotted on 9-NOV-92 15:17 from file [ANDREW]ANDREW.FIELDS;2 4-NOV-1992 12:18

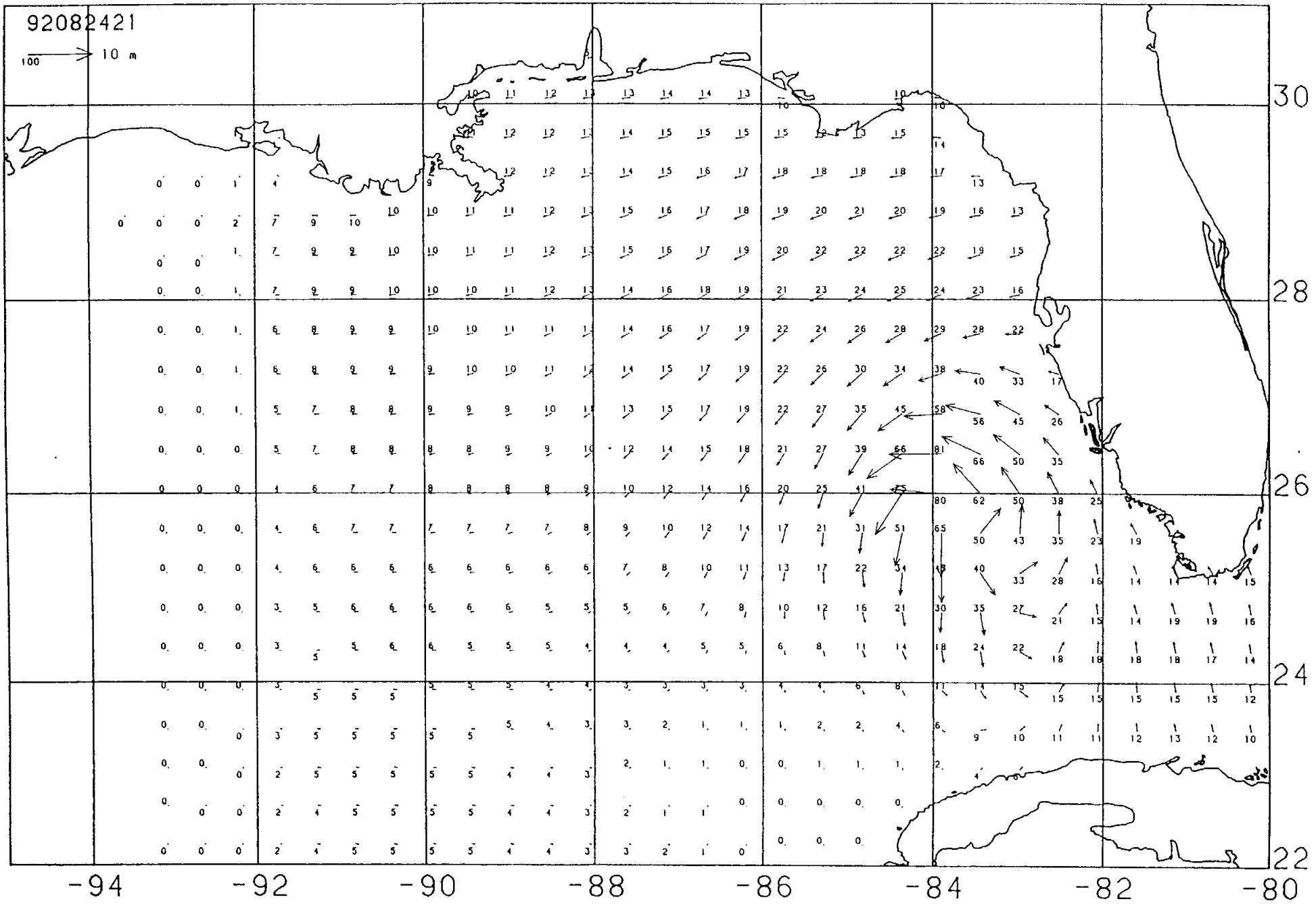

Plotted on 9-NOV-92 15:25 from file [ANDREW]ANDREW.FIELDS;2 4-NOV-1992 12:18

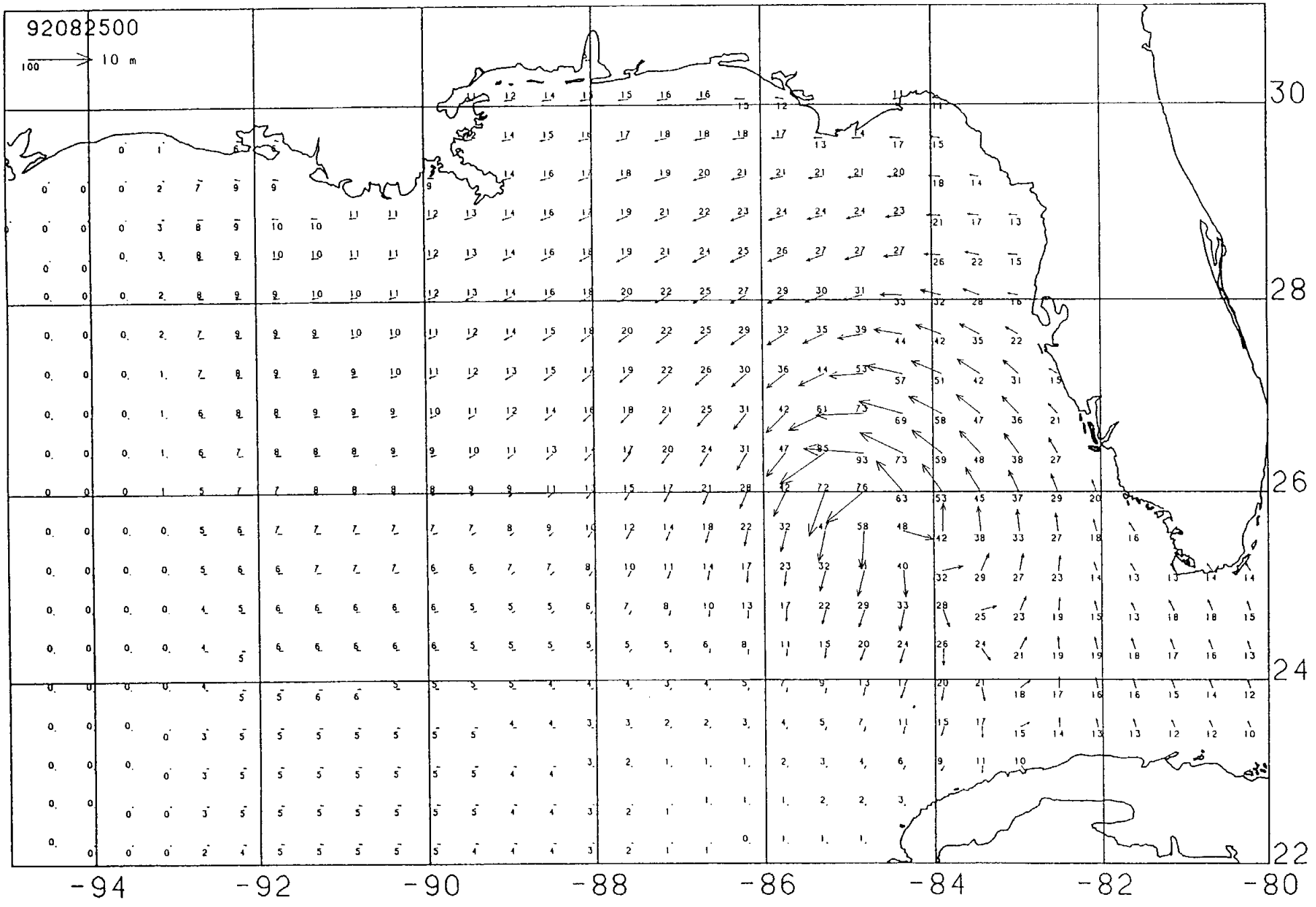

Plotted on 9-NOV-92 15:33 from file [ANDREW]ANDREW.FIELDS;2 4-NOV-1992 12:18

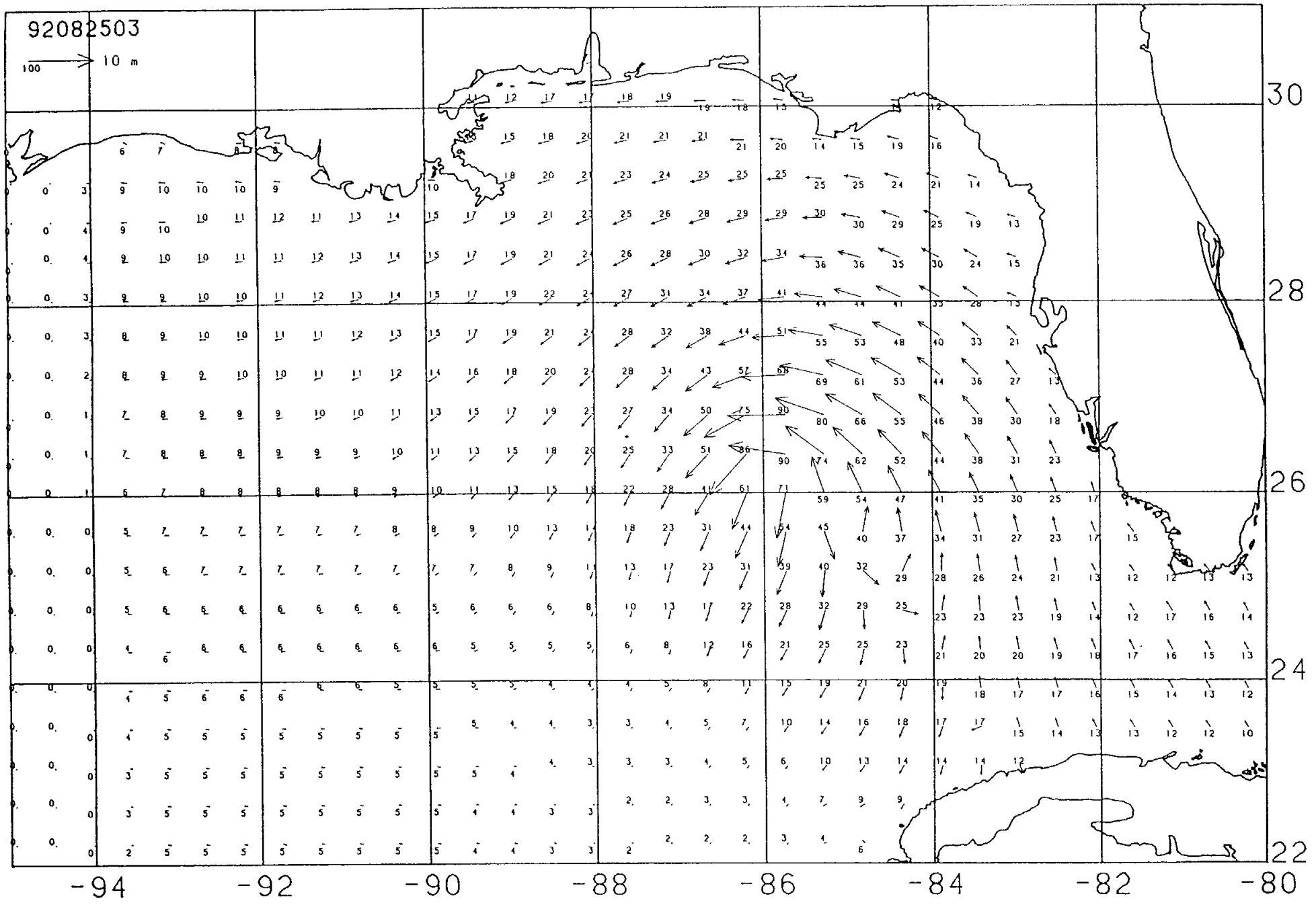

Plotted on -NOV-92 15:42 from file [ANDREW]ANDREW.FIELDS;2 4-NOV-2 12:18

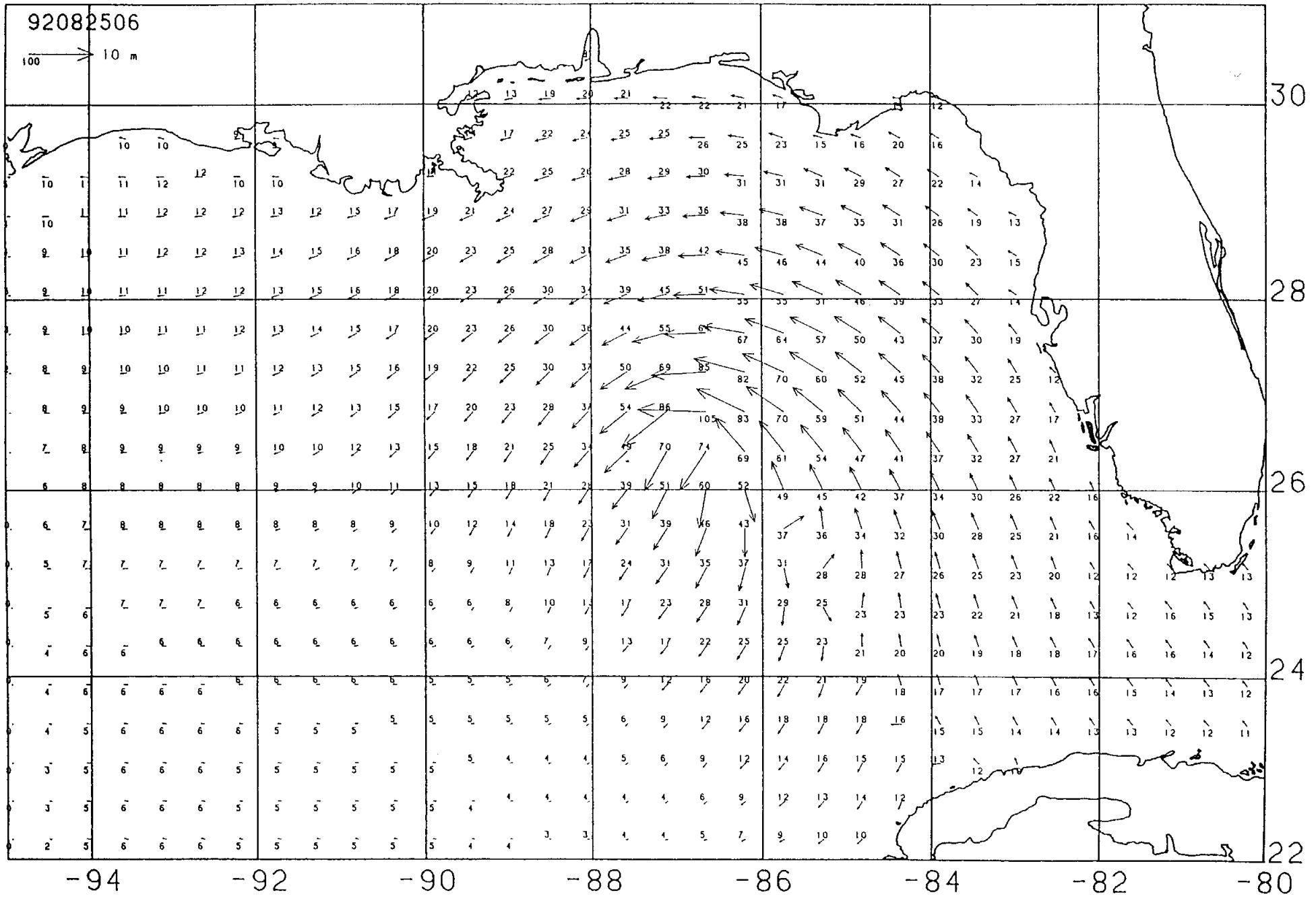

Plotted on 9-NOV-92 15:51 from file CANDREW]ANDREW.FIELDS;2 4-NOV-1992 12:18

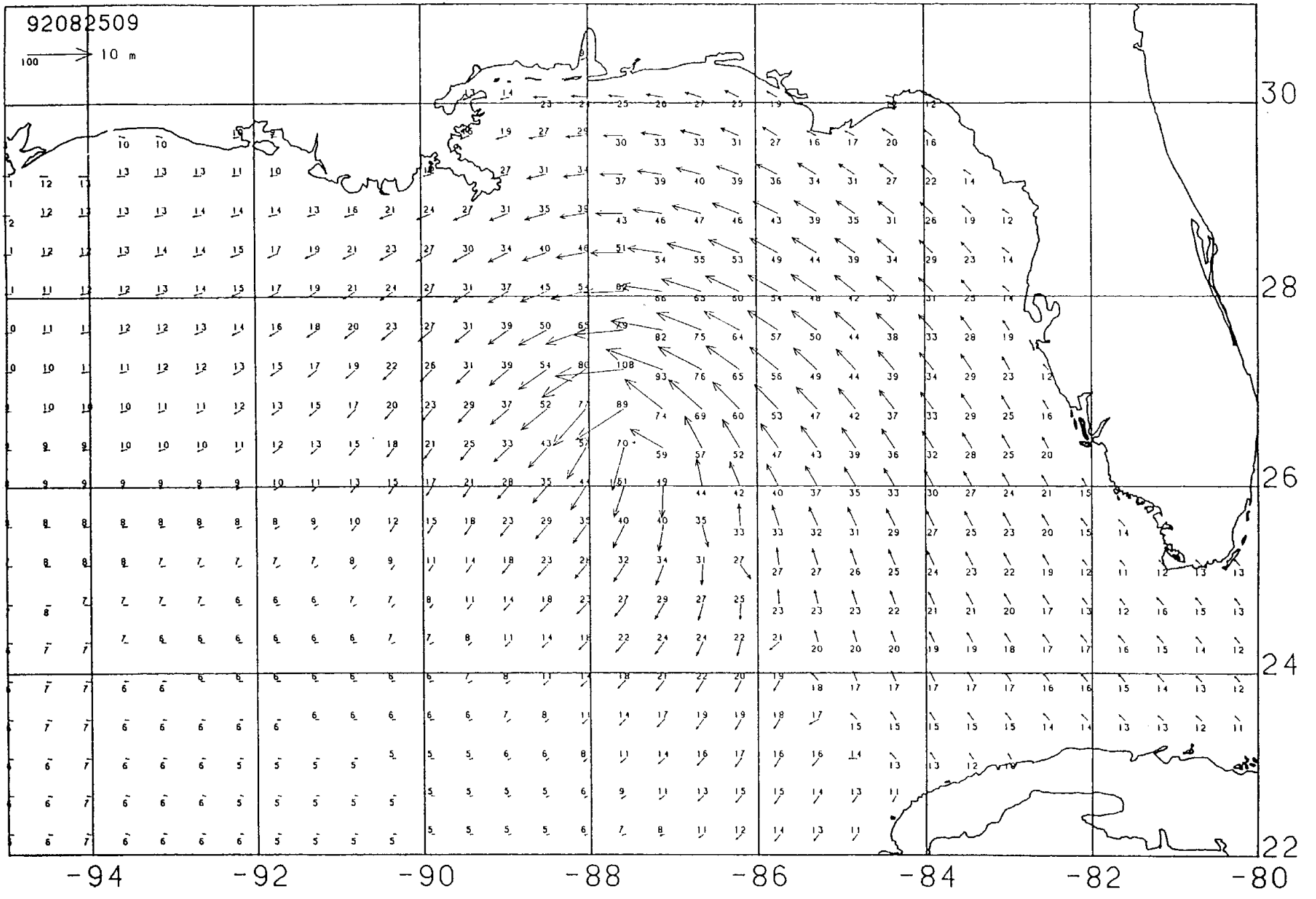

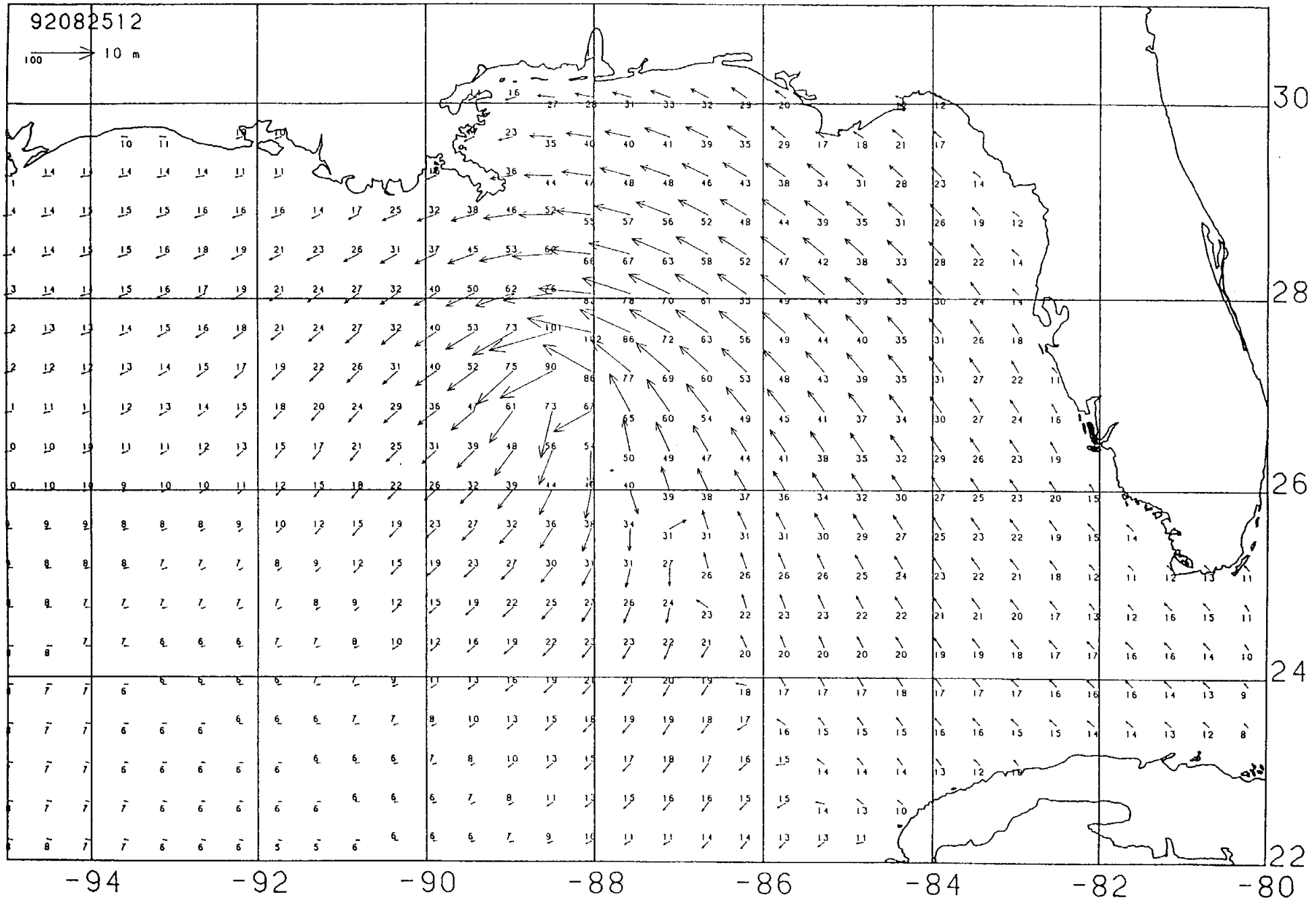
Plotted(9-NOV-92 12:22 from file [ANDREW]ANDREW.FIELDS;2 4-NO 992 12:18
92082512
100
10 m
30
28
26
24
22
-94
-92
-90
-88
-86
-84
-82
-80

Plotted on 9-NOV-92 12:31 from file CANDREW]ANDREW.FIELDS;2 4-NOV-92 12:18

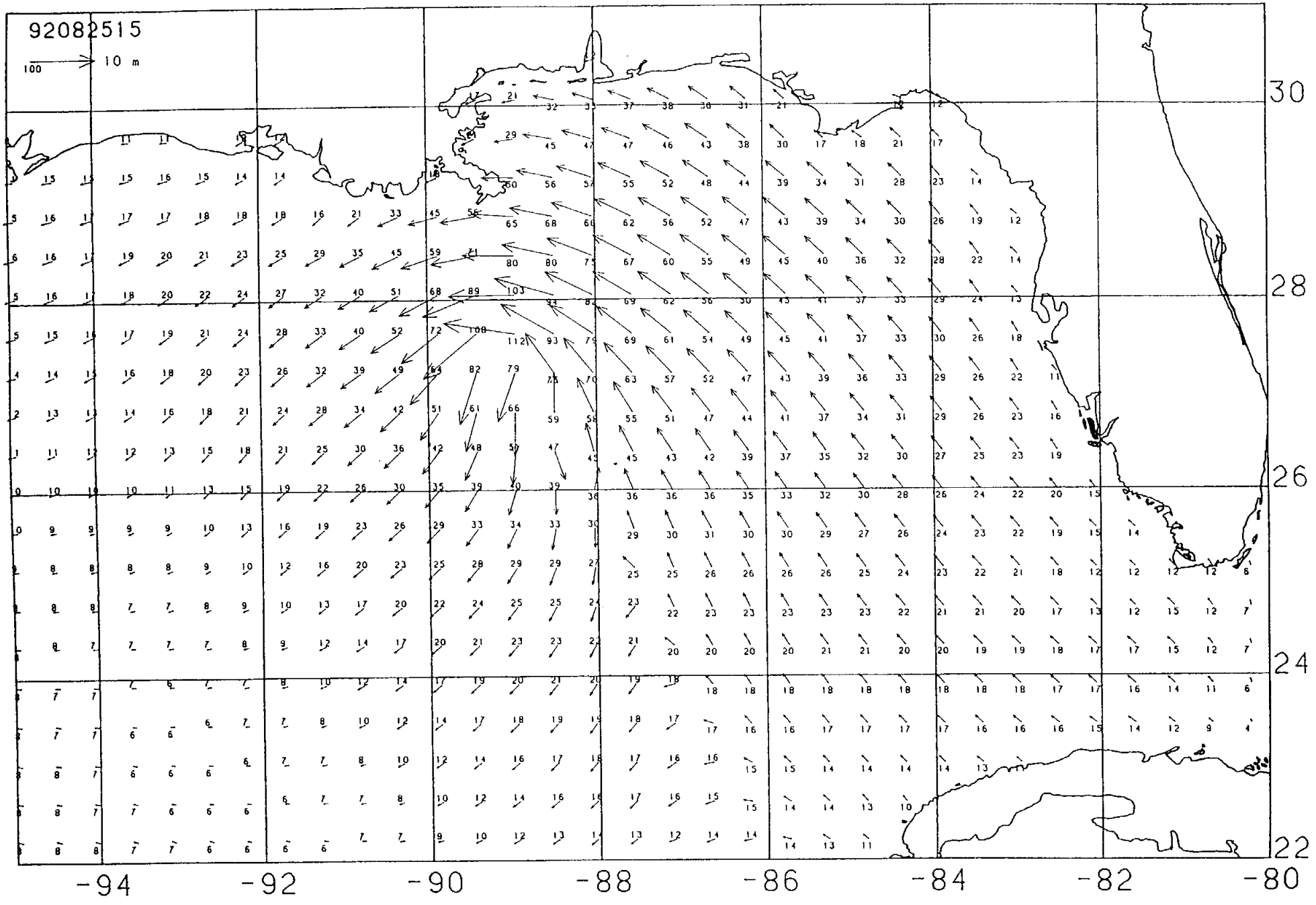

Plotted on 9-NOV-92 12:41 from file [ANDREW]ANDREW.FIELDS;2 4-NOV-1992 12:18

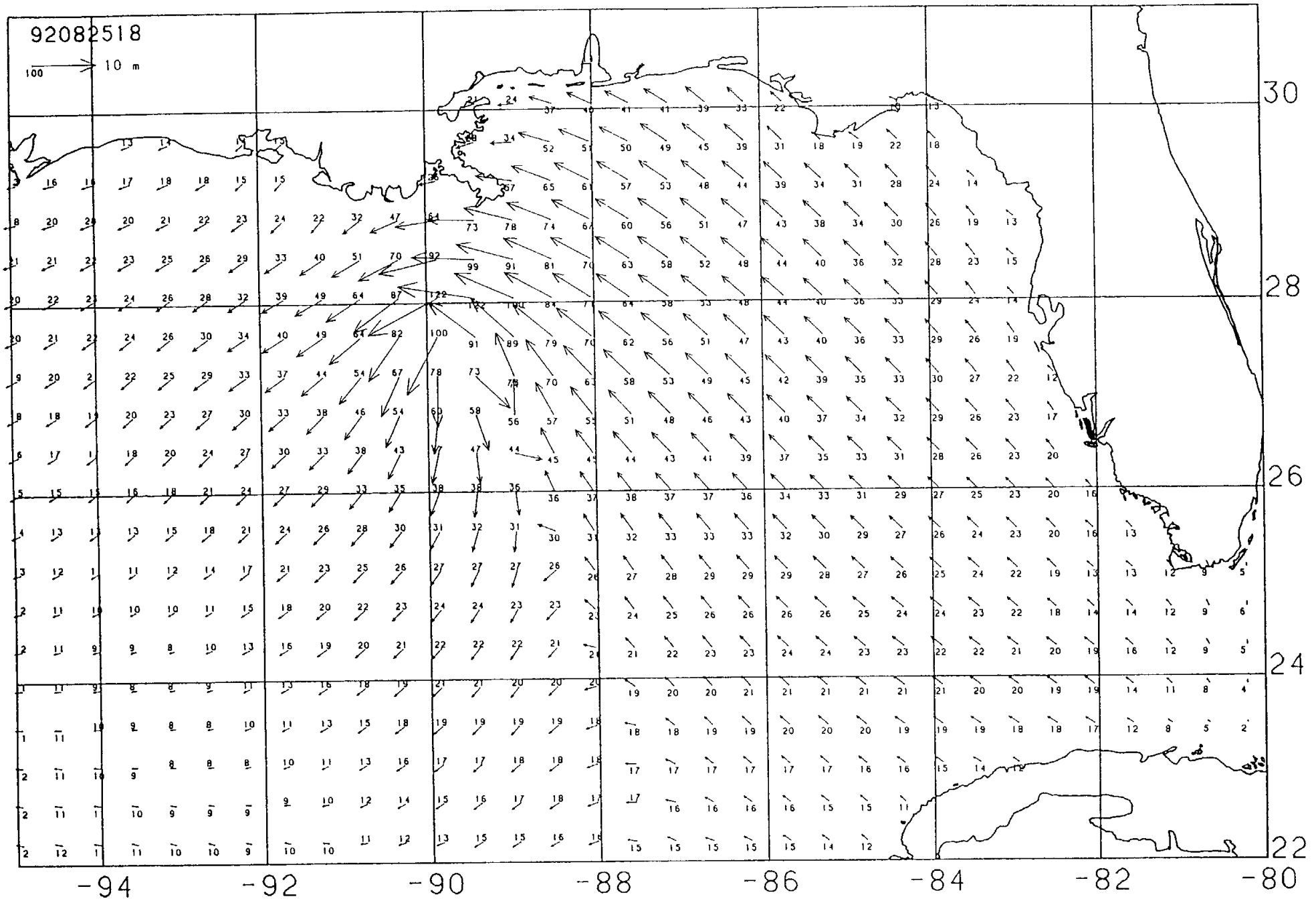

Plotted on 9-NOV-92 12:51 from file [ANDREW]ANDREW.FIELDS;2 4-NOV-1992 12:18

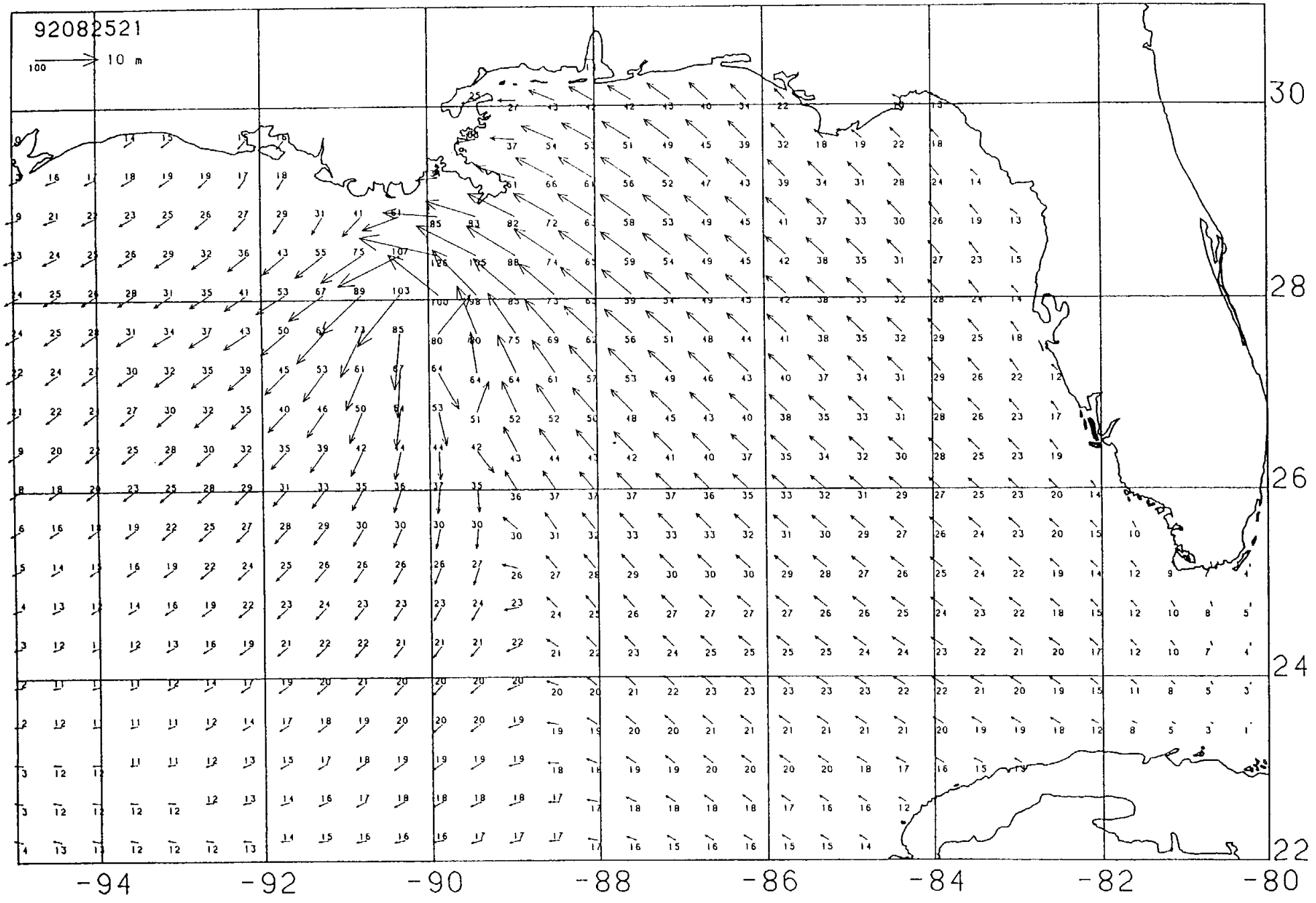

Plotted on 9-NOV-92 13:01 from file [ANDREW]ANDREW.FIELDS;2 4-NOV-1992 12:18

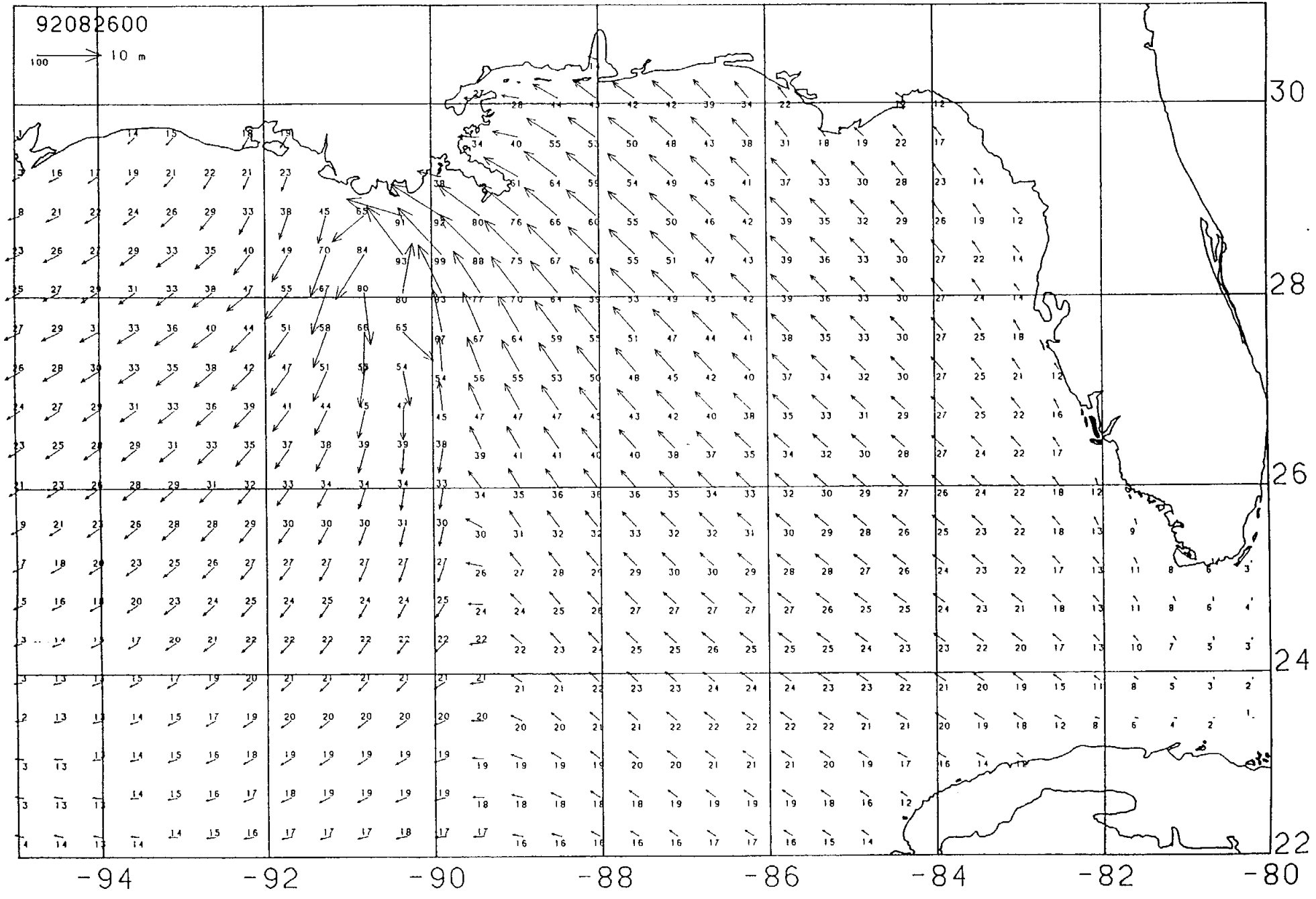

Plotted on 9-NOV-92 13:11 from file [ANDREW]ANDREW.FIELDS;2 4-NOV-1992 12:18

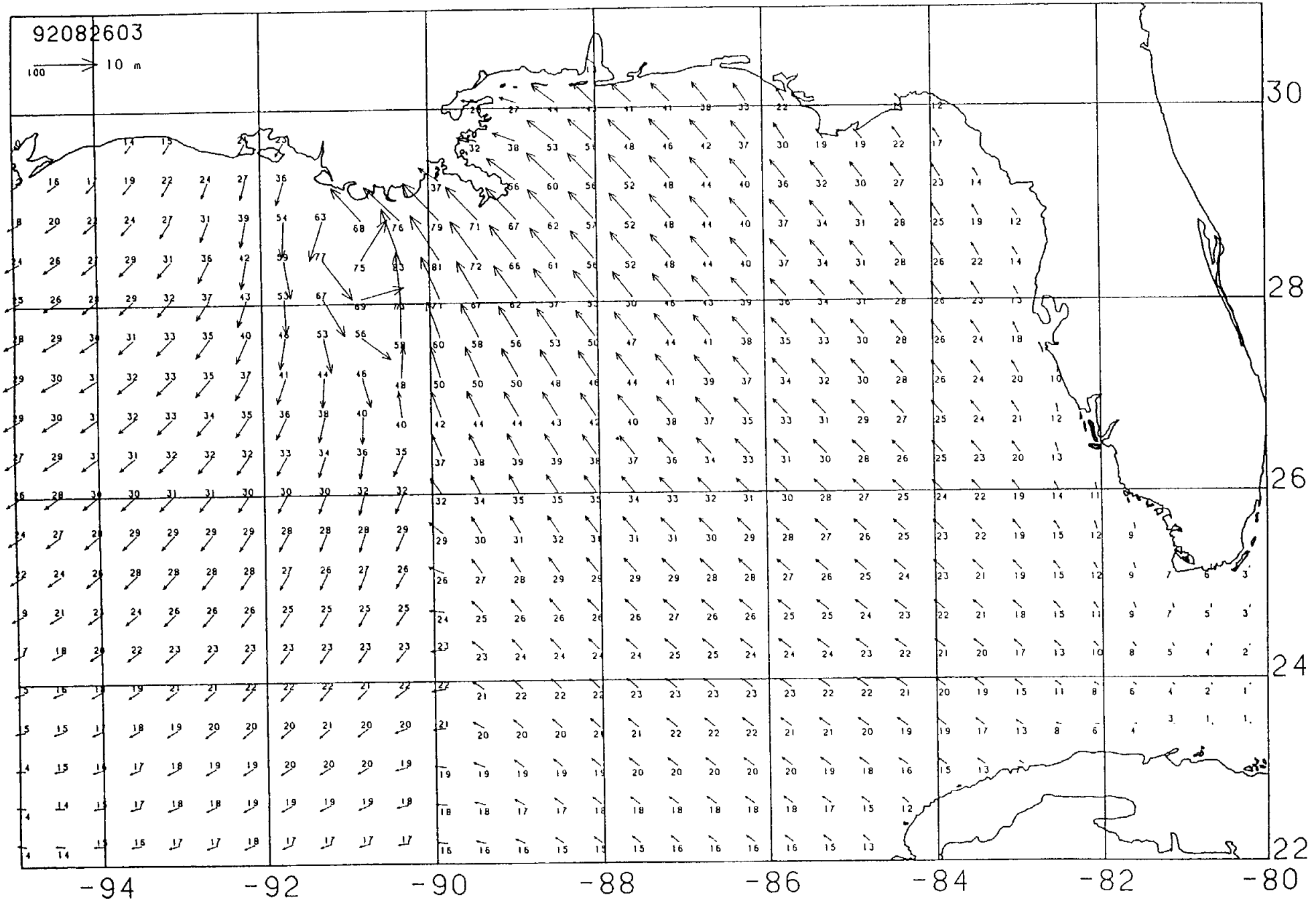

Plotted 9-NOV-92 13:21 from file [ANDREW]ANDREW.FIELDS;2 4-NOV 992 12:18

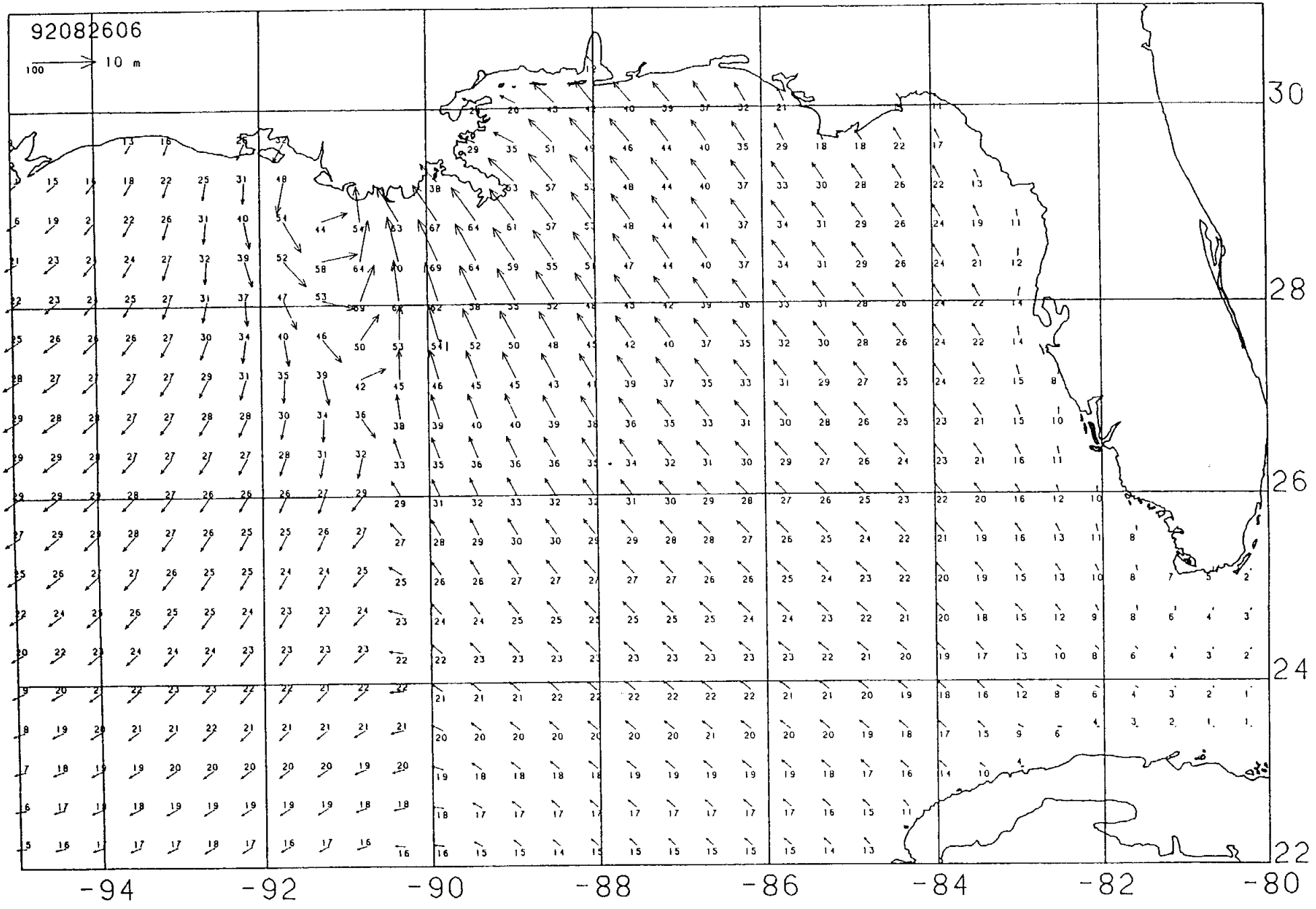

Plotted on 9-NOV-92 13:30 from file [ANDREW]ANDREW.FIELDS;2 4-NOV-1992 12:18

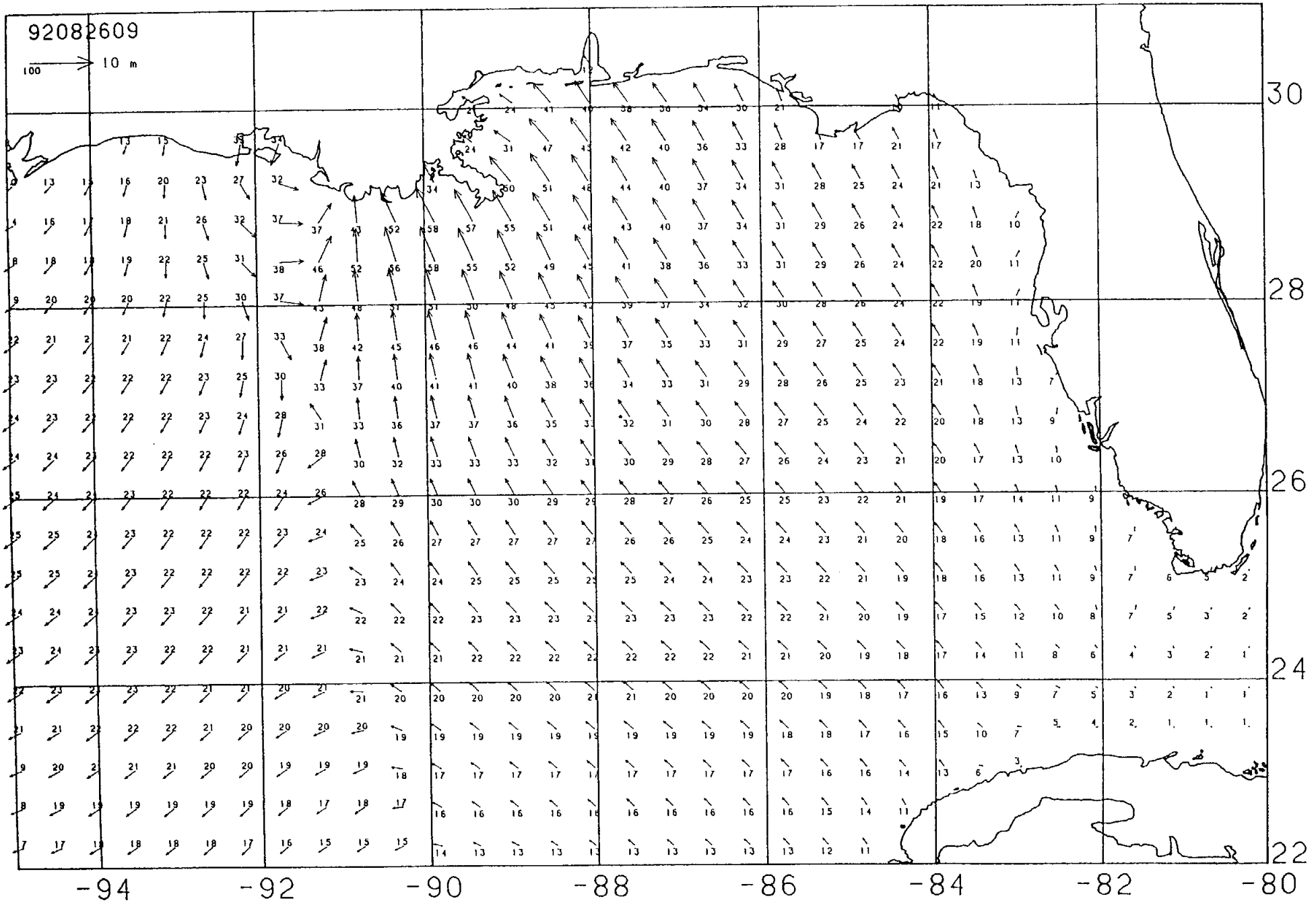

Plotted on 9-NOV-92 13:40 from file [ANDREW]ANDREW.FIELDS;2 4-NOV-1992 12:18

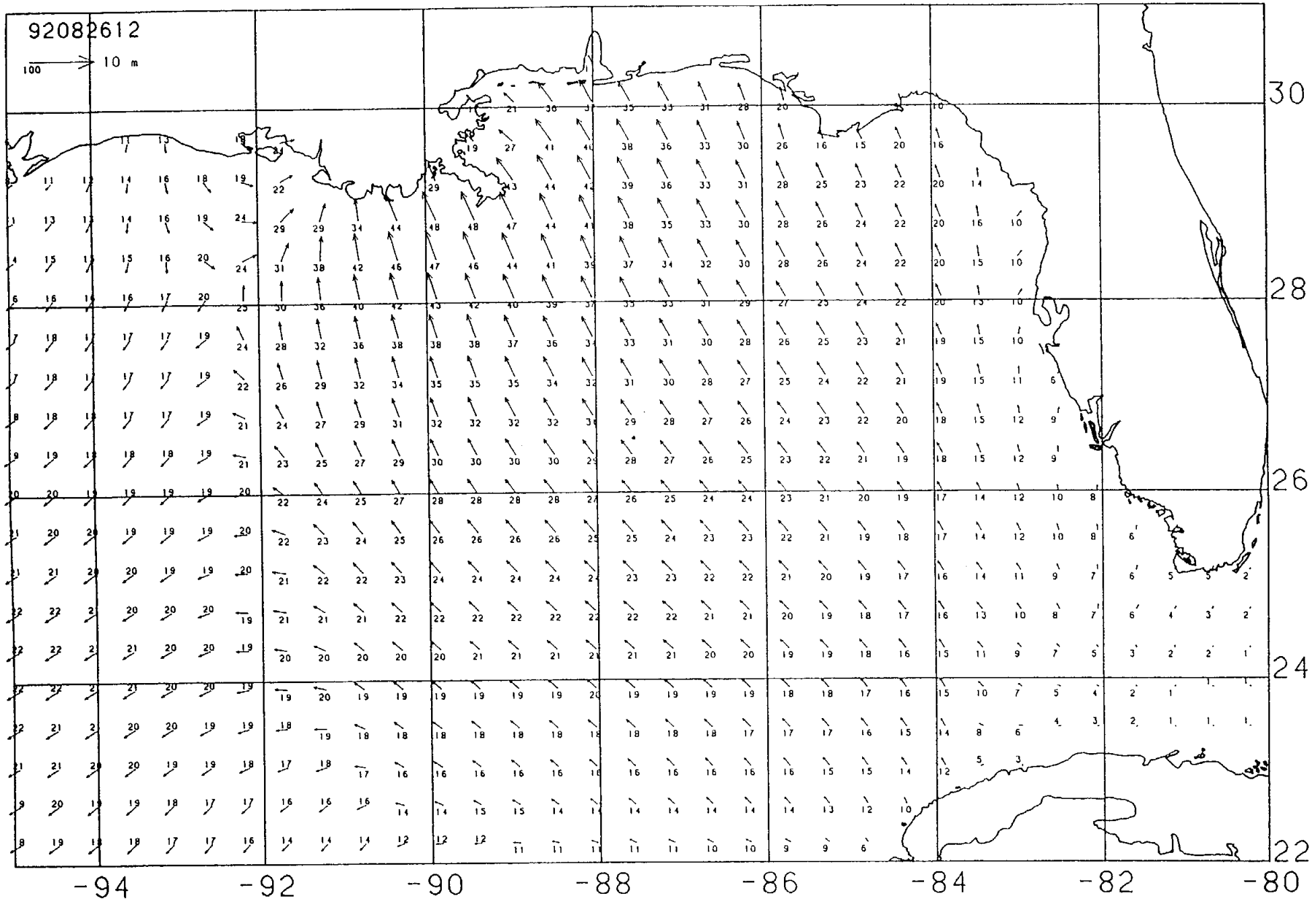

Plotted on 9-NOV-92 13:50 from file [ANDREW]ANDREW.FIELDS;2 4-NOV-1992 12:18

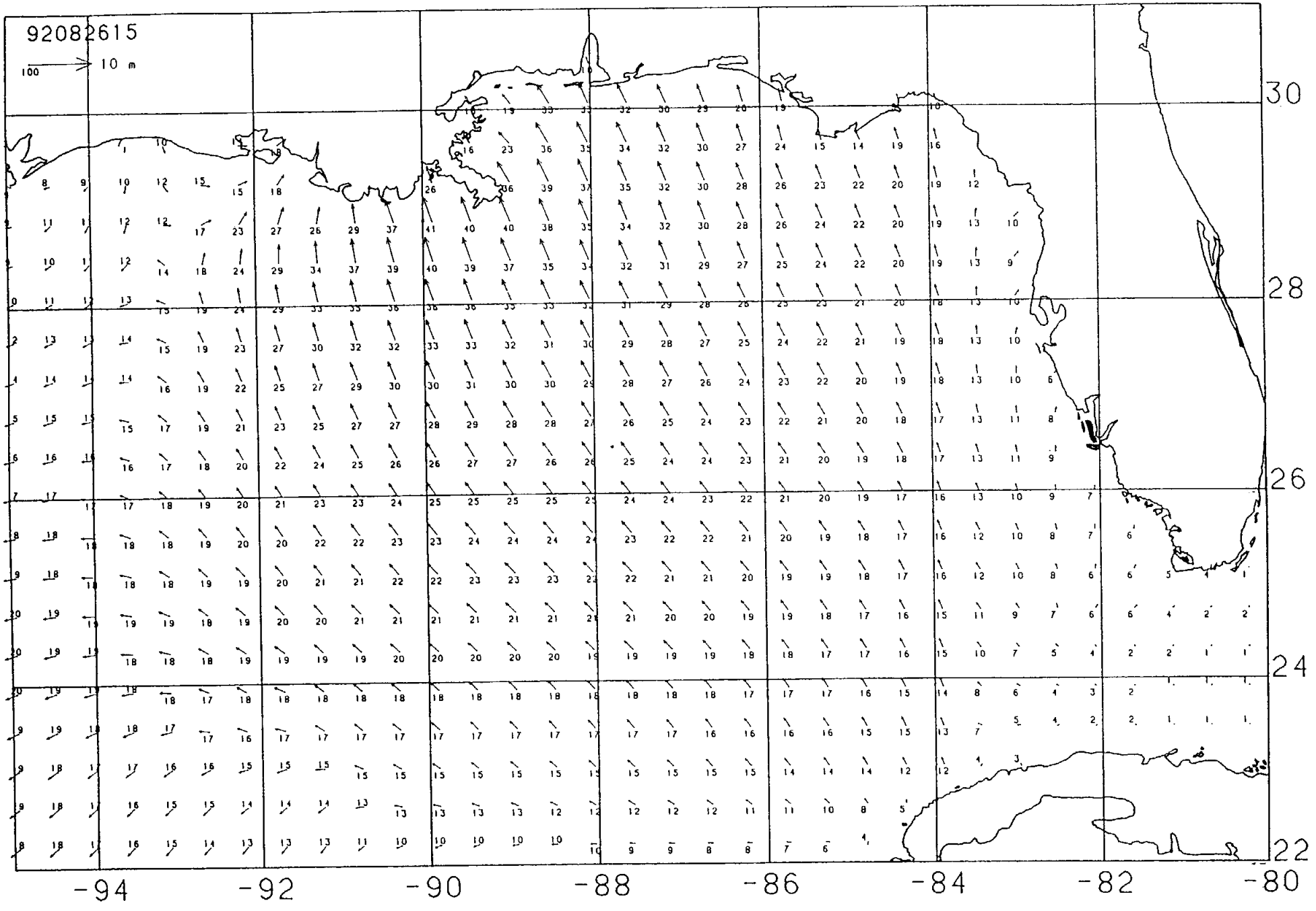

Plotted on 9-NOV-92 14:00 from file [ANDREW]ANDREW.FIELDS;2 4-NOV-1992 12:18

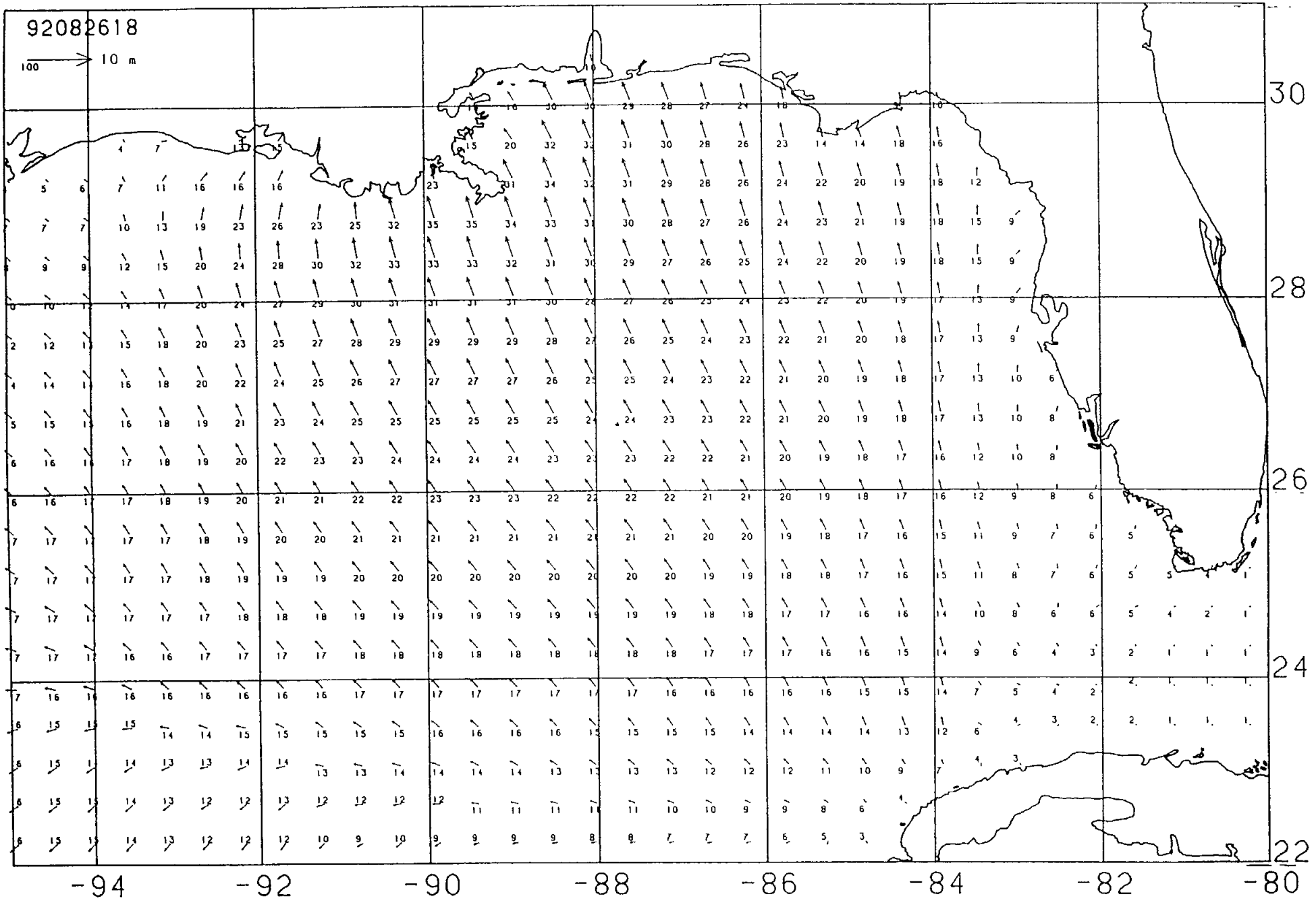

Appendix H

Listing of hindcast peak winds, sea states, currents and surge at 317 model grid points located in the area: 27N - 31N, 87W - 92W.

Explanation of Table.

Each line gives all hindcast and computed peaks at a grid point, including storm peak individual wave height and crest height computed from the time history using the Forristall distribution (1978) for wave height and the Haring et al. distribution (1978) for crest height.

GP	grid point number of 12-nm GUMSHOE grid
LAT	North latitude of grid point degrees (decimal)
LONG	West longitude of grid point degrees (decimal)
MAX WS	maximum average wind speed in storm at point, m/sec
ASSO WD	wind direction associated with MAX WS, degrees from which

The following nine quantities apply at time step of maximum HS

WS, WD	average wind speed (m/sec) and direction
MAX HS	maximum storm significant wave height, meters
TS	significant wave period, seconds
.74*TP	spectral peak period multiplied by 0.74, seconds (this is an approximation of zero-crossing period)
VMD	vector mean wave direction, degrees true, toward which
HSUR	surge with respect to mean sea level, centimeters
CS	depth averaged current speed, cm/sec
CD	depth averaged current direction, degrees true, toward which

The following quantities are storm maxima

MAX HSUR	maximum positive surge height in storm at point
MAX CS	maximum depth averaged current speed in storm at point cm/s
ASSO CD	current direction of MAX CS, degrees true,
FORR	maximum (median) individual wave height at point in storm, meters
HARING	maximum (median) individual crest height (with respect to still water) in storm at point), meters
W/HS	ratio of FORR/MAX HS
C/HS	ratio of HARING/HS

Hurricane ANDREW
Final Hindcast Results

gp	lat	long	max ws	asso wd	(ws	wd	max hs	ts	.74*tp	vmd	hsur	cs	cd)	max hsur	max cs	asso cd	forr	haring	w/hs	c/hs
3265.	27.03	-91.95	14.29	347.	13.51	308.	4.23	9.9	10.4	225.	10.3	0.6	202.	10.4	1.3	209.	7.51	4.15	1.7750	0.9807
3266.	27.03	-91.72	15.11	326.	14.31	299.	4.50	9.9	10.3	221.	11.3	0.9	193.	11.3	2.2	195.	7.92	4.38	1.7602	0.9724
3267.	27.03	-91.49	16.17	326.	15.15	289.	4.70	9.8	10.1	216.	12.4	0.4	206.	12.4	1.4	198.	8.33	4.61	1.7739	0.9807
3268.	27.03	-91.26	17.41	326.	16.34	290.	5.01	9.9	10.1	214.	13.2	0.3	199.	13.3	1.6	189.	8.83	4.88	1.7622	0.9747
3269.	27.03	-91.03	18.82	318.	17.87	290.	5.28	9.8	10.1	211.	12.6	1.5	182.	12.6	2.2	181.	9.34	5.17	1.7669	0.9779
3270.	27.03	-90.80	20.36	309.	18.86	279.	5.57	9.7	9.9	204.	14.1	0.7	179.	14.1	1.9	183.	9.87	5.47	1.7725	0.9826
3271.	27.03	-90.57	22.17	300.	20.80	278.	5.88	9.6	9.9	200.	12.7	1.5	178.	13.3	2.9	173.	10.43	5.78	1.7732	0.9824
3272.	27.03	-90.34	24.07	289.	22.80	276.	6.20	9.5	9.7	196.	15.3	1.4	171.	15.7	2.3	164.	10.96	6.07	1.7690	0.9802
3273.	27.03	-90.11	25.81	276.	23.81	262.	6.54	9.5	9.3	185.	16.6	1.2	166.	17.9	2.0	160.	11.51	6.38	1.7610	0.9761
3274.	27.03	-89.88	27.06	275.	26.92	260.	6.83	9.4	9.2	182.	19.2	1.2	166.	19.2	1.8	156.	11.95	6.62	1.7487	0.9697
3275.	27.03	-89.65	28.70	277.	28.21	259.	7.14	9.4	9.1	182.	23.3	1.4	167.	23.3	1.5	161.	12.39	6.87	1.7351	0.9629
3276.	27.03	-89.42	30.34	279.	29.94	260.	7.34	9.4	9.0	180.	24.2	1.1	169.	24.2	1.5	165.	12.64	7.01	1.7214	0.9552
3277.	27.03	-89.19	32.09	286.	31.13	259.	7.60	9.4	9.0	186.	25.9	0.4	167.	25.9	1.2	74.	12.94	7.18	1.7035	0.9448
3278.	27.03	-88.96	33.92	294.	33.32	266.	7.78	9.4	9.0	188.	28.4	1.1	179.	28.4	1.7	173.	13.27	7.37	1.7058	0.9473
3279.	27.03	-88.73	35.45	305.	34.68	274.	8.04	9.3	9.0	191.	29.8	0.4	194.	29.8	1.6	170.	13.76	7.64	1.7121	0.9504
3280.	27.03	-88.50	37.58	323.	35.11	287.	8.66	9.7	9.1	206.	29.8	0.2	275.	32.0	1.2	174.	14.62	8.11	1.6880	0.9362
3281.	27.03	-88.27	37.83	337.	37.83	337.	8.53	9.9	10.1	226.	24.9	0.5	243.	43.7	1.9	187.	14.57	8.08	1.7073	0.9467
3282.	27.03	-88.04	37.35	351.	36.93	350.	9.46	10.1	9.8	231.	38.3	0.5	249.	54.1	1.8	23.	15.60	8.64	1.6501	0.9138
3283.	27.03	-87.81	42.81	18.	42.81	18.	10.36	10.3	9.8	236.	28.3	0.7	233.	63.3	2.0	194.	16.73	9.25	1.6146	0.8931
3284.	27.03	-87.58	41.68	19.	40.88	95.	11.10	10.5	9.8	270.	54.6	0.8	238.	54.6	2.1	195.	18.05	10.01	1.6257	0.9014
3285.	27.03	-87.35	43.31	68.	43.31	68.	11.19	10.5	9.9	260.	36.2	1.8	204.	36.2	1.9	336.	18.16	10.06	1.6219	0.8989
3286.	27.03	-87.12	41.27	54.	38.55	110.	10.37	10.2	9.4	283.	35.2	0.8	277.	35.2	1.1	222.	17.57	9.75	1.6940	0.9401
3344.	27.23	-91.95	15.20	337.	14.80	311.	4.48	9.8	10.5	226.	9.5	0.8	211.	9.9	1.7	217.	7.93	4.38	1.7690	0.9762
3345.	27.23	-91.72	16.28	330.	15.79	302.	4.75	9.8	10.4	222.	9.6	1.3	198.	10.0	2.6	201.	8.39	4.63	1.7656	0.9754
3346.	27.23	-91.49	17.53	322.	17.09	303.	5.07	9.8	10.3	221.	11.0	0.4	260.	11.4	1.9	205.	8.95	4.95	1.7652	0.9762
3347.	27.23	-91.26	18.92	314.	18.19	293.	5.38	9.9	10.2	215.	11.8	0.5	214.	12.5	2.1	198.	9.52	5.27	1.7698	0.9793
3348.	27.23	-91.03	20.44	315.	19.97	295.	5.78	9.9	10.1	213.	12.3	1.5	189.	12.3	2.3	189.	10.18	5.64	1.7613	0.9761
3349.	27.23	-90.80	22.31	316.	21.31	283.	6.14	9.8	10.0	204.	14.1	1.2	189.	14.3	2.8	191.	10.84	6.01	1.7660	0.9798
3350.	27.23	-90.57	24.67	307.	23.90	283.	6.56	9.8	10.0	201.	14.6	1.5	184.	15.3	3.0	178.	11.55	6.41	1.7587	0.9761
3351.	27.23	-90.34	27.34	297.	25.34	270.	6.98	9.7	9.8	190.	17.5	1.9	174.	19.6	2.6	169.	12.26	6.81	1.7567	0.9755
3352.	27.23	-90.11	29.84	285.	28.07	268.	7.46	9.7	9.6	185.	20.9	1.8	173.	22.3	2.6	165.	12.98	7.21	1.7401	0.9666
3353.	27.23	-89.88	31.47	286.	31.41	268.	7.80	9.6	9.2	180.	24.4	1.8	174.	24.4	2.4	168.	13.56	7.53	1.7389	0.9658
3354.	27.23	-89.65	34.00	292.	32.92	268.	8.08	9.6	9.2	182.	30.2	1.1	172.	30.2	1.3	155.	14.00	7.78	1.7333	0.9630
3355.	27.23	-89.42	36.26	298.	35.32	274.	8.44	9.6	9.1	186.	31.6	1.5	179.	31.6	2.2	174.	14.44	8.02	1.7101	0.9499
3356.	27.23	-89.19	37.87	311.	37.87	311.	8.52	9.7	9.8	206.	27.4	0.4	234.	34.6	1.6	169.	14.61	8.11	1.7148	0.9526
3357.	27.23	-88.96	39.41	325.	39.41	325.	8.98	9.9	9.9	218.	32.5	0.7	218.	41.3	2.4	182.	15.26	8.48	1.6998	0.9443
3358.	27.23	-88.73	40.32	338.	40.32	338.	9.05	10.0	10.1	223.	27.8	0.5	238.	43.3	1.8	188.	15.26	8.47	1.6861	0.9361
3359.	27.23	-88.50	40.46	354.	40.46	354.	9.20	10.0	9.9	229.	22.8	0.6	231.	51.2	0.8	197.	15.68	8.70	1.7043	0.9463
3360.	27.23	-88.27	40.41	31.	40.41	31.	10.56	10.5	9.8	242.	48.5	0.9	225.	54.9	1.7	15.	17.15	9.52	1.6252	0.9016
3361.	27.23	-88.04	43.88	33.	40.25	115.	10.91	10.3	9.7	276.	64.3	0.7	274.	64.3	1.0	217.	18.26	10.13	1.6732	0.9281
3362.	27.23	-87.81	42.73	86.	42.73	86.	11.27	10.5	9.8	269.	42.3	1.6	204.	42.3	1.6	204.	18.33	10.17	1.6267	0.9024
3363.	27.23	-87.58	41.34	71.	41.34	71.	10.78	10.5	9.9	265.	31.1	1.3	213.	31.1	1.3	213.	17.86	9.92	1.6564	0.9195
3364.	27.23	-87.35	38.52	57.	37.60	99.	10.26	10.2	9.6	281.	26.0	0.9	307.	26.0	1.1	355.	17.15	9.52	1.6716	0.9274
3365.	27.23	-87.12	36.89	83.	36.89	83.	9.87	10.1	9.7	274.	23.0	0.8	246.	23.0	0.9	268.	16.47	9.14	1.6686	0.9260
3423.	27.44	-91.95	16.29	334.	16.15	315.	4.68	9.6	10.7	227.	12.1	1.2	262.	13.1	3.8	231.	8.27	4.57	1.7680	0.9773

Hurricane ANDREW
Final Hindcast Results

gp	lat	long	max ws	asso wd	(ws	wd	max hs	ts	.74*tp	vmd	hsur	cs	) cd	max hsur	max cs	asso cd	forr	haring	w/hs	c/hs
3424.	27.44	-91.72	17.56	327.	17.37	307.	5.02	9.7	10.4	222.	11.3	2.4	208.	12.1	3.6	223.	8.89	4.92	1.7707	0.9790
3425.	27.44	-91.49	18.99	319.	18.80	308.	5.37	9.8	10.6	222.	14.1	1.2	248.	14.8	4.6	212.	9.50	5.26	1.7687	0.9791
3426.	27.44	-91.26	20.58	320.	20.27	299.	5.76	9.8	10.3	216.	16.4	1.7	217.	17.1	3.9	215.	10.25	5.68	1.7808	0.9865
3427.	27.44	-91.03	22.49	312.	22.42	301.	6.28	9.9	10.3	214.	18.4	1.9	213.	18.4	3.1	207.	11.06	6.14	1.7621	0.9776
3428.	27.44	-90.80	24.88	303.	24.40	290.	6.82	9.9	10.0	205.	20.2	2.7	201.	20.2	4.5	197.	11.97	6.65	1.7539	0.9745
3429.	27.44	-90.57	27.51	305.	27.32	291.	7.35	9.9	10.0	203.	22.3	1.6	214.	23.0	4.0	191.	12.82	7.13	1.7452	0.9706
3430.	27.44	-90.34	30.85	310.	30.46	294.	7.84	9.9	10.0	200.	29.7	1.9	206.	29.7	4.0	183.	13.74	7.65	1.7523	0.9752
3431.	27.44	-90.11	34.85	300.	32.73	279.	8.47	9.9	9.8	188.	33.5	3.9	191.	33.5	5.7	182.	14.62	8.14	1.7269	0.9618
3432.	27.44	-89.88	37.17	306.	37.09	285.	8.98	9.9	9.6	186.	38.2	1.9	206.	38.9	3.5	179.	15.44	8.60	1.7189	0.9575
3433.	27.44	-89.65	39.54	319.	39.54	319.	9.30	10.0	9.9	205.	35.4	1.0	244.	50.4	2.1	189.	15.96	8.89	1.7175	0.9560
3434.	27.44	-89.42	41.00	333.	41.00	333.	9.33	9.9	9.4	210.	31.4	1.9	210.	54.3	2.8	193.	15.92	8.87	1.7053	0.9501
3435.	27.44	-89.19	42.37	347.	42.37	347.	9.96	10.2	9.9	223.	28.1	1.1	239.	63.2	1.4	220.	16.30	9.06	1.6367	0.9096
3436.	27.44	-88.96	42.67	359.	42.67	359.	9.95	10.2	9.9	228.	32.0	1.4	217.	55.8	1.8	217.	16.44	9.15	1.6514	0.9190
3437.	27.44	-88.73	41.07	6.	37.66	46.	10.78	10.7	9.9	248.	42.5	1.5	218.	60.2	1.5	218.	17.76	9.88	1.6477	0.9171
3438.	27.44	-88.50	44.36	46.	44.36	46.	11.29	10.6	10.0	250.	31.2	1.1	220.	50.5	1.3	227.	18.75	10.42	1.6600	0.9224
3439.	27.44	-88.27	42.75	42.	42.13	99.	11.34	10.5	9.8	275.	36.6	0.9	246.	36.6	1.4	231.	18.68	10.38	1.6472	0.9153
3440.	27.44	-88.04	41.82	81.	41.82	81.	11.06	10.5	9.9	270.	26.1	0.9	233.	30.6	1.3	229.	18.19	10.10	1.6451	0.9140
3441.	27.44	-87.81	39.55	67.	37.77	104.	10.30	10.2	9.5	285.	23.8	0.7	279.	24.4	1.1	275.	17.49	9.71	1.6979	0.9429
3442.	27.44	-87.58	37.01	90.	37.01	90.	10.00	10.1	9.7	279.	16.0	0.7	262.	16.1	1.0	271.	16.76	9.30	1.6757	0.9303
3443.	27.44	-87.35	34.47	79.	34.47	79.	9.34	10.1	9.8	275.	14.1	0.6	266.	14.1	1.1	298.	16.00	8.88	1.7131	0.9514
3444.	27.44	-87.12	32.63	71.	31.84	93.	9.00	9.9	9.2	284.	12.4	0.7	273.	12.4	1.0	289.	15.32	8.51	1.7030	0.9455
3502.	27.64	-91.95	17.55	293.	17.52	320.	4.87	9.5	10.5	228.	13.6	1.8	266.	15.2	5.8	218.	8.62	4.77	1.7698	0.9795
3503.	27.64	-91.72	19.01	312.	18.89	323.	5.19	9.5	10.7	228.	10.6	2.7	218.	14.9	4.6	228.	9.28	5.14	1.7870	0.9899
3504.	27.64	-91.49	20.62	303.	20.62	303.	5.67	9.6	10.2	218.	14.5	2.2	236.	15.6	6.3	213.	10.12	5.61	1.7835	0.9895
3505.	27.64	-91.26	22.52	305.	22.52	305.	6.18	9.8	10.3	217.	16.2	2.9	219.	17.2	5.5	215.	10.95	6.08	1.7732	0.9847
3506.	27.64	-91.03	24.90	309.	24.78	295.	6.74	9.9	10.1	210.	18.8	2.9	221.	19.1	4.2	230.	11.95	6.65	1.7746	0.9870
3507.	27.64	-90.80	27.66	299.	27.66	299.	7.33	10.0	10.2	207.	21.0	3.9	207.	21.0	5.7	199.	12.97	7.22	1.7707	0.9856
3508.	27.64	-90.57	31.13	304.	31.13	304.	8.13	10.1	10.1	208.	24.2	2.4	226.	25.4	5.3	196.	14.26	7.95	1.7531	0.9770
3509.	27.64	-90.34	34.97	310.	34.97	310.	8.83	10.2	10.1	208.	34.9	2.6	227.	36.2	5.7	191.	15.35	8.57	1.7394	0.9706
3510.	27.64	-90.11	40.03	324.	40.03	324.	9.72	10.3	10.0	212.	32.7	3.8	211.	41.2	7.0	191.	16.75	9.35	1.7228	0.9622
3511.	27.64	-89.88	42.29	336.	37.72	318.	10.02	10.3	9.8	209.	46.1	2.8	227.	54.5	4.6	194.	17.07	9.53	1.7035	0.9514
3512.	27.64	-89.65	43.71	352.	43.71	352.	10.61	10.4	9.9	224.	37.5	1.9	240.	75.5	3.3	212.	17.67	9.87	1.6655	0.9303
3513.	27.64	-89.42	43.97	7.	43.97	7.	10.76	10.5	10.0	231.	29.9	2.5	214.	73.6	3.0	220.	17.93	10.01	1.6663	0.9302
3514.	27.64	-89.19	42.38	12.	40.67	59.	11.63	10.9	10.1	253.	40.7	2.2	221.	64.9	2.5	305.	19.09	10.65	1.6418	0.9155
3515.	27.64	-88.96	44.88	53.	44.88	53.	11.76	10.8	10.2	253.	37.4	2.5	208.	43.1	2.5	208.	19.51	10.87	1.6597	0.9247
3516.	27.64	-88.73	43.85	50.	42.64	98.	11.49	10.6	9.8	275.	38.2	1.5	230.	38.2	1.8	256.	19.26	10.73	1.6764	0.9343
3517.	27.64	-88.50	42.23	86.	42.23	86.	11.35	10.6	9.9	273.	32.7	1.4	220.	32.7	1.6	294.	18.79	10.46	1.6550	0.9212
3518.	27.64	-88.27	40.66	75.	40.66	75.	10.71	10.4	9.9	270.	25.9	0.8	244.	25.9	1.5	306.	18.01	10.01	1.6816	0.9347
3519.	27.64	-88.04	37.43	95.	37.43	95.	10.19	10.2	9.7	282.	23.6	0.8	258.	23.6	1.4	243.	17.18	9.55	1.6866	0.9371
3520.	27.64	-87.81	35.27	83.	35.27	83.	9.61	10.1	9.7	278.	18.5	0.7	270.	20.5	1.5	317.	16.38	9.10	1.7044	0.9471
3521.	27.64	-87.58	33.34	76.	32.38	95.	9.09	9.9	9.2	286.	14.5	0.7	277.	15.2	1.1	252.	15.62	8.68	1.7175	0.9542
3522.	27.64	-87.35	31.15	88.	31.15	88.	8.72	9.8	9.2	283.	11.2	0.7	281.	13.5	1.1	318.	14.93	8.29	1.7123	0.9510
3523.	27.64	-87.12	29.32	82.	29.32	82.	8.20	9.7	9.4	280.	9.8	0.6	274.	12.1	0.9	271.	14.25	7.91	1.7382	0.9653
3582.	27.84	-91.72	21.03	290.	20.65	319.	5.50	9.4	10.3	226.	17.0	3.6	253.	18.8	10.6	222.	9.75	5.45	1.7722	0.9906
3583.	27.84	-91.49	22.75	288.	22.28	322.	6.03	9.7	10.4	228.	15.6	4.4	228.	18.5	9.4	227.	10.68	5.97	1.7722	0.9901

Hurricane ANDREW
Final Hindcast Results

gp	lat	long	max ws	asso wd	(ws	wd	max hs	ts	.74*tp	vmd	hsur	cs	) cd	max hsur	max cs	asso cd	forr	haring	w/hs	c/hs
3584.	27.84	-91.26	25.20	302.	24.78	314.	6.60	9.8	10.3	222.	18.4	5.8	223.	20.7	9.4	222.	11.74	6.58	1.7796	0.9970
3585.	27.84	-91.03	27.86	305.	27.86	305.	7.35	9.9	10.0	214.	22.4	5.6	226.	24.3	9.1	224.	12.95	7.26	1.7610	0.9878
3586.	27.84	-90.80	31.10	312.	31.10	312.	8.18	10.2	10.2	216.	23.3	6.9	211.	24.9	9.4	203.	14.23	7.97	1.7400	0.9750
3587.	27.84	-90.57	35.31	302.	35.31	302.	9.08	10.1	9.9	205.	27.9	5.3	221.	28.3	8.5	202.	15.68	8.78	1.7268	0.9668
3588.	27.84	-90.34	40.38	317.	40.38	317.	10.27	10.4	10.0	211.	44.3	5.9	221.	44.8	9.4	199.	17.39	9.76	1.6938	0.9503
3589.	27.84	-90.11	43.44	350.	42.91	340.	10.91	10.6	9.9	217.	49.0	6.4	218.	55.6	9.2	199.	18.40	10.35	1.6865	0.9481
3590.	27.84	-89.88	44.04	2.	43.82	18.	11.79	10.8	9.9	233.	47.7	4.4	233.	72.6	7.2	210.	19.36	10.88	1.6420	0.9224
3591.	27.84	-89.65	46.92	40.	46.92	40.	12.29	10.9	10.2	244.	52.7	3.8	229.	76.4	4.8	249.	20.07	11.25	1.6322	0.9149
3592.	27.84	-89.42	47.27	47.	45.26	100.	12.31	10.8	9.9	273.	58.8	3.6	234.	58.8	4.3	278.	20.77	11.63	1.6863	0.9444
3593.	27.84	-89.19	45.54	88.	45.54	88.	12.05	10.7	9.9	272.	43.7	2.9	228.	48.8	4.0	276.	20.30	11.35	1.6845	0.9424
3594.	27.84	-88.96	42.67	84.	42.67	84.	11.53	10.7	9.9	272.	30.6	2.2	228.	30.6	3.3	254.	19.42	10.85	1.6848	0.9415
3595.	27.84	-88.73	40.78	74.	40.78	74.	10.88	10.5	9.9	270.	25.5	1.5	224.	25.5	2.7	259.	18.51	10.32	1.7008	0.9484
3596.	27.84	-88.50	37.95	68.	37.82	92.	10.31	10.3	9.8	282.	22.6	1.2	236.	22.6	2.1	263.	17.62	9.81	1.7101	0.9519
3597.	27.84	-88.27	35.92	85.	35.92	85.	9.87	10.2	9.8	280.	19.2	0.8	255.	19.2	1.9	303.	16.83	9.36	1.7063	0.9490
3598.	27.84	-88.04	34.20	79.	34.20	79.	9.28	10.0	9.8	278.	17.8	0.7	255.	17.8	1.6	294.	16.07	8.93	1.7306	0.9621
3599.	27.84	-87.81	31.79	91.	31.79	91.	8.90	9.9	9.3	285.	16.2	0.7	275.	16.2	1.7	308.	15.31	8.51	1.7204	0.9563
3600.	27.84	-87.58	30.06	85.	30.06	85.	8.41	9.7	9.3	283.	12.7	0.6	278.	12.8	1.2	287.	14.61	8.12	1.7363	0.9650
3601.	27.84	-87.35	28.53	80.	27.95	93.	7.97	9.5	8.9	288.	11.5	0.7	293.	11.5	1.3	307.	13.94	7.75	1.7498	0.9723
3602.	27.84	-87.12	26.89	88.	26.89	88.	7.65	9.4	8.9	286.	8.9	0.6	281.	10.4	1.0	292.	13.36	7.42	1.7459	0.9702
3660.	28.05	-91.95	21.49	298.	20.13	333.	5.19	9.1	10.8	236.	11.6	7.8	248.	20.0	19.0	249.	9.12	5.27	1.7589	1.0170
3661.	28.05	-91.72	23.59	287.	22.20	327.	5.70	9.3	10.8	232.	15.7	8.3	248.	18.9	21.6	226.	10.12	5.89	1.7751	1.0326
3662.	28.05	-91.49	25.81	287.	23.82	331.	6.33	9.7	10.9	236.	17.1	9.6	238.	20.6	20.7	236.	11.26	6.52	1.7793	1.0306
3663.	28.05	-91.26	28.14	298.	26.83	325.	7.06	9.9	10.7	231.	26.2	12.7	237.	27.8	22.0	250.	12.58	7.32	1.7811	1.0363
3664.	28.05	-91.03	31.62	304.	29.33	332.	7.76	10.1	10.8	231.	21.9	12.8	235.	29.4	21.8	249.	13.86	8.25	1.7870	1.0640
3665.	28.05	-90.80	35.37	312.	34.11	329.	8.94	10.4	10.6	227.	28.5	13.3	226.	37.4	21.6	207.	15.45	8.97	1.7283	1.0037
3666.	28.05	-90.57	40.30	327.	40.30	327.	9.86	10.3	10.1	214.	31.4	15.6	217.	36.3	23.9	202.	17.04	9.95	1.7285	1.0093
3667.	28.05	-90.34	45.20	349.	45.20	349.	11.42	10.8	10.3	227.	45.5	13.7	215.	56.0	20.5	201.	18.79	10.80	1.6446	0.9457
3668.	28.05	-90.11	48.40	14.	48.40	14.	12.28	11.1	10.5	235.	46.8	9.6	226.	70.8	14.0	214.	19.91	11.34	1.6219	0.9236
3669.	28.05	-89.88	48.89	33.	43.65	69.	12.76	11.3	10.6	260.	62.5	9.2	227.	82.6	13.0	240.	21.22	12.00	1.6623	0.9404
3670.	28.05	-89.65	50.51	71.	50.51	71.	13.08	11.1	10.3	263.	50.6	5.5	235.	55.1	8.1	257.	21.79	12.30	1.6659	0.9404
3671.	28.05	-89.42	47.23	95.	47.23	95.	12.23	10.7	9.9	279.	45.1	4.2	255.	45.1	6.7	280.	20.86	11.70	1.7052	0.9569
3672.	28.05	-89.19	43.44	89.	43.44	89.	11.38	10.5	9.8	278.	37.5	3.2	246.	37.5	5.7	279.	19.61	11.00	1.7233	0.9664
3673.	28.05	-88.96	39.51	84.	39.51	84.	10.56	10.3	9.8	278.	26.7	2.2	237.	26.7	3.9	250.	18.42	10.30	1.7451	0.9760
3674.	28.05	-88.73	36.33	84.	36.33	84.	9.98	10.2	9.8	279.	21.6	1.4	244.	22.4	2.9	257.	17.40	9.71	1.7426	0.9725
3675.	28.05	-88.50	34.51	78.	34.51	78.	9.47	10.1	9.8	278.	18.0	1.1	236.	18.7	2.4	278.	16.54	9.22	1.7469	0.9735
3676.	28.05	-88.27	32.54	75.	32.23	89.	9.06	9.9	9.4	284.	13.3	0.9	256.	15.0	2.0	293.	15.75	8.77	1.7384	0.9679
3677.	28.05	-88.04	30.76	86.	30.76	86.	8.64	9.8	9.4	284.	13.3	0.8	253.	13.7	1.8	287.	15.03	8.36	1.7402	0.9683
3678.	28.05	-87.81	29.35	82.	29.35	82.	8.16	9.7	9.3	283.	12.7	0.6	275.	12.7	1.7	299.	14.36	7.99	1.7595	0.9789
3679.	28.05	-87.58	27.56	90.	27.56	90.	7.81	9.5	8.9	288.	10.2	0.7	271.	10.5	1.2	282.	13.72	7.63	1.7558	0.9764
3680.	28.05	-87.35	26.18	86.	25.70	96.	7.46	9.3	8.8	292.	9.3	0.7	289.	10.0	1.3	300.	13.15	7.31	1.7639	0.9809
3681.	28.05	-87.12	25.01	83.	24.67	93.	7.13	9.2	8.8	290.	8.9	0.7	289.	8.9	1.1	287.	12.61	7.01	1.7694	0.9837
3739.	28.25	-91.95	23.67	307.	23.03	316.	4.87	7.7	8.8	198.	16.7	8.4	248.	21.8	22.1	184.	8.98	5.56	1.8441	1.1419
3740.	28.25	-91.72	26.47	297.	24.88	287.	5.58	8.1	7.8	161.	25.9	10.2	192.	25.9	24.0	191.	10.13	6.34	1.8174	1.1371
3741.	28.25	-91.49	29.22	298.	29.13	285.	6.64	8.7	8.5	160.	27.7	17.9	202.	32.1	26.7	193.	11.69	7.23	1.7600	1.0879
3742.	28.25	-91.26	32.08	299.	32.04	285.	7.40	8.9	8.6	156.	38.8	38.5	204.	38.8	38.5	204.	13.19	8.22	1.7838	1.1117

Hurricane ANDREW
Final Hindcast Results

gp	lat	long	max ws	asso wd	(ws	wd	max hs	ts	.74*tp	vmd	hsur	cs	) cd	max hsur	max cs	asso cd	forr	haring	w/hs	c/hs
3743.	28.25	-91.03	35.89	303.	35.89	303.	8.23	9.3	8.9	189.	45.2	52.2	223.	46.8	56.6	209.	14.51	9.26	1.7627	1.1254
3744.	28.25	-90.80	40.40	321.	40.40	321.	9.48	9.8	9.3	206.	47.8	67.3	227.	57.9	77.5	217.	16.28	10.53	1.7178	1.1109
3745.	28.25	-90.57	43.22	352.	43.22	352.	10.54	10.4	10.1	230.	40.4	58.5	235.	69.2	95.0	220.	17.73	11.59	1.6813	1.0989
3746.	28.25	-90.34	46.20	21.	46.20	21.	11.90	10.8	9.7	240.	60.3	79.2	233.	87.2	101.0	241.	19.58	12.51	1.6448	1.0508
3747.	28.25	-90.11	50.67	45.	50.67	45.	12.99	11.1	10.7	251.	46.3	49.9	234.	76.0	79.1	246.	21.30	13.01	1.6398	1.0015
3748.	28.25	-89.88	49.17	89.	49.17	89.	13.26	11.2	10.4	274.	47.5	30.1	240.	53.8	45.1	260.	22.04	12.79	1.6625	0.9646
3749.	28.25	-89.65	47.80	79.	47.80	79.	12.40	10.9	10.1	273.	30.9	7.0	247.	32.9	11.7	273.	21.16	11.97	1.7061	0.9650
3750.	28.25	-89.42	43.27	94.	43.27	94.	11.45	10.5	9.8	284.	27.6	6.1	263.	27.6	10.3	283.	19.79	11.14	1.7288	0.9727
3751.	28.25	-89.19	39.61	87.	39.61	87.	10.50	10.2	9.7	282.	22.1	5.2	245.	22.1	9.2	276.	18.50	10.40	1.7619	0.9906
3752.	28.25	-88.96	36.38	86.	36.38	86.	9.81	10.0	9.6	282.	18.3	3.1	233.	18.3	5.4	246.	17.38	9.73	1.7718	0.9924
3753.	28.25	-88.73	33.57	84.	33.57	84.	9.25	9.9	9.5	283.	16.5	1.8	245.	16.5	3.9	254.	16.43	9.18	1.7759	0.9920
3754.	28.25	-88.50	31.15	85.	31.15	85.	8.78	9.8	9.5	283.	14.0	1.3	254.	14.8	3.1	262.	15.58	8.70	1.7743	0.9900
3755.	28.25	-88.27	29.77	81.	29.77	81.	8.34	9.7	9.4	283.	10.8	0.8	266.	11.8	2.2	274.	14.82	8.26	1.7784	0.9912
3756.	28.25	-88.04	28.25	79.	28.04	89.	7.98	9.5	8.9	288.	9.6	0.8	261.	10.5	1.9	269.	14.16	7.89	1.7757	0.9889
3757.	28.25	-87.81	26.93	78.	26.86	87.	7.62	9.4	8.9	287.	9.5	0.7	275.	9.8	1.6	271.	13.55	7.55	1.7784	0.9901
3758.	28.25	-87.58	25.81	85.	25.30	93.	7.31	9.3	8.8	291.	7.8	0.8	266.	8.0	1.5	256.	13.00	7.24	1.7781	0.9898
3759.	28.25	-87.35	24.46	82.	24.44	91.	7.00	9.2	8.8	290.	7.6	0.9	286.	7.6	1.7	269.	12.47	6.94	1.7803	0.9911
3760.	28.25	-87.12	23.38	88.	23.08	96.	6.72	9.0	8.7	294.	7.2	1.1	278.	7.2	1.9	266.	11.96	6.66	1.7817	0.9922
3818.	28.45	-91.95	25.78	318.	25.78	318.	4.87	7.4	6.4	182.	14.9	3.7	230.	21.1	22.7	170.	8.78	5.58	1.8019	1.1457
3819.	28.45	-91.72	29.47	311.	28.05	299.	5.88	8.0	7.7	158.	25.6	14.3	171.	25.6	29.3	168.	10.38	6.78	1.7653	1.1520
3820.	28.45	-91.49	33.41	302.	33.41	302.	7.06	8.5	8.6	158.	27.6	22.9	191.	32.0	32.2	160.	12.15	8.10	1.7218	1.1486
3821.	28.45	-91.26	37.18	309.	37.18	309.	7.77	8.8	8.4	160.	45.1	57.5	202.	48.6	57.5	202.	13.59	9.21	1.7489	1.1854
3822.	28.45	-91.03	40.77	332.	40.77	332.	8.35	9.1	8.9	196.	45.4	70.7	228.	59.5	82.4	215.	14.42	9.93	1.7257	1.1888
3823.	28.45	-90.80	45.09	356.	45.09	356.	9.36	9.7	9.2	222.	53.0	90.0	235.	78.4	111.4	227.	15.59	10.70	1.6648	1.1431
3824.	28.45	-90.57	48.04	17.	48.04	17.	10.42	10.2	9.8	238.	47.2	93.4	236.	98.3	136.4	235.	17.00	11.68	1.6306	1.1203
3825.	28.45	-90.34	48.03	32.	45.61	70.	11.42	10.6	10.2	263.	73.2	119.1	240.	88.8	136.4	249.	19.09	13.10	1.6715	1.1472
3826.	28.45	-90.11	50.20	67.	50.20	67.	12.39	10.8	10.6	265.	48.0	65.8	235.	63.6	87.0	256.	21.06	13.92	1.7006	1.1242
3827.	28.45	-89.88	47.29	91.	47.29	91.	12.60	11.0	10.2	283.	42.3	29.0	242.	46.8	35.6	254.	21.19	12.27	1.6818	0.9742
3828.	28.45	-89.65	43.16	82.	42.28	101.	11.51	10.6	9.8	292.	30.5	13.3	270.	30.9	15.3	278.	19.90	11.27	1.7294	0.9798
3829.	28.45	-89.42	39.37	79.	39.15	92.	10.63	10.3	9.7	288.	26.5	13.1	267.	26.5	17.3	279.	18.59	10.59	1.7497	0.9966
3830.	28.45	-89.19	36.36	89.	36.36	89.	9.81	10.0	9.3	286.	19.2	10.1	256.	21.8	14.9	278.	17.45	9.88	1.7783	1.0067
3831.	28.45	-88.96	33.68	86.	33.68	86.	9.14	9.8	9.0	285.	15.5	4.4	231.	17.2	6.4	240.	16.45	9.23	1.7999	1.0105
3832.	28.45	-88.73	31.34	86.	31.34	86.	8.62	9.7	9.0	286.	14.2	2.4	243.	14.8	4.1	249.	15.54	8.70	1.8036	1.0092
3833.	28.45	-88.50	29.28	92.	29.23	86.	8.16	9.6	8.9	287.	13.1	1.5	257.	13.2	3.0	259.	14.76	8.24	1.8080	1.0097
3834.	28.45	-88.27	27.48	92.	27.48	92.	7.79	9.4	8.8	291.	11.1	1.2	281.	11.3	2.0	272.	14.07	7.85	1.8065	1.0074
3835.	28.45	-88.04	26.28	84.	25.82	92.	7.48	9.3	8.8	291.	9.2	0.9	274.	10.2	1.8	268.	13.46	7.50	1.8003	1.0034
3836.	28.45	-87.81	25.16	83.	24.96	90.	7.18	9.3	8.8	290.	7.7	0.8	281.	9.8	1.6	265.	12.90	7.18	1.7963	1.0006
3837.	28.45	-87.58	24.16	82.	23.63	95.	6.88	9.1	8.7	294.	5.8	1.0	271.	8.1	1.9	254.	12.37	6.89	1.7983	1.0019
3838.	28.45	-87.35	23.17	87.	22.82	94.	6.60	9.0	8.7	293.	6.3	1.2	278.	7.7	2.4	259.	11.88	6.63	1.8001	1.0046
3839.	28.45	-87.12	22.13	86.	22.09	92.	6.33	8.9	8.7	292.	6.1	1.3	276.	6.5	2.9	265.	11.43	6.39	1.8070	1.0102
3897.	28.65	-91.95	27.52	332.	27.14	323.	4.92	7.3	6.4	173.	12.9	11.0	110.	23.8	30.0	144.	8.82	5.81	1.7937	1.1820
3898.	28.65	-91.72	32.06	329.	31.22	317.	6.06	8.0	7.8	165.	19.3	22.5	152.	27.3	38.7	153.	10.56	7.21	1.7420	1.1890
3899.	28.65	-91.49	37.59	327.	35.52	310.	6.95	8.5	8.3	154.	29.1	41.6	167.	30.9	49.5	154.	12.09	8.30	1.7410	1.1956
3900.	28.65	-91.26	41.64	342.	41.64	342.	7.47	8.6	8.9	177.	42.2	80.1	207.	58.5	80.1	207.	12.65	8.43	1.6944	1.1292
3901.	28.65	-91.03	43.46	359.	42.69	2.	7.59	8.5	8.2	201.	55.1	107.3	227.	82.4	108.1	227.	12.86	8.38	1.6942	1.1036

Hurricane ANDREW
Final Hindcast Results

gp	lat	long	max ws	asso wd	(ws	wd	max hs	ts	.74*tp	vmd	hsur	cs	) cd	max hsur	max cs	asso cd	forr	haring	w/hs	c/hs
3902.	28.65	-90.80	44.68	16.	43.93	34.	7.94	9.0	9.0	235.	60.3	132.0	238.	97.4	146.0	243.	13.46	8.29	1.6948	1.0444
3903.	28.65	-90.57	49.53	51.	41.70	109.	9.18	10.0	11.7	289.	93.3	175.0	249.	119.1	175.0	249.	15.71	9.59	1.7108	1.0448
3904.	28.65	-90.34	48.57	89.	48.57	89.	10.78	10.2	10.9	279.	83.8	142.6	252.	96.0	146.9	262.	18.00	11.81	1.6695	1.0949
3905.	28.65	-90.11	46.83	78.	44.86	105.	11.51	10.5	10.2	292.	67.9	90.0	256.	73.2	90.0	256.	19.67	13.15	1.7094	1.1428
3906.	28.65	-89.88	42.55	92.	42.55	92.	11.40	10.6	10.0	290.	42.2	42.6	249.	51.4	45.7	253.	19.53	11.51	1.7134	1.0099
3907.	28.65	-89.65	39.38	85.	38.20	100.	10.59	10.3	9.8	296.	30.4	47.1	277.	30.4	49.9	279.	18.44	11.24	1.7425	1.0617
3908.	28.65	-89.42	36.09	82.	35.95	93.	9.89	10.1	9.4	292.	23.6	44.6	272.	24.1	52.3	276.	17.42	10.56	1.7609	1.0679
3909.	28.65	-89.19	33.56	81.	33.47	90.	9.18	9.8	9.0	290.	20.3	24.9	264.	22.1	32.0	272.	16.46	9.45	1.7929	1.0301
3910.	28.65	-88.96	31.45	88.	30.92	95.	8.62	9.6	8.8	294.	12.6	7.4	229.	16.5	8.2	232.	15.59	8.79	1.8073	1.0189
3911.	28.65	-88.73	29.54	87.	29.37	93.	8.16	9.4	8.8	293.	10.6	3.9	238.	14.4	4.7	244.	14.79	8.29	1.8130	1.0162
3912.	28.65	-88.50	27.84	92.	27.84	92.	7.77	9.3	8.8	292.	11.2	2.4	250.	13.2	3.3	257.	14.08	7.87	1.8130	1.0136
3913.	28.65	-88.27	26.25	96.	26.24	92.	7.42	9.2	8.8	293.	10.6	1.5	278.	11.1	2.2	271.	13.44	7.50	1.8117	1.0115
3914.	28.65	-88.04	24.82	96.	24.76	92.	7.07	9.1	8.7	293.	10.2	1.1	275.	10.2	1.9	268.	12.85	7.16	1.8166	1.0130
3915.	28.65	-87.81	23.69	87.	23.36	93.	6.76	9.1	8.7	293.	9.3	1.0	289.	9.8	1.7	264.	12.31	6.86	1.8206	1.0148
3916.	28.65	-87.58	22.78	86.	22.63	91.	6.48	9.0	8.7	293.	6.6	1.0	277.	8.4	2.2	255.	11.84	6.60	1.8264	1.0183
3917.	28.65	-87.35	21.95	85.	21.59	95.	6.22	8.8	8.3	296.	6.1	1.5	283.	8.1	3.0	252.	11.39	6.37	1.8330	1.0245
3918.	28.65	-87.12	21.12	89.	20.89	94.	5.98	8.7	8.3	295.	5.5	1.6	270.	7.4	3.5	265.	10.97	6.15	1.8349	1.0278
3976.	28.86	-91.95	28.79	338.	28.78	327.	4.79	7.0	6.6	170.	3.7	34.0	101.	27.4	47.5	93.	8.59	5.86	1.7929	1.2236
3977.	28.86	-91.72	33.73	337.	33.23	323.	5.73	7.7	7.8	161.	9.7	47.5	129.	30.2	57.5	115.	10.09	6.85	1.7611	1.1955
3978.	28.86	-91.49	40.26	353.	39.70	343.	6.25	8.2	9.0	173.	14.8	57.4	159.	35.3	66.6	151.	10.82	6.58	1.7296	1.0515
3979.	28.86	-91.26	43.60	9.	42.30	18.	6.30	8.3	10.0	199.	22.7	104.4	234.	77.9	104.4	234.	10.68	5.68	1.6965	0.9022
3980.	28.86	-91.03	46.23	25.	46.23	25.	5.53	7.6	8.8	209.	11.4	106.7	249.	144.2	155.9	266.	9.41	4.75	1.7023	0.8584
3981.	28.86	-90.80	48.46	67.	45.77	104.	7.40	9.1	10.9	286.	90.5	204.9	275.	166.1	204.9	275.	12.77	6.67	1.7245	0.9004
3982.	28.86	-90.57	48.41	72.	47.16	101.	8.10	9.4	11.0	289.	121.6	214.6	267.	163.9	214.6	267.	13.93	7.68	1.7203	0.9490
3983.	28.86	-90.34	45.34	93.	45.34	93.	9.07	9.5	11.0	287.	108.4	142.8	263.	127.1	142.8	263.	15.44	9.37	1.7026	1.0332
3984.	28.86	-90.11	41.58	83.	40.44	103.	9.04	9.5	10.2	295.	83.3	116.4	262.	90.1	117.5	259.	15.70	10.61	1.7365	1.1733
3985.	28.86	-89.88	38.56	80.	37.94	93.	9.29	9.7	9.9	293.	54.2	99.7	258.	63.2	99.7	258.	16.28	11.12	1.7524	1.1975
3986.	28.86	-89.65	35.71	89.	34.43	100.	9.29	9.8	9.8	301.	34.8	77.8	285.	40.9	77.8	285.	16.33	10.71	1.7578	1.1535
3987.	28.86	-89.42	33.57	85.	32.80	95.	8.39	9.5	9.7	294.	27.6	73.7	280.	36.0	75.0	282.	15.00	10.21	1.7864	1.2160
3988.	28.86	-89.19	31.28	84.	31.23	91.	8.54	9.6	8.9	294.	24.7	45.0	256.	25.6	47.3	257.	15.36	9.43	1.7987	1.1050
3989.	28.86	-88.96	29.48	83.	29.09	96.	8.18	9.5	8.8	296.	17.0	13.9	219.	18.0	14.5	193.	14.78	8.49	1.8081	1.0388
3990.	28.86	-88.73	27.96	89.	27.63	94.	7.77	9.3	8.8	295.	14.3	6.2	234.	15.5	6.6	235.	14.12	7.98	1.8169	1.0270
3991.	28.86	-88.50	26.57	88.	26.44	93.	7.40	9.2	8.7	294.	11.7	3.7	247.	13.8	4.1	252.	13.48	7.57	1.8213	1.0230
3992.	28.86	-88.27	25.28	92.	25.28	92.	7.05	9.1	8.7	295.	10.1	1.9	271.	11.2	2.5	270.	12.87	7.20	1.8252	1.0213
3993.	28.86	-88.04	24.06	95.	23.92	93.	6.73	9.0	8.6	295.	9.3	1.4	271.	10.1	2.1	268.	12.32	6.88	1.8321	1.0233
3994.	28.86	-87.81	22.95	98.	22.65	93.	6.42	8.9	8.6	296.	9.3	1.2	285.	9.3	1.9	262.	11.84	6.61	1.8437	1.0290
3995.	28.86	-87.58	21.95	100.	21.43	94.	6.16	8.8	8.5	295.	8.2	1.1	285.	8.3	2.3	254.	11.41	6.36	1.8526	1.0335
3996.	28.86	-87.35	21.02	102.	20.80	93.	5.91	8.7	8.5	295.	7.1	1.3	289.	8.1	3.6	215.	10.98	6.14	1.8587	1.0387
3997.	28.86	-87.12	20.18	87.	19.96	96.	5.67	8.5	8.1	298.	6.5	1.7	280.	7.4	3.8	262.	10.57	5.92	1.8653	1.0450
4055.	29.06	-91.95	30.30	335.	30.30	335.	4.37	6.6	6.5	171.	-14.4	62.5	96.	35.1	67.4	85.	7.82	5.33	1.7896	1.2189
4056.	29.06	-91.72	35.94	348.	35.94	348.	5.14	7.5	8.5	180.	-17.8	65.4	122.	41.0	70.1	111.	8.93	5.41	1.7376	1.0534
4057.	29.06	-91.49	41.53	10.	41.53	10.	5.65	8.0	9.1	195.	-38.6	75.7	147.	49.5	75.7	147.	9.68	5.14	1.7137	0.9100
4058.	29.06	-91.26	45.33	33.	45.33	33.	6.13	8.5	10.2	218.	-132.2	29.6	143.	141.5	65.2	342.	10.18	4.94	1.6603	0.8065
4059.	29.06	-91.03	47.84	70.	47.84	70.	6.52	8.6	10.3	253.	-132.2	29.6	143.	141.5	65.2	342.	11.01	5.16	1.6888	0.7906
4060.	29.06	-90.80	46.09	73.	46.09	73.	6.26	8.3	10.0	259.	-11.0	28.1	0.	314.8	44.5	0.	10.70	5.08	1.7094	0.8112

Hurricane ANDREW
Final Hindcast Results

gp	lat	long	max ws	asso wd	(ws	wd	max hs	ts	.74*tp	vmd	hsur	cs	) cd	max hsur	max cs	asso cd	forr	haring	w/hs	c/hs
4061.	29.06	-90.57	43.39	76.	43.39	76.	5.42	7.7	8.8	264.	206.9	64.4	235.	226.5	68.4	236.	9.42	4.76	1.7386	0.8780
4062.	29.06	-90.34	40.39	77.	40.22	90.	5.12	7.5	8.7	281.	151.9	105.0	267.	153.8	119.7	266.	9.15	5.11	1.7870	0.9973
4063.	29.06	-90.11	37.54	88.	37.54	88.	7.13	8.5	10.0	287.	98.0	115.8	266.	112.5	117.6	265.	12.47	7.64	1.7476	1.0703
4064.	29.06	-89.88	34.94	84.	34.36	96.	7.72	8.9	9.9	299.	78.2	98.1	247.	82.1	101.1	249.	13.62	9.26	1.7634	1.1997
4065.	29.06	-89.65	32.94	82.	32.45	92.	7.27	8.7	9.8	302.	41.2	89.3	296.	50.4	89.3	296.	12.97	8.88	1.7849	1.2217
4066.	29.06	-89.42	31.00	80.	30.06	97.	5.47	7.6	8.8	291.	41.4	93.8	277.	45.8	97.4	276.	9.88	5.97	1.8057	1.0911
4067.	29.06	-89.19	29.46	86.	28.94	94.	6.99	8.8	8.8	293.	32.3	75.8	262.	35.9	75.9	263.	12.75	8.78	1.8236	1.2564
4068.	29.06	-88.96	27.86	86.	27.12	98.	7.54	9.2	8.7	298.	19.9	45.7	214.	19.9	48.2	218.	13.67	8.74	1.8113	1.1584
4069.	29.06	-88.73	26.55	85.	26.26	95.	7.38	9.2	8.7	297.	14.5	17.0	231.	15.0	19.8	247.	13.45	7.86	1.8224	1.0654
4070.	29.06	-88.50	25.36	90.	25.36	90.	7.04	9.1	8.7	294.	11.0	7.1	243.	12.4	10.0	260.	12.90	7.30	1.8324	1.0371
4071.	29.06	-88.27	24.29	89.	24.29	89.	6.72	9.0	8.7	294.	8.1	2.5	267.	10.0	4.1	263.	12.36	6.94	1.8387	1.0322
4072.	29.06	-88.04	23.27	93.	23.27	93.	6.43	8.8	8.3	297.	7.2	2.0	265.	9.5	3.5	246.	11.88	6.65	1.8475	1.0339
4073.	29.06	-87.81	22.31	95.	22.09	93.	6.15	8.7	8.2	297.	6.5	1.5	276.	8.6	3.2	249.	11.44	6.39	1.8600	1.0391
4074.	29.06	-87.58	21.42	98.	21.21	96.	5.90	8.5	8.0	300.	5.6	1.4	270.	8.0	3.9	226.	11.02	6.15	1.8667	1.0424
4075.	29.06	-87.35	20.59	100.	20.59	100.	5.66	8.3	7.9	303.	5.7	2.1	263.	7.2	5.1	230.	10.61	5.93	1.8758	1.0483
4076.	29.06	-87.12	19.82	102.	19.82	102.	5.43	8.2	7.8	304.	5.2	2.8	264.	7.2	5.2	243.	10.22	5.72	1.8820	1.0542
4134.	29.26	-91.95	31.33	341.	31.33	353.	3.67	6.4	7.0	184.	-144.6	71.9	92.	67.4	76.4	88.	6.51	3.84	1.7716	1.0456
4135.	29.26	-91.72	37.74	3.	37.74	3.	4.80	7.3	8.6	191.	-182.4	61.5	101.	94.5	61.5	101.	8.14	4.37	1.6960	0.9110
4136.	29.26	-91.49	42.50	28.	42.50	28.	5.38	7.8	9.8	203.	-215.1	41.4	147.	140.8	53.1	357.	9.10	4.64	1.6918	0.8635
4143.	29.26	-89.88	32.08	88.	25.88	128.	3.80	6.3	8.1	318.	61.6	27.0	227.	100.3	40.3	231.	7.13	4.27	1.8737	1.1220
4144.	29.26	-89.65	30.33	86.	30.30	78.	3.45	6.2	6.1	275.	23.7	37.8	308.	57.9	40.9	309.	6.46	3.92	1.8710	1.1357
4147.	29.26	-88.96	26.52	87.	26.06	94.	6.19	8.3	8.8	291.	32.6	68.3	181.	33.4	69.1	181.	11.39	7.78	1.8397	1.2562
4148.	29.26	-88.73	25.30	87.	24.70	97.	6.74	8.8	8.6	299.	22.6	53.4	221.	25.2	55.7	221.	12.34	7.85	1.8312	1.1653
4149.	29.26	-88.50	24.29	87.	24.06	95.	6.63	8.8	8.3	299.	15.9	42.8	241.	18.5	48.3	240.	12.24	7.36	1.8458	1.1094
4150.	29.26	-88.27	23.34	91.	23.34	91.	6.40	8.8	8.5	297.	10.8	23.2	268.	12.2	30.2	268.	11.87	6.91	1.8552	1.0801
4151.	29.26	-88.04	22.49	91.	22.42	94.	6.16	8.7	8.1	299.	10.6	16.1	275.	12.1	22.6	272.	11.46	6.55	1.8609	1.0624
4152.	29.26	-87.81	21.67	93.	21.54	96.	5.93	8.5	8.0	300.	8.3	11.6	277.	11.3	19.7	265.	11.06	6.25	1.8660	1.0539
4153.	29.26	-87.58	20.90	96.	20.73	98.	5.71	8.4	7.9	302.	6.9	4.5	268.	12.4	15.0	234.	10.67	5.98	1.8684	1.0483
4154.	29.26	-87.35	20.17	98.	20.17	98.	5.49	8.3	7.9	303.	6.5	2.9	253.	10.7	12.5	229.	10.27	5.75	1.8715	1.0482
4155.	29.26	-87.12	19.48	100.	19.48	100.	5.28	8.2	7.8	304.	6.3	2.6	257.	9.8	9.6	240.	9.89	5.55	1.8751	1.0512
4213.	29.46	-91.95	32.80	349.	32.80	349.	3.79	6.4	7.2	183.	-96.4	65.5	83.	67.4	76.4	88.	6.74	3.92	1.7805	1.0360
4214.	29.46	-91.72	38.56	18.	38.56	18.	4.88	7.4	8.8	206.	-156.7	51.9	93.	94.5	61.5	101.	8.21	4.39	1.6812	0.8985
4215.	29.46	-91.49	41.43	43.	41.43	43.	5.29	7.7	9.1	217.	-227.0	34.2	134.	140.8	53.1	357.	9.08	4.65	1.7174	0.8788
4224.	29.46	-89.42	27.19	81.	27.03	88.	3.51	6.2	6.8	262.	145.9	35.8	181.	145.9	35.8	181.	6.42	3.98	1.8257	1.1326
4225.	29.46	-89.19	26.14	80.	26.12	86.	3.11	6.0	6.1	264.	109.5	35.8	173.	111.8	35.8	173.	5.73	3.55	1.8455	1.1434
4226.	29.46	-88.96	25.25	85.	24.98	91.	3.80	6.2	8.7	277.	42.5	59.4	208.	45.2	59.4	208.	6.88	4.18	1.8088	1.0981
4227.	29.46	-88.73	24.27	89.	22.68	105.	5.69	8.2	8.2	300.	32.1	57.0	229.	32.4	58.7	231.	10.64	7.33	1.8697	1.2888
4228.	29.46	-88.50	23.31	89.	22.79	97.	6.03	8.4	8.0	299.	24.4	52.8	237.	26.7	53.5	237.	11.17	7.24	1.8540	1.2017
4229.	29.46	-88.27	22.51	89.	22.32	95.	5.89	8.4	8.0	298.	15.8	37.7	265.	18.7	38.6	266.	10.98	7.09	1.8651	1.2046
4230.	29.46	-88.04	21.73	89.	21.43	98.	5.73	8.3	7.9	300.	13.1	35.4	273.	16.3	36.2	273.	10.72	6.82	1.8696	1.1904
4231.	29.46	-87.81	21.03	92.	20.82	97.	5.59	8.3	7.9	301.	12.5	31.9	276.	14.7	33.6	277.	10.46	6.54	1.8723	1.1704
4232.	29.46	-87.58	20.36	94.	20.26	97.	5.48	8.3	7.9	302.	10.4	14.9	272.	12.0	24.3	240.	10.26	6.18	1.8709	1.1267
4233.	29.46	-87.35	19.71	96.	19.58	99.	5.31	8.2	7.9	304.	8.9	6.7	244.	9.7	22.4	217.	9.95	5.64	1.8737	1.0627
4234.	29.46	-87.12	19.10	98.	18.96	100.	5.11	8.1	7.8	306.	8.6	4.4	248.	8.9	14.7	225.	9.58	5.40	1.8750	1.0566
4292.	29.66	-91.95	33.82	2.	33.82	2.	4.64	7.3	8.2	196.	-19.1	39.3	77.	67.4	76.4	88.	7.86	4.78	1.6962	1.0316

Hurricane ANDREW
Final Hindcast Results

gp	lat	long	max ws	asso wd	(ws	wd	max hs	ts	.74*tp	vmd	hsur	cs	cd)	max hsur	max cs	asso cd	forr	haring	w/hs	c/hs
4293.	29.66	-91.72	38.90	34.	38.90	34.	4.71	7.3	8.7	210.	-67.3	26.2	66.	94.5	61.5	101.	7.80	4.25	1.6553	0.9022
4302.	29.66	-89.65	26.58	86.	26.47	80.	3.14	5.8	6.5	263.	145.9	35.8	181.	145.9	35.8	181.	5.83	3.58	1.8572	1.1386
4303.	29.66	-89.42	25.57	80.	25.57	80.	3.42	6.1	6.5	263.	105.1	17.6	182.	108.8	19.6	185.	6.34	4.06	1.8519	1.1869
4304.	29.66	-89.19	24.80	84.	24.56	89.	3.44	6.3	6.3	271.	108.4	16.5	177.	108.8	19.6	185.	6.39	4.14	1.8573	1.2014
4305.	29.66	-88.96	24.05	83.	23.53	93.	4.01	6.5	8.0	278.	58.6	40.4	217.	59.3	43.5	222.	7.36	4.65	1.8376	1.1607
4306.	29.66	-88.73	23.30	87.	22.54	97.	4.77	7.4	8.2	290.	44.0	42.8	233.	44.0	44.9	236.	9.00	5.89	1.8882	1.2356
4307.	29.66	-88.50	22.48	90.	21.60	99.	5.48	8.0	7.9	299.	34.4	43.5	230.	35.4	44.1	231.	10.27	6.95	1.8766	1.2699
4308.	29.66	-88.27	21.70	90.	21.25	97.	5.44	8.0	7.8	299.	21.8	37.9	264.	25.2	37.9	264.	10.24	6.83	1.8838	1.2565
4309.	29.66	-88.04	21.05	90.	20.46	100.	5.31	8.0	7.8	301.	19.2	37.9	273.	22.8	37.9	273.	10.02	6.68	1.8859	1.2564
4310.	29.66	-87.81	20.41	93.	20.18	98.	5.20	7.9	7.8	300.	18.0	35.9	276.	21.1	36.0	276.	9.81	6.50	1.8852	1.2491
4311.	29.66	-87.58	19.83	93.	19.50	100.	5.10	8.0	7.8	302.	13.1	19.8	271.	16.5	19.9	270.	9.60	6.19	1.8811	1.2139
4312.	29.66	-87.35	19.27	95.	19.18	97.	5.10	8.2	7.9	304.	10.1	10.0	239.	15.3	27.4	202.	9.58	5.61	1.8775	1.1000
4313.	29.66	-87.12	18.73	97.	18.44	101.	4.94	8.0	7.8	307.	9.7	7.4	239.	12.9	20.0	219.	9.27	5.28	1.8776	1.0703
4383.	29.86	-89.19	23.56	83.	21.86	106.	3.22	6.0	6.2	285.	97.4	6.9	216.	108.4	13.8	229.	6.10	3.99	1.8916	1.2381
4384.	29.86	-88.96	22.92	82.	21.87	100.	3.49	6.3	6.5	285.	64.7	21.4	236.	66.4	35.0	245.	6.51	4.28	1.8682	1.2275
4385.	29.86	-88.73	22.34	85.	21.42	99.	4.18	6.9	7.8	289.	50.4	25.9	240.	50.7	33.7	246.	7.90	5.09	1.8874	1.2165
4386.	29.86	-88.50	21.72	89.	20.59	102.	5.05	7.7	7.8	299.	39.8	29.0	225.	41.5	32.3	230.	9.50	6.49	1.8812	1.2836
4387.	29.86	-88.27	21.03	91.	19.81	104.	5.07	7.8	7.7	304.	28.4	33.5	265.	31.2	35.8	266.	9.55	6.42	1.8849	1.2670
4388.	29.86	-88.04	20.41	89.	19.53	102.	4.94	7.7	7.7	302.	26.4	37.1	274.	28.4	37.9	273.	9.35	6.32	1.8923	1.2797
4389.	29.86	-87.81	19.86	92.	19.32	100.	4.86	7.7	7.7	301.	21.4	36.3	272.	25.5	36.9	273.	9.19	6.21	1.8911	1.2768
4390.	29.86	-87.58	19.32	92.	19.12	98.	4.74	7.7	7.7	300.	16.4	21.7	269.	19.9	21.7	268.	8.95	5.95	1.8880	1.2546
4391.	29.86	-87.35	18.82	94.	18.55	100.	4.74	7.8	7.8	304.	13.8	16.0	235.	16.0	26.4	206.	8.93	5.65	1.8841	1.1912
4392.	29.86	-87.12	18.34	96.	18.15	99.	4.72	7.9	7.8	307.	11.1	10.4	239.	14.8	25.5	229.	8.87	5.16	1.8807	1.0934
4460.	30.06	-89.65	0.00	0.	0.00	0.	0.00	0.0	0.0	0.	0.0	0.0	0.	0.0	0.0	0.	0.00	0.00	0.0000	0.0000
4461.	30.06	-89.42	0.00	0.	0.00	0.	0.00	0.0	0.0	0.	0.0	0.0	0.	0.0	0.0	0.	0.00	0.00	0.0000	0.0000
4462.	30.06	-89.19	0.00	0.	0.00	0.	0.00	0.0	0.0	0.	0.0	0.0	0.	0.0	0.0	0.	0.00	0.00	0.0000	0.0000
4463.	30.06	-88.96	0.00	0.	0.00	0.	0.00	0.0	0.0	0.	0.0	0.0	0.	0.0	0.0	0.	0.00	0.00	0.0000	0.0000
4464.	30.06	-88.73	21.47	85.	20.38	101.	3.65	6.3	7.7	290.	54.4	21.1	258.	56.0	33.7	263.	6.74	4.33	1.8446	1.1851
4465.	30.06	-88.50	20.99	88.	20.05	100.	4.45	7.2	7.8	299.	44.8	26.6	231.	46.2	31.0	239.	8.42	5.78	1.8936	1.2990
4466.	30.06	-88.27	20.40	90.	19.36	102.	4.42	7.3	7.7	305.	35.0	36.4	269.	36.5	39.2	269.	8.40	5.71	1.9014	1.2930
4467.	30.06	-88.04	19.84	93.	18.72	104.	4.30	7.2	7.7	307.	32.0	39.9	275.	33.9	42.7	272.	8.22	5.64	1.9107	1.3112
4468.	30.06	-87.81	19.32	91.	18.51	102.	4.25	7.2	7.7	304.	27.9	41.6	271.	31.8	43.8	271.	8.13	5.59	1.9139	1.3161
4469.	30.06	-87.58	18.84	93.	18.37	100.	4.25	7.2	7.7	303.	20.6	28.7	263.	24.1	30.1	263.	8.08	5.53	1.9014	1.3016
4470.	30.06	-87.35	18.39	93.	18.23	98.	4.25	7.3	7.7	302.	16.8	27.3	250.	20.1	27.3	247.	8.05	5.43	1.8919	1.2769
4471.	30.06	-87.12	17.97	95.	17.74	100.	4.26	7.5	7.7	306.	14.2	22.7	250.	16.9	30.8	249.	8.06	5.16	1.8890	1.2098
4540.	30.26	-89.42	0.00	0.	0.00	0.	0.00	0.0	0.0	0.	0.0	0.0	0.	0.0	0.0	0.	0.00	0.00	0.0000	0.0000
4541.	30.26	-89.19	0.00	0.	0.00	0.	0.00	0.0	0.0	0.	0.0	0.0	0.	0.0	0.0	0.	0.00	0.00	0.0000	0.0000
4542.	30.26	-88.96	0.00	0.	0.00	0.	0.00	0.0	0.0	0.	0.0	0.0	0.	0.0	0.0	0.	0.00	0.00	0.0000	0.0000
4543.	30.26	-88.73	0.00	0.	0.00	0.	0.00	0.0	0.0	0.	0.0	0.0	0.	0.0	0.0	0.	0.00	0.00	0.0000	0.0000
4544.	30.26	-88.50	0.00	0.	0.00	0.	0.00	0.0	0.0	0.	0.0	0.0	0.	0.0	0.0	0.	0.00	0.00	0.0000	0.0000
4545.	30.26	-88.27	0.00	0.	0.00	0.	0.00	0.0	0.0	0.	0.0	0.0	0.	0.0	0.0	0.	0.00	0.00	0.0000	0.0000
4546.	30.26	-88.04	0.00	0.	0.00	0.	0.00	0.0	0.0	0.	0.0	0.0	0.	0.0	0.0	0.	0.00	0.00	0.0000	0.0000
4547.	30.26	-87.81	0.00	0.	0.00	0.	0.00	0.0	0.0	0.	0.0	0.0	0.	0.0	0.0	0.	0.00	0.00	0.0000	0.0000
4548.	30.26	-87.58	0.00	0.	0.00	0.	0.00	0.0	0.0	0.	0.0	0.0	0.	0.0	0.0	0.	0.00	0.00	0.0000	0.0000
4549.	30.26	-87.35	0.00	0.	0.00	0.	0.00	0.0	0.0	0.	0.0	0.0	0.	0.0	0.0	0.	0.00	0.00	0.0000	0.0000

Hurricane ANDREW
Final Hindcast Results

gp	lat	long	max ws	asso wd	(ws	wd	max hs	ts	.74*tp	vmd	hsur	cs	cd)	max hsur	max cs	asso cd	forr	haring	w/hs	c/hs
4550.	30.26	-87.12	0.00	0.	0.00	0.	0.00	0.0	0.0	0.	0.0	0.0	0.	0.0	0.0	0.	0.00	0.00	0.0000	0.0000
4625.	30.46	-88.04	0.00	0.	0.00	0.	0.00	0.0	0.0	0.	0.0	0.0	0.	0.0	0.0	0.	0.00	0.00	0.0000	0.0000